Conjugate effect of fluctuating thermal and mass diffusion on the viscous fluid flow along flat and cylindrical surfaces

Ph.D DISSERTATION

by

Sharmina Hussain

to

The Department of Mathematics

in partial fulfillment of the requirements

for the Degree of

Doctor of Philosophy

in the subject of

Mathematics.

UNIVERSITY OF DHAKA

Ramna, Dhaka-1000

February 2018

Dedication:

I would like to dedicate this work
to my beloved husband and my three angels.

Abstract

Numerical investigations have been carried out to look into the effect of double-diffusion on laminar flow along vertical flat and cylindrical surfaces. Conventional convective processes i.e. natural convection, mixed convection and magnetohydrodynamic (MHD) natural convection have been considered and six different models are studied deeming oscillating surface temperature and species concentration boundary conditions. In each case, extensive parametric simulations are performed in order to elucidate the effects of some important parameters i.e. Prandtl number, Schmidt number, buoyancy ratio parameter, Straouhal number, and magnetic parameter on flow field in conjunction with heat and mass transfer. Different numerical techniques are applied to solve the governing equations. Asymptotic solutions for low and high frequencies are obtained for the conveniently transformed governing coupled equations. Solutions are also obtained for wide ranged values of the frequency parameter.

At the very outset of this dissertation, natural convection flow along vertical flat plate is considered. The surface temperature and species concentrations are assumed to be of small amplitude oscillation. In this study, the similar boundary conditions are imposed for surface temperature and concentration as well as surface heat and mass flux. Finally, comparative study has been made to find a correlation between these two cases. Comparison between the perturbation solutions and the solutions for the wide ranged values are made in terms of the amplitude and phase of the shear stress, surface heat transfer and surface mass transfer coefficient. It has been found that the amplitudes and phase angles obtained from asymptotic solutions are in good agreement with the finite difference solutions obtained for wide ranged values of the frequency parameter. This simulated results are validated against some published results.

Flow along a vertical wedge is taken into account and the convective process is deemed as mixed convection in the subsequent model study. In this study also, the surface temperature and velocity boundary conditions are assumed to be sinusoidal and amplitude of the oscillation is considered very small. Implicit finite difference method is used to solve the governing equations of the entire flow field and results obtained from this method are

compared with the perturbation solutions which are calculated for low and high frequency regions of the flow field, respectively. To study the parametric effects on the heat transfer rate, results are calculated in terms of amplitude and phase angles of shear stress and heat transfer coefficient.

In the next investigation, the preceding model is extended to study heat and mass transfer simultaneously. In order to take into account the concentration field, another convection-diffusion equation is added with the governing set of equations and corresponding boundary condition is assumed to be similar to surface temperature boundary condition. Wide-ranging parametric studies have been carried out and results are presented in both tabular and graphical forms.

Magnetohydrodynamic (MHD) natural convection flow is investigated considering fluctuating surface temperature and concentration boundary condition. Results obtained in the present investigation are compared with some other published results and further numerical investigations are accomplished to study the both heat and mass transfer by using implicit finite difference method. It has been assumed in this study that, in some undisturbed flow region, there is an uniform magnetic field making a non-zero angle with it.

Mixed convection flow along horizontal heated cylinder have been considered in the last two models and full set of Navier-Stokes equations in terms of vorticity and stream function is solved. Parametric studies have been carried out in these cases and heat and mass transfer rates are observed by calculating the Nusselt number and Sherwood number. In the first investigation of these type of flow, non-uniform surface temperature and concentration are considered with no oscillations. After that, the same problem is studied by allowing small amplitude oscillations in surface velocity, temperature and species concentration. In both the cases, isothermal lines and isoconcentration contours are drawn to visualize the temperature and concentration distribution by varying the relevant parameters.

Important findings are listed after each investigation and finally concluding remarks are brought out based on the overall investigation and understanding. Almost all the cases, the present simulations are validated either qualitatively or quantitatively by comparing with some published results.

Acknowledgements

It is a matter of great pleasure for me to acknowledge my thankfulness to my honorable supervisor Professor Amulya Chandra Mandal, Department of Mathematics, University of Dhaka. I would like to offer my special thanks to the members of my examining committee for taking all the troubles to read through my thesis and for traveling all way through from different corners of the world to here at Dhaka, Bangladesh. My sincere gratitude to all of them.

The work compiled here would not have been materialized without the untiring support,valuable guidance and sincere supervision that have been received by me from my mentor Professor Anwar Hossain. So my heart full gratitude and profound respect to him. His flexibility, dedication, and encouragement have pushed me far beyond my expectations.

Heartfelt thanks to my fellow colleague Dr.Nepal Chandra Roy for his cordial support and important suggestions that he provided throughout my Ph.D period. My genuine thankfulness towards my brother like colleagues Mr. Shamim Kaiser, Mr. Lutfor Rahman, Mr. Fysol Ibn Abbas and Mr. Hasan Murad for their very kind and cordial gesture en route to me!

I wish to express my sincere gratitude to my husband for taking all the troubles of baby seating for last six years and for holding my hands with his divine love and for offering me moral support and mental strength to overcome all the hurdles whenever it comes. Sincere gratitude to all of my family members, specially, my brothers and sister(who is the second Mom of my son!) for their true love, appreciation, co-operation and encouragement throughout the journey of my life.

Sincere gratitude to the BRAC university authority for providing me all sorts of technical supports, specially, for granting me sabbatical leave for one year during the preparation of this dissertation. Heart full gratitude to our former department chair, Professor A.A.Z. Ahmad for his father like encouragement to complete my Ph.D thesis.

Appreciativeness are due to the department of Mathematics and Natural Sciences, BRAC University, for their co-operation and technical support and material support in different stages of this work. Finally, to those unnamed or unreferenced (and there will

always be someone), my apologies and thanks. You know who you are !

Last but not the least gratefulness to Abbu and Ammu for giving me birth in this wonderful world because I always find my life in this planet very beautiful.

Finally, I would like to apologize to anyone whose rights I may have unwittingly infringed.

Table of Contents

List of Figures

List of Tables

List of Symbols

B_0	Magnetic field
$\bar{C}$	Dimensional Species concentration in the boundary layer
C	Species concentration in the boundary layer
C_w	Species concentration at the surface
C_∞	Species concentration at the ambient fluid
D	Concentration Diffusivity
g	Acceleration due to gravity
Gr_T	Grashof number for thermal diffusion
Gr_C	Grashof number for mass diffusion
Gr_x	Grashof number for combined thermal and mass diffusion
M	magnetic parameter
m_w	Dimensionless Sherwood number
n	Flux exponent parameter
Pr	Prandtl number
q_w	Dimensionless heat transfer rate
Sc	Schmidt number
St	Strouhal number
$\bar{T}$	Dimensioless temperature of the fluid in the boundary layer
T	Dimensioless temperature of the fluid in the boundary layer
T_w	Temperature at the surface
T_∞	Temperature of the ambient fluid
$\bar{u},\ \bar{v}$	Dimensional velocity in the $\bar{x},\ \bar{y}$ direction respectively.

$u,\ v$	Dimensionless fluid velocities in the $x,\ y$ direction respectively
t	Time
w	Buoyancy ratio parameter
$\bar{x},\ \bar{y}$	Dimensional Cartesian coordinates
$x,\ y$	Dimensionless Cartesian coordinates
Greek letters	
ξ	Scaled streamwise variable
η	Pseudo similarity variable
δ_M	Momentum boundary layer thickness
δ_T	Thermal boundary layer thickness
δ_C	Concentration boundary layer thickness
τ_w	Dimensionless shear stress
ϕ	Dimensionless concentration
θ	Dimensionless temperature
ψ	Stream function
γ	Wavelength of the applied magnetic field
$\bar{\alpha}$	Dimensional thermal diffusivity
β_T	Volumetric coefficient of thermal expansion
β_C	Volumetric coefficient of expansion with concentration
μ	Dynamical viscosity
ν	Kinematic viscosity
ρ	Density of the fluid
σ	Electrical conductivity
Subscripts	
w	Wall condition
∞	Ambient condition

Chapter 1

Introduction

1.1 Introduction

Fluid Dynamics is the study of dynamics of things that flow and react. This branch of science co-relate the theoretical aspects of fluid flow (for both liquid and gas) to the mathematical and physical approach. Modern efficient computational skills and technology enables us to study even the dynamics of very complicated flows. Fluid dynamics offers a systematic structure which underlies a number of practical disciplines that embraces empirical and semi-empirical laws derived from flow measurement and used to solve practical problems. The solution to a fluid dynamics problem typically involves calculating various properties of the fluid, such as velocity, pressure, density and temperature as functions of space and time. Fluid mechanics, like the study of any other branch of science, needs mathematical analysis as well as experimentation. The analytical approaches help in finding the solutions to certain idealized and simplified problems, and in understanding the unity behind apparently dissimilar phenomena. In fact, fluid dynamics study involves such a large number of fields that have no strict border line. Applications of fluid mechanics include a variety of machines, ranging from the water-wheel to the airplane. In addition, the study of fluids provides an understanding of a number of everyday phenomena, such as why an open window and door together create a draft in a room etc.

Aerospace engineers may be interested in designing airplanes that have low resistance

and, at the same time, high"lift" force to support the weight of the plane. Civil engineers may be interested in designing irrigation canals, dams, and water supply systems. Pollution control engineers may be interested in saving our planet from the constant dumping of industrial sewage into the atmosphere and the ocean. Mechanical engineers may be interested in designing turbines, heat exchangers, and fluid cooling. Chemical engineers may be interested in designing efficient devices to mix industrial chemicals. All these works are highly involved with fluid flow and all of their jobs require a very clear understanding and knowledge of physics of fluid flow, mathematics in conjunction with engineering. The objectives of physicists and engineers, however, are not quite separable because the engineers need to understand and the physicists need to be motivated through applications. Needless to say, drastic simplifications are frequently necessary because of the complexity of real phenomena. The mathematicians help both engineers and physicist by their mathematical skills and knowledge, they help extensively how to solve or simulate the model equations so that the physicists can have a clear insight about the flow behavior and the engineers can apply the model in a most efficient manner. A good under-standing of mathematical techniques is definitely helpful here, although it is probably fair to say that some of the greatest theoretical contributions have come from the people who depended rather strongly on their unusual physical intuition, some sort of a"visio" by which they were able to distinguish between what is relevant and what is not.

By solving the governing equation of the flow, some coefficients, which are important in practical point of view, are calculated. If the desired quantities are related to some reference values, then the dimensionless solutions can be obtained. These dimensionless solutions are dependent only on dimensionless position coordinates and on some other dimensionless values, which are known as similarity parameters. The knowledge of the relevant coefficients for a flow problem is of fundamental importance in carrying out modeling. In general, similar types but smaller in size model is studied first then results are examined in a water or wind tunnel. Thus the question of the physical similarity of flows arises, and with it the question of whether the results from modeling can be carried over to full-scale construction. By introducing the dimensionless quantities in the fundamental set of governing equation-

s, some very important dimensionless characteristics number appear, these are, Reynolds number, Froude number, Prandtl number, Eckert number, thermal expansion number etc. It can be inferred physically similar flows from the flow passing through geometrically similar types of flow by examining the above mentioned dimensionless numbers. The main concern of fluid mechanics is to determine the dependence of the solutions of the equations of motion on the characteristics numbers. In order to reduce the number of characteristics number, it is usual to investigate the asymptotic behaviour of the solutions for very large or very small values of the similarity variables.

To study the flow behavior, heat and mass transfer, (such as in transpiration or dissolution), phase change (such as in freezing or boiling), chemical reaction (such as combustion), mechanical movement (such as an impeller turning), and stress or deformation of related solid structures (such as a mast bending in the wind), computational model is built that represents a system or device that we want to study. Then we apply the fluid flow physics to this virtual prototype, and the computational skills produce the outputs of a prediction of the fluid dynamics.

Fluid normally flows from high velocity to lower, as a result momentum transfer occurs and one can get the experience of problem of momentum transfer during pressure drop in systems, determination of flow rate measurements and control, motion of solid particles in fluids, flow over immersed bodies, flow through porous media and channels, examining rate of heat and mass transfer between flowing streams and the motion of drops and bubbles. Two important mechanisms that arise in most transport processes are *diffusion* and *convection*. Diffusive flow is caused by the action of density gradients in conjunction with a gravitational field. In these kind of flow, the driving forces arise not only from temperature gradients, but also from composition gradients even in an isothermal system etc. In convective flow, there must be some transfer of thermal energy (species concentration) in a moving fluid (liquid or gas). Internal stresses, namely , hydrostatic pressure and the viscous stresses are responsible for momentum transfer to, from or within a fluid. Fluid flows due to only pressure gradient are relatively easier to study whereas the viscous fluid flows arises with certain complexities. Velocity gradient in the direction normal to the ve-

locity itself results into the "***shear***" which is confined to a thin layer adjacent to the solid surface along which the fluid flows. Shear layers in which the flow is steady or varies with time only in a simple way are called *laminar* shear layers. In the cases, where, though the external stream may be steady or smoothly varying in time, the velocity within the shear layer fluctuates irregularly but continuously in magnitude and direction both in time and in space are called *turbulent* flows.

It has been observed that heat and mass transfer mechanism are almost similar in nature so that identical mathematical expressions can be made for both. So this advantageous factor is exploited for studying heat and mass transfer. There also some significant differences between these two, for example, one of them is the large number of chemical and physical processes that essentially requires the analysis of mass transfer. The stability of this type of flow is also depends on the specific chemical system involved as well as on the temperature and the pressure. Transported particle size of the pure species relative to the mean free path in the neighboring environment is another influential factor for this kind of flow. Considering all these factors, study of heat and mass transfer along with velocity field is classified into three subsequent branches namely, *natural convection*, *forced convection* and *mixed convection* depending upon the physical system that initiated the motion of the fluid.

Natural or "Buoyant" or "Free" convection is a very important mechanism that is operative in a variety of environments from cooling electronic circuit boards in computers to causing large scale circulation in the atmosphere as well as in lakes and oceans that influences the weather. "Buoyancy force", due to the density gradient, act as the driving force in natural convection flow. The presence of some accelerating forces such as appears from resistance to gravity, or an equivalent force (arising from centrifugal or Coriolis force), is also important for this kind of flow. In natural convection situations, an important dimensionless group is the Grashof number which is the ratio of buoyancy force to the viscous force and is denoted as Gr. The Grashof number is related to the Reynolds number, and in heat transfer, the Prandtl number, plays a significant role. Therefore, in natural convection heat transfer, we encounter another dimensionless group, called the Rayleigh

number, abbreviated by Ra, which is the product of the Grashof and Prandtl numbers: $Ra = Gr \times Pr = \frac{\beta \triangle T g L^3}{\nu \alpha}$. Here, α is the thermal diffusivity of the fluid and β is the co-efficient of volumetric expansion.

When the fluid flow occurs due to the effects of some external forces which may be in the form of pressure differences (created by an external device, fan or pump, then the convection is termed as forced convection. The fundamental difference between natural and forced convection flow is being conceived through the governing equations of the two convection modes. The buoyancy parameter for this type of flow is the ratio of Grashof number to the Reynolds number, i.e. $\frac{Gr}{Re^n}$, where n is a positive constant which depends on the surface heating conditions and flow configuration.

Mixed (combined) convection is a combination of forced and free convection which is the general case of convection when a flow is determined simultaneously by both an outer forcing system (i.e., outer energy supply to the fluid-streamlined body system) and inner volumetric (mass) forces, viz., by the nonuniform density distribution of a fluid medium in a gravity field. The most vivid manifestation of mixed convection is the motion of the temperature stratified mass of air and water areas of the earth that the traditionally studied in geophysics. Moreover, in micro meteorological and industrial applications, fluid flow along both horizontal and vertical surfaces bounded by an extensive body of fluid due to free or mixed convection are of significant importance and interest.

1.2 A wide reaching literature review

Flows arising from differences in concentration of material constitution, alone or in conjunction with temperature effects, are today receiving much attention by researchers. This is because, such buoyancy effects occur in many processes. Clearly atmospheric flows at all scales are driven appreciably by both temperature and water concentration differences. Flows in bodies of water are driven through the comparable effects upon density of temperature, concentration of dissolved materials and suspended particulate matter. Buoyancy induced convective flow has become isolated as a self-sustained research area not for so long, so it requires continuous development of mathematical methods to study these prob-

lems and also advanced equipment for solving modern practical problems. The transport processes due to double diffusion occurs both in nature and many engineering applications. Some very important examples of engineering applications include chemical reactions in reactor chamber, chemical vapor deposition of solid layers, combustion of atomized liquid fuels and dehydration operations in chemical and foundry plants etc. And, therefore, till today, a number of investigators are interested in the combined buoyancy forces arising from diffusion due to both thermal and concentration gradients, as this is very important from practical point of view. Before ensuing to the original work of present dissertation, an wide spreading literature review is presented here.

1.2.1 Convective flow due to double diffusion

An extensive literature survey on the topic of double diffusive flow has been carried out by Ostrach *et al.* (1980) [1], Huppert *et al.*(1981) [2], Gebhart *et al.* (1971) [3], Bejan (1995) [4], Mongruel *et al.* (1996) [5]. Important information and a frame work of this type of flow can also be found in the works of these investigators. In their studies, simultaneous heat and mass transfer in buoyancy induced laminar boundary layer flow along a vertical plate is studied substantially. The contributions of Turner (1973) [6], Gebhart (1973) [7], Nakayama (1995) [8], Goldstein and Volino (1995) [9], Hossain *et al.* [10] etc. are remarkable and provided basic frame work of studying double diffusive fluid flow problems. Some complexity arises during solving these problems because of the nonlinear nature of the governing equations and usually do not allow to use the superposition principal to solve the governing equations. Good information on recent investigations on the studies of simultaneous heat and mass transfer in laminar free convection boundary layer flows for plates can be found in the works of Khair and Bejan [11], in the monograph of Gebhart *et al.* [3], Chen Lin and Wu [12]- [13], and Mongruel *et al.* [5]. In the above studies, simultaneous heat and mass transfer in buoyancy induced laminar boundary layer flow along a vertical plate have been considered. Chen, [14] directed his attention towards the forced convection along vertical and inclined plates for which the plate is either maintained at a uniform temperature and concentration or subjected to a uniform surface heat and mass

flux. Khair and Bejan [11] (1985) was the first who considered the free convection boundary-layer along an isothermal vertical surface in a porous medium. They have deliberated the combined heat and mass transfer effect based on the similarity analysis of Cheng and Minkowycz [15] (1982). Angirasa *et al.* [16] (1997) studied numerically the double diffusive problem along a vertical flat plate. They have considered the porosity of the surface and has given special attention to the opposing buoyancy effects which are of the same order of magnitude and unequal thermal and concentration coefficients. S.Hussain *et.al* [17] investigated the steady natural convection flow due to combined effects of thermal and mass diffusion from a permeable vertical flat plate. This study focused on the boundary -layer regime promoted by the combined events in the permeable surface when the surface is at a non-uniform temperature, a non-uniform mass diffusion but with a uniform rate of suction. Natural convection flow through a vertical flat plate with oscillating surface heat flux was premeditated by Hossain *et al.* [18] (1998).

1.2.2 Double diffusive flow with oscillating boundary condition

The study of laminar boundary layer flow in presence of an oscillatory potential flow with a steady mean component was first undertaken by Lighthill [19] (1954). He considered the effect of small fluctuation in the free stream velocity on the skin friction and the heat transfer for plates and cylinders by employing the Karman-Pohlhausen approximate integral method. Nanda and Sharma [20] (1963) and Eshghy *et al.* [21] (1965) later extended Lighthill's theory for free convection flows. Muhuri and Maiti (1967) [22] investigated the free convection flow and heat transfer along a semi infinite horizontal plate with small amplitude surface temperature oscillation about a non zero mean, with the same method that has been mentioned. The problem of natural convection flow with an oscillating surface heat flux has been studied by Hossain *et al.* [23] (1988). Combined heat and mass transfer above a near-horizontal surface in a fluid saturated media was also studied by Hossain *et al.* (1999) [24]. Ackerberg and Phillips [25] found the solutions for the velocity flow field in presence of small oscillation in surface velocity. They calculated the asymptotic solutions of the boundary layer equations by implementing the matched asymptotic expansions

method. Furthermore, in their work, the numerical solution to the steady Blasius flow is also presented.

Less attention has been given to the study of unsteady flow due to double diffusion. Moreover, only the search of similarity solutions have attracted much attention. This is because similarity formulation transform easily the transport equations into a set of ordinary differential equations which can be solved numerically for different values of the parameters involved. However, some researchers, for example, Khair and Bejan (1985) [11], Trevisan and Bejan [26] (1987) set out a frame work to solve non similarity solutions for depicting heat and mass transfer with great success. Mongruel *et al.* (1996) [5], as stated earlier of this chapter, have proposed a novel method to solve double diffusive boundary layer flow over a vertical flat plate. They considered a vertical flat plate which is immersed in a viscous fluid or in a fluid-saturated porous medium. They proposed the integral boundary layer equations and scaling analysis approach. Hossain *et al.* [27] (2001) presented the results of unsteady natural convection flow along vertical flat plate subjected to the oscillatory boundary conditions on both surface temperature and species concentration. In their work, it is assumed that both the surface temperature and species concentration have small amplitude temporal oscillations with non-zero means. The mean temperature and mean species concentration are assumed to vary as a power of n of the distance measured from the leading edge. Numerical calculations were carried out by applying different techniques and results were compared in terms of amplitude and phase angles of heat and mass transfer coefficient.

1.2.3 Flow along wedges and boundary layer control

Ishigaki published a series of papers [28]- [32] on unsteady laminar boundary layer flow in the presence of free-stream oscillations. He investigated the time-mean characteristics of the periodic boundary layer near a two-dimensional stagnation point [28]. Later, Ishigaki, [29] focused on the temperature field in the laminar boundary layer near a two-dimensional stagnation point due to main-stream oscillation. He observed a time-mean modification in the temperature field through two effects, such as, the heat convection by the secondary

flow induced by the oscillation which consists in the nonlinearity of the governing equation, and the other effect results from the combined influence between the fluctuations of velocity and temperature. Ishigaki [30] theoretically examined the effect of oscillation on the time-mean skin friction and surface temperature of an insulated flat plate, taking into account the fluctuating stream velocity and the viscous dissipation in kinetic energy. In the subsequent study of the author [31], the oscillating heat transfer mechanism was investigated assuming the previous problem while the plate is kept at constant temperature instead of being insulated.

It was noted that the analysis is applicable to the fluctuations in relative velocity that arise from oscillations of a body parallel to a steady oncoming stream and when a body having variable speed as well as constant orientation and direction moves through a fluid at rest. Using this concept, Glauert [33] examined the laminar boundary layer on oscillating plates and cylinders. A comprehensive description shows how the results for a flat plate can be used to illustrate the boundary layer in the neighbourhood of the front stagnation point on a cylinder making transverse or rotational oscillations.

From a practical point of view, the flow oscillation is seen not only along the horizontal and vertical plate but also in an inclined plate or wedge-type flow. Gersten [35] theoretically investigated the time-mean heat transfer in a wedge-type flow with small amplitude oscillation and found that the time-mean heat-transfer rate is smaller than that without oscillation. Kumari and Gorla [36] carried out a boundary layer analysis considering the combined convection along a vertical non-isothermal wedge embedded in a fluid-saturated porous medium. Hossain *et al.* [37] examined a steady two dimensional laminar forced flow of a viscous incompressible fluid past a horizontal wedge with uniform surface heat flux. A steady mixed convection boundary layer flow over a vertical wedge with the effect of magnetic field embedded in a porous medium was studied by Kumari *et al.* [38]. Kandasamy *et al.* [39] presented the effects of variable viscosity and thermophoresis on magneto-hydrodynamics mixed convective heat and mass transfer past a porous wedge in the presence of chemical reaction. However, it should be mentioned here that Nanda and Sharma [20] first analyzed the free convection laminar boundary layers on a flat plate

assuming the oscillating plate temperature and isothermal free-stream. Also, the free convection flow and heat transfer from a semi-infinite vertical plate moving arbitrarily in its own plane and having variable surface temperature was examined by Sinha and Singh [40]. Roy *et al.* [41] studied the mixed convection flow due to surface temperature and free stream velocity oscillations along a vertical wedge. In this paper, parametric studies were carried out and the effects of some important parameters, i.e. Richardson number, Prandtl number on the amplitude and phase angles of skin friction were elucidated. Results obtained from different numerical techniques were also compared and good agreement were found to be noted.

The importance of suction and blowing in controlling the boundary-layer thickness and the rate of heat transfer has motivated many researchers to investigate its effects on forced and free convection flow. Flow control play very important role in combustion chamber of a aircraft and usually transpiration is the way to control the flow. Clarke and Riley [62] deliberated this kind of flow along a heated horizontal surface. Eichhorn [42] (1960) was the first to consider power law variations in the plate temperature and transpiration velocity, and gave similarity solutions of the problem. Sparrow and Cess [43], discussed the case of constant plate temperature and transpiration velocity distributions in powers of $x^{1/2}$, where x is the distance in the stream wise direction measured from the leading edge. Later, Merkin [44], Parikh *et al.* [45] presented numerical solutions for free convection heat transfer with blowing along an isothermal vertical flat plate. Hartnett and Eckert [46], Sparrow and Starr [47] reported the characteristics of heat transfer and skin friction for pure forced convection with blowing; the former dealt with a similar solution and the later with non similar one. Solutions of the problem on natural convection flow with arbitrary transpiration velocity were obtained by Kao [48], applying Meksin transformations. Free convection flow along a vertical plate with arbitrary blowing and wall temperature has also been investigated by Vedhanayagam *et. al* [49]. Lin and Yu [50] investigated the free convection flow over a horizontal plate, considering temperature and transpiration rates both of which followed power law variations. Tsuruno and Iguchi [51] were the first to predict the effects of uniform blowing on combined forced and free convection heat transfer

along a vertical isothermal plate, using methods similar to that of Terril [52], paying special attention to clarification of the limit between the combined convection and the effectively pure (either forced and free) convection region of flow. Kelleher and Yang [53] used series expansion technique to present the result for laminar free convection flow in presence of variable surface temperature along heated vertical flat plate. The efficient coordinate transformation procedure was adopted by Yang [54] and subsequently Merk-type series was applied to solve the problem along an inclined surface. Mixed convection flow of viscous incompressible fluid along a vertical permeable plate under the combined effects of thermal and mass diffusion and subjected to uniform wall temperature and species concentration has greatly fascinated the researchers and engineers due to its versatile applications. Hossain [55] studied the effect of uniform transpiration rate on the heat and mass transfer characteristics. In this analysis, the author considered the transpiration parameter of the type, given by : $V_0 = \left(\frac{V_w}{U_0}\right)\sqrt{\frac{Re_x}{\xi}}$ which is the ratio of the transpiration rate $\left(\frac{V_w}{U_0}\right)\sqrt{Re_x}$ and $\sqrt{\xi}$, where ξ is the mixed convection parameter that represents the thermal buoyancy effect, U_0 is the free stream velocity and V_w is the transpiration velocity at the plate. Hossain *et al.* [56] investigated the steady natural convection flow due to combined effects of thermal and mass diffusion from a permeable vertical flat plate. This study focused on the boundary -layer regime promoted by the combined events in the permeable surface when the surface is at a non-uniform temperature, a non-uniform mass diffusion but with a uniform rate of suction. Kimura and Bejan [57] developed the idea of heat and mass lines which can be very effectively used to visualize the path followed by heat and mass within the boundary layer. This concept can be used as a very useful tools to analyze the convective heat and mass transfer. Trevisan and Bejan [26] used this idea to depict the mass transfer in a rectangular enclosure. Unsteady natural convection flow in a cylindrical enclosure was also studied by Aggarwal and Manhapra , [58]. They have also applied the concept of heat lines to analyze the heat transfer phenomena. Mulaweh [59] presented a comprehensive review of the flow and heat transfer results of single-phase laminar mixed convection flow over vertical, horizontal and inclined backward-and forward-facing steps that have been published in different sources. The main perseverance of his study is to give

a detailed summary of the effect of several parameters such as, Prandtl number, Reynolds number, inclination angle, expansion ratio, step height, temperature difference between the heated wall and the free stream, and buoyancy force (assisting and opposing) on the flow and thermal fields downstream of the step. To measure the reattachment lengths of the recirculation regions that may develop upstream and/or downstream of the step are also noted in this review paper.

1.2.4 Magnetohydrodynamic (MHD) convective flow

Continuous development of MHD flow is opening new horizon to the technical development. Most recent research have been conducting in MHD flow so that it can be used in seawater propulsion and control of turbulent boundary layers to reduce drag. MHD applies quite well to astrophysics and cosmology. Because of wide range of practical applications, MHD flow has drawn significant attention by many researchers. Hossain and Mandal [60] (1986) investigated the effect of mass transfer and free convection on the unsteady MHD flow past a vertical plate with constant suction. Later on, the same problem considering variable suction was also investigated by the same authors. Fundamental directions of MHD natural convection flow along vertical flat plate can be obtained from the papers of Singh and Cowling [61], Riley [62], and Kuiken [63]. Singh and Cowling and Riley discovered that the major (outer) part of the flow in presence of strong cross magnetic field can be illustrated by Blasius's equation with appropriate boundary conditions for a moving plate while the fluid is at rest. The effects of transverse magnetic field on the natural convection flow due to osciallting surface heat flux was imposed by Kelleher and Yang (1968) [53] and more recently this was also premeditated by Hossain *et al.* [69] (1998). The problems involving magnetohydrodynamic natural convection flow of an electrically conducting fluid in presence of strong cross field due to surface heat flux have been discussed elaborately in many literatures. Very recently, Palani and Srikanth [64] investigated the MHD natural convection flow field due to double diffusion. They have considered the flow past a semi infinite vertical flat plate in presence of a magnetic field which was applied uniformly in transverse direction of the flow. Implicit finite difference method was applied to simulate

the flow field and the value of the parameter Pr was chosen as 0.7 and 7.0 which represents the air and water respectively. S.Siddiqa and Hossain [65] studied the effects of thermal radiation on free convection flow of electrically conducting and optically dense gray fluid in a strong cross magnetic field. This types of flow occurs in space technology and processes involving high temperatures. In recent times S. Siddiqa *et al.* [66] studied the MHD flow field in presence of uniform surface temperature, surface concentration and also with uniform surface heat and mass flux. Free variable formulation (FVF) and stream function formulation (SFF) were applied in these work to transform the governing equations and finally the numerical solutions were obtained by applying the *Thomas* algorithm. The main objective of their work was to observe the boundary layer behavior of electrically conducting fluid in the strong cross field by taking into consideration of liquid metals. In their work, it has also been drawn both the heat flux lines and mass flux lines so that the path followed by heat and mass can be elucidated within the boundary layer. Hossain *et al.* [68] (1985), studied the effects of viscous dissipation and free convection currents on the flow of an electrically conducting fluid. In their work, it has been produced the numerical results of the MHD flow past an accelerated vertical porous plate in presence of strong magnetic field. Later on Hossain *et al.* [69] (1996) investigated the MHD flow along vertical porous plate. They considered a variable transverse magnetic field along with a power law surface temperature. The flow field was simulated by applying two techniques: namely perturbation method with perturbation parameter ξ and finite difference method. Zeeshan and Ellahi [70] (2011) studied the non-newtonian fluid flow with slip boundary conditions. They have applied the series solution method for calculating the flow parameters along a porous surface and assumed the existence of cross magnetic field.

1.2.5 Convective flow along cylindrical surface

Amongst quite a number of scientists, Merkin [71] was the first who studied the free convection boundary layer on an isothermal horizontal circular cylinder in viscous fluid. In his paper, the complete solution to this problem for Newtonian fluid using Blasius and Grtler series expansion methods along with an integral method and a finite difference scheme was

presented for the first time. Hossain *et al.* [72] investigated the same problem posed above for steady free convection flow by bringing the effect of radiative heat transfer. In their work, they showed that the rate of heat transfer from the slender body is higher than from the blunt body due to increase of radiation parameter. The same problem with the cylinder of elliptic cross section over isothermal bodies was studied by the same authors. In this investigation the heat transfer from isothermal cylinder of elliptic cross section of various eccentricities were discussed. Saville and Churchill [73] and Lin and Chao [74] also studied the free convection flow from a horizontal cylinder and from axisymmetric bodies of arbitrary contours respectively with isothermal surface condition. Jaman *et al.* [75]- [76] studied the free convection flow of a viscous incompressible flow along an infinite horizontal cylinder considering sinosoidical oscillations in the surface temperature of the cylinder. In their subsequent work, the authors studied the similar type of problem assuming the flow over a cylinder of elliptic cross section of various eccentricities. In this investigation, the two different configuration of the cylinder, when the major axis is horizontal and vertical, were considered. A theoretical study of mixed convection flow along an isothermal circular cylinder was conducted in [82]. In this study, full set of Navier stokes equations were solved with a wide ranges of both Reynolds number and Grashof number. To solve the governing equations, the method of series truncation developed by the same authors were applied. The values of these two non-dimensional parameters, Reynolds number and Grashof number were chosen based on the free stream condition and the values were chosen as 1-40 for Reynolds number and 0-5 for Grashof numbers respectively. The computed results for stream lines and isotherms were also compared with some experimental correlations. Similar solution procedure was adopted by the same author to study the laminar combined convection flow from a horizontal cylinder [83]. In this paper, two cases of forced flow were considered, in parallel flow, the forced flow was directed vertically upward and in contra flow, the direction was taken as vertically downwards. Full vorticity transport equations accompanied with the stream function and energy equation were solved. The calculated values of average Nusselt number were compared with the available experimental data. Mahfouz *et al.* [84] studied the flow behaviour in the wake associated with a circular cylin-

der. It was assumed a rotational oscillation of the cylinder in the cross stream. In this work, an integral condition was introduced to estimate accurately the surface vorticity. In the case of lower velocity gradient, the solution methodology did not impose any explicit boundary condition for the vorticity at the cylinder surface, rather this quantity was computed from the known stream function distribution near the wall. Transient laminar natural convection flow from a heated horizontal cylinder was investigated in the paper of Wang *et al.* [85]. In this study, numerical results were carried out by using different types of boundary conditions with the help of spline fractional step method. Scale analysis was done to predict some important characteristics of the boundary layer and complete range of Rayleigh number was covered for the case of transient flow. Steady viscous flow past a circular cylinder at high Reynolds number (up to 300) was reported by Fornberg [86]. Remedies of some numerical difficulties which usually occurred during simulation were discussed and modified approach to solve the problem have been commenced by the author. A notable phenomenon of the vorticity was marked for higher Reynolds number which was the shortening of the wake region with vorticity being convected into its interior. It was also observed that, as the vorticity starts to recirculate back from the end of the wake region, this region becomes wider and shorter. In the case of transversely oscillating cylinder, the flow behaviour and the heat transfer characteristics of cross flow was presented in [88]. Numerical calculations were performed to predict the lock-on incident and its effect on the heat transfer. Numerical data were also validated against some experimental data presented by some other scientists. John Patterson *et al.* [89] presented detailed scale analysis to elucidate the possible transient behaviour for the case of aspect ratio $A \leq 1$ where they considered the transient natural convection flow in a cavity. In this paper, a modified version of the finite difference method was taken into action in order to solve the problem and the choice of the parametric values are made in such a way that the divisions in flow regimes were traversed.

1.3 Scope and Contribution of the Thesis

The study of this dissertation is devoted to perform an extensive numerical investigation on laminar flow along a vertical flat plate and cylinder in conjunction with heat and mass transfer. Several models have been developed in association with different geometrical configurations as well as boundary conditions. It is worth noting that for each case the computations are carried out by considering only the positive values of the dimensions of the computational domain, i.e. for $x \geq 0$ and $y \geq 0$.

In the first model, problem of double diffusive natural convection flow have been considered with non uniform surface heat and mass transfer. Similar type of boundary condition are imposed for the surface heat and mass flux and comparative studies between these two cases also presented and correlation are drawn by calculating the heat and mass transfer coefficient parameters.

Forced convective flow along a vertical wedge with oscillating surface heat and mass flux is studied in the second problem. Parametric studies are carried out to study the effects on surface shear stress and heat transfer. Different numerical techniques are applied to calculate the results and simulated results, obtained from different methods are compared in terms of amplitude and phase angels of shear stress and heat transfer coefficients.

Later on, the model, developed in the second problem is extended to study the mass transfer in presence of heat transfer. Conjugate heat and mass transfer study is performed considering double diffusive forced convection flow. Here also calculated results attained from different numerical methods are compared and nice agreement is found among all these results.

Afterwards, magnetohydrodynamic free convection flow is studied with small amplitude oscillation in both surface temperature and concentration. Each of the chapters include formulation of the problem, solution procedure, representation of the simulated results accompanying with intricate discussions. Parametric studies have been carried out for each of the problems and asymptotic solutions for the flow variables as well as some important associated coefficients of physical interests are calculated. Different numerical techniques are applied and for some cases results obtained from these different techniques are validated

through comparisons.

In the study of mixed convection flow along the heated horizontal cylinder, full set of Navier stokes equation in terms of vorticity and stream function is solved for mixed convection flow along horizontal heated circular cylinder. Implicit finite difference method is applied to solve the set of governing equation and results are compared with some published results in order to validate the present simulation. Since the similar problem is studied earlier by some other researchers in which only heat transfer is considered, Here the investigation is broaden by taking into account of mass transfer. Variable surface temperature without oscillation is considered and results are carried out in terms of heat and mass transfer coefficient parameter, $Nu_x,\ Sh_x$.

Subsequently, the same problem, considered in previous model, is investigated by considering the surface temperature and species concentration of the cylinder with small amplitude oscillation. The effects of fluctuating surface temperature and species concentration on heat and mass transfer is explored in this chapter and produced results are presented in graphical forms in terms of isothermal lines, iso concentration lines etc.

1.4 Numerical Techniques Engaged

Is has already been mentioned earlier that, all the model studies involving in this dissertation are carried out numerically and physical interpretation of the numerical results and conclusions are drawn based on these numerical simulations. All he methods which are taken into action here for analyzing the flow behavior are listed below:

- Implicit finite difference method together with Keller box scheme.
- Implicit finite difference method together with Gaussian elimination method.
- Linear and nonlinear shooting method.
- Regular perturbation method.
- Matched asymptotic expansion method.

The details of the computing techniques are discussed with the related chapters and problems. The repetition of the details calculation procedures are avoided when similar techniques are used for solving different problems.

1.5 Organization of the Thesis

The whole dissertation is organized in the following manner:

In Chapter 1, the brief introduction regarding the fluid dynamics has been presented. A comprehensive literature review on related topics has also been written in order to get a proper frame work and direction of the proposed research for this thesis work. Basic transport equations are derived with the help of Newton's law of motion in Chapter 2. Concepts of boundary layer and related discussions also presented shortly. In Chapter 3, model has been developed to study the natural convection flow along a vertical flat plate in presence of oscillating surface heat and mass transfer. The mixed convection flow due to thermal diffusion along a vertical wedge have been investigated with unsteady surface heat transfer boundary conditions in Chapter 4. This model has been extended to study both thermal and mass diffusion with oscillating surface boundary condition for velocity, temperature and concentration in Chapter 5. To study the heat and mass transfer response due to oscillating surface temperature and concentration in MHD natural convection flow is the substance of the Chapter 6. Mixed convection flow along a heated circular cylinder in presence of heat and mass diffusion is the subject matter of the chapter 7. In this study, it has been assumed that, the surface temperature and concentration are time dependent but there is no oscillation in these quantities. The same model has been studied in presence of small amplitude oscillation in both surface temperature and concentration in Chapter 8. Each chapters are ended with concise conclusions. In Chapter 9, summarization and concluding remarks have been listed of this whole thesis work and pointed out some directions for future research work.

Chapter 2

Basic transport equation and boundary layer concept

The mathematical basis of modeling fluid flow to study heat and mass transfer is to develop the governing equation in conjunction with the necessary supporting conditions: initial and boundary condition. To derive the fundamental set of governing equation, the importance is given to the resulting conservation equations and finally the transport equations are derived. These transport equations are the basic elements for developing the numerical algorithm that are to follow to analyze a fluid flow problem. The details of the basic transport equations are presented in this chapter.

2.1 Basic Transport Equation

This chapter seeks to present a short overview of the fundamental governing equations which govern the flow. It has been considered the basic equations of laminar boundary layer flow. Three fundamental conservation laws of physics, known as conservation of mass, conservation of momentum and conservation of energy are used to derive the governing fundamental set of equations considering the viscous fluid subject to a body force in natural or free convection. The governing equations of fluid flow represent the mathematical statement of the conservation laws of physics:

- The mass of fluid is conserved.
- The rate of change of momentum equals the sum of the forces on a fluid particle (Newton's second law).
- The rate of change of energy is equal to the sum of the rate of heat addition to and the rate of work done on a fluid particle (first law of thermodynamics).

Furthermore, in all the models investigated in present dissertation, the following assumptions are also made:

- Fluid is incompressible in the sense that the density does not change appreciably with pressure. The density is therefore considered to be a function of temperature only, i.e. $\rho = \rho(T)$
- Fluid properties, for example, specific heat, thermal conductivity, viscosity are constant.
- Viscous dissipation is negligible.

Since the details derivation of all these basic transport equations are unnecessary, only the most intuitive form of these equations are presented here. In these equations, all the terms are very general and all-encompassing. The most primitive form of the transport equations are as follows [100]:

$$\text{Mass equation}: \ \frac{\partial\, \rho}{\partial\, t} + \nabla.\ (\rho\ u) = 0 \tag{2.1}$$

$$\begin{aligned}\text{Momentum equation}: \frac{\partial \mathbf{u}}{\partial t} + \mathbf{u}.\nabla\mathbf{u} = &-\frac{1}{\rho}\nabla\bar{p} + \nu\nabla^2\mathbf{u} + \frac{1}{\rho}(\mathbf{j}\times\mathbf{B}) \\ &+ \mathbf{g}\beta_T(\bar{T} - T_\infty) + \mathbf{g}\beta_C(\bar{C} - C_\infty)\end{aligned} \tag{2.2}$$

$$\text{Energy equation}: \ u.\nabla\bar{T} = \bar{\alpha}\left(\nabla^2\bar{T}\right) \tag{2.3}$$

$$\text{Concentration equation}: \ u\ .\ \nabla\bar{C} = D\ \nabla^2\bar{C} \tag{2.4}$$

where, $\nabla = \left(\frac{\partial}{\partial\bar{x}}, \frac{\partial}{\partial\bar{y}}, \frac{\partial}{\partial\bar{z}}\right)$, $\mathbf{u} = (\bar{u}, \bar{v}, \bar{w})$ is the velocity vector, $\bar{T}$ the temperature field in the boundary layer, T_∞ the temperature of the ambient fluid, $\bar{C}$ the species concentration

in the boundary layer, C_∞ the species concentration of the ambient fluid, $\bar{p}$ the pressure, ρ the density of the fluid, ν the kinematic coefficient of viscosity, $\mathbf{g} = (-g, 0, 0)$ identifies the gravitational vector, β_T the volumetric coefficient of thermal expansion, β_C the volumetric coefficient of concentration expansion, $\bar{\alpha}$ the thermal diffusivity and D the diffusion coefficient.

As one of the models, studied in this dissertation in chapter 6 is concerned with magnetohydrodynamic flow, it is required to present the Ohm's Law and Maxwell's equation to take into account the effect of magnetic field that significantly act on the fluid and remarkable modification is made into fluid motion. These two equations are defined as:

$$\text{Maxwell's equation} : \nabla\times\mathbf{E} = 0 \quad , \quad \nabla.\mathbf{B} = 0 \quad , \quad \nabla\times\mathbf{B} = \mu_0\mathbf{j} \tag{2.5}$$

$$\text{Ohm's Law} : \mathbf{j} = \bar{\sigma}\left(\mathbf{E} + \mathbf{u}\times\mathbf{B}\right) \tag{2.6}$$

where, $\mathbf{j}$ is the electric current density, $\mathbf{B} = (B_{\bar{x}}, B_{\bar{y}}, B_{\bar{z}})$ represents the magnetic induction vector, $\mathbf{E}$ the applied electric field. In equation (2.2), magnetohydrodynamic (MHD) body force *i.e* $\mathbf{j} \times \mathbf{B}$ is included which has significant effect on fluid motion and this force is termed as Lorentz force. In order to consider the magnetohydrodynamic flow, an induced magnetic fields is considered and the relative strength of the induced field is characterized by the magnetic Reynolds number ($R_m = \mu_0\bar{\sigma}\bar{u}\gamma$, where γ is the wavelength of the applied magnetic field). Additionally, the applied magnetic field vector applied normal to the surface is of the form $\mathbf{B} = (0, B_{\bar{y}}, 0)$, in which $B_{\bar{y}}$ is the strength of constant or variable magnetic field.

Now, considering all the assumptions and simplifications that can be made, the two dimensional Navier-Stokes equations (2.1)-(2.2) coupled with energy and concentration equations (2.3)-(2.5) for the unsteady flow in the Cartesian coordinates along with the magnetic field becomes:

$$\frac{\partial\bar{u}}{\partial\bar{x}} + \frac{\partial\bar{v}}{\partial\bar{y}} = 0 \tag{2.7}$$

$$\frac{\partial\bar{u}}{\partial t} + \bar{u}\frac{\partial\bar{u}}{\partial\bar{x}} + \bar{v}\frac{\partial\bar{u}}{\partial\bar{y}} = -\frac{1}{\rho}\frac{\partial\bar{p}}{\partial\bar{x}} + \nu\left(\frac{\partial^2\bar{u}}{\partial\bar{x}^2} + \frac{\partial^2\bar{u}}{\partial\bar{y}^2}\right) - \frac{\bar{\sigma}B_{\bar{y}}^2}{\rho}\bar{u} + g\beta_T(\bar{T} - T_\infty) + g\beta_C(\bar{C} - C_\infty) \tag{2.8}$$

$$\frac{\partial \bar{v}}{\partial t} + \bar{u}\frac{\partial \bar{v}}{\partial \bar{x}} + \bar{v}\frac{\partial \bar{v}}{\partial \bar{y}} = -\frac{1}{\rho}\frac{\partial \bar{p}}{\partial \bar{y}} + \nu\left(\frac{\partial^2 \bar{v}}{\partial \bar{x}^2} + \frac{\partial^2 \bar{v}}{\partial \bar{y}^2}\right) \tag{2.9}$$

$$\frac{\partial \bar{T}}{\partial t} + \bar{u}\frac{\partial \bar{T}}{\partial \bar{x}} + \bar{v}\frac{\partial \bar{T}}{\partial \bar{y}} = \bar{\alpha}\left(\frac{\partial^2 \bar{T}}{\partial \bar{x}^2} + \frac{\partial^2 \bar{T}}{\partial \bar{y}^2}\right) \tag{2.10}$$

$$\frac{\partial \bar{C}}{\partial t} + \bar{u}\frac{\partial \bar{C}}{\partial \bar{x}} + \bar{v}\frac{\partial \bar{C}}{\partial \bar{y}} = D\left(\frac{\partial^2 \bar{C}}{\partial \bar{x}^2} + \frac{\partial^2 \bar{C}}{\partial \bar{y}^2}\right) \tag{2.11}$$

It can be observed that the Navier-Stokes equations are second order PDE and according to the problems this PDE's are classified into three types: elliptic, parabolic and hyperbolic equations. The steady-state problems are governed by elliptic equations. Parabolic or Hyperbolic equations govern the marching or propagation problems. However, all unsteady problems do not always represent marching problems. Parabolic equations are involved with significant amount of dissipation and describe time dependent problems. Analysis of vibration problems involve with Hyperbolic equations. Hyperbolic equations are different from the other two types because these equations possesses a special behaviour which is associated with the finite speed, namely the wave speed, at which information travels through the problem.

2.2 Boundary condition

Every well imposed fluid problem is described with proper boundary conditions. The following types of boundary conditions in the computational domain of the fluid problem are used with the governing equations of the motion:

- **No-slip condition**: This type of boundary condition states that the velocity component u , tangential to the wall vanishes at the wall. If x, y are considered as tangential and normal direction to the wall then

$$y = 0: \quad u(x, y, t) = 0, \; y \to \infty: \; u(x, \infty, t) = 0$$

This type of boundary condition satisfied very well within the framework of continuum mechanics. At extremely low gas densities the no-slip condition is no longer satisfied.

- **Normal component of the velocity**: The velocity component v normal to the wall generally vanishes where the walls are impermeable, i.e.

$$y = 0: \quad v(x, y, t) = 0, \; y \to \infty: \; v(x, \infty, t) = 0$$

  However they are non-zero iff the wall is permeable and fluid is either sucked or blown through it. The normal components of the velocity can also be non-zero in the case of non-porous walls if mass transfer processes are taken into account, as in the case of binary or multi-fluid flows. For example, condensation corresponds to suction and evaporation , to blowing [95]

- **Different kinds of temperature boundary conditions are specified in different cases**:

  - Boundary conditions of the first kind: In this case, the wall temperature is stipulated. Usually, it is assumed that fluid takes the wall temperature at the wall. For the case of very low density gases, there is a jump in temperature. For example,

$$y = 0: \quad T = T_w(x)[1 + \varepsilon\,(\exp(i\omega t) + c.c)], \; y \to \infty: \; T(x, \infty, t) = 0$$

  - Boundary conditions of second kind: In this case, the heat flux, $q_w = (\bar{q}.\bar{n})$, where, $\bar{n}$ is the normal unit vector at the wall, is set down,i.e.:

$$y = 0: \quad -\kappa\frac{\partial T}{\partial y} = q_w(x)[1 + \varepsilon\,(\exp(i\omega t) + c.c)], \; y \to \infty: -\kappa\frac{\partial T}{\partial y} = 0$$

  - Boundary conditions of the third kind: This type of boundary condition is a blending of above mentioned two types of boundary conditions, i.e. a combination of wall temperature and the heat flux at the wall. However, such boundary conditions could also be coupling conditions with the temperature field inside the wall.

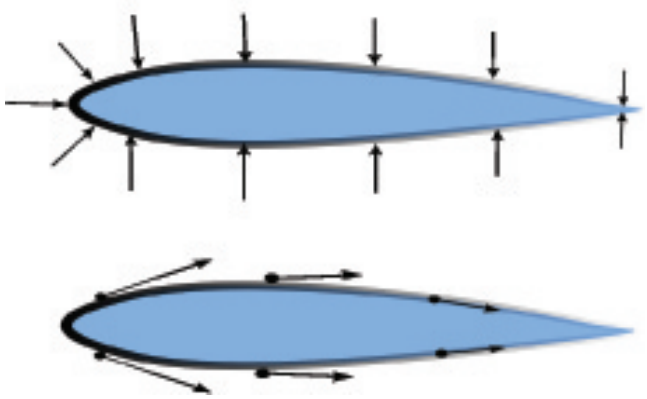

Figure 2.1: Pressure and shear stress distributions, [100]

2.3 Boundary layer Concept and approximation

To analyze a fluid flow problem, the biggest challenge is to solve the governing equations of the flow field which are derived from the general Navier-Stoke's equation. The limiting solution as $Re = \infty$ is often a good approximation of the Navier-Stokes equations. But a very notable inadequacy of this type of limiting solution is the violation of no-slip condition. Therefore, while solving the Navier-Stokes equations, instabilities occur for most of the practical flow problem. Virtually, this type of shortcoming of the solution became quite powerful when the first practical aircraft was invented and consequently the calculation of the drag and the lift on aircraft becomes necessary. For instance, consider that the airfoil shaped body is immersed in a fluid which exerts a net force (or aerodynamic force) on the surface of the airfoil as shown in the Figure 2.1. Two types of forces namely, the fluid pressure and the shear stress are originated due to the friction between the surface of the body and the flow. These two types of forces are the driving forces to hold the airfoil and also exerts a force on it. To get a notion about these forces, aerodynamicists required to calculate both the pressure distribution and shearing stress at the surface and then integrate them over the surface of the airfoil. A number of approximations can be made to calculate that pressure distributions within the flow. While determining pressure distribution one can assume that the flow is frictionless or inviscid. Because of this assumption the pressure becomes comparatively less problematic than the shear stress. However, the distribution

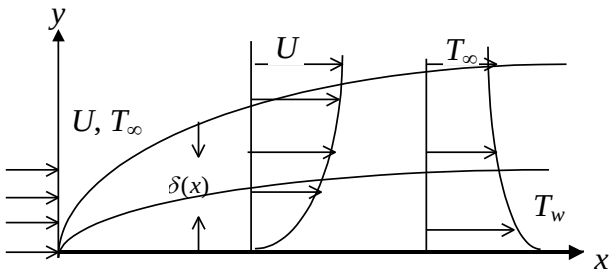

Figure 2.2: Flow of a viscous fluid parallel to a flat surface.

of the shearing stress can be calculated when the viscous flow and the internal friction are taken into consideration. All these assumptions suggests to tackle the Navier-Stokes equations consciously.

Consider the flow of a viscous fluid over a stationary smooth plate surface as illustrated in Figure 2.2. It is worth mentioning that, during this type of flow, at the surface the fluid particles adhere to it and the frictional forces between the fluid layers retard the motion of the fluid within a thin layer near the surface. In this thin layer, which is termed the boundary layer, the velocity of the fluid decreases form its free-stream value U_∞ to a value of zero at the surface (no-slip condition). Figure 2.3 shows diagrammatically the variation of the velocity component parallel to the surface in the boundary layer at a given location on the surface.

According to Prandtl's boundary-layer concept, under certain conditions viscous forces are of importance only in the immediate vicinity of a solid surface where velocity gradients are large. This region near the surface is referred to as the boundary layer. In regions removed from the solid surface where there exist no large gradients in fluid velocity, the fluid motion may be consider frictionless i.e. potential flow. Prandtl estimated various terms in the Navier-Stokes equations with the help of order of magnitude analysis and thus derived the so called equations for boundary layer in which the inertial effects are comparable to the viscous effects. By doing these *order-of-magnitude* analysis, the terms can be dropped which are negligibly small in the computations as compared to the terms in the same

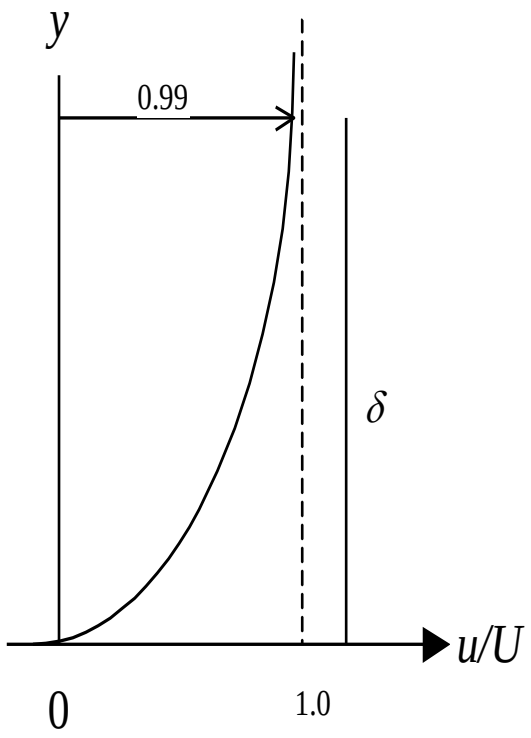

Figure 2.3: Velocity boundary layer thickness

equation. Prandtl approximations took up the idea that in the boundary layer $\bar{u} = O(\bar{\delta})$ and $bary = O(\bar{\delta})$ and in locations removed from the leading edge $\bar{x} = O(1)$, where the symbol O( ) stands for the "order of". Here, $\bar{\delta} = \frac{\delta}{L} << 1$ and L is the length of the surface in $\bar{x}$ direction. Considering the order of magnitudes of $\bar{u}$ and $\bar{x}$ we observe that $\frac{\partial \bar{u}}{\partial \bar{x}} \approx \frac{O(1)}{O(1)} = O(1)$ thus, it follows that $\frac{\partial^2 \bar{u}}{\partial \bar{x}^2} = O(1)$. Likewise, $\bar{y} = O(\bar{\delta})$ and $\frac{\partial \bar{u}}{\partial \bar{y}} = O\left(\frac{1}{\bar{\delta}}\right)$ and $\frac{\partial^2 \bar{u}}{\partial \bar{y}^2} = O\left(\frac{1}{\bar{\delta}^2}\right)$. From the continuity equation (2.7) it can be inferred that $\frac{\partial \bar{u}}{\partial \bar{x}}$ and $\frac{\partial \bar{v}}{\partial \bar{y}}$ should be of same order of magnitude. Therefore, $\frac{\partial \bar{v}}{\partial \bar{y}} = O(1)$ and $\bar{v} = O(\bar{\delta})$. It can also be concluded that, $\frac{\partial \bar{v}}{\partial \bar{x}} = O(\bar{\delta})$, $\frac{\partial^2 \bar{v}}{\partial \bar{y}^2} = O\left(\frac{1}{\bar{\delta}}\right)$ and $\frac{\partial^2 \bar{v}}{\partial \bar{x}^2} = O\left(\bar{\delta}\right)$.

Introducing all these dimensions in the equation (2.8) and omitting the time dependent term and the terms on the right hand side of the equation involving thermal and mass diffusion we can have:

$$\begin{array}{ccccc} \bar{u}\dfrac{\partial \bar{u}}{\partial \bar{x}} + \bar{v}\dfrac{\partial \bar{u}}{\partial \bar{y}} = -\dfrac{\partial \bar{p}}{\partial \bar{x}} + \nu\left(\dfrac{\partial^2 \bar{u}}{\partial \bar{x}^2} + \dfrac{\partial^2 \bar{u}}{\partial \bar{y}^2}\right) \\ \dfrac{1}{1} \quad + \quad \bar{\delta}\,\dfrac{1}{\bar{\delta}} \qquad\qquad \left(\dfrac{1}{1} \quad + \quad \dfrac{1}{\bar{\delta}^2}\right) \end{array} \tag{2.12}$$

Since $\bar{\delta} << 1$, from equation (2.12) it can be concluded that

$$\frac{\partial^2 \bar{u}}{\partial \bar{x}^2} << \frac{\partial^2 \bar{u}}{\partial \bar{y}^2}$$

In general, according to the Prandtl boundary layer approximation, it can be shown that the derivatives of any quantity with respect to the independent variable y are much larger as compared to the derivatives with respect to the independent variable x. Thus the following estimation is applicable within the boundary-layer region:

$$\left|\frac{\partial \Gamma}{\partial \bar{x}}\right| << \left|\frac{\partial \Gamma}{\partial \bar{y}}\right|, \quad \left|\frac{\partial^2 \Gamma}{\partial \bar{x}^2}\right| << \left|\frac{\partial^2 \Gamma}{\partial \bar{y}^2}\right| \tag{2.13}$$

where Γ is any flow quantity. By applying the above mentioned techniques of magnitude analysis, the final form of the boundary-layer equations of different convective flow are derived in the following sections.

2.3.1 Equations for MHD Natural Convection Flow Along Vertical Surface

The order of magnitude analysis of the Navier-Stokes equations of viscous fluid flow along with the energy and concentration equations can be simplified to the convenient boundary layer equations. Consider now the case of unsteady two-dimensional incompressible laminar boundary layer MHD natural convection flow over a semi-infinite vertical surface. Thermal radiation effects are also taken into account. Further, assume that all the thermophysical properties of the fluid are constant. Under the usual Boussinesq approximation the continuity equation (2.7) and the Navier-Stokes Eqs. (2.8-2.9) coupled with the energy and concentration equations (2.10-2.11) may now be written in the following dimensionless form

$$\frac{\partial u}{\partial x}+\frac{\partial v}{\partial y}=0 \tag{2.14}$$

$$u\frac{\partial u}{\partial x}+v\frac{\partial u}{\partial y}=\frac{1}{Gr^{1/2}}\left(\frac{\partial^2 u}{\partial x^2}+\frac{\partial^2 u}{\partial y^2}\right)-Mu+\left(\frac{T+NC}{1+N}\right) \tag{2.15}$$

$$u\frac{\partial v}{\partial x}+v\frac{\partial v}{\partial y}=-\frac{\partial p}{\partial y}+\frac{1}{Gr^{1/2}}\left(\frac{\partial^2 v}{\partial x^2}+\frac{\partial^2 v}{\partial y^2}\right) \tag{2.16}$$

$$u\frac{\partial T}{\partial x}+v\frac{\partial T}{\partial y}=\frac{1}{Gr^{1/2}\mathrm{Pr}}\left(\frac{\partial^2 T}{\partial x^2}+\frac{\partial^2 T}{\partial y^2}\right) \tag{2.17}$$

$$u\frac{\partial C}{\partial x}+v\frac{\partial C}{\partial y}=\frac{1}{Gr^{1/2}\mathrm{Sc}}\left(\frac{\partial^2 C}{\partial x^2}+\frac{\partial^2 C}{\partial y^2}\right) \tag{2.18}$$

where

$$\begin{aligned}
&x=\frac{\bar{x}}{L},\quad y=\frac{\bar{y}}{L},\quad u=\frac{\bar{u}}{U_0},\quad v=\frac{\bar{v}}{U_0},\quad p=\frac{\bar{p}}{\rho U_0^2},\\
&T=\frac{\bar{T}-T_\infty}{T_w-T_\infty},\quad C=\frac{\bar{C}-C_\infty}{C_w-C_\infty},\quad M=\frac{\bar{\sigma}B_y^2 L}{\rho U_0},\\
&Gr_t=\frac{g\beta_T(T_w-T_\infty)L^3}{\nu^2},\quad Gr_c=\frac{g\beta_C(C_w-C_\infty)L^3}{\nu^2}\\
&Pr=\frac{\nu}{\alpha},\quad Sc=\frac{\nu}{D},\quad \triangle=\frac{T_w}{T_\infty}-1,\\
&Gr=Gr_T+Gr_C,\quad N=\frac{Gr_C}{Gr_T}
\end{aligned} \tag{2.19}$$

Here $U_0 = \nu Gr^{1/2}/L$ is the boundary layer velocity scale, T_w the temperature at the surface, C_w the species concentration at the surface, M the magnetic field parameter, Gr_T the Grashof number for thermal diffusion, Gr_C the Grashof number for mass diffusion, Pr the Prandtl number, Sc the Schmidt number, N the buoyancy ratio parameter.

Assuming that Gr becomes asymptotically large, therefore retaining only the leading order terms in equations (2.14)-(2.19). The boundary layer equations are obtained by introducing the scalings given in (2.20) into the equations (2.14)-(2.18).

$$\begin{gathered} u = u^*, \quad v = Gr^{-1/4}v^*, \quad x = x^*, \quad y = Gr^{-1/4}y^*, \\ p = Gr^{-1/2}p^*, \quad T = T^*, \quad C = C^* \end{gathered} \tag{2.20}$$

The final form of the boundary layer equations by commencing the scalings given in (2.19) into the equations (2.12)-(2.17) and dropping the asterisk:

$$\frac{\partial u}{\partial x} + \frac{\partial v}{\partial y} = 0 \tag{2.21}$$

$$\frac{\partial u}{\partial t} + u\frac{\partial u}{\partial x} + v\frac{\partial u}{\partial y} = \frac{\partial^2 u}{\partial y^2} - Mu + \left(\frac{T + NC}{1 + N}\right) \tag{2.22}$$

$$\frac{\partial v}{\partial t} + u\frac{\partial v}{\partial x} + v\frac{\partial v}{\partial y} = -\frac{\partial p}{\partial y} + \frac{\partial^2 v}{\partial y^2} \tag{2.23}$$

$$\frac{\partial T}{\partial t} u\frac{\partial T}{\partial x} + v\frac{\partial T}{\partial y} = \frac{1}{Pr}\frac{\partial^2 T}{\partial y^2} \tag{2.24}$$

$$\frac{\partial C}{\partial t} + u\frac{\partial C}{\partial x} + v\frac{\partial C}{\partial y} = \frac{1}{Sc}\frac{\partial^2 C}{\partial y^2} \tag{2.25}$$

It can be noted that equation (2.23) serves to define the pressure field in terms of the two velocity components and is decoupled from the other three equations. Therefore equation (2.23) is not considered during the analysis of laminar boundary layer natural convection flow over a semi-infinite vertical surface.

By omitting the MHD body force and the resultant parameter M in equation (2.15), the set of non dimensional boundary layer equation can be derived for simple natural convection flow along semi infinite, vertical flat plate.

2.3.2 Equations for Mixed Convection Flow Along Inclined Surface

Consider the two dimensional unsteady mixed convection flow of a viscous, incompressible fluid with constant thermo-physical properties over a semi-infinite heated horizontal plate, which is inclined at an angle ϕ to the horizontal. For this case, the continuity and the momentum equations coupled with energy equation are:

$$\frac{\partial \bar{u}}{\partial \bar{x}} + \frac{\partial \bar{v}}{\partial \bar{y}} = 0 \tag{2.26}$$

$$\bar{u}\frac{\partial \bar{u}}{\partial \bar{x}} + \bar{v}\frac{\partial \bar{u}}{\partial \bar{y}} = \nu\left(\frac{\partial^2 \bar{u}}{\partial \bar{x}^2} + \frac{\partial^2 \bar{u}}{\partial \bar{y}^2}\right) + \frac{\partial U}{\partial t} + U\frac{\partial U}{\partial x} + g\beta_T\left(\bar{T} - T_\infty\right)\sin\phi \tag{2.27}$$

$$\bar{u}\frac{\partial \bar{v}}{\partial \bar{x}} + \bar{v}\frac{\partial \bar{v}}{\partial \bar{y}} = -\frac{1}{\rho}\frac{\partial \bar{p}}{\partial \bar{y}} + \nu\left(\frac{\partial^2 \bar{v}}{\partial \bar{x}^2} + \frac{\partial^2 \bar{v}}{\partial \bar{y}^2}\right) + g\beta_T\left(\bar{T} - T_\infty\right)\cos\phi \tag{2.28}$$

$$\bar{u}\frac{\partial \bar{T}}{\partial \bar{x}} + \bar{v}\frac{\partial \bar{T}}{\partial \bar{y}} = \bar{\alpha}\left(\frac{\partial^2 \bar{T}}{\partial \bar{x}^2} + \frac{\partial^2 \bar{T}}{\partial \bar{y}^2}\right) \tag{2.29}$$

In the equation (2.27), $u = U(x,t)$ is the ambient fluid velocity. Introducing the following dimensionless dependent and independent variables

$$\begin{aligned} &x = \frac{\bar{x}}{L}, \quad y = \frac{\bar{y}}{L}, \quad u = \frac{\bar{u}}{U_0}, \quad v = \frac{\bar{v}}{U_0}, \quad p = \frac{\bar{p}}{\rho U_0^2}, \quad T = \frac{\bar{T} - T_\infty}{T_w - T_\infty} \\ &Gr = \frac{g\beta_T(T_w - T_\infty)L^3}{\nu^2}\cos\phi, \quad Pr = \frac{\nu}{\bar{\alpha}}, \quad \triangle = \frac{T_w}{T_\infty} - 1 \end{aligned} \tag{2.30}$$

Therefore, with the help of (2.30) equations (2.26)-(2.29) can be written as

$$\frac{\partial u}{\partial x} + \frac{\partial v}{\partial y} = 0 \tag{2.31}$$

$$\frac{\partial u}{\partial t} + u\frac{\partial u}{\partial x} + v\frac{\partial u}{\partial y} = \frac{\partial U}{\partial t} + U\frac{\partial U}{\partial x} + \frac{1}{Gr^{1/2}}\left(\frac{\partial^2 u}{\partial x^2} + \frac{\partial^2 u}{\partial y^2}\right) + \tan\phi T \tag{2.32}$$

$$\frac{\partial v}{\partial t} + u\frac{\partial v}{\partial x} + v\frac{\partial v}{\partial y} = -\frac{\partial p}{\partial y} + \frac{1}{Gr^{1/2}}\left(\frac{\partial^2 v}{\partial x^2} + \frac{\partial^2 v}{\partial y^2}\right) + T \tag{2.33}$$

$$\frac{\partial T}{\partial t} + u\frac{\partial T}{\partial x} + v\frac{\partial T}{\partial y} = \frac{1}{Gr^{1/2}Pr}\frac{\partial^2 T}{\partial x^2} + \frac{\partial^2 T}{\partial y^2} \tag{2.34}$$

Again $U_0 = \nu Gr^{1/2}/L$ is the boundary layer velocity scale. Now introduce the following scaled variables into equations (2.31)-(2.33).

$$\begin{aligned} u^* = Gr^{-2/5}u, \quad v^* = Gr^{-1/5}v, \quad x^* = x, \quad y^* = Gr^{1/5}y, \\ p^* = Gr^{-4/5}p, \quad T^* = T \end{aligned} \tag{2.35}$$

Assuming that Gr becomes asymptotically large and retaining only the leading order terms in equations. (2.31)-(2.33) to obtain the following boundary layer equations (dropping asterisk).

$$\frac{\partial u}{\partial x} + \frac{\partial v}{\partial y} = 0 \tag{2.36}$$

$$\frac{\partial u}{\partial t} + u\frac{\partial u}{\partial x} + v\frac{\partial u}{\partial y} = -\frac{\partial p}{\partial x} + \frac{\partial^2 u}{\partial y^2} + \frac{\partial U}{\partial t} + \Lambda T \tag{2.37}$$

$$\frac{\partial p}{\partial y} = T \tag{2.38}$$

$$u\frac{\partial T}{\partial x} + v\frac{\partial T}{\partial y} = \frac{1}{Pr}\frac{\partial^2 T}{\partial y^2} \tag{2.39}$$

where $\Lambda = Gr^{-4/5}\tan\phi$ is the inclination parameter.

In order to take into account the mass transfer, the concentration equation should be added with the above mentioned set of equations (2.26)-(2.29). This set of equations are valid for adequately large Reynolds numbers. Present thesis work is mostly aimed to study the boundary layer equations under different convection phenomena and for different geometries.

2.4 Summary

In this chapter the complete transport equations have been derived shortly from the basic conservation laws. In order to incorporate with mathematics, Newtonian model of viscous stresses and thermodynamic equilibrium assumptions are made. Finally boundary layer concept is introduced and discussed how boundary layer approximations are made to make the whole set of Navier-Stokes equation simpler and solvable.

Chapter 3

Effect of fluctuating surface heat and mass flux on natural convection flow along a vertical flat plate

3.1 Introduction

Heat and mass transfer are kinetic processes that may occur in nature which has been studied separately or jointly. Studying them apart is simpler, however, it is more efficient to consider them jointly. Double diffusive convection, which create a buoyancy force so that fluid flow occurs and can be seen in many natural and technological processes. Besides, heat and mass transfer must be jointly considered in some cases like evaporative cooling and ablation. Because of the coupling between the fluid velocity field and the diffusive fields, flow becomes more complicated than the convective flow. Therefore, many different behavior may be expected and thus, many investigators are still interested in double diffusive flow.

In this present problem, double diffusive flow through a vertical flat plate has been studied extensively. Similar type of boundary conditions for two different cases are considered and results are produced accordingly. Firstly, surface temperature and surface species concentration are assumed to have small amplitude oscillation and secondly, these

quantities are reflected on the surface heat and mass flux. The most important parameter that determines the relative strength of the two buoyancy forces, is the ratio parameter w, and for a positive w, the buoyancy forces are cooperating and drive the flow in the same direction which is considered in this present investigation. This parameter measures the relative importance of solutal and thermal diffusion in causing the density changes which drive the flow. It can be observed that, w=0 corresponds to no species diffusion and ∞ to no thermal diffusion. Similar to any double diffusive study, the governing equations of the flow field is simulated for two different diffusive parameters, Pr and Sc. The values of these two parameters depend on the nature of the fluid and on the physical mechanisms governing the diffusion of the heat and chemical species. As the most important fluids are atmospheric air and water, the results are presented here mostly for $Pr = 0.7$ that represent the air at 20^0C at 1 atmosphere against the transpiration parameter ξ and Sc is ranged from 0.1-1.6. Another important parameter, n, which is termed as exponent parameter, has also been taken into account widely. In this present study, numerical simulations are carried out in details and results are illustrated in both figures and tabular forms.

3.2 Formulation of the problem

A two dimensional unsteady free convection flow of a viscous incompressible fluid flow along a vertical flat plate in the presence of a soluble species is considered in this present study. A semi infinite vertical flat plate is placed at y=0 in Cartesian coordinate system. Also, it is considered $x \geq 0$, so that the distance from the leading edge along the plate measured the x and y is measured in outward normal direction from the plate. The ambient fluid temperature and species concentration are taken as T_∞ and C_∞. Similar type of boundary conditions for two different cases have been considered. In the **case 1**, where it has been assumed that the surface temperature and surface species concentration are time dependent and have small amplitude oscillation. Surface heat flux and mass flux are considered with exactly similar type of boundary conditions in **case 2**. For both the cases, the governing

equations of the flow is given by the following sets of Navier-Stokes equations:

$$\frac{\partial u}{\partial x} + \frac{\partial v}{\partial y} = 0 \tag{3.1}$$

$$\frac{\partial u}{\partial t} + u\frac{\partial u}{\partial x} + v\frac{\partial u}{\partial y} = \nu\frac{\partial^2 u}{\partial y^2} + g\beta_T(T - T_\infty) + g\beta_C(C - C_\infty) \tag{3.2}$$

$$\frac{\partial T}{\partial t} + u\frac{\partial T}{\partial x} + v\frac{\partial T}{\partial y} = \alpha\frac{\partial^2 T}{\partial y^2} \tag{3.3}$$

$$\frac{\partial C}{\partial t} + u\frac{\partial C}{\partial x} + v\frac{\partial C}{\partial y} = D\frac{\partial^2 C}{\partial y^2} \tag{3.4}$$

where$u$ and v are the x and y components of velocity field, respectively, g is the gravitational acceleration, β_T and β_C are the volumetric expansion coefficients for temperature and concentration respectively, α is the thermal diffusivity and D is the molecular diffusivity of the species concentration. Moreover $\theta = T - T_\infty$ and $\phi = C - C_\infty$ are the differences of temperature and species concentration between fluid and ambient flow. Considered boundary conditions for two differen cases, under which the equations (3.1)-(3.4) are solved listed below:

Case 1: When the surface temperature and concentration have small amplitude oscillation:

$$\begin{aligned} &y = 0: \ u(x,y,t) = v(x,y,t) = 0, \quad T = T_w(x)[1 + \varepsilon\,(\exp(i\omega t) + c.c)] \\ &C = C_w(x)[1 + \varepsilon\,(\exp(i\omega t) + c.c)] \\ &y \to \infty: \quad u(x,\infty,t) = v(x,\infty,t) = 0 \end{aligned} \tag{3.5}$$

Case 2: When the surface heat and mass flux have small amplitude oscillation:

$$\begin{aligned} &y = 0: \ u(x,y,t) = v(x,y,t) = 0, \quad -\kappa\frac{\partial T}{\partial y} = q_w(x)[1 + \varepsilon\,(\exp(i\omega t) + c.c)] \\ &-D\frac{\partial C}{\partial y} = c_w(x)[1 + \varepsilon\,(\exp(i\omega t) + c.c)] \\ &y \to \infty: \quad u(x,\infty,t) = v(x,\infty,t) = 0 \end{aligned} \tag{3.6}$$

Here c.c stands for complex conjugate. For both the cases, ε is real and much less than unity so that amplitude of oscillation is small. Here ω is the frequency of oscillation. $T_w(x),\ C_w(x)$ are the mean surface temperature and concentration and $q_w(x)$ and $c_w(x)$ are respectively, the mean temperature flux and mean concentration flux as given by Gebhart and Pera [3], and

$$T_w(x) = T_0\ x^n,\quad C_w(x) = C_0\ x^n,\quad q_w(x) = q_0\ x^n,\quad c_w(x) = c_0\ x^n \tag{3.7}$$

$T_0,\ q_0$ and $C_0,\ c_0$ are respectively, the scaled form of the temperature and species concentration at the surface of the plate. The exponent n in equation (3.7) can be expressed as:

$$n = \frac{d\ \ln q_w(x)}{d\ \ln x} = \frac{d\ \ln c_w(x)}{d\ \ln x} \tag{3.8}$$

and may be considered as the temperature as well as the concentration gradient at the surface of the plate.

The above mentioned sets of boundary conditions suggest the form of the solutions of the equations (3.1)-(3.4) as:

$$\begin{aligned}
&u = u_0(x,y) + \varepsilon\,(\exp(i\omega t) + c.c)\,u_1(x,y),\ \ v = v_0(x,y) + \varepsilon\,(\exp(i\omega t) + c.c)\,v_1(x,y)\\
&T - T_\infty = \theta_0(x,y) + \varepsilon\,(\exp(i\omega t) + c.c)\,\theta_1(x,y)\\
&C - C_\infty = \phi_0(x,y) + \varepsilon\,(\exp(i\omega t) + c.c)\,\phi_1(x,y)
\end{aligned} \tag{3.9}$$

where, ω represents the frequency of oscillation and , ε, which is very small positive number measures the amplitude. The calculations are restricted here by linearizing the equations for small values of ε, thus the c.c terms are omitted hereafter. Considering these form of solutions, the steady mean flow is governed by the following set of equations:

$$\frac{\partial u_0}{\partial x} + \frac{\partial v_0}{\partial y} = 0 \tag{3.10}$$

$$u_0\frac{\partial u_0}{\partial x} + v_0\frac{\partial u_0}{\partial y} = \nu\frac{\partial^2 u_0}{\partial y^2} + g\beta_T\theta_0 + g\beta_C\phi_0 \tag{3.11}$$

$$u_0\frac{\partial\theta_0}{\partial x}+v_0\frac{\partial\theta_0}{\partial y}=\alpha\frac{\partial^2\theta_0}{\partial y^2} \tag{3.12}$$

$$u_0\frac{\partial\phi_0}{\partial x}+v_0\frac{\partial\phi_0}{\partial y}=D\frac{\partial^2\phi_0}{\partial y^2} \tag{3.13}$$

Subject to the boundary conditions:

$$\begin{aligned} &y=0:\ u_0=v_0=0,\quad \theta_0=-q_w(x),\quad \phi_0=-c_w(x)\\ &y\to\infty:\ u_0\to 0,\quad \theta_0\to 0,\quad \phi_0\to 0 \end{aligned} \tag{3.14}$$

The unsteady flow field is governed by the set of following differential equations and corresponding boundary conditions:

$$\frac{\partial u_1}{\partial x}+\frac{\partial v_1}{\partial y}=0 \tag{3.15}$$

$$\begin{aligned} u_0\frac{\partial u_1}{\partial x}+u_1\frac{\partial u_0}{\partial x}+v_0\frac{\partial u_1}{\partial y}+v_1\frac{\partial u_0}{\partial y}+i\omega u_1\\ =\nu\frac{\partial^2 u_1}{\partial y^2}+g\beta_T\theta_1+g\beta_C\phi_1 \end{aligned} \tag{3.16}$$

$$u_0\frac{\partial\theta_1}{\partial x}+u_1\frac{\partial\theta_0}{\partial x}+v_0\frac{\partial\theta_1}{\partial y}+v_1\frac{\partial\theta_0}{\partial y}+i\omega\theta_1=\alpha\frac{\partial^2\theta_1}{\partial y^2} \tag{3.17}$$

$$u_0\frac{\partial\phi_1}{\partial x}+u_1\frac{\partial\phi_0}{\partial x}+v_0\frac{\partial\phi_1}{\partial y}+v_1\frac{\partial\phi_0}{\partial y}+i\omega\phi_1=D\frac{\partial^2\phi_1}{\partial y^2} \tag{3.18}$$

$$\begin{aligned} y=0: u_1=v_1=0,\quad \theta_1=-q_w(x),\quad \phi_1=-c_w(x)\\ y\to\infty: u_1\to 0,\quad \theta_1\to 0,\quad \phi_1\to 0 \end{aligned} \tag{3.19}$$

For the **case 1**, the associated boundary conditions given by equation (3.5) for the surface temperature and concentration suggests the following group of transformations:

$$\begin{aligned} &\Psi(x,y,t)=\nu Gr_x^{1/4}\left[F(\eta)+\varepsilon\exp(i\omega t)f(\xi,\eta)\right]\\ &\theta(x,y)=q_w(x)\left[\Theta(\eta)+\theta(\xi,\eta)\right],\ \phi(x,y)=c_w(x)\left[\Phi(\eta)+\phi(\xi,\eta)\right]\\ &\eta=\frac{y}{x}Gr_x^{1/4},\xi=\frac{\omega}{\nu}Gr_x^{-\ 1/4}x,\ Gr_x=\frac{g\left(\beta_T q_w+\beta_C c_w\right)}{\nu^2}x^3 \end{aligned} \tag{3.20}$$

Now substituting the above group of transformations into (3.10)-(3.14), one first obtain the following similarity equations for steady flow:

$$F''' + \frac{n+3}{4}FF'' - \frac{n+1}{2}(F')^2 + (1-w)\Theta + w\Phi = 0 \tag{3.21}$$

$$\frac{1}{Pr}\Theta'' + \frac{n+3}{4}F\Theta' - nF'\Theta = 0 \tag{3.22}$$

$$\frac{1}{Sc}\Phi'' + \frac{n+3}{4}F\Phi' - nF'\Phi = 0 \tag{3.23}$$

Associated boundary conditions are:

$$\begin{aligned} &F(0) = F'(0) = 0, \Theta(0) = \Phi(0) = -1 \\ &F'(\infty) = \Theta(\infty) = \Phi(\infty) = 0 \end{aligned} \tag{3.24}$$

The following set of non-similarity equations can be obtained for governing the unsteady flow field by introducing the above mentioned transformations into equations (3.15)-(3.19):

$$\begin{aligned} f''' + \frac{n+3}{4}(Ff'' + F''f) - (n+1)F'f' + (1-w)\theta + w\phi - i\xi f' \\ = \frac{(1-n)}{4}\xi(F'\frac{\partial f'}{\partial \xi} - F''\frac{\partial f}{\partial \xi}) \end{aligned} \tag{3.25}$$

$$\begin{aligned} \frac{1}{Pr}\theta'' + \frac{n+3}{4}(F\theta' + \Theta' f) - n(F'\theta + \Theta f') - i\xi\theta \\ = \frac{(1-n)}{4}\xi(F'\frac{\partial \theta}{\partial \xi} - \Theta'\frac{\partial f}{\partial \xi}) \end{aligned} \tag{3.26}$$

$$\begin{aligned} \frac{1}{Sc}\phi'' + \frac{n+3}{4}(F\phi' + \Phi' f) - n(F'\phi + \Phi f') - i\xi\phi \\ = \frac{(1-n)}{4}\xi(F'\frac{\partial \phi}{\partial \xi} - \Phi'\frac{\partial f}{\partial \xi}) \end{aligned} \tag{3.27}$$

Corresponding boundary conditions are:

$$\begin{aligned} &f(\xi,0) = f'(\xi,0) = 0, \theta(\xi,0) = \phi(\xi,0) = -1 \\ &f'(\xi,\infty) = \theta(\xi,\infty) = \phi(\xi,\infty) = 0 \end{aligned} \tag{3.28}$$

In the above equation (3.25), $w = \frac{N}{1+N}$, where $N = \frac{Gr_{x,C}}{Gr_{x,T}}$, which measures the relative importance of solutal and thermal diffusion in causing the density changes which drive the flow.

Now, for **case 2** the following transformations are introduced in order to achieve the governing equations for steady flow:

$$\psi_0 = C_2 x^{\frac{4}{5}} F(\eta),\ \Theta(\eta) = \frac{C_1\theta_0}{x^{1/5}(q_w/\kappa)},\ \Phi(\eta) = \frac{C_1\phi_0}{x^{1/5}(c_w/D)},\ \eta = \frac{C_1 y}{x^{\frac{1}{5}}},\ \text{where}$$
$$\beta = \beta_T + \beta_C,\ C_1 = (\frac{g\beta q_w}{\kappa\nu^2})^{\frac{1}{5}},\ C_2 = (\frac{g\beta q_w \nu^3}{\kappa})^{\frac{1}{5}} \tag{3.29}$$

where, ψ_0 is the stream function which satisfies the continuity equation (3.10) and q_0 and c_0 are the constants related to mean surface heat flux and mass flux respectively. By introducing the above mentioned set of transformations, the following equations along with the boundary conditions are found for the steady flow:

$$F''' + \frac{n+4}{5}FF'' - \frac{2n+3}{5}(F')^2 + (1-w)\Theta + w\Phi = 0 \tag{3.30}$$

$$\frac{1}{Pr}\Theta'' + \frac{n+4}{5}F\Theta' - \frac{4n+1}{5}F'\Theta = 0 \tag{3.31}$$

$$\frac{1}{Sc}\Phi'' + \frac{n+4}{5}F\Phi' - \frac{4n+1}{5}F'\Phi = 0 \tag{3.32}$$

$$F(0) = F'(0) = 0, \Theta'(0) = \Phi'(0) = -1$$
$$F'(\infty) = \Theta(\infty) = \Phi(\infty) = 0 \tag{3.33}$$

The transformations for the non similarity equations for the unsteady flow are as follows:

$$\Psi_1 = C_2 x^{\frac{4}{5}} f(\eta,\xi),\ \theta(\eta) = \frac{C_1\theta_1}{x^{1/5}q_w/\kappa},\ \phi(\eta) = \frac{C_1\phi_1}{x^{1/5}c_w/D}$$
$$\eta = \frac{C_1 y}{x^{\frac{1}{5}}},\ \xi = \omega(\frac{\kappa x}{g\beta q_w \nu})^{\frac{2}{5}} \tag{3.34}$$

Equations for the unsteady flow field are the following:

$$f''' + \frac{n+4}{5}Ff'' - (i\xi + \frac{4n+6}{5}F')f' + \frac{n+4}{5}F''f + (1-w)\theta + w\phi = \frac{2(1-n)}{5}\xi(F'\frac{\partial f'}{\delta\xi} - F''\frac{\partial f}{\partial\xi}) \tag{3.35}$$

$$\frac{1}{Pr}\theta'' + \frac{n+4}{5}F\theta' - (i\xi + \frac{4n+1}{5}F')\theta + \frac{n+4}{5}\Theta' f - \frac{4n+1}{5}\Theta f' = \frac{2(1-n)}{5}\xi(F'\frac{\partial\theta}{\partial\xi} - \Theta'\frac{\partial f}{\partial\xi}) \tag{3.36}$$

$$\frac{1}{Sc}\phi'' + \frac{n+4}{5}F\phi' - (i\xi + \frac{4n+1}{5}F')\Phi + \frac{n+4}{5}\Phi' f - \frac{4n+1}{5}\Phi f' = \frac{2(1-n)}{5}\xi(F'\frac{\partial\phi}{\partial\xi} - \Phi'\frac{\partial f}{\partial\xi}) \tag{3.37}$$

Corresponding boundary conditions are:

$$f(\xi,0) = f'(\xi,0) = 0, \theta'(\xi,0) = \phi'(\xi,0) = -1$$
$$f'(\xi,\infty) = \theta(\xi,\infty) = \phi(\xi,\infty) = 0 \tag{3.38}$$

Unsteady shear stress, surface heat transfer and surface mass transfer coefficients are the most important quantities which should be taken into account to understand the flow field associated with heat and mass transfer clearly, and to elucidate the effects of corresponding important parameters on the flow pattern, heat and mass transfer. These quantities can be calculated from the solutions of the equations (3.21)-(3.28) and (3.30)-(3.38). In this present study, these quantities are calculated and presented in terms of amplitude and phase angels. The following expressions are used to calculate the amplitude and phase of shear stress, local heat transfer coefficient and mass transfer coefficient respectively:

$$A_u = \sqrt{(f_r'')^2 + (f_i'')^2}|_{\eta=0}, \quad A_t = \sqrt{(\theta_r^2) + (\theta_i^2)}|_{\eta=0}, \quad A_c = \sqrt{(\phi_r^2) + (\phi_i^2)}|_{\eta=0} \tag{3.39}$$

and

$$\phi_u = \tan^{-1}(\frac{f_i''}{f_r''}), \quad \phi_t = \tan^{-1}(\frac{\theta_i}{\theta_r}), \quad \phi_c = \tan^{-1}(\frac{\phi_i}{\phi_r}) \tag{3.40}$$

where (f_r, f_i), (θ_r, θ_i) and (ϕ_r, ϕ_i) represent the real and imaginary part of $f(\xi, \eta)$, $\theta(\xi, \eta)$,and $\phi(\xi, \eta)$ respectively.

A dimensionless representation of the results for surface heat and mass transfer parameter, Nu_x and Sh_x can be achieved by using the definition of local heat transfer coefficient and mass transfer coefficient, which are expressed in the following usual manner:

$$\begin{aligned} h_x &= \frac{q_w}{T_w - T_\infty}, \; Nu_x = \frac{h_x x}{\kappa} \\ m_x &= \frac{c_w}{C_w - C_\infty}, \; Sh_x = \frac{m_x x}{\kappa} \end{aligned} \tag{3.41}$$

Using these definitions of h_x, m_x and Nu_x, Sh_x it can be obtained for the **case 1** that:

$$Nu_x = -\theta'(0) Gr_x^{1/4}, \quad Sh_x = -\phi'(0) Gr_x^{1/4}$$

For the **case 2**, flow adjacent to a vertical surface, the local heat transfer parameter, the Nusselt number $Nu_{x,T}$, or the local Nusselt number Nu_x and the local chemical species transfer parameter $Nu_{x,C}$, or the local Sherwood Number Sh_x can be found in terms of modified Grashof number, Gr^* as :

$$\begin{aligned} \frac{Nu_x}{Gr_x^{*1/5}} &= \frac{1}{\theta(0)}, \quad Nu_x = \frac{h_x x}{\kappa} = \frac{q_w x}{\kappa(T_w - T_\infty)} \\ \frac{Sh_x}{Gr_x^{*1/5}} &= \frac{1}{\phi(0)}, \quad Sh_x = \frac{m_x x}{D} = \frac{c_w x}{D(C_w - C_\infty)} \\ Gr^*_{x,T} &= \frac{g\beta_T q_w x^4}{\nu^2 \kappa}, \; Gr^*_{x,C} = \frac{g\beta_C c_w x^4}{\nu^2 D}, \; Gr^* = Gr^*_{x,T} + Gr^*_{x,C} \end{aligned} \tag{3.42}$$

The solution methodologies for different parts of the flow field to attain the required quantities are discussed in brief in the following sections.

3.3 Solution methodologies

Three different techniques are used in both these two cases to solve the governing equations of the flow field. The implicit finite difference method of Keller and Cebeci, (1978) [93], [94] (1984) is put into operation for the entire regime, extended series solution (ESS) for small

ξ which corresponds the region near the leading edge and asymptotic solution (ASS) for large ξ, corresponding the region far from the leading edge. Comparison amongst the results simulated by these three different techniques are elucidated in tabular form as well as by graphs. Excellent agreement amongst the simulated results by different numerical techniques ensured the validity of the model assumptions and efficiency of the numerical techniques that are applied here. The details of the calculation for both the cases have been presented in the following sections.

3.3.1 Extended series solutions(ESS)

Case 1:

For the effect of free convection on the flow near the leading edge or, equivalently, for small frequencies of oscillation, i.e. when ξ is small, we expand the functions f, θ, ϕ in powers of ξ as given below:

$$f(\xi,\eta)=\sum_{n=0}^{\infty}(\xi)^m f_m(\eta),\ \theta(\xi,\eta)=\sum_{n=0}^{\infty}(\xi)^m\theta_m(\eta),\ \phi(\xi,\eta)=\sum_{n=0}^{\infty}(\xi)^m\phi_m(\eta) \tag{3.43}$$

On substituting these into equations (3.25)-(3.28) and equating the terms of like powers of ξ to zero, the following sets of equations are obtained:

$$f_0'''+\frac{(n+3)}{4}\left(Ff_0''+f_0F''\right)-(n+1)F'f_0'+(1-w)\theta_0+w\phi_0=0 \tag{3.44}$$

$$\frac{1}{Pr}\theta_0''+\frac{(n+3)}{4}\left(F\theta_0'+\Theta' f_0\right)-n\left(\theta_0F'+\Theta f_0'\right)=0 \tag{3.45}$$

$$\frac{1}{Sc}\phi_0''+\frac{(n+3)}{4}\left(F\phi_0'+\Phi f_0'\right)-n\left(\phi_0F'+\Phi f_0'\right)=0 \tag{3.46}$$

$$f_m''' + \frac{n+3}{4} F f_m'' + \left\{ \frac{n+3}{4} + \frac{1}{2}(n-1)m \right\} F'' f_m$$
$$- \left\{ (n+1) + \frac{1}{2}(1-n)m \right\} F' f_m' + (1-w)\theta_m + w\phi_m = f_{m-1}' \tag{3.47}$$
$$\frac{1}{Pr}\theta_m'' + \frac{n+3}{4} F \theta_m' + \left\{ \frac{n+3}{4} + \frac{1}{2}(n-1)m \right\} \Theta' f_m$$
$$- \left\{ n + \frac{1}{2}(n-1)m \right\} F' \theta_m + n\Theta f_m' = \theta_{m-1} \tag{3.48}$$
$$\frac{1}{Sc}\phi_m'' + \frac{n+3}{4} F \phi_m' + \left\{ \frac{n+3}{4} + \frac{1}{2}(n-1)m \right\} \Phi' f_m$$
$$- \left\{ n + \frac{1}{2}(n-1)m \right\} F' \phi_m + n\Phi f_m' = \phi_{m-1} \tag{3.49}$$

$$f_0(0) = f_0'(0) = 0, \quad \theta_0 = -1, \quad \phi_0 = -1, \quad f_0'(\infty) = \theta_0(\infty) = \phi_0(\infty) = 0$$
$$f_m(0) = f_m'(0) = \theta_m(0) = \phi_m(0) = 0, \quad f_m'(\infty) = \theta_m(\infty) = \phi_m(\infty) = 0 \tag{3.50}$$

Case 2:

The results considering finite number of terms are valid only for very small range of frequencies. Since small values of ξ corresponds small frequencies ω also, it can be predicted that the flow to be adjusted quasi-statically to the fluctuating rate of both heat and mass transfer in the boundary layer. For small values of ξ which corresponds to near the leading edge, the functions f, g, h are expanded in powers of ξ as given below:

$$f(\xi,\eta) = \sum_{n=0} (2i\xi)^m f_m(\eta), \ \theta(\xi,\eta) = \sum_{n=0} (2i\xi)^m \theta_m(\eta)$$
$$\phi(\xi,\eta) = \sum_{n=0} (2i\xi)^m \phi_m(\eta) \tag{3.51}$$

Introducing the above mentioned series in the equations (3.35)-(3.38) and equating the terms of similar powers of ξ to zero, the following sets of equations can be obtained:

$$f_0''' + \frac{(n+4)}{5} F f_0'' - \frac{(4n+6)}{5} F' f_0' + \frac{(n+4)}{5} F'' f_0 + (1-w)\theta_0 + w\phi_0 = 0 \tag{3.52}$$

$$\frac{1}{Pr}\theta_0'' + \frac{(n+4)}{5}F\theta_0' - \frac{(4n+1)}{5}\theta_0 F' - \frac{4n+1}{5}\Theta f_0' + \frac{n+4}{5}\Theta' f_0 = 0 \tag{3.53}$$

$$\frac{1}{Sc}\phi_0'' + \frac{(n+4)}{5}F\phi_0' - \frac{(4n+1)}{5}\phi_0 F' - \frac{4n+1}{5}\Phi f_0' + \frac{n+4}{5}\Phi' f_0 = 0 \tag{3.54}$$

$$\begin{aligned} &f_m''' + \frac{n+4}{5}Ff_m'' + \frac{2m(n-1)}{5} - \frac{4n+6}{5}F'f_m' \\ &\quad + \frac{n+4}{5} - \frac{2m(n-1)}{5}F''f_m + \theta_m = \frac{1}{2}f_{m-1}' \end{aligned} \tag{3.55}$$

$$\begin{aligned} &\frac{1}{Pr}\theta_m'' + \frac{n+4}{5}F\theta_m' + \frac{2m(n-1}{5} - \frac{4n+1}{5}F'\theta_m \\ &\quad - \frac{4n+1}{5}\Theta f_m' + \frac{n+4}{5} - \frac{2m(n-1)}{5}\Theta' f_m = \frac{1}{2}\theta_{m-1} \end{aligned} \tag{3.56}$$

$$\begin{aligned} &\frac{1}{Sc}\phi_m'' + \frac{n+4}{5}F\phi_m' + \frac{2m(n-1}{5} - \frac{4n+1}{5}F'\phi_m \\ &\quad - \frac{4n+1}{5}\Phi f_m' + \frac{n+4}{5} - \frac{2m(n-1)}{5}\Phi' f_m = \frac{1}{2}\phi_{m-1} \end{aligned} \tag{3.57}$$

where m=1,2,3... and the respective boundary conditions are:

$$\begin{aligned} &f_0(0) = f_0'(0) = 0, \quad \theta_0' = -1, \quad \phi_0' = -1, \quad f_0'(\infty) = \theta_0(\infty) = \phi_0(\infty) = 0 \\ &f_m(0) = f_m'(0) = \theta_m(0) = \phi_m(0) = 0, \quad f_m'(\infty) = \theta_m(\infty) = \phi_m(\infty) = 0 \end{aligned} \tag{3.58}$$

where, primes denote the derivatives with respect to η as convention.

In the above, $f_0,\ \theta_0,\ \phi_0$ are the well known free convection similarity solutions for steady flow field and the functions $f_m,\ \theta_m,\ \phi_m$ are the higher order corrections to the flow due to the effect of the transpiration of fluid through the surface of the plate. Moreover it can be observed that the equations are linear but coupled. Thus it can be assumed that the solutions can be calculated by pair-wise sequential solution. Here, pair of equations are integrated using implicit Rungee-Kutta Butcher (Butcher,1964) initial value solver together with Nachtsheim and Swigert, [91] (1965). In this investigation, 8 pairs of equations are considered and solved numerically. Simulated results are compared with the results that are obtained by finite difference method and nice agreement found in the midst of these two types of results.

3.3.2 Asymptotic solution for large ξ

To study the flow pattern far from the leading edge i.e when the values of ξ are large, the asymptotic solutions are carried out. From the results that obtained by Keller box method shows that for larger values of ξ the unsteady response is confined to a thin layer adjacent to the surface. Thus as frequency approaches towards infinity, the solutions tend to be independent of the distance measured downstream from the leading edge, similar to the shear wave solution in the corresponding forced flow problem. This suggested once again another set of series expansion for both the cases, utilizing the limiting solutions as the zeroth-order approximation:

$$\begin{aligned} &Y = \xi^{1/2}\eta,\ \varphi(\xi, Y) = \xi^{3/2} f(\xi, \eta),\ \theta(\xi, Y) = \theta(\xi, \eta) \\ &\phi(\xi, Y) = \phi(\xi, \eta) \end{aligned} \tag{3.59}$$

Introducing these transformations, the equations (3.25)-(3.28) (which corresponds to **case:1**) take the form:

$$\begin{aligned} &\frac{\partial^3 \varphi}{\partial Y^3} + \frac{n+3}{4} F \xi^{-1/2} \frac{\partial^2 \varphi}{\partial Y^2} - i \frac{\partial \varphi}{\partial Y} \\ &\quad + \frac{3n+1}{4} F'' \xi^{-3/2} \varphi - \frac{n+3}{4} \xi^{-1} F' \frac{\partial \varphi}{\partial Y} + (1-w)\theta + w\phi \\ &\quad = \frac{(1-n)}{4} \left[F' \left(\frac{\partial^2 \varphi}{\partial Y \partial \xi} + \frac{Y}{2\xi} \frac{\partial^2 \varphi}{\partial Y^2} \right) - F'' \xi^{-1/2} \left(\frac{\partial \varphi}{\partial \xi} + \frac{Y}{2\xi} \frac{\partial \varphi}{\partial Y} \right) \right] \end{aligned} \tag{3.60}$$

$$\begin{aligned} &\frac{1}{Pr} \frac{\partial^2 \theta}{\partial Y^2} + \frac{n+3}{4} F \xi^{-1/2} \frac{\partial \theta}{\partial Y} - i\theta + n \xi^{-5/2} \theta \frac{\partial \varphi}{\partial Y} \\ &\quad = \frac{(1-n)}{4} \left[F' \left(\frac{\partial \theta}{\partial \xi} + \frac{Y}{2\xi} \frac{\partial \theta}{\partial Y} \right) - \Theta' \xi^{-3/2} \left(\frac{\partial \varphi}{\partial \xi} + \frac{Y}{2\xi} \frac{\partial \varphi}{\partial Y} \right) \right] \end{aligned} \tag{3.61}$$

$$\begin{aligned} &\frac{1}{Sc} \frac{\partial^2 \phi}{\partial Y^2} + \frac{n+3}{4} F \xi^{-1/2} \frac{\partial \phi}{\partial Y} - i\phi + n \xi^{-5/2} \phi \frac{\partial \varphi}{\partial Y} \\ &\quad = \frac{(1-n)}{4} \left[F' \left(\frac{\partial \phi}{\partial \xi} + \frac{Y}{2\xi} \frac{\partial \phi}{\partial Y} \right) - \Phi' \xi^{-3/2} \left(\frac{\partial \varphi}{\partial \xi} + \frac{Y}{2\xi} \frac{\partial \varphi}{\partial Y} \right) \right] \end{aligned} \tag{3.62}$$

And for **case 2**, the equations (3.35)-(3.38) take the form:

$$\frac{\partial^3\varphi}{\partial Y^3}+\frac{n+4}{5}F\xi^{-1/2}\frac{\partial^2\varphi}{\partial Y^2}-i\frac{\partial\varphi}{\partial Y}-\frac{6n+4}{5}F'\xi^{-1}\frac{\partial\varphi}{\partial Y}$$
$$+\frac{4n+1}{5}F''\xi^{-3/2}\varphi+(1-w)\theta+w\phi$$
$$=\frac{2(1-n)}{5}\left[F'\left(\frac{\partial^2\varphi}{\partial Y\partial\xi}+\frac{Y}{2\xi}\frac{\partial^2\varphi}{\partial Y^2}\right)-F''\xi^{-1/2}\left(\frac{\partial\varphi}{\partial\xi}+\frac{Y}{2\xi}\frac{\partial\varphi}{\partial Y}\right)\right] \quad (3.63)$$

$$\frac{1}{Pr}\frac{\partial^2\theta}{\partial Y^2}+\frac{n+4}{5}F\xi^{-1/2}\frac{\partial\theta}{\partial Y}-i\theta$$
$$-\frac{4n+1}{5}F'\xi^{-1}\theta-\frac{4n+1}{5}\Theta\xi^{-2}\frac{\partial\varphi}{\partial Y}+\frac{4n+1}{5}\Theta'\xi^{-5/2}\varphi$$
$$=\frac{2(1-n)}{5}\left[F'\left(\frac{\partial\theta}{\partial\xi}+\frac{Y}{2\xi}\frac{\partial\theta}{\partial Y}\right)-\Theta'\xi^{-3/2}\left(\frac{\partial\varphi}{\partial\xi}+\frac{Y}{2\xi}\frac{\partial\varphi}{\partial Y}\right)\right] \quad (3.64)$$

$$\frac{1}{Sc}\frac{\partial^2\phi}{\partial Y^2}+\frac{n+4}{5}F\xi^{-1/2}\frac{\partial\phi}{\partial Y}-i\phi$$
$$-\frac{4n+1}{5}F'\xi^{-1}\phi-\frac{4n+1}{5}\Phi\xi^{-2}\frac{\partial\varphi}{\partial Y}+\frac{4n+1}{5}\phi'\xi^{-5/2}\varphi$$
$$=\frac{2(1-n)}{5}\left[F'\left(\frac{\partial\phi}{\partial\xi}+\frac{Y}{2\xi}\frac{\partial\phi}{\partial Y}\right)-\Phi'\xi^{-3/2}\left(\frac{\partial\varphi}{\partial\xi}+\frac{Y}{2\xi}\frac{\partial\varphi}{\partial Y}\right)\right] \quad (3.65)$$

We can express the functions $F,\ \Theta,\ \Phi$ with fine accuracy as power series. This is because the above equations represent the region which is confined to a thin layer adjacent to the surface. Here, the following series representations are used:

$$\textbf{Case:1}: \quad F=a_2\eta^2+a_3\eta^3+a_4\eta^4...$$
$$\Theta=1+b_1\eta+b_2\eta^2...,\quad \Phi=1+c_1\eta+c_2\eta^2...\ \text{ where}$$
$$a_2=\frac{1}{2}F''(0),\ a_3=-1/6,\ a_4=1/24\left((1-w)G'(0)+wH'(0)\right)$$
$$b_1=\Theta'(0),\ c=\Phi'(0) \quad (3.66)$$
$$\textbf{Case 2:}\quad F=a_2\eta^2+...,\ \Theta=b-\eta+...,\quad \Phi=c-\eta+...\ \text{ where}$$
$$a_2=\frac{1}{2}F''(0),\ b=\Theta(0)=-1,\ c=\Phi(0)=-1 \quad (3.67)$$

Implementing those above expansions, solutions of the equations (3.25)-(3.28) and (3.35)-(3.38) can be found in the form of:

$$\varphi(\xi,Y)=\sum_{n=0}\xi^{-m/2}\bar{f}_m(Y),\ \theta(\xi,Y)=\sum_{n=0}\xi^{-m/2}\bar{\theta}_m(Y)$$
$$\phi(\xi,Y)=\sum_{n=0}\xi^{-m/2}\bar{\phi}_m(Y) \tag{3.68}$$

When equation (3.65) are surrogated in equations (3.25)-(3.28) and terms of like powers of ξ are collected, it can be obtained:

$$\bar{f}_0'''-i\bar{f}_0'=-(1-w)\bar{\theta}_0-w\bar{\phi}_0 \tag{3.69}$$
$$\bar{f}_1'''-i\bar{f}_1'=-(1-w)\bar{\theta}_1-w\bar{\phi}_1 \tag{3.70}$$
$$\bar{f}_2'''-i\bar{f}_2'=-(1-w)\bar{\theta}_2-w\bar{\phi}_2 \tag{3.71}$$
$$\bar{f}_3'''-i\bar{f}_3'=-\frac{3n+1}{4}a_2Y^2\bar{f}_0''+\frac{(3n+5)}{2}a_2Y\bar{f}_0'-\frac{(3n+1)}{2}a_2\bar{f}_0-(1-w)\bar{\theta}_3-w\bar{\phi}_3 \tag{3.72}$$
$$\frac{1}{Pr}\bar{\theta}_0''-i\bar{\theta}_0=0 \tag{3.73}$$
$$\frac{1}{Pr}\bar{\theta}_1''-i\bar{\theta}_1=0 \tag{3.74}$$
$$\frac{1}{Pr}\bar{\theta}_2''-i\bar{\theta}_2=0 \tag{3.75}$$
$$\frac{1}{Pr}\bar{\theta}_3''-i\bar{\theta}_3=-\frac{3n+1}{4}a_2Y^2\bar{\Theta}_0'+2na_2Y\bar{\Theta}_0 \tag{3.76}$$
$$\frac{1}{Sc}\bar{\phi}_0''-i\bar{\phi}_0=0 \tag{3.77}$$
$$\frac{1}{Sc}\bar{\phi}_1''-i\bar{\phi}_1=0 \tag{3.78}$$
$$\frac{1}{Sc}\bar{\phi}_2''-i\bar{\phi}_2=0 \tag{3.79}$$
$$\frac{1}{Sc}\bar{\phi}_3''-i\bar{\phi}_3=-\frac{3n+1}{4}a_2Y^2\bar{\Phi}_0'+\frac{8n+2}{5}2na_2Y\bar{\Phi}_0 \tag{3.80}$$

After substituting equation (3.65) into the equations (3.35)-(3.38) (which corresponds to **case 2**), and collecting the similar powers of ξ, the following equations are acquired:

$$\bar{f}_0''' - i\bar{f}_0' = -(1-w)\bar{\theta}_0 - w\bar{\phi}_0 \tag{3.81}$$

$$\bar{f}_1''' - i\bar{f}_1' = -(1-w)\bar{\theta}_1 - w\bar{\phi}_1 \tag{3.82}$$

$$\bar{f}_2''' - i\bar{f}_2' = -(1-w)\bar{\theta}_2 - w\bar{\phi}_2 \tag{3.83}$$

$$\begin{aligned}\bar{f}_3''' - i\bar{f}_3' = &-\frac{3n+2}{5}a_2Y^2\bar{f}_0'' + \frac{2(7n+3)}{5}a_2Y\bar{f}_0' \\ &- \frac{2(4n+1)}{5}a_2\bar{f}_0 - (1-w)\bar{\theta}_3 - w\bar{\phi}_3\end{aligned} \tag{3.84}$$

$$\frac{1}{Pr}\bar{\theta}_0'' - i\bar{\theta}_0 = 0 \tag{3.85}$$

$$\frac{1}{Pr}\bar{\theta}_1'' - i\bar{\theta}_1 = 0 \tag{3.86}$$

$$\frac{1}{Pr}\bar{\theta}_2'' - i\bar{\theta}_2 = 0 \tag{3.87}$$

$$\frac{1}{Pr}\bar{\theta}_3'' - i\bar{\theta}_3 = -\frac{3n+2}{5}a_2Y^2\bar{\Theta}_0' + \frac{8n+2}{5}a_2Y\bar{\Theta}_0 \tag{3.88}$$

$$\frac{1}{Sc}\bar{\phi}_0'' - i\bar{\phi}_0 = 0 \tag{3.89}$$

$$\frac{1}{Sc}\bar{\phi}_1'' - i\bar{\phi}_1 = 0 \tag{3.90}$$

$$\frac{1}{Sc}\bar{\phi}_2'' - i\bar{\phi}_2 = 0 \tag{3.91}$$

$$\frac{1}{Sc}\bar{\phi}_3'' - i\bar{\phi}_3 = -\frac{3n+2}{5}a_2Y^2\bar{\Phi}_0' + \frac{8n+2}{5}a_2Y\bar{\Phi}_0 \tag{3.92}$$

In these equations, primes denote the differentiation with respect to Y, and the associated boundary conditions are:

$$\begin{aligned}&\textbf{case:1} \quad \bar{f}_m(0) = \bar{f}_m'(0) = \bar{f}_m'(\infty) = 0, \quad m = 0,1,2,3,4... \\ &\bar{\theta}_0 = -1,\ \bar{\theta}_m(0) = \bar{\theta}_m(\infty) = 0, \quad m = 0,1,2,3,4... \\ &\bar{\phi}_0(0) = -1,\ \bar{\phi}_m(0) = \bar{\phi}_m(\infty) = 0, \quad m = 0,1,2,3,4.. \\ &\textbf{case:2} \quad \bar{f}_m(0) = \bar{f}_m'(0) = \bar{f}_m'(\infty) = 0, \quad m = 0,1,2,3,4... \\ &\bar{\theta}_0'(0) = -1,\ \bar{\theta}_m(0) = \bar{\theta}_m(\infty) = 0, \quad m = 0,1,2,3,4... \\ &\bar{\phi}_0'(0) = -1,\ \bar{\phi}_m(0) = \bar{\phi}_m(\infty) = 0, \quad m = 0,1,2,3,4...\end{aligned} \tag{3.93}$$

Solution of the above equations (3.69)-(3.71), yield the following relation:

$$f''(0) = f_0''(0)\xi^{-1/2} + f_3''(0)\xi^{-3/2} + O(\xi^{-5/2}), \quad \text{where} \tag{3.94}$$

$$f_0''(0) = \frac{1}{\sqrt{i}}\left\{\frac{1-w}{1+\sqrt{Pr}} + \frac{w}{1+\sqrt{Sc}}\right\}$$

$$f_3''(0) = \frac{(1-w)i}{(Pr-1)}\left\{\frac{3a_2(5n-1)(1+3\sqrt{Pr})}{16\sqrt{i}Pr(Pr-1)(\sqrt{Pr}-1)} - \frac{a_2(5n-1)i}{4}\left(1+\frac{2\sqrt{Pr}}{Pr-1}\right)\left(\frac{1}{4i}-\frac{Pr}{Pr-1}\right)\right\}$$

$$+\frac{wi}{Sc-1}\left\{\frac{3a_2(5n-1)(1+3\sqrt{Sc})}{16\sqrt{i}Sc(Sc-1)(\sqrt{Sc}-1)} - \frac{a_2(5n-1)i}{4}\left(1+\frac{2\sqrt{Sc}}{Sc-1}\right)\left(\frac{1}{4i}-\frac{Sc}{Sc-1}\right)\right\}$$

$$+\frac{(3n+1)a_2}{2}\left[\left\{\frac{1-w}{Pr-1}\left(\frac{1}{8}+\frac{\sqrt{Pr}(3\sqrt{Pr}-1)}{(Pr-1)^2}+\right)+\frac{w}{Sc-1}\left(\frac{1}{8}+\frac{\sqrt{Sc}(3\sqrt{Sc}-1)}{(Sc-1)^2}+\right)\right\}\right]$$

$$+\frac{(3n+1)a_2}{2}\left[\frac{1-w}{2(\sqrt{Pr}+1)^2}+\frac{w}{2(\sqrt{Sc}+1)^2}\right] + \frac{(3n+5)a_2}{2}\left\{\frac{1-w}{Pr-1}\left(\frac{1}{(\sqrt{Pr}+1)^2}-\frac{1}{4}\right)\right\}$$

$$\frac{(3n+5)a_2}{2}\left\{\frac{w}{Sc-1}\left(\frac{1}{(\sqrt{Sc}+1)^2}-\frac{1}{4}\right)\right\}$$

$$\theta'(\xi,0) = -\sqrt{iPr} - \frac{ia_2}{16}(1+5n)\xi^{-1} + O(\xi^{-3/2})$$

$$\phi'(\xi,0) = -\sqrt{iSc} - \frac{i\ a_2}{16}(1+5n)\xi^{-1} + O(\xi^{-3/2})$$

The solutions of the equations (3.66)-(3.78) subject to the boundary conditions (3.79), gives the following expressions for shear stress, surface temperature and species concentration coefficient respectively:

$$f''(\xi,0) = -i(\frac{1-w}{\sqrt{Pr}(1+\sqrt{Pr})} + \frac{w}{\sqrt{Sc}(1+\sqrt{Sc})})\xi^{-1/2} + 2(C_{12}+C_{22}+C_{32})$$
$$- 2\sqrt{i}(C_{13} + \sqrt{Pr}\ C_{23} + \sqrt{Sc}\ C_{33}) + O(\xi^{-5/2}) \tag{3.95}$$

$$\theta(\xi,0) = \frac{1}{\sqrt{iPr}}\,\xi^{-1/2} + \frac{(11n+4)\,a_2}{20\ Pr}\,\xi^{-5/2} + O(\xi^{-7/2}) \tag{3.96}$$

$$\phi(\xi,0) = \frac{1}{\sqrt{iSc}}\,\xi^{-1/2} + \frac{(11n+4)\,a_2}{20\ Sc}\,\xi^{-5/2} + O(\xi^{-7/2}) \tag{3.97}$$

$$A = \frac{(1-w)}{Pr(1-Pr)},\ B = \frac{w}{Sc(1-Sc)},\ C_3 = \frac{(1-w)\ \sqrt{Pr}}{Pr(1-Pr)} - \frac{w\ \sqrt{Sc}}{Sc(1-Sc)}$$

$$A_1 = -\frac{(3n+2)\ a_2\ \sqrt{Pr}}{30\ \sqrt{i}},\ B_1 = \frac{(11n+4)\ a_2\ i}{20},\ C_1 = \frac{(11n+4)\ a_2\ \sqrt{i}}{20\sqrt{Pr}}$$

$$A_2 = -\frac{(3n+2)\ a_2\ \sqrt{Sc}}{30\ \sqrt{i}},\ B_2 = \frac{(11n+4)\ a_2\ i}{20},\ C_2 = \frac{(11n+4)\ a_2\ \sqrt{i}}{20\sqrt{Sc}}$$

$$P_1 = -\frac{(3n+2)\ a_2}{5},\ P_2 = -\frac{2(7n+3)\ a_2}{5},\ P_3 = -\frac{2(4n+1)\ a_2}{5}$$

$$C_{11} = \frac{P_1\ C_3}{6},\ C_{12} = \frac{1}{4\sqrt{i}}P_2\ C_3 + 18\ C_{11}$$

$$C_{13} = \frac{1}{2i}P_3\ C_3 + 6\sqrt{i}C_{12} - 6\ C_{11}$$

$$C_{21} = -\frac{(1-w)\ (3n+2)\ a_2}{30(1-Pr)},\ C_{22} = -\frac{(1-w)\ a_2\ K_1}{20\ \sqrt{iPr}\ (1-Pr)^2}$$

$$C_{23} = -\frac{(1-w)\ a_2\ K_2}{20\ i\ Pr\ (1-Pr)^3}$$

$$C_{31} = -\frac{w\ (3n+2)\ a_2}{30(1-Sc)},\ C_{32} = -\frac{w\ a_2\ K_{11}}{20\ \sqrt{iSc}\ (1-Sc)^2}$$

$$C_{33} = -\frac{w\ a_2\ K_{22}}{20\ i\ Sc\ (1-Sc)^3}$$

$$K_1 = 4(3n+2) + (1-Pr)(11n+4) + 2(3n+2)(1-3Pr)$$

$$K_2 = 8(1-Pr)(7n+3) + (11n+4)(1-Pr)^2 + 4(1-3Pr)K_1 + 12\ Pr(1-Pr)(3n+2)$$

$$K_{11} = 4(3n+2) + (1-Sc)(11n+4) + 2(3n+2)(1-3Sc)$$

$$K_{22} = 8(1-Sc)(7n+3) + (11n+4)(1-Sc)^2 + 4(1-3Sc)K_1 + 12\ Sc\ (1-Sc)\ (3n+2)$$

The above expressions are valid only for $Pr \neq 1$ and $Sc \neq 1$. If it is necessary to calculate the values for $Pr = 1$ and $Sc = 1$ then the limiting values as $Pr \to \infty$ and $Sc \to \infty$ should be calculated.

Exactly in the similar procedure, the equations (3.60)-(3.63) (for **case 1**) are solved and the required quantities are calculated. The details presentation of the calculations are exempted here in order to avoid the repetition.

3.4 Results and discussion

Since natural convection flow due to combined effects of thermal and mass diffusion is very important from practical point of view, an extensive investigation for this type of model flow field have been carried out through numerical simulations. In view of the fact that, Hossain *et.al* [18], also examined this type of flow field only for thermal diffusion. In the present investigation, as mentioned earlier, similar types of boundary conditions for two different cases are considered and calculations are performed accordingly. In **case 1**, oscillating surface temperature and species concentration are considered and these small amplitude oscillations are imposed on the surface heat and mass flux in **case 2**. Comparative numerical results for these two cases are presented in tabular form. Few graphical representation of the results considering the boundary condition for **case 1** have been illustrated at the beginning of the discussions.

The effect of varying buoyancy parameter, w, on the amplitude and phase of the rates of heat and mass transfer(case 1)are depicted in Figure 3.2 and 3.3 respectively, for the case Pr=0.7, Sc=0.22, and n=0.5. In these figures, the dotted curves and the broken curves represent the solutions obtained for the low frequency and high frequency cases, respectively. From Figure 3.2(a) and 3.3(a) it can be seen that there is an increase in the local amplitude for both the heat and mass transfer rates due to increase in the buoyancy parameter, w. This effect is most significant near the leading edge, i.e. in the low-frequency range. As the values of the frequency parameter increase, these values tend toward the asymptotic state. For **case 2**, in this present investigation, similar types of results, discussed by the authors [18], are produced first. Then the model has been extended to study the flow field with both thermal and mass diffusion. All the model assumptions are kept similar to [18]. Both the steady and fluctuating part of the problem are analyzed by the keller-box method for the entire frequency regime. The fluctuating part of the problem is investigated by three different methodologies. Results are presented in in terms of amplitude and phase angles for variation of different parameters both in tabular and graphical forms. The forgoing formulations may be analyzed to indicate the nature of the interaction of the various contributions to buoyancy. These may aid or oppose one

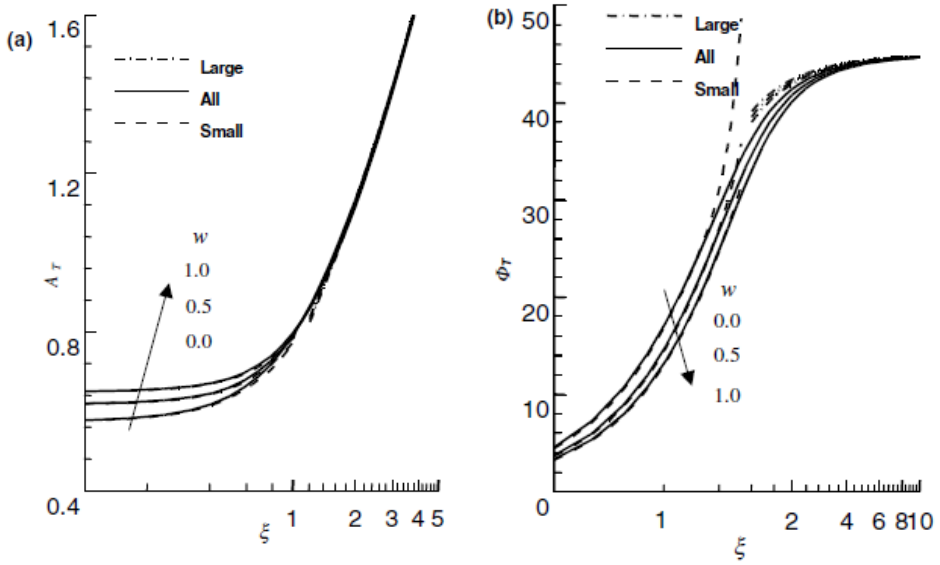

Figure 3.1: (a) Amplitude, (b) Phase angles, local heat flux against ξ for different values of w, while, Pr=0.7, Sc=0.22,n=0.5.

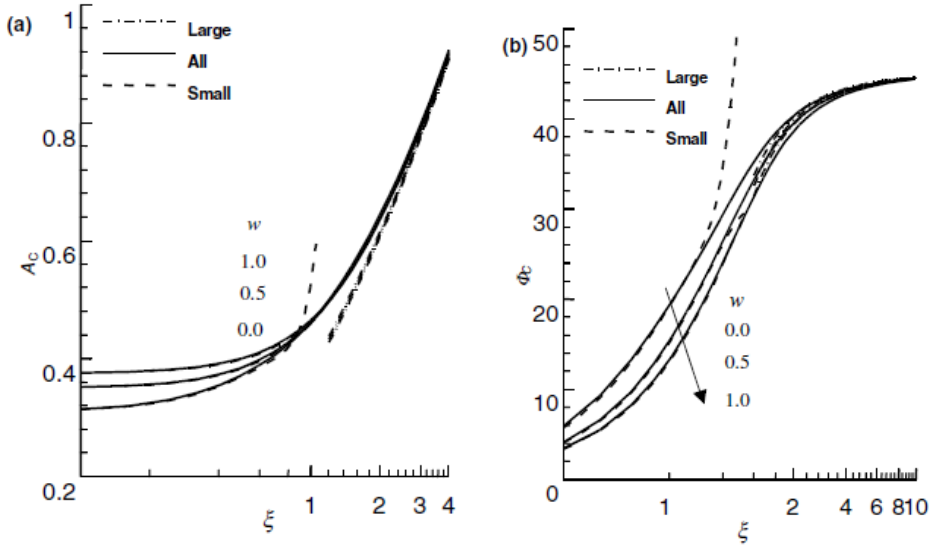

Figure 3.2: (a) Amplitude, (b) Phase angles, of local mass flux against ξ for different values of w, while, Pr=0.7, Sc=0.22, n=0.5.

Table 3.1: Values of shear stress, surface temperature and surface concentration for the steady flow field for variation of different parameters, while, Pr=0.7.

w	shear stress	surface heat transfer	surface mass transfer
0.0000	0.56578	0.33272	0.59525
0.2500	0.50978	0.31013	0.54862
0.7500	0.46897	0.29386	0.51562
1.000	.41226	0.27140	0.47100
n			
0.0000	0.44347	0.38467	0.72034
0.2500	0.40040	0.35692	0.66014
0.7500	0.36891	0.33708	0.61773
1.000	.0.32501	0.30994	0.56078
Sc			
0.1000	0.56920	0.26926	0.68102
0.6000	37955	0.33184	0.35711
1.1000	.34202	0.35068	0.28454
1.6000	.32396	0.35963	0.24756

another and be of different magnitudes characterized by the value of w. When the thermal and solutal effects are opposed, the value of w is negative in order to assure that the flow is in positive x direction. The relative physical extent η of the two effects in convection region is governed by the magnitudes of the Prandtl number and Schimdt number and their relative values. Here, discussions are restricted for favorable case only (w is positive) for the fluids with Prandtl number Pr=0.9 to 0.25. Here, the values of Prandtl numbers are chosen to represent the fluid as air and liquid which are currently used as coolant in nuclear engineering. Although the diffusing chemical species of most common interest in air has Schmidt numbers in the range from 0.1 to 10.0, the present investigation considered a range from 0.1 to 1.60. Some values of shear stress, surface temperature and surface concentration for the steady flow field are listed in Table 3.2. During the simulations, the value of Prandtl number, Pr is chosen as constant value 0.7, representing air, and all other parameters are varied. It can be observed from the Table 3.2 that the values of shear stress, surface temperature and surface concentration decrease as the values of w,n and Sc become higher. Table 3.3 and Table 3.4 show the comparison of the results obtained by keller-Box method and perturbation method for local surface heat transfer and local mass

Table 3.2: Comparison of the values of amplitude and phase angels of the local surface heat transfer, obtained by finite difference method, while, Pr=0.7, Sc=0.94, w=0.5, n=0.5.

ξ	A_T		ϕ_T	
—-	Surface heat transfer	Surface temperature	Surface heat transfer	Surface temperature
0.0000	1.4273	1.42738^1	0.00000	0.00000^1
0.1002	1.42469	1.42627^1	2.99340	2.68514^1
0.2013	1.41650	1.42292^1	5.99132	5.37870^1
0.3045	1.40272	1.40877^1	8.99521	7.08826^1
0.4108	1.38327	1.38864^1	12.00221	9.81945^1
0.5024	1.36270	1.36990^1	14.50581	8.39808^1
0.5975	1.33815	1.33728^1	17.00177	9.81636^1
0.6967	1.30965	1.31337^1	19.48248	11.24410^1
0.8009	1.27723	1.29649^1	21.93677	12.84996^1
0.9105	1.24099	1.25415^1	24.34766	14.08462^1
1.0028	1.20936	1.23616^2	26.22925	15.45600^2
2.0143	0.89404	1.4176^2	38.25065	24.8384^2
6.0502	0.49349	0.5428^2	43.94037	39.2737^2
8.0555	0.42544	0.4281^2	44.32133	41.2201^2
10.0179	0.38044	0.3979^2	44.51393	42.1542^2
20.2113	0.26657	0.2708^2	44.83141	43.9730^2
30.1619	0.21795	0.2198^2	44.90746	44.4320^2
40.0461	0.18905	0.1885^2	44.93943	44.6366^2
50.5732	0.16818	0.1603^2	44.95727	44.7304^2
60.7511	0.15342	0.1539^2	44.96755	44.8000^2
70.5839	0.14232	0.1427^2	44.97404	44.84020^2

[1] stands for series solution and [2] stands for asymptotic solution

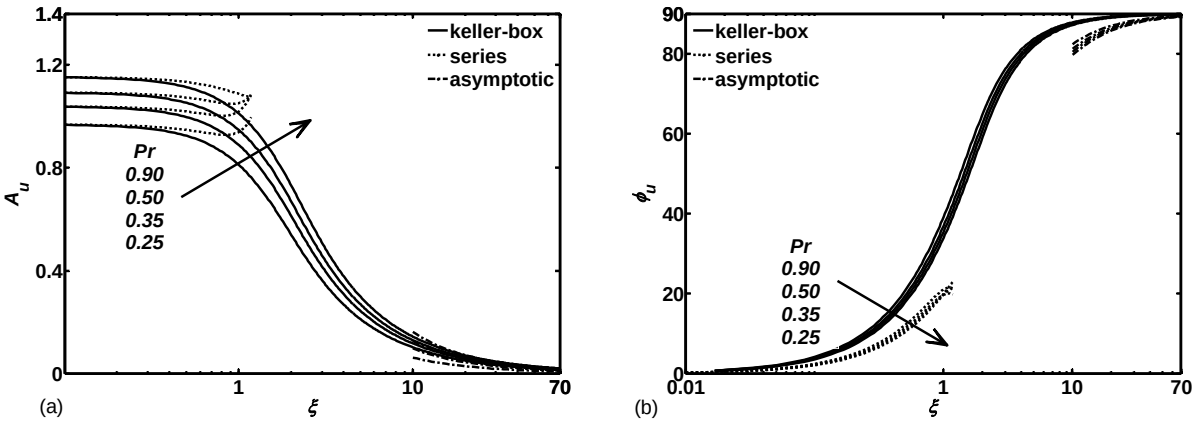

Figure 3.3: (a) Amplitude, (b) Phase angles, of shear stress for different values of Pr, while, Sc=0.6, w=0.5, n=0.5.

transfer respectively. For these simulations, the values of parameters w, n,Pr,Sc are taken as 0.5,0.5.0.7 and 0.22 respectively and the quantities represented against ξ ranging from 0.00 to 70.00. The required quantities for the small value of ξ (0.0 to 0.9) are obtained from extended series solution method and for the higher values of ξ (1.0 to 70.0) the respective quantities are taken from the results by asymptotic series solution method. For both amplitude and phase angles of the respective quantities, nice agreement is found amongst the results calculated by different methodologies. Here also plodding decrement of amplitude of shear stress, surface temperature and surface concentration and increment of phase angles of the respective quantities along with the increment of the values of ξ can be observed.

The effect of Prandtl number Pr, and the exponent parameter n on the shear stress are presented in Figures 3.3-3.4. All the graphs for depicting the amplitudes and phase angles of shear stress are drawn for the results obtained from numerical simulations by Keller-box method, extended series solution method and asymptotic series solution method. All the figures clearly show that results obtained for the entire regime are significantly close to the results that are calculated for the region near and far from the leading edge.

For different values of Pr, while all other parameters are kept constant(w=*0.5, n=0.5, Sc=0.6*), it can be seen remarkable increase in amplitudes of the shear stress due to the increment of the Prandtl number, Pr. The phase angles are zero under quasi-steady conditions and decrease monotonically towards the asymptotic value 90^0 as $\xi \to \infty$. From

Table 3.3: Comparison of the values of amplitude and phase angels of the local surface mass transfer, obtained by perturbation method and finite difference method, while, Pr=0.7, Sc=0.22, w=0.5, n=0.5.

ξ	A_c		ϕ_c	
—-	Keller	Series and asymp.	Keller	Series and asymp.
0.0000	1.53621	1.53620^{1}	0.00000	0.00000^{1}
0.1002	1.53298	1.53484^{1}	3.02864	3.42313^{1}
0.2013	1.52326	1.53484^{1}	6.04759	5.00983^{1}
0.3045	1.50730	1.52422^{1}	9.04992	5.13372^{1}
0.4108	1.48535	1.51529^{1}	12.03249	6.83417^{1}
0.5024	1.46265	1.50561^{1}	14.50248	8.33942^{1}
0.5975	1.43599	1.49615^{1}	16.95796	9.79256^{1}
0.6967	1.40540	1.48654^{1}	19.39603	10.85799^{1}
0.8009	1.37088	1.47676^{1}	21.80920	11.00362^{1}
0.9105	1.33244	1.47121^{1}	24.18315	12.87376^{1}
1.0995	1.26326	1.46922^{2}	27.84154	13.63863^{2}
2.0143	0.96403	1.5857^{2}	38.02563	23.9307^{2}
4.0219	0.66171	0.7996^{2}	42.83438	34.6990^{2}
6.0502	0.53315	0.5914^{2}	43.86996	38.8672^{2}
8.0555	0.45964	0.4867^{2}	44.27340	40.9397^{2}
10.0179	0.41102	0.4315^{2}	44.47848	41.9387^{2}
20.2113	0.28796	0.2929^{2}	44.81842	43.8923^{2}
30.1619	0.23543	0.2376^{2}	44.90023	44.3870^{2}
40.0461	0.20421	0.2037^{2}	44.93467	44.6077^{2}
50.5732	0.18167	0.1840^{2}	44.95390	44.7089^{2}
60.7511	0.16572	0.1663^{2}	44.96498	44.7840^{2}
70.5839	0.15373	0.1541^{2}	44.97199	44.8274^{2}

[1] stands for series solution and [2] stands for asymptotic solution

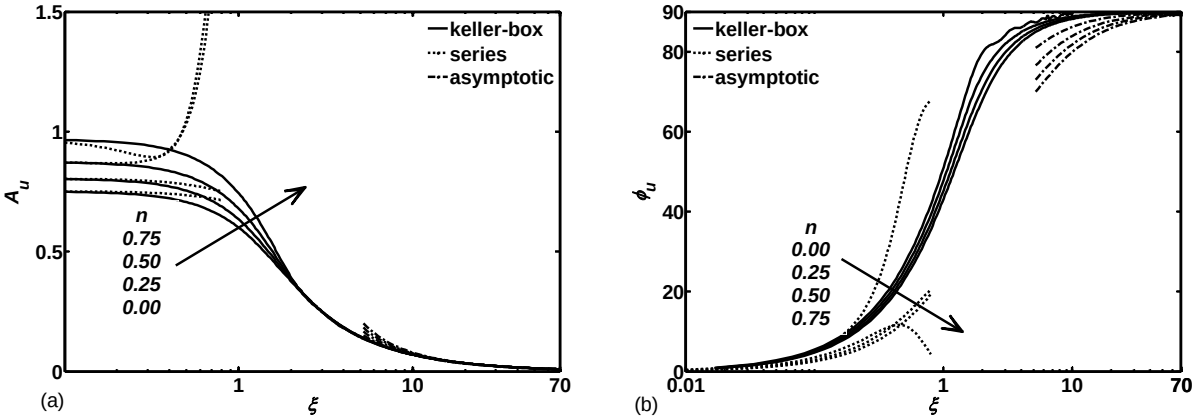

Figure 3.4: (a) Amplitude, (b) Phase angels, of shear stress for different values of n, while, Pr=0.7, Sc=0.6, w=0.5.

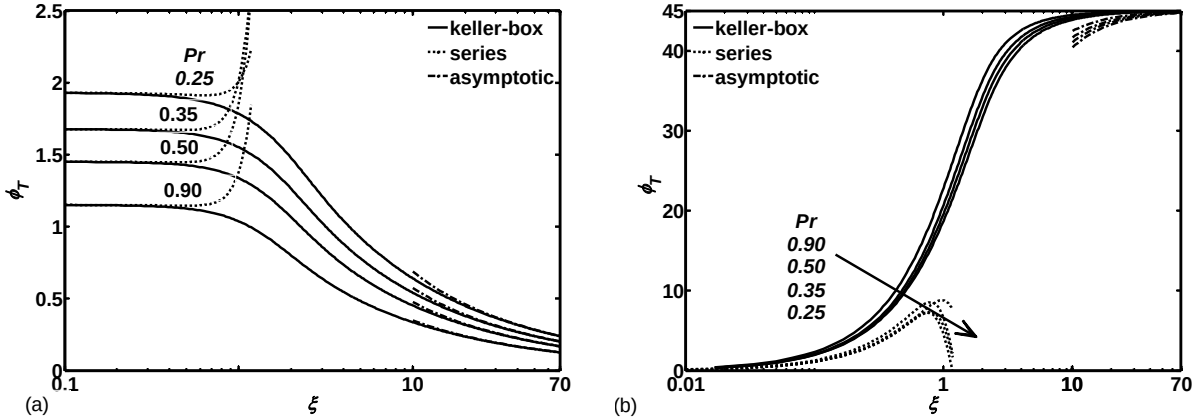

Figure 3.5: (a) Amplitude, (b) Phase angles, of surface heat transfer for different values of Pr, while, Sc=0.6, w=0.5, n=0.5.

Figures 6.5, it can be observed that the amplitudes of the shear stress are decreased while the exponent parameter n of the surface heat and mass flux are increased. But the values of phase angle of shear stress are increased as the value of exponent increase. For much higher values of ξ, i.e, far from the leading edge, there is almost no change in values of amplitude for variation of n and tends to zero for all values of n.

The effects of Prandtl number, Pr on the amplitudes and phase angles of the surface heat transfer is illustrated in the Figure 3.5. For these simulations, the values of w and n is taken as 0.5 and the value of Sc is chosen as 0.6. In these figures also, results are presented for three different methodologies, as described in the previous sections. For the

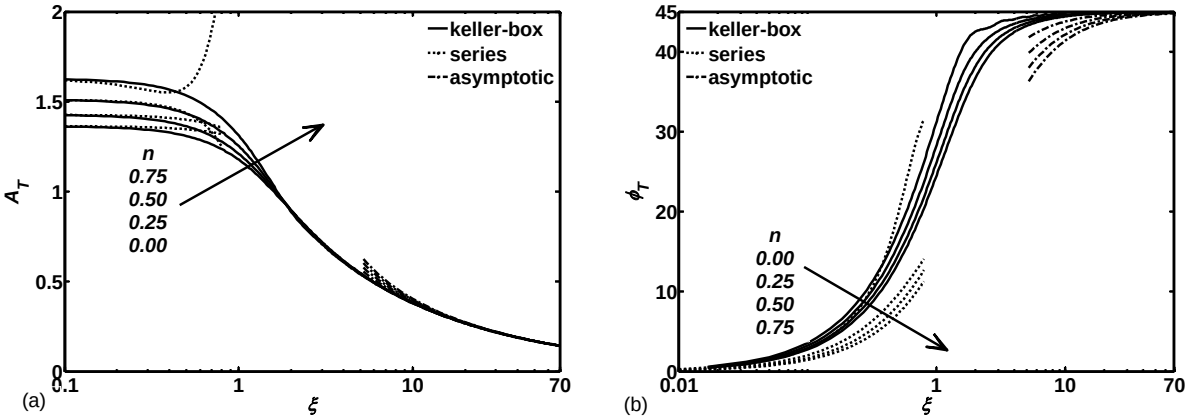

Figure 3.6: (a) Amplitude, (b) Phase angles of surface heat transfer for different values of n, while, Pr=0.7, Sc=0.6, w=0.5.

very low frequency region, i.e. for the very small values of ξ , the results obtained by extended series solution method are very much close to the solutions that are obtained from keller-box method. Far from the leading edge, i.e. for the large values of ξ, we can see very nice agreement between the results obtained from the asymptotic solutions and keller-box solutions. It can also be seen from these figures that, the values of amplitude of surface temperature decrease as the value of Pr increases. The values of phase angles for surface temperature increase for the decrement of the values of Pr. The values of phase angles tends towards the value of 45^0 as the value of $\xi \to \infty$.

In Figure 3.6, the effect of exponent parameter n on the surface heat transfer is presented. Similar to shear stress, here also the values of amplitude of surface temperature become little smaller as the values of n become higher and far from the leading edge, i,e for the large values of ξ , these changes become ignorable for the variation of n and tends toward the value of zero. For the phase angles, as expected, the opposite behavior is observed, i.e very small increment of the quantities are achieved because of small decrement of values of n.

Similar types of behavior can be observed for the surface mass transfer for different values of Schmidt number, Sc and n in Figures 3.7-3.8. During the simulation, to predict the effects of Schmidt numbers on both the surface mass transfer and shear stress, the value of Prandtl number is taken as 0.7 and the values of w and n are chosen as 0.5. We can

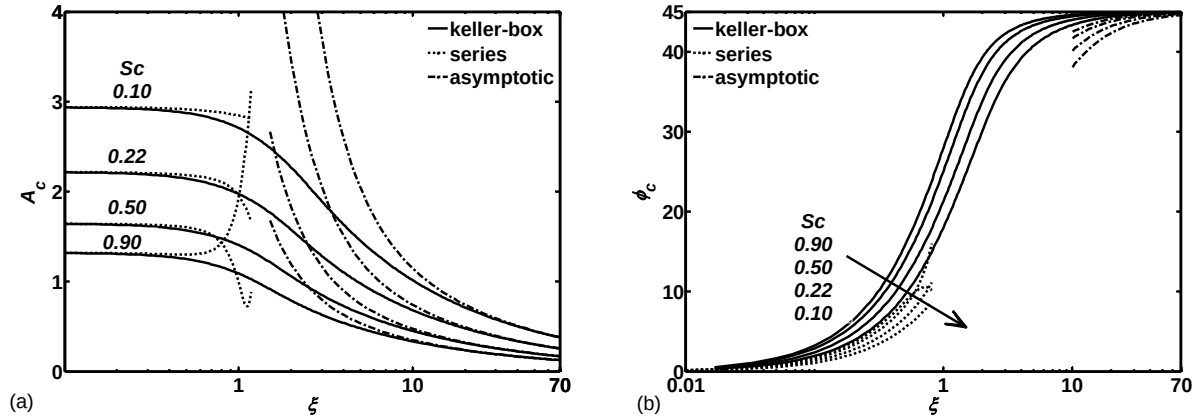

Figure 3.7: (a) Amplitude, (b) Phase angles of surface mass transfer for different values of Sc, while, Pr=0.7, w=0.5, n=0.5.

monitor the increment of the values of amplitude of surface species transfer as the values of Sc is decreased while the values of phase angle increased in small amount. As it is marched towards the higher values of ξ, the value of the phase angles of the surface mass concentration reached to the asymptotic value 45^0. For the case of n, just as surface temperature, we can see that, the values of amplitude of surface concentration become little smaller and phase angles become little higher while the values of n are taken in ascending order.

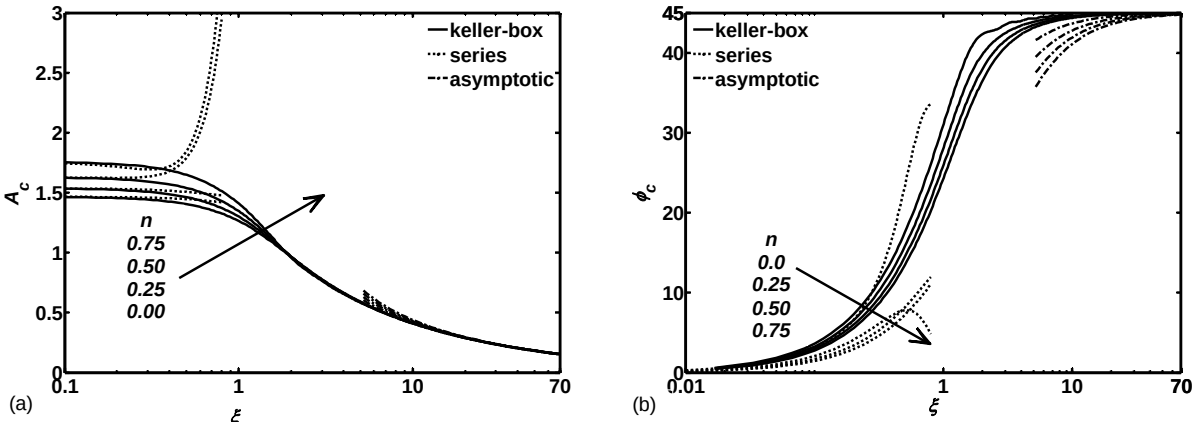

Figure 3.8: (a) Amplitude, (b) Phase angles, of surface mass transfer for different values of n, while, Pr=0.7, Sc=0.6, w=0.5.

3.4.1 Effects of different parameters on transient shear stress,transient surface temperature and transient surface concentration

In this section, the effects of some parameters, such as, Schmidt number Sc, amplitude of surface temperature and concentration ε, buoyancy ratio parameter, w and the flux exponent parameter n on the transient shear stress, transient heat transfer and transient mass transfer are discussed at $\xi = 1.00$. All these results are presented here for a fixed Prandtl number, Pr, which is taken once again as 0.70. The definition for transient shear stress, τ, transient heat transfer, θ_w, transient mass transfer, ϕ_w have been used as follows:

$$\tau = \tau_s + \varepsilon A_u \cos(\omega t + \phi_u),\ \theta_w = \theta_s + \varepsilon A_t \cos(\omega t + \phi_t)$$
$$\phi_w = \phi_s + \varepsilon A_c \cos(\omega t + \phi_c) \tag{3.98}$$

where, τ_s is the steady mean shear stress, θ_s is the steady heat transfer and θ_s is the steady mass transfer respectively. The values of τ_s, θ_s, ϕ_s are calculated first and then the required quantities are obtained accordingly from the simulations by using the implicit finite difference method together with the Keller-box for the entire regime [93].

From Figures 3.9, 3.10, 3.11 (a), it can be seen that the increase in the values of amplitude of oscillation of surface heat flux and surface mass flux cause increment in the oscillation of transient skin friction, transient heat transfer and transient mass transfer respectively. The oscillations with different values of amplitude and phase with regular periodic maxima and minima are visualized in Figure 3.9, 3.10, 3.11(b) for the heat and mass flux exponent parameter n. The oscillations pattern of the transient skin friction, surface temperature and surface concentration are similar. From Figures 3.9, 3.10, 3.11 (c), it can be seen that, the oscillations of the amplitude of transient shear stress, transient surface temperature and transient surface concentration decrease as the values of Sc increase. For each values of Sc, these oscillations attain a maximum and a minimum values periodically. For buoyancy ratio parameter w, a periodic oscillation for transient skin friction, transient heat transfer and transient mass transfer are shown. For the variation of the values of w, no significant changes are occurred for the corresponding maximum and minimum values

Table 3.4: Computed surface heat flux, for both the cases, obtained by perturbation methods and finite difference method, while Pr=0.7, Sc=0.94, w=0.5, n=0.5.

ξ	Amplitude		Phase Angles	
—-	Heat Transfer Coefficient) (Case:1)	Heat Transfer Coefficient (Case:2)	Heat Transfer Coefficient (Case:1)	Heat Transfer Coefficient (Case:2)
0.0000	0.5640	1.4841	0.0000	0.00000
0.2000	0.5757	1.4693	9.4097	6.57415
0.4000	0.6081	1.4265	17.7448	13.0214
0.6000	0.6569	1.3653	24.5914	18.7786
0.8000	0.7208	1.3005	29.9354	23.3428
1.0000	0.8002	1.2234	33.8894	27.6700
2.0000	1.3381	0.8903	41.5582	38.9819
3.0000	1.4159	0.7096	43.2498	42.0514
4.0000	1.6483	0.6109	44.2149	43.1387
5.0000	1.8507	0.5581	44.4054	43.6964
6.0000	2.0326	0.5327	44.5290	44.0268]
7.0000	2.1992	0.4885	44.6147	44.2304
8.0000	2.3538	0.4687	44.6771	44.3737
9.0000	2.4988	0.4479	44.7242	44.4763
10.0000	2.6357	0.4238	44.8913	44.5503

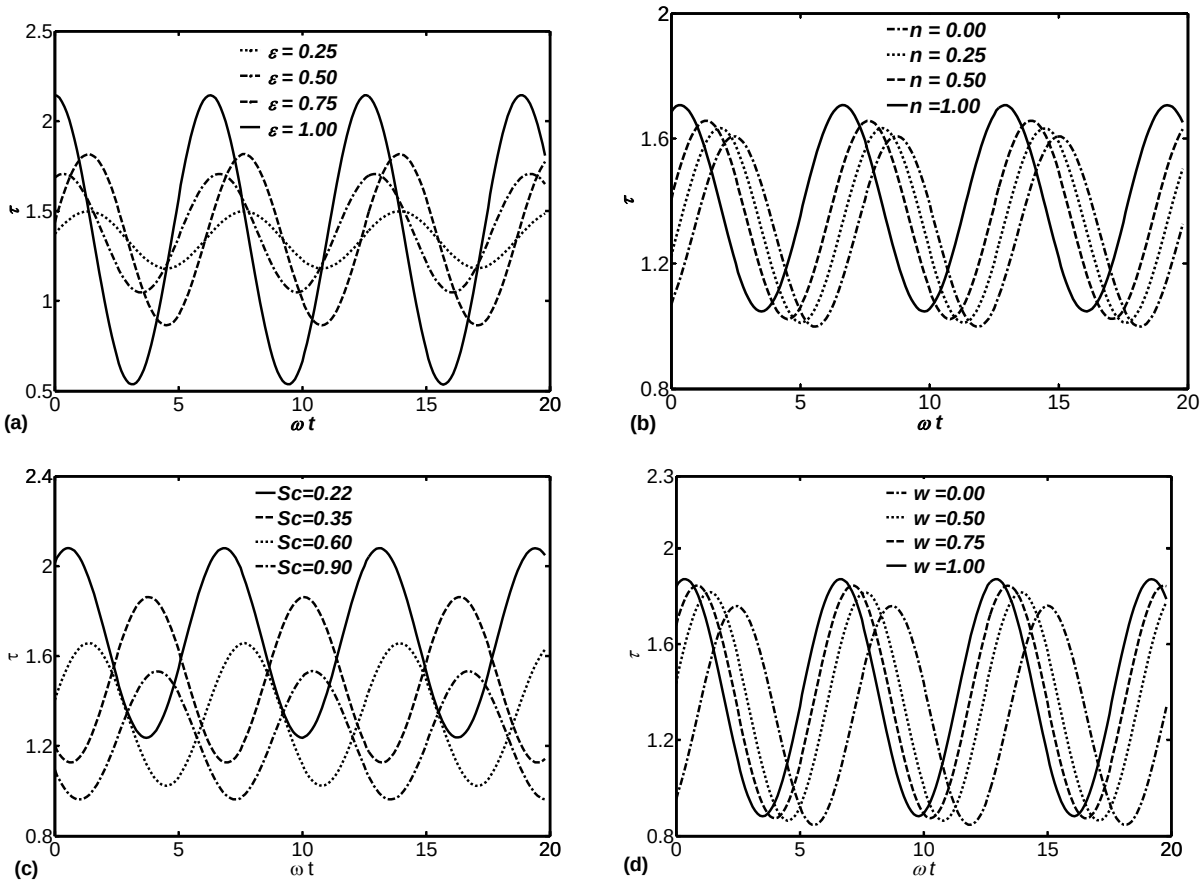

Figure 3.9: Transient shear stress at $\xi = 1.0$ for different (a) ϵ, while, Pr=0.7, Sc=0.6, w=0.5, n=0.5 (b) n, while Pr=0.7, Sc=0.6, w=0.0, (c) Sc, while, Pr=0.7, w=0.5,n=0.5 (d) w, while Pr=0.7, n=0.5, Sc=0.6.

of the oscillations.

Finally in Table 3.4, a comparative presentation of numerical values of amplitude and phase angle of surface heat flux for two different cases have been illustrated. Here both the values of amplitude and phase angles of surface heat and mass flux as well as surface temperature and concentration are listed against the non similarity parameter ξ. From this comparative studies, it can be observed that, for case 1, i.e. for the surface heat flux, the values of amplitude increased as the value of ξ increased. But for case 2, i.e. for surface temperature, the opposite behaviour can be monitored. But for the phase angles, for both the cases, the values are increased as it is marched towards far from the leading edge and finally asymptotic values are attained.

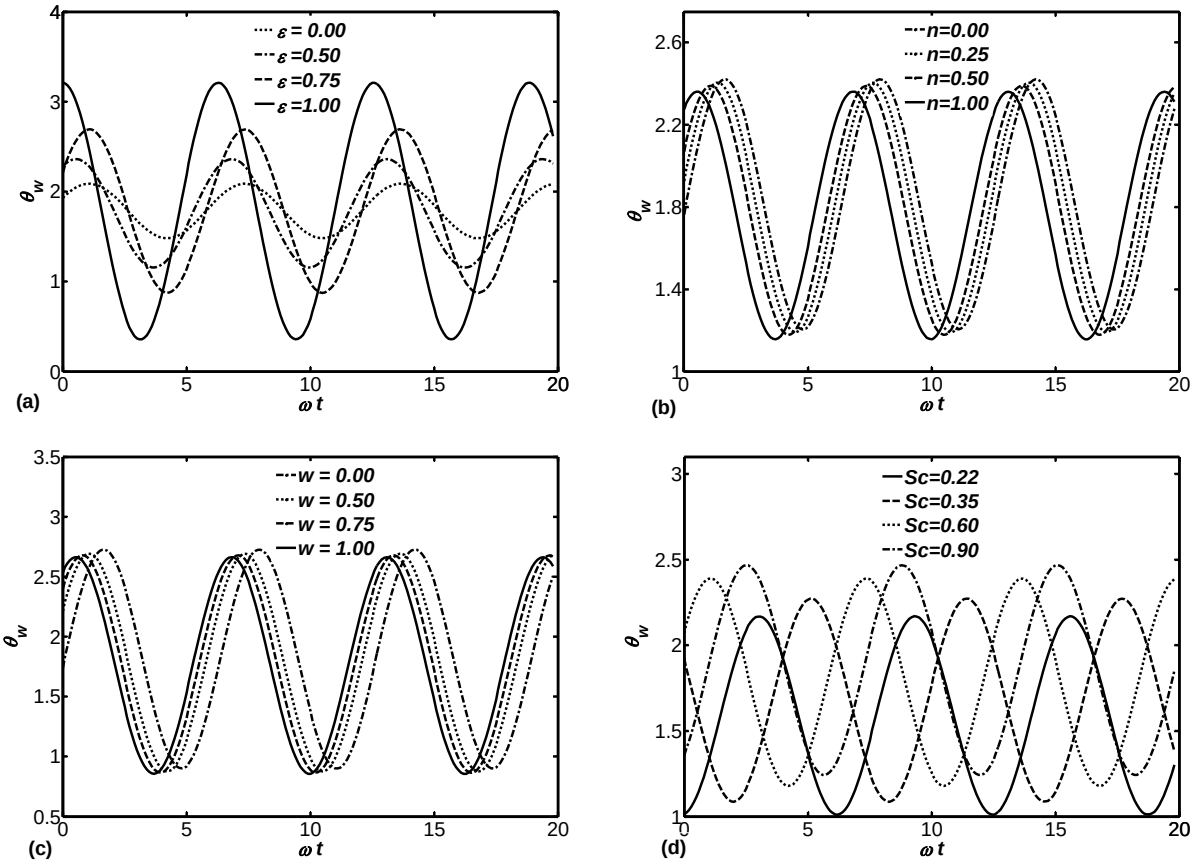

Figure 3.10: Transient heat transfer at $\xi = 1.0$ for different (a) ϵ, while, Pr=0.7, Sc=0.6, w=0.5, n=0.5 (b) n, while Pr=0.7, Sc=0.6, w=0.0, (c) w, while, Pr=0.7, Sc=0.6, n=0.5 (d) w, while, Pr=0.7, n=0.5, Sc=0.6.

In Table 3.5, computed heat transfer coefficient parameter (Nu_x) and mass transfer coefficient parameter (Sh_x)are presented for portraying a correlation between these two cases. The calculations are carried out with the small amplitude oscillation $\varepsilon = 0.25$. The rest of the parameters were taken as, $Pr = 0.7,\ Sc = 0.94,\ w = 0.5,\ n = 0.5$ respectively. As it can be observed from this table that, the computed values of both the Nusselt number and Sherwood number are for both the cases are almost same, as expected. This nice agreement of these two quantities for these two cases, surely establish a very strong correlation between the simulation of these two cases.

Table 3.5: Computed heat transfer coefficient, (Nu_x), and mass transfer coefficient (Sh_x) for both the cases, obtained by perturbation methods and finite difference method, while, Pr=0.7, Sc=0.94, w=0.5, n=0.5.

ξ	Amplitude		Phase Angles	
—-	Heat Transfer Parameter (Case:1)	Heat Transfer Parameter (Case:2)	Mass Transfer Parameter (Case:1)	Mass Transfer Parameter (Case:2)
0.0000	0.0000	0.0000	0.0000	
0.0200	0.1721	0.18781	0.1693	0.1700
0.4000	0.3259	0.3368	0.3198	0.3235
0.64000	0.4478	0.4867	0.4432	0.4517
0.86000	0.6097	0.6432	0.6614	0.6602
1.0000	0.8002	0.8173	0.8238	0.8698
2.0000	1.7504	1.9556	1.0471	1.0861
3.0000	3.2275	3.3937	3.1106	3.1313
4.0000	4.6621	4.9622	4.2822	4.3812
5.0000	6.1881	6.4932	6.0451	6.1636
6.0000	7.7922	7.8711	7.6984	7.8645
7.0000	9.4642	9.7098	9.2560	9.3271
8.0000	11.1966	11.2610	11.4625	11.4830
9.0000	12.9841	12.9483	13.1969	13.4025
10.0000	14.8216	14.8881	15.2816	15.3110

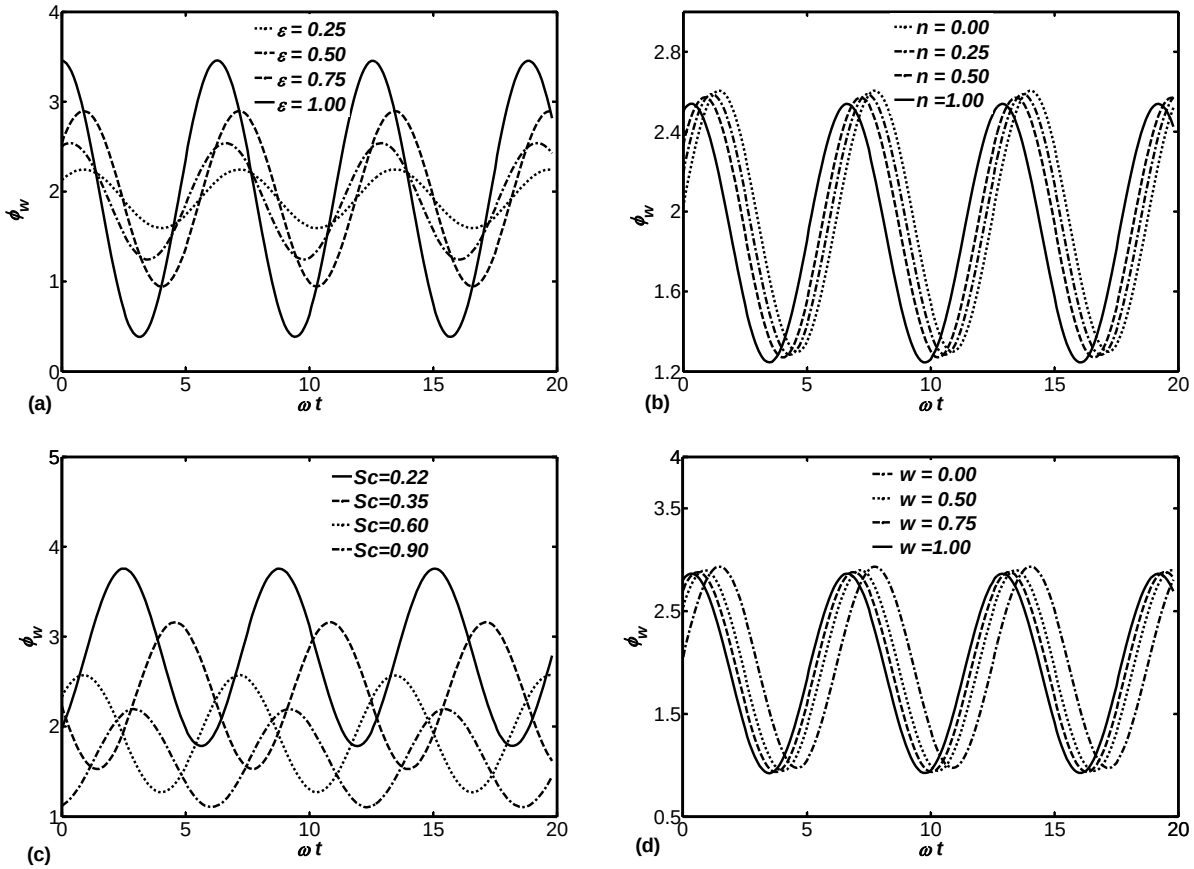

Figure 3.11: Transient mass transfer at $\xi = 1.0$ for different (a) ε, while, Pr=0.7, Sc=0.6, w=0.5, n=0.5 (b) n, while Pr=0.7, Sc=0.6, w=0.0, (c) Sc, while, Pr=0.7, w=0.5, n=0.5 (d) w, while, Pr=0.7, n=0.5, Sc=0.6.

3.5 Summary

The purpose of this study is to investigate the velocity flow field in terms of local shear stress. Local heat and mass transfer coefficient, resulting from buoyancy forces which arise from a combination of temperature and species concentration effects of comparable magnitude are also studied rigorously. The summarization of the whole work has been listed below:

- A linearized theory has been utilized and detailed numerical calculations are carried out for wide ranges of parameters. Similar type of boundary condition have been considered for two different cases. Exceptive agreement amongst all the results calculated by different numerical methods establish the validity of the simulations as well

as the assumptions of the mathematical model that are made for the respective flow field.

- A correlation between the two cases have been drawn by calculating the local heat and mass transfer coefficient parameter, $Nu_x,\ Sh_x$ respectively.

- From the observations of the simulated results it can be concluded that, the amplitude of the shear stress, local heat transfer and local mass transfer decrease as the frequency increases despite the consequences of the Prandtl number, Schimdt number and the surface heat and mass flux exponent. But for surface heat and mass flux, the values of the amplitude get higher as the values of ξ also become higher. The phase angles for both heat and mass transfer decrease towards the asymptotic value 45^0, while the respective quantity for shear stress reaches to the value of 90^0 in a decreasing manner.

- The heat and mass flux exponent parameter n has no significant effects on both amplitude and phase angles as the values of ξ become very large.

Chapter 4

Unsteady laminar mixed convection boundary layer flow near a vertical wedge due to oscillations in velocity and surface temperature

4.1 Introduction

Over a few decades, oscillating flow and heat transfer under the influence of free-stream oscillation have been the focus of research due to its occurrence in many interesting and important fluid-mechanical problems, for example, the accelerating and decelerating phases of missile flight, the intermittent flow in an engine during unstable combustion, heat transfer encountered in liquid rocket and turbo-jet engines, and thermal failure of the resonance tube heating in which the effect of heat generation appears to be significant. Many studies were devoted to unsteady laminar boundary layer characteristics (e.g., fluctuating skin-friction and heat transfer) between 1950 and 1980 as a result of its practical applications. Due to lack of the development of numerical simulation up to the early 1970s, this issue was mainly investigated theoretically. As a result, a simplified problem was formulated of the actual technological problems and the complexity in obtaining the solutions was thus

circumvented by imposing restrictions on oscillation amplitude or a frequency [28]. Accordingly, a body of knowledge about the problems was not fully uncovered. Even, there is still scope for further investigation about this large subject.

Since, in practice, unsteady heat transfer and flow field are encountered in some machinery, so it is expected that both the stream velocity and surface temperature can be oscillatory. Moreover, the effect of buoyancy driven flow has to be incorporated into the mathematical formulation as the aforementioned engineering problems take place under the gravitational field. Nevertheless, the previous studies did not consider mixed convection induced by buoyancy force and the oscillating free-stream velocity and surface temperature. Thus the purpose of this study is to investigate the oscillating laminar boundary layer of mixed convection flow past a vertical wedge under the influence of free-stream and surface temperature oscillations. The effects of the Richardson number, Ri, introduced to measure the effect of mixed convection and the Prandtl number, Pr, have been presented in terms of amplitudes and phase angles of skin-friction and heat transfer. The transient skin-friction and heat transfer are also shown for different values of Ri and Pr.

4.2 Formulation of the problem

Let us consider a two-dimensional unsteady laminar boundary layer flow of an incompressible fluid with constant properties. To describe the flow configuration, we assume that x denotes the distance along the surface from the leading edge, y denotes the distance normal from the surface, u and v are the corresponding velocity components, T is the temperature, t is the time, U is the velocity at the edge of the boundary layer, ν is the kinematic viscosity, α is the thermal diffusivity, g is the acceleration due to gravity, β is the coefficient of volumetric expansion. The coordinate system and the flow configuration are shown in figure 4.1.

Under the usual Boussinesq approximation along with the above assumptions the bound-

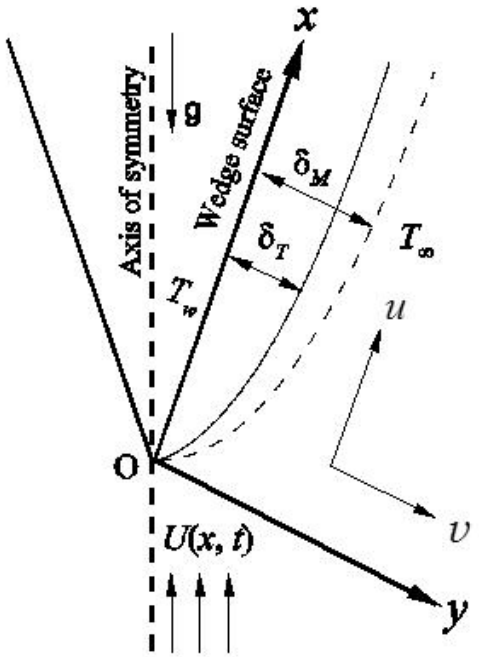

Figure 4.1: Physical configuration and coordinate system

ary layer equations for mass, momentum and energy can be written as:

$$\frac{\partial u}{\partial x} + \frac{\partial v}{\partial y} = 0 \tag{4.1}$$

$$\frac{\partial u}{\partial t} + u\frac{\partial u}{\partial x} + v\frac{\partial u}{\partial y} = \nu\frac{\partial^2 u}{\partial y^2} + \frac{\partial U}{\partial t} + U\frac{\partial U}{\partial x} + g\beta\left(T - T_\infty\right)\cos\left(\frac{\pi}{4}\right) \tag{4.2}$$

$$\frac{\partial T}{\partial t} + u\frac{\partial T}{\partial x} + v\frac{\partial T}{\partial y} = \alpha\frac{\partial^2 T}{\partial y^2} \tag{4.3}$$

where u and v are the x and y components of velocity field, respectively, in the momentum boundary layer; $\bar{T} = T - T_\infty$, T and T_∞ being the temperature in the thermal boundary layer and ambient fluid respectively, ν is the kinematic viscosity of the fluid, g the acceleration due to gravity, α the thermal diffusivity, β_T, β_C are the coefficient of volume expansion

due to temperature and species concentration. The associated boundary conditions are:

$$\begin{aligned} &y = 0: \quad u = v = 0,\ T = T_\infty + (T_w - T_\infty)\,(1 + \varepsilon\ \ (\exp i\ \omega t + c.c)) \\ &y = \infty: \quad u = U(x,t),\ \ T = T_\infty \end{aligned} \tag{4.4}$$

where,

$$U = U_0\ x^{1/2}[1 + \varepsilon\,(\exp i\omega t + c.c)], \quad T_w = T_0[1 + \varepsilon\,(\exp i\omega t + c.c)]$$

Above, T_0 and U_0 are, respectively the mean temperature and mean velocity ; $\varepsilon(<< 1)$ is the amplitude and ω is the frequency of oscillations in the surface temperature and free stream velocity. Equation (4.4) suggests the solutions to be of the form:

$$\begin{aligned} \psi(x,y,t) &= \psi_0(x,y) + \varepsilon\ \psi_1(x,y)\,(\exp(i\omega t) + c.c) \\ T(x,y,t) &= T_0(x,y) + \varepsilon\ T_1(x,y)\,(\exp(i\omega t) + c.c) \end{aligned} \tag{4.5}$$

where only the real part is to be taken as it has physical meaning. Now we substitute equations (4.6)-(4.8) into equations (4.1)-(4.3) and equate the coefficient of ε^0 that give

$$\frac{\partial\psi_0}{\partial y}\frac{\partial^2\psi_0}{\partial x\partial y} - \frac{\partial\psi_0}{\partial x}\frac{\partial^2\psi_0}{\partial y^2} = \frac{1}{2}U_0^2 + \nu\frac{\partial^3\psi_0}{\partial y^3} + g\beta\,(T_0 - T_\infty)\cos\left(\frac{\pi}{4}\right) \tag{4.6}$$

$$\frac{\partial\psi_0}{\partial y}\frac{\partial T_0}{\partial x} - \frac{\partial\psi_0}{\partial x}\frac{\partial T_0}{\partial y} = \alpha\frac{\partial^2 T_0}{\partial y^2} \tag{4.7}$$

The set of equations for ψ_0 and T_0 represents the steady state solution that can be determined by the following functions

$$\psi_0 = (\nu U_0)^{1/2}\,x^{3/4} f(\eta), \quad \frac{T_0 - T_\infty}{T_w - T_\infty} = \theta(\eta); \quad \eta = \left(\frac{U_0}{\nu}\right)^{1/2} x^{-1/4} y \tag{4.8}$$

using equation (4.8) in equations (4.6) and (4.7), we obtain the dimensionless equations:

$$f''' + \frac{3}{4}ff'' + \frac{1}{2}(1 - F'^2) + Ri\theta = 0 \tag{4.9}$$

$$\frac{1}{Pr}\theta'' + \frac{3}{4}f\Theta' = 0 \tag{4.10}$$

Corresponding boundary conditions are given by:

$$\begin{aligned} f = f' = 0, \quad \theta = 1 \quad \text{at} \quad \eta = 0 \\ f' = 1, \theta = 0 \quad \text{at} \quad \eta \to \infty \end{aligned} \tag{4.11}$$

Substituting the expressions (4.6)-(4.8) into equations (4.2),(4.3) and equating the coefficients of ε give equations for time dependent components $\psi_1,\ T_1$ as

$$\begin{aligned} i\omega\frac{\partial\psi_1}{\partial y} + \frac{\partial\psi_0}{\partial y}\frac{\partial^2\psi_1}{\partial x\partial y} + \frac{\partial\psi_1}{\partial y}\frac{\partial^2\psi_0}{\partial x\partial y} - \frac{\partial\psi_0}{\partial x}\frac{\partial^2\psi_1}{\partial y^2} \\ = i\omega U_0 x^{1/2} + U_0^2 + \nu\frac{\partial^3\psi_1}{\partial y^3} + g\beta T_1 \end{aligned} \tag{4.12}$$

$$i\omega T_1 + \frac{\partial\psi_0}{\partial y}\frac{\partial T_1}{\partial x} + \frac{\partial\psi_1}{\partial y}\frac{\partial T_0}{\partial x} - \frac{\partial\psi_0}{\partial x}\frac{\partial T_1}{\partial y} - \frac{\partial\psi_1}{\partial x}\frac{\partial T_0}{\partial y} = \alpha\frac{\partial^2 T_1}{\partial y^2} \tag{4.13}$$

The associated boundary conditions become

$$\begin{aligned} \psi_1 = \frac{\partial\psi_1}{\partial y} = 0, \quad T_1 = T_w - T_\infty \quad \text{at} \quad \text{y} = 0 \\ \frac{\partial\psi_1}{\partial y} = U_0 x^{1/2}, \quad T_1 = 0 \quad \text{as} \quad \text{y} \to \infty \end{aligned} \tag{4.14}$$

To non-dimensionalize equations (4.12) and (4.13), we introduce the following expressions

$$\psi_1 = (\nu U_0)^{1/2}\, x^{3/4} F(\xi,\ \eta), \quad \frac{T_1}{T_w - T_\infty} = \Theta(\xi,\ \eta) \tag{4.15}$$

Using equations (4.15) into equations (4.12) and (4.13), we obtain

$$\begin{aligned} F''' + \frac{3}{4}\left(fF'' + f''F\right) - f'F' + Ri\Theta + 1 \\ + i\xi(1 - F') = \frac{1}{2}\xi\left(f'\frac{\partial F'}{\partial\xi} - f''\frac{\partial F}{\partial\xi}\right) \end{aligned} \tag{4.16}$$

$$\frac{1}{Pr}\Theta'' + \frac{3}{4}\left(f\Theta' + F\theta'\right) - i\xi\ \Theta = \frac{1}{2}\xi\left(f'\frac{\partial\Theta}{\partial\xi} - \theta'\frac{\partial F}{\partial\xi}\right) \tag{4.17}$$

Here, $\xi = \omega x^{1/2}/U_0$, $Gr_x = g\beta\,(T_w - T_\infty)\cos(\pi/4)x^3/\nu^2$ is the Grashof number, $Re_x = U_0 x^{3/2}/\nu$ is the Reynolds number and $Pr = \nu/\alpha$ is the Prandtl number. The mixed convection parameter Ri is defined as $\frac{Gr_x}{Re_x^2}$. Typically, the natural convection is negligible when $Ri < 0.1$, forced convection is negligible when $Ri < 10$ and neither is negligible when $0.1 < Ri < 10$. In the present problem, the values of Ri is chosen from 0.0-4.0. Corresponding boundary conditions need to be satisfied:

$$\begin{aligned} &F(\xi,0) = F'(\xi,0) = 0, \quad \Theta(\xi,0) = 1 \\ &F'(\xi,\infty) = 1, \quad \Theta(\xi,\infty) = 0 \end{aligned} \tag{4.18}$$

Now we obtain the appropriate equations for all Pr by introducing

$$(f,F) = (1+Pr)^{-3/4}\left(\hat{f},\ \hat{F}\right), \quad \hat{\eta} = (1 = pr)^{1/4}\,\eta \tag{4.19}$$

into the set of equations (4.9)-(4.10) and(4.16)-(4.17) as well as the corresponding boundary conditions. Thus we get,

$$(1+Pr)\,\hat{f}''' + \frac{3}{4}\hat{f}\hat{f}'' + \frac{1}{2}\left(\hat{f}'^2 - (1+Pr)\right) + Ri(1+Pr)\hat{\theta} = 0 \tag{4.20}$$

$$\frac{1+Pr}{Pr}\hat{\theta}'' + \frac{3}{4}\hat{f}\hat{\theta}' = 0 \tag{4.21}$$

Corresponding boundary conditions are given by:

$$\begin{aligned} &\hat{f} = \hat{f}' = 0, \quad \hat{\theta} = 1 \quad \eta = 0 \\ &\hat{f}' = (1+Pr)^{1/2}, \quad \hat{\theta} = 0, \quad \eta \to \infty \end{aligned} \tag{4.22}$$

and

$$(1+Pr)\hat{F}''' + \frac{3}{4}\left(\hat{f}\hat{F}'' + \hat{f}''\hat{F}\right) - \hat{f}'\hat{F}' + i\xi\left\{(1+Pr) - \sqrt{1+Pr}\hat{F}'\right\} + Ri(1+Pr)\hat{\Theta} + (1+Pr) = \frac{1}{2}\xi\left(\hat{f}'\frac{\partial\hat{F}'}{\partial\xi} - \hat{f}''\frac{\partial\hat{F}}{\partial\xi}\right) \tag{4.23}$$

$$\frac{1+Pr}{Pr}\hat{\Theta}'' + \frac{3}{4}\left(\hat{f}\hat{\Theta}' + \hat{F}\hat{\theta}'\right) - i\xi\sqrt{1+Pr}\hat{\Theta} = \frac{1}{2}\xi\left(\hat{f}'\frac{\partial\hat{\Theta}}{\partial\xi} - \hat{\theta}'\frac{\partial\hat{F}}{\partial\xi}\right) \tag{4.24}$$

Corresponding boundary conditions are given by:

$$\begin{aligned} &\hat{F} = \hat{F}' = 0, \quad \hat{\Theta} = 1 \quad \hat{\eta} = 0 \\ &\hat{F}' = (1+Pr)^{1/2}, \quad \hat{\Theta} = 0, \quad \hat{\eta} \to \infty \end{aligned} \tag{4.25}$$

Once the solutions of the sets of equation (4.20) to equation (4.22) and (4.23) to equation (4.25) are known, the values of the physical quantities, namely, the skin friction and the rate of heat transfer at the surface of the plate, are readily obtained. These are important not only from the physical point of view but also from the experimental point of view. In this study, the results will be presented in terms of amplitudes and phases of the skin friction and the heat transfer rate having the following relations:

$$A_u = \sqrt{\tau_r^2 + \tau_i^2}, \quad A_t = \sqrt{q_r^2 + q_i^2}, \quad \phi_u = \tan^{-1}\left(\frac{\tau_i}{\tau_r}\right), \quad \phi_u = \tan^{-1}\left(\frac{q_i}{q_r}\right) \tag{4.26}$$

where $(\tau_r,\ \tau_i)$ and $q_r,\ q_i$ are the corresponding real and imaginary parts of the transverse velocity and temperature gradients at the surface.

4.3 Solution methodologies

The set of equation (4.20) to equation (4.22) represents the steady mean flow and temperature fields which are solved by employing the straightforward finite difference method for different values of the physical parameters Pr and Ri. The resulting solutions are then used in finding the solutions of equation.(4.23) to equation (4.25) that provide the oscillating

parts of the flow and the temperature fields. With a view to validating the numerical solutions equation (4.23) to equation (4.25) are also solved using the extended series expansion method for small ξ and the asymptotic method for large ξ. Details of the solutions are discussed in the following sections.

4.3.1 Extended series solution (ESS) for small ξ

The results considering finite number of terms will be valid only for very small range of frequencies. Since small values of ξ corresponds small frequencies ω also, we can predict the flow to be adjusted quasi-statically to the fluctuating rate of heat transfer in the boundary layer. For small values of ξ which corresponds to near the leading edge, we expand the functions $F,\ \Theta$ in powers of ξ as given below:

$$\hat{F}(\xi,\hat{\eta}) = \sum_{m=0}^{\infty} (2i\xi)^m\ F_m(\hat{\eta}), \quad \hat{\Theta}(\xi,\hat{\eta}) = \sum_{m=0}^{\infty} (2i\xi)^m\ \Theta_m(\hat{\eta}) \tag{4.27}$$

Implementing these into the equations (4.20)-(4.22) and collecting the terms of similar powers of ξ, the following sets of equations and their corresponding boundary conditions can be obtained:

$$(1+Pr)F_0''' + \frac{3}{4}\left[\hat{f}F_0'' + \hat{f}''F_0\right] - \hat{f}'F_0' + Ri(1+Pr)\Theta_0 + 1 + Pr = 0 \tag{4.28}$$

$$\frac{1+Pr}{Pr}\Theta_0'' + \frac{3}{4}\left[\hat{f}\Theta_0' + F_0\hat{\theta}'\right] = 0 \tag{4.29}$$

$$(1+Pr)F_1''' + \frac{3}{4}\hat{f}F_1'' + \frac{5}{4}\hat{f}''F_1 - \frac{3}{2}\hat{f}'F_1' + Ri(1+Pr)\Theta_1 + \frac{1}{2}(1+Pr) = \frac{1}{2}\sqrt{1+Pr}F_0' \tag{4.30}$$

$$\frac{1+Pr}{Pr}\Theta_1'' + \frac{3}{4}\hat{f}\Theta_1' + \frac{5}{4}\hat{\theta}'F1 - \frac{1}{2}\hat{f}'\Theta_1 = \frac{1}{2}\sqrt{1+Pr}\Theta_0 \tag{4.31}$$

for $m \geq 2$

$$(1+Pr)F_m''' + \frac{3}{4}\hat{f}F_m'' + \left(\frac{3}{4}+\frac{m}{2}\right)\hat{f}''F_m - \left(1+\frac{m}{2}\right)\hat{f}'F_m' + Ri(1+Pr)\Theta_m = \frac{1}{2}\sqrt{1+Pr}F_{m-1}' \tag{4.32}$$

$$\frac{1+Pr}{Pr}\Theta_m'' + \frac{3}{4}\hat{f}\theta_m' + \left(\frac{3}{4}+\frac{m}{2}\right)\hat{\theta}'F_m - \frac{m}{2}\hat{f}'\Theta_M = \frac{1}{2}\sqrt{1+Pr}\Theta_{m-1} \tag{4.33}$$

$$F_m(0) = F_m'(0) = \Theta_m(0) = 0, \quad \Theta_0(0) = 1$$

$$F_m'(\infty) = (1+Pr)^{1/2}, \ \Theta_m(\infty) = 0 \tag{4.34}$$

In the above equations (4.28)-(4.34), $m = 0, 1, 2, ..., n$. Here primes denote derivative with respect to $\hat{\eta}$. Evidently, equation (4.28) to equation (4.34) are linear, but coupled, and so these are solved independently pair-wise one after another. In this study, the implicit RungeKuttaButcher [92] initial value solver together with NachtsheimSwigert [91] iteration scheme is utilized to solve equation (4.28) to equation (4.34), up to $O(\xi^{10})$.

4.3.2 Asymptotic series solution (ASS) for large ξ

This section concerns the behavior of the solutions of equations (4.23) and (4.24) when ξ is large. As the frequency of surface temperature oscillation becomes very high, the boundary layer response should be confined in a very thin region adjacent to the surface. Thus, as the frequency approaches infinity, the solution becomes independent of x. Now, a series solution in the high frequency range, utilizing the limiting solution as the zero-th order approximation, is sought. Accordingly, the following transformations are introduced in equation (4.23) and (4.24).

$$F(\xi,\hat{\eta}) = \xi^{-1/2}\phi(\xi,Y), \quad \Theta(\xi,\hat{\eta}) = \Theta(\xi,Y), \quad Y = \xi^{1/2}\hat{\eta} \tag{4.35}$$

Thus we have,

$$(1+Pr)\frac{\partial^3\phi}{\partial Y^3}+\frac{3}{4}\xi^{-1/2}f\frac{\partial^2\phi}{\partial Y^2}+\xi^{-1}\left(1-f'\frac{\partial\phi}{\partial Y}\right)+\frac{1}{2}\xi^{-3/2}f''\phi$$
$$+i\left\{(1+Pr)-\sqrt{1+Pr}\frac{\partial\phi}{\partial Y}\right\}+Ri(1+Pr)\xi^{-1}\Theta$$
$$=\frac{1}{2}\left\{f'\left(\frac{\partial^2\phi}{\partial Y\partial\xi}+\frac{Y}{2\xi}\frac{\partial^2\phi}{\partial Y^2}\right)-\xi^{-1/2}f''\left(\frac{\partial\phi}{\partial\xi}+\frac{Y}{2\xi}\frac{\partial\phi}{\partial Y}\right)\right\} \quad (4.36)$$

$$\frac{(1+Pr)}{Pr}\frac{\partial^2\Theta}{\partial Y^2}+\frac{3}{4}\xi^{-1/2}f'\frac{\partial\Theta}{\partial Y}+\frac{1}{2}\xi^{-3/2}\theta'\phi+i\sqrt{1+Pr}\Theta$$
$$=\frac{1}{2}\left\{f'\left(\frac{\partial^2\phi}{\partial Y\partial\xi}+\frac{Y}{2\xi}\frac{\partial^2\phi}{\partial Y^2}\right)-\xi^{-1/2}\theta'\left(\frac{\partial\phi}{\partial\xi}+\frac{Y}{2\xi}\frac{\partial\phi}{\partial Y}\right)\right\} \quad (4.37)$$

For smaller values of $\hat{\eta}$, the solutions for the functions $f,\ \theta$ can be expanded in terms of power series of $\hat{\eta}$ as follows:

$$\hat{f}=a_2\hat{\eta}^2+a_3\hat{\eta}^3+a_4\hat{\eta}^4+a_5\hat{\eta}^5\cdots \quad (4.38)$$
$$\theta=1+b_1\eta+b_2\eta^2+b_3\eta^3+b_4\eta^4+b_5\eta^5\cdot\cdot\cdot, \quad (4.39)$$

The solutions of the above equations can be found as follows:

$$\phi(\xi,Y)=\sum_{m=0}^{\infty}\xi^{-\frac{m}{2}}E_m(Y),\quad \theta(\xi,Y)=\sum_{m=0}^{\infty}\xi^{-\frac{m}{2}}L_m(Y), \quad (4.40)$$

Surrogating the above form into the equations (4.36)-(4.37) and equating the like powers of ξ, the following sets of equations can be obtained:

$$E_0'''-\frac{i}{\sqrt{1+Pr}}E_0'=-i$$
$$E_1'''-\frac{i}{\sqrt{1+Pr}}E_1'=0$$
$$E_2'''-\frac{i}{\sqrt{1+Pr}}E_2'=-\left(1+Ri\ L_0\right)$$
$$E_3'''-\frac{i}{\sqrt{1+Pr}}E_3'=-\frac{a_2}{4(1+Pr)}\left(Y^2E_0''-6YE_0'+4E_0\right)-Ri\ L_1\cdot\cdot$$

and

$$L_0'' - \frac{i\ Pr}{\sqrt{1+Pr}} L_0 = 0$$
$$L_1'' - \frac{i\ Pr}{\sqrt{1+Pr}} L_1 = 0$$
$$L_2'' - \frac{i\ Pr}{\sqrt{1+Pr}} i L_2 = 0$$
$$L_3'' - \frac{i\ Pr}{\sqrt{1+Pr}} i L_3 = -\frac{Pr}{4(1+Pr)} \left(a_2 Y^2 L_0' + b_1 \left(Y E_0' + 2E_0\right)\right) \cdots$$

The associated boundary conditions are:

$$E_m(0) = E_m'(0) = 0,\ E_0'(\infty) = (1+Pr)^{1/2}$$
$$E_m'(\infty) = 0,\ \text{for } m = 1, 2, \cdots$$
$$L_0(0) = 1,\ L_m(0) = L_m(\infty) = 0 \text{ for } m = 1, 2, \cdots$$

Solving the above set of equations, it can be obtained the values of $F''(\xi, 0),\ \Theta'(\xi, 0)$ as:

$$(1+Pr)^{1/4} \xi^{-\frac{1}{2}} F\prime\prime(\xi, 0) = \sum_{m=0}^{\infty} \xi^{-\frac{m}{2}} E_m''(0) \tag{4.41}$$
$$(1+Pr)^{-1/4} \xi^{-\frac{1}{2}} \Theta'(\xi, 0) = \sum_{m=0}^{\infty} \xi^{-\frac{m}{2}} L_m'(0) \tag{4.42}$$

where,

$$E_0''(0) = \sqrt{i}(1+Pr)^{1/4},\ E_1''(0) = 0$$
$$E_2''(0) = \frac{(1+Pr)^{1/4}\left(G_0 - G_1\right)}{(1-Pr)i}$$
$$E_3''(0) = \frac{-9\ a_2}{16i}$$
$$L_0'(0) = -\frac{\sqrt{iPr}}{(1+Pr)^{1/4}},\ L_1'(0) = 0,\ L_2'(0) = 0$$
$$L_3'(0) = \frac{G_2 + G_3}{8i(1+\sqrt{Pr})^2\sqrt{1+Pr}}$$

where,

$$G_0 = \sqrt{i}\left\{(1-Pr)+Ri\right\}, \quad G_1 = \sqrt{i}\ Ri\ \sqrt{Pr}$$
$$G_2 = -\frac{1}{2}\left(1+\sqrt{Pr}\right)^2 a_2, \quad G_3 = 2b_1\sqrt{1+Pr}\left(4\sqrt{Pr}-1\right)$$

4.4 Results and discussion

The governing equations of the unsteady laminar mixed convection boundary layer flow past a vertical wedge have been solved by two distinct methods, namely, the straightforward finite difference method for the entire frequency range, and the extended series solution for low frequency range and the asymptotic series expansion method for high frequency range. It is worthwhile to note that the effect of the constant coefficients $(1+Pr)^{1/4}$ and $(1+Pr)^{-1/4}$ within the definitions of the skin friction and heat transfer (equations (4.41) and (4.42)), respectively, have not been included during the presentation of the results.

With a view to validating the numerical solution, a comparison of the amplitudes and phase angles of skin friction obtained by the SFF (stream function formulation) and the series solutions for small and large ξ is shown in Figure 4.2. It is evident from the figures that the solutions are in excellent agreement. In addition, Figure 4.2 exhibits the effects of varying the Prandtl number, Pr, on amplitudes and phase angles of the skin friction. When the Prandtl number is increased, the amplitudes and phase angles of skin friction increase. This is because the Prandtl number becomes high due to either an increase of the kinematic viscosity or a decrease of the thermal diffusivity of the fluid, and the increase of the skin friction is the result of this change of the fluid property.

Figure 4.3 presents a comparison between the SFF and the series solutions for small and large ξ in terms of the amplitudes and phase angles of heat transfer. Evidently, the solutions obtained by the SFF provide a good agreement with the series solutions. Also, the effects of the Prandtl number on the heat transfer are comprehensible from Figure 4.3. It is seen that the increment of the Prandtl number causes an increase of the amplitudes and phase angles of heat transfer near the leading edge. Since the Prandtl number increases owing to either an increase of the kinematic viscosity or a decrease of the thermal diffusivity of the

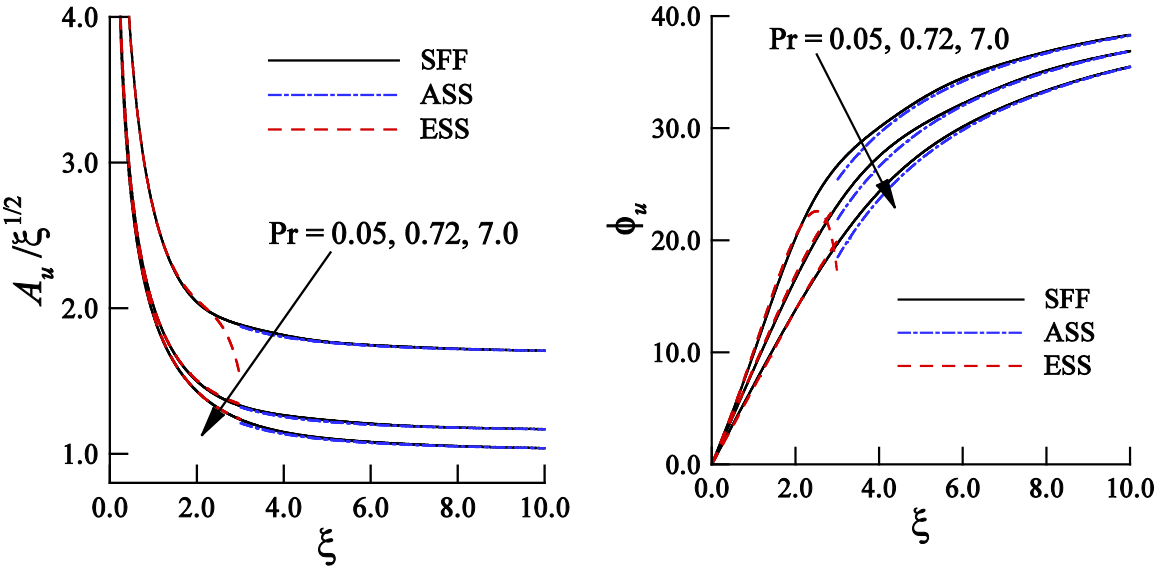

Figure 4.2: Amplitude and phase angle of skin friction for different values of Pr, while, Ri = 1.0. The solid (black) lines are for SFF, the dashed (red) lines are for extended series solution (ESS) for small ξ, and the dashed-dot (blue) lines are for asymptotic solution (ASS) for large ξ.

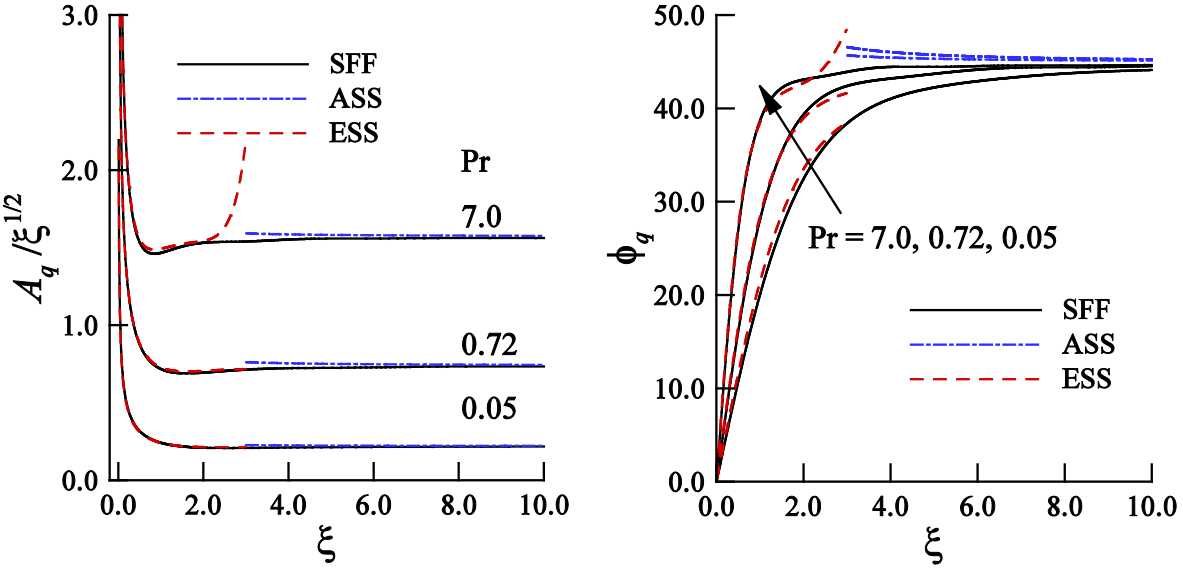

Figure 4.3: Amplitude and phase angle of heat transfer for different values of Pr, while, Ri = 1.0. The solid (black) lines are for SFF, the dashed (red) lines are for extended series solution (ESS) for small ξ, and the dashed-dot (blue) lines are for asymptotic solution (ASS) for large ξ.

Table 4.1: Amplitude and phase angle of skin friction for different Ri, while, Pr=0.7

ξ	A_U		ϕ_U	
—-	FDF	Series and asymp.	FDF	Series and asymp.
		Ri=0.0		
0.01	15.44288	15.45543[1]	0.12	0.16[1]
0.10	4.88661	4.89135[1]	1.51	1.61[1]
0.50	2.22211	2.22875[1]	7.64	7.87[1]
1.00	1.64739	1.65818[1]	14.45	14.66[1]
2.00	1.33356	1.34454[1]	24.02	23.96[1]
3.00	1.24320	1.30423[1]	29.41	30.41[1]
4.00	1.20444	1.19947[2]	32.69	32.45[2]
6.00	1.17383	1.17256[2]	36.40	36.32[2]
8.00	1.16167	1.16202[2]	38.36	38.37[2]
10.00	1.15546	1.15673[2]	39.58	39.64[2]
		Ri=2.0		
0.01	24.1966	24.23397[1]	0.04	0.05[1]
0.10	7.65152	7.66298[1]	0.46	0.46[1]
0.50	3.41938	3.42219[1]	2.34	2.31[1]
1.00	2.41382	2.41203[1]	4.824	4.81[1]
2.00	1.71211	1.70855[1]	10.49	10.78[1]
3.00	1.43917	1.44512[1]	16.71	17.28[2]
4.00	1.32304	1.31958[2]	22.17	21.08[2]
6.00	1.24484	1.23342[2]	28.42	27.83[2]
8.00	1.20174	1.19909[2]	31.77	31.67[2]
10.00	1.18296	1.18188[2]	34.43	34.8022[2]
		Ri=4.0		
0.01	32.33106	32.39354[1]	0.01	0.01[1]
0.10	10.22308	10.24231[1]	0.11	0.08[1]
0.50	4.55937	4.56520 [1]	0.52	0.44[1]
1.00	3.19704	3.19606[1]	1.17	1.05[1]
2.00	2.19798	2.18744[1]	3.31	3.32[1]
3.00	1.74511	1.73463[1]	7.01	7.44[1]
4.00	1.50073	1.48039[2]	11.97	11.57[2]
6.00	1.31603	1.31690[2]	21.16	20.09[2]
8.00	1.26245	1.25015[2]	25.88	25.32[2]
10.00	1.21931	1.21638[2]	28.83	28.79[2]

Here and hereafter [1] for series solution and [2] stands for asymptotic solution

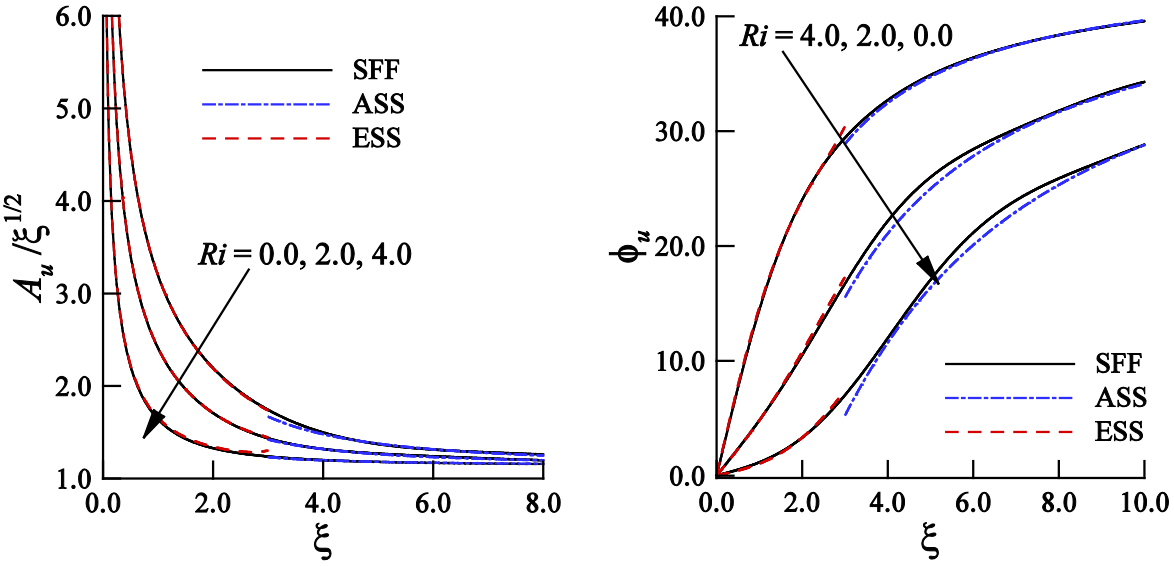

Figure 4.4: Amplitude and phase angle of skin friction for different values of Ri, while, Pr = .70. The solid (black) lines are for SFF, the dashed (red) lines are for extended series solution (ESS) for small ξ, and the dashed-dot (blue) lines are for asymptotic solution (ASS) for large ξ.

fluid, hence heat is accumulated near the leading edge that results in the increase of the amplitudes and phase angles of heat transfer. The effects of Richardsons number, Ri, on the amplitudes and phase angles of the skin friction are shown in Figure 4.4. From the figure and Table 4.1, it is observed that for higher Richardsons number, Ri, the amplitudes of skin friction are higher while the phase angles are lower. As Richardsons number, Ri, increases, mixed convection of flow and heat transfer increases. Accordingly, the amplitudes of skin friction are higher for higher Ri. But the rate of change of skin friction from the leading edge to the downstream region is higher for lower Ri so that the phase angles of skin friction are higher for lower Ri.

Figure 4.5 exhibits the change of amplitudes and phase angles of heat transfer against Richardsons number, Ri. With an increase of Ri, the amplitudes of heat transfer are higher near the leading edge while the reverse case is observed in the downstream region. On the other hand, for smaller Ri the phase angles are higher near the leading edge and then they become lower in the downstream region. Finally, the amplitudes and phase angles tend to an asymptotic value for all Ri.

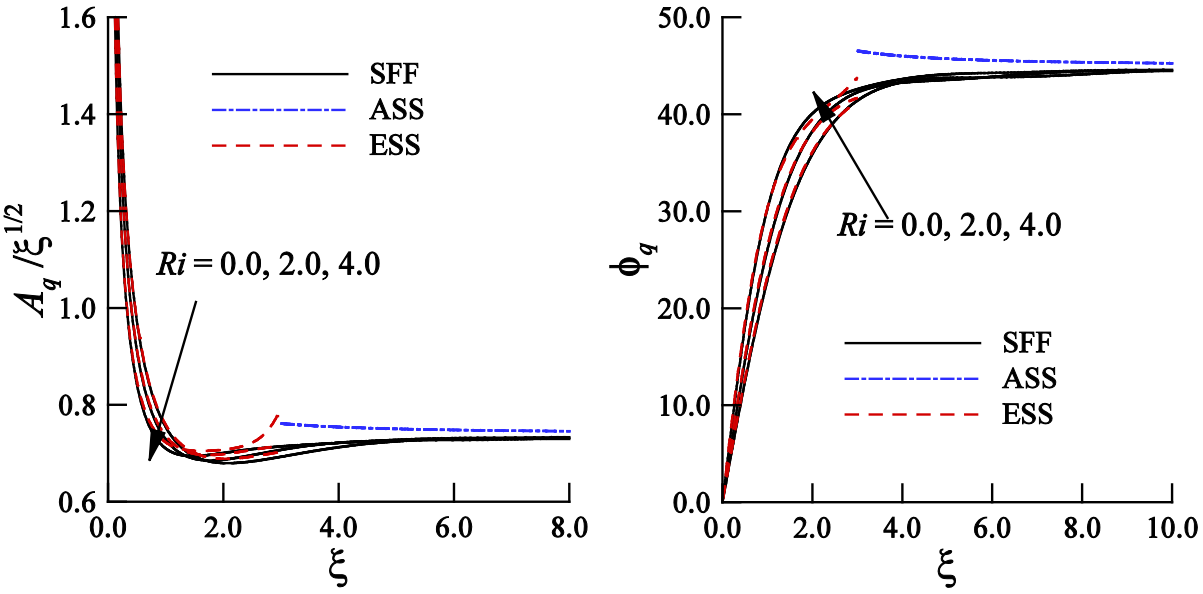

Figure 4.5: Amplitude and phase angle of skin friction for different values of Ri, while, Pr = .70. The solid (black) lines are for SFF, the dashed (red) lines are for extended series solution (ESS) for small ξ, and the dashed-dot (blue) lines are for asymptotic solution (ASS) for large ξ.

4.4.1 Effects of different physical parameters on transient skin friction and heat transfer

From a practical point of view, transient skin friction and heat transfer are important. The reason is that the unsteady behavior of these two properties over a wide region from the leading edge might damage a system. However, the transient skin friction and heat transfer are evaluated here by the following relations:

$$\tau = \tau_s + \varepsilon A_u cos(\omega t + \phi_u)$$

$$\theta_w = \theta_s + \varepsilon A_t cos(\omega t + \phi_t)$$

where τ_s and q_s are, respectively, the steady-state skin friction and heat transfer.

Numerical values of transient skin friction and heat transfer against ωt have been presented in Figures 4.6 and 4.7, respectively, for $Ri = 0.0$ and 2.0 taking $Pr = 0.72$. It is clear from the figures that the amplitudes of oscillation of transient skin friction, τ, and heat

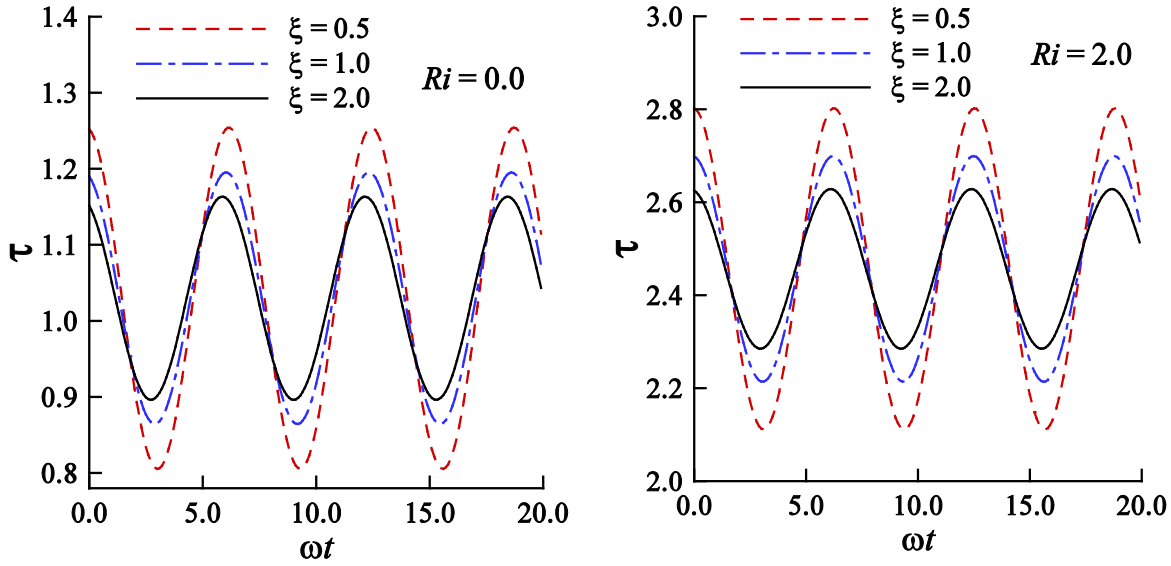

Figure 4.6: Numerical values of transient skin friction for different values of ξ, while, Pr=0.72, Ri=0.0 and 2.0.

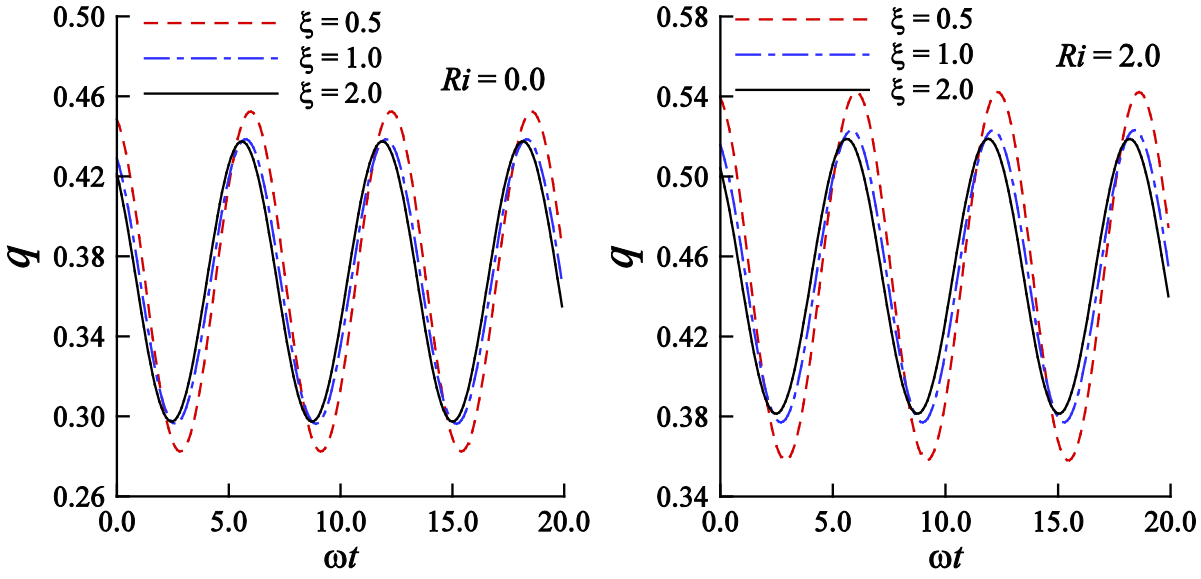

Figure 4.7: Numerical values of transient heat transfer for different values of ξ, while, Pr=0.72, Ri=0.0 and 2.0.

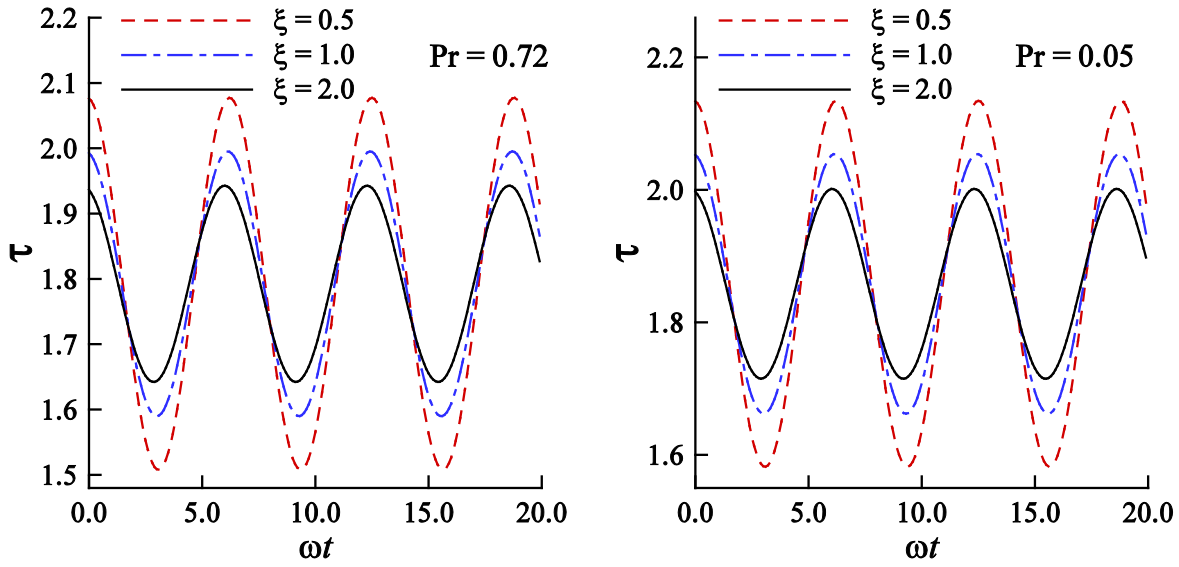

Figure 4.8: Numerical values of transient skin friction for different values of ξ, while, Pr=0.72, Ri=0.0 and 2.0.

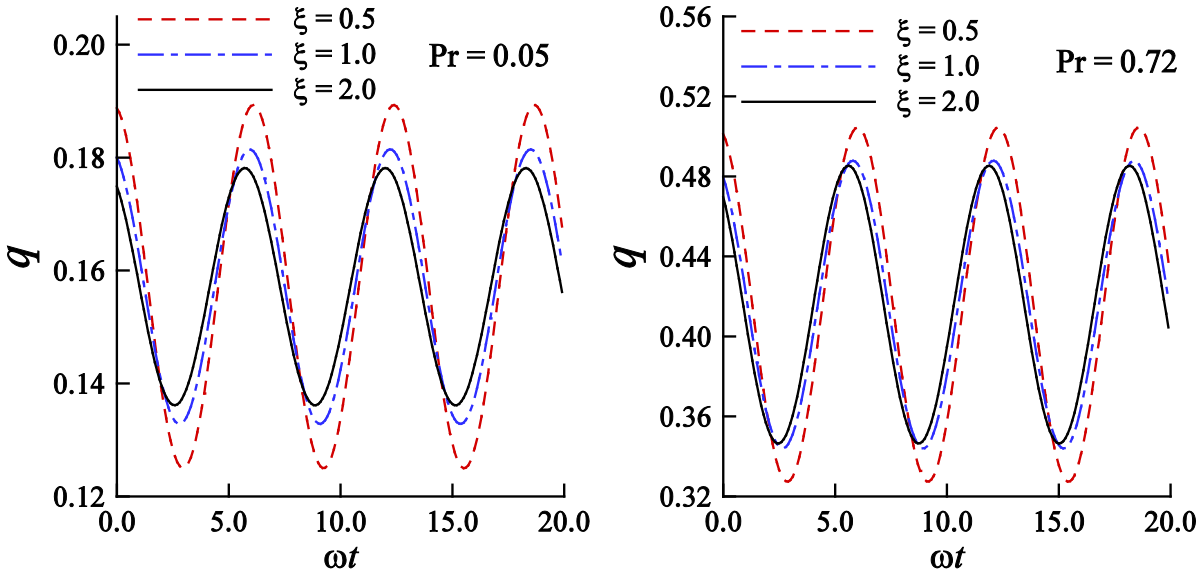

Figure 4.9: Numerical values of transient heat transfer for different values of ξ, while, Pr=0.72, Ri=0.0 and 2.0.

transfer, q, increase owing to the increase of Richardsons number, Ri. Also the intensity of oscillation of both transient skin friction and heat transfer subsides quickly away from the leading edge for a small value of Ri compared to a higher value of Ri. The reason is that the impact of mixed convection of flow and heat transfer is strong near the leading edge.

The effects of varying the Prandtl number, Pr, on the transient skin friction and heat transfer are shown in Figures 4.8 and 4.9, respectively. The figures suggest that the amplitudes of oscillation of transient skin friction,τ, and heat transfer, q, increase with an increase of the Prandtl number, Pr. The amplitudes of oscillation die down slowly from the leading edge to the downstream region but it happens swiftly for higher Pr.

4.5 Summary

The periodic laminar boundary layer mixed convection flow past a vertical wedge with the effect of the fluctuations in the free-stream produced by fluctuations of the oncoming stream has been investigated numerically. The governing equations have been solved by the straightforward finite difference method for the entire frequency range, the extended series solution for low frequency range and the asymptotic series expansion method for high frequency range. The solutions obtained by the straightforward finite difference method provide good agreement with the series solutions. The effects of varying Richardsons number, Ri, introduced to quantify the influence of mixed convection and the Prandtl number, Pr, on the amplitudes and phase angles of the skin friction and heat transfer as well as on the transient skin friction and heat transfer are examined. Based on the results, the following conclusions can be drawn.

- The amplitudes and phase angles of skin friction and heat transfer increase with an increase of the Prandtl number, Pr
- When Richardsons number, Ri, is increased, the amplitudes of skin friction become large but the phase angles are small. On the other hand, for higher values of Ri, the amplitudes of heat transfer are higher near the leading edge while the reverse circumstance is observed in the downstream region. Moreover, the phase angles are

higher near the leading edge for smaller Ri and then they are lower in the downstream region. Finally, both the amplitudes and phase angles of skin friction and heat transfer reach the corresponding asymptotic values.

- The amplitudes of oscillation of transient skin friction, τ, and heat transfer, q, are found to increase owing to the increase of Richardsons number,Ri, and Prandtl number, Pr. Moreover, the amplitudes of oscillation of both transient skin friction and heat transfer subside quickly away from the leading edge for a small value of Ri compared to a higher value of Ri while the reverse situation is seen for the Prandtl number, Pr.

Chapter 5

Velocity, heat transfer and mass transfer response in periodic boundary layer along a vertical wedge for mixed convection flow

5.1 Introduction

Both in natural and artificial flow situation, there is almost always unsteadiness occurs and examples of unsteady free and mixed convection flows are in abundant. One of the general case of convection is mixed convection in which flow is driven concurrently by both an applied forcing system externally (i.e., outer energy supply to the fluid-streamlined body system) and inner volumetric (mass) forces, viz., by the non homogeneous density distribution of a fluid medium in a gravity field. In micro meteorological and industrial applications, fluid flow along both horizontal and vertical surface bounded by an extensive body of fluid due to free or mixed convection are of significant importance and interest. It has already been mentioned in Chapter 1 that mixed convection flow is characterized by the parameter $\lambda = \frac{Gr}{Re^n}$. This characteristic parameter λ provides a measure of the influence of the free convection compare to forced convection on the fluid flow. The mixed

convection regime of the flow field is generally divided into the region based on the range of $\lambda_{min} \leq \lambda \leq \lambda_{max}$. The upper bound and lower bound of this type of region is described by the value of λ_{max} and λ_{min} respectively. In order to analyze the flow field along with temperature and concentration transfer outside the mixed convection region, either the pure forced convection or the pure free convection can be taken into account. When the value of $\lambda \to 0$, represents the dominance of forced convection for heat and mass transfer, where as the value of $\lambda \to \infty$ indicates the natural convection as dominant mode. From this point of view, it can be inferred that buoyancy forces can enhance the surface heat and mass transfer rate when they assist the forced flow, and vice versa. The parameter λ, which is the ratio of buoyancy forces to the inertial forces inside the boundary layer, provides a measure of the influence of the free convection in comparison with that of forced convection on the fluid flow.

This present study is devoted to investigate mixed convective flow along vertical wedge with small amplitude oscillations of velocity, surface temperature and surface concentration. Two different important diffusive parameters, Pr and Sc, which are appearing in the governing equations have been considered broadly during the simulation. Another two important parameters, w and the Richardson number, Ri have also been taken into account extensively. To derive the governing equations, the boussinesq approximations are made, that is, it is assumed that the fluid property variations are limited to firstly the density which is taken into account only in so far as its effects the buoyancy term and secondly the viscosity.

5.2 Formulation of the problem

In this work, consideration has been given to unsteady two dimensional mixed convection flow of a viscous incompressible fluid over a semi infinite vertical wedge. It is assumed that both the surface temperature, concentration as well as the free stream velocity have small amplitude oscillations about a mean value. The ambient fluid is maintained at uniform temperature, T_∞, and concentration, C_∞ and the free stream velocity is taken as $U(x,t)$. However, all the thermo-physical fluid properties are considered to be constant and viscous

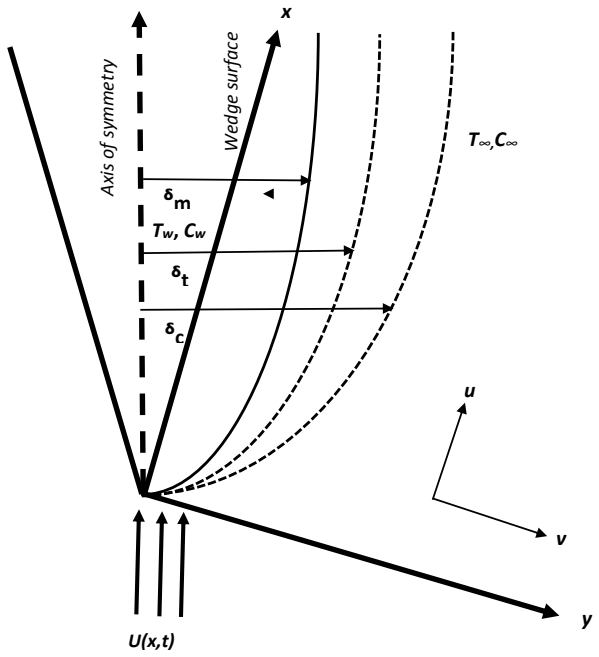

Figure 5.1: Physical configuration and coordinate system

dissipation effect is neglected. The coordinate system and flow configuration of the problem are kept exactly similar to the problem described in chapter 4.

Under the usual Boussinesq approximation along with the above assumptions the boundary layer equations for mass, momentum and energy can be written as:

$$\frac{\partial u}{\partial x} + \frac{\partial v}{\partial y} = 0 \tag{5.1}$$

$$\frac{\partial u}{\partial t} + u\frac{\partial u}{\partial x} + v\frac{\partial u}{\partial y} = \nu\frac{\partial^2 u}{\partial y^2} + \frac{\partial U}{\partial t} + U\frac{\partial U}{\partial x} + \left(g\beta_T\bar{T} + g\beta_C\bar{C}\right)\cos(\pi/4) \tag{5.2}$$

$$\frac{\partial \bar{T}}{\partial t} + u\frac{\partial \bar{T}}{\partial x} + v\frac{\partial \bar{T}}{\partial y} = \kappa\frac{\partial^2 \bar{T}}{\partial y^2} \tag{5.3}$$

$$\frac{\partial \bar{C}}{\partial t} + u\frac{\partial \bar{C}}{\partial x} + v\frac{\partial \bar{C}}{\partial y} = D\frac{\partial^2 \bar{C}}{\partial y^2} \tag{5.4}$$

where, u and v are the x and y components of velocity field, respectively, in the momentum boundary layer; $\bar{T} = T - T_\infty$, $\bar{C} = C - C_\infty$, T, C and T_∞, C_∞ being the temperature, concentration in the thermal boundary layer and ambient fluid respectively, ν is the kinematic

viscosity of the fluid, g is the acceleration due to gravity, κ the thermal diffusivity, β_T, β_C are the coefficient of volume expansion due to temperature and species concentration. The associated boundary conditions are:

$$\begin{aligned} &y = 0 : u = v = 0,\ \bar{T} = T_w(t),\ \bar{C} = C_w(t) \\ &y = \infty : \quad u = U(x,t),\ \bar{T} = 0, \quad \bar{C} = 0 \end{aligned} \tag{5.5}$$

where,

$$\begin{aligned} U = U_0\ x^{1/2}[1 + \varepsilon\,(\exp i\omega t + c.c)],\ \ T_w = T_0[1 + \varepsilon\,(\exp i\omega t + c.c)] \\ C_w = C_0[1 + \varepsilon\,(\exp i\omega t + c.c)] \end{aligned} \tag{5.6}$$

Above, T_0, U_0 , and C_0 are, respectively the mean temperature, mean velocity and mean surface concentration ; $\varepsilon(<< 1)$ is the amplitude and ω is the frequency of oscillations in the surface temperature, species concentration and free stream velocity. Equation (5.5) suggests the solutions of the governing equations to be of the form:

$$\begin{aligned} u(x,y,t) &= u_0(x,y) + \varepsilon\,(\exp i\omega t + c.c)\,u_1(x,y) \\ v(x,y,t) &= v_0(x,y) + \varepsilon\,(\exp i\omega t + c.c)\,v_1(x,y) \\ \bar{T}(x,y,t) &= \theta_0(x,y) + \varepsilon\,(\exp i\omega t + c.c)\,\theta_1(x,y) \\ \bar{C}(x,y,t) &= \phi_0(x,y) + \varepsilon\,(\exp i\omega t + c.c)\,\phi_1(x,y) \end{aligned} \tag{5.7}$$

where, u_0, v_0, θ_0 and ϕ_0 represent the steady mean flow and only real parts are to be considered since these parts have significant physical meanings. Considering these form of

solutions, the steady mean flow is governed by the following set of equations:

$$\frac{\partial u_0}{\partial x} + \frac{\partial v_0}{\partial y} = 0 \tag{5.8}$$

$$u_0\frac{\partial u_0}{\partial x} + v_0\frac{\partial u_0}{\partial y} = \nu\frac{\partial^2 u_0}{\partial y^2} + (g\beta_T\theta_0 + g\beta_C\phi_0)\cos(\pi/4) + \frac{1}{2}U_0^2 \tag{5.9}$$

$$u_0\frac{\partial \theta_0}{\partial x} + v_0\frac{\partial \theta_0}{\partial y} = \alpha\frac{\partial^2 \theta_0}{\partial y^2} \tag{5.10}$$

$$u_0\frac{\partial \phi_0}{\partial x} + v_0\frac{\partial \phi_0}{\partial y} = D\frac{\partial^2 \phi_0}{\partial y^2} \tag{5.11}$$

Corresponding boundary conditions are:

$$\begin{aligned} &y = 0 : u_0 = v_0 = 0, \quad \theta_0 = T_0 \\ &y \to \infty : u_0 = U_0\, x^{\frac{1}{2}}, \quad \theta_0 = 0, \quad \phi_0 = 0 \end{aligned} \tag{5.12}$$

The set of differential equations and corresponding boundary conditions, which govern the unsteady flow field are in the form of equations (5.13)-(5.17):

$$\frac{\partial u_1}{\partial x} + \frac{\partial v_1}{\partial y} = 0 \tag{5.13}$$

$$\begin{aligned} &u_0\frac{\partial u_1}{\partial x} + u_1\frac{\partial u_0}{\partial x} + v_0\frac{\partial u_1}{\partial y} + v_1\frac{\partial u_0}{\partial y} + i\omega u_1 \\ &+ \nu\frac{\partial^2 u_1}{\partial y^2} + i\omega x^{\frac{1}{2}}U_0 + U_0^2 + g\beta_T\theta_1 + g\beta_C\phi_1 \end{aligned}$$

$$u_0\frac{\partial \theta_1}{\partial x} + u_1\frac{\partial \theta_0}{\partial x} + v_0\frac{\partial \theta_1}{\partial y} + v_1\frac{\partial \theta_0}{\partial y} + i\omega\theta_1 = \alpha\frac{\partial^2 \theta_1}{\partial y^2} \tag{5.14}$$

$$u_0\frac{\partial \phi_1}{\partial x} + u_1\frac{\partial \phi_0}{\partial x} + v_0\frac{\partial \phi_1}{\partial y} + v_1\frac{\partial \phi_0}{\partial y} + i\omega\phi_1 = D\frac{\partial^2 \phi_1}{\partial y^2} \tag{5.15}$$

$$\begin{aligned} &y = 0 : u_1 = v_1 = 0, \quad \theta_1 = T_0, \quad \phi_1 = C_0 \\ &y \to \infty : u_1 = U_0\, x^{\frac{1}{2}}, \quad \theta_1 = 0, \quad \phi_1 = 0 \end{aligned} \tag{5.16}$$

The following transformations are commenced in order to get the solutions of the equations (5.8)-(5.11) along with the boundary condition given in equation(5.12):

$$\psi_0(x,y) = \sqrt{\nu x^{3/2} U_0} F(\xi,\eta), \quad \theta_0(x,y) = T_0\Theta(\xi,\eta)$$
$$\phi_0(x,y) = C_0\Phi(\xi,\eta), \quad \eta = y\sqrt{\frac{U_0 x^{1/2}}{\nu}}, \quad Ri = \frac{Gr_L}{Re_L^2}, \quad X = x/L \tag{5.17}$$

where, $Gr_T(= g\beta_T T_0 L^3/\nu^2)$, $Gr_C(= g\beta_C C_0 L^3/\nu^2)$ and $Re_L = (U_0 L^{\frac{3}{2}}/\nu)$ are, respectively, the Grashof numbers for thermal and concentration diffusion and Reynolds number. ψ_0 is the stream function which satisfies the continuity equation (5.8). $\xi = \frac{\omega\ x^{1/2}}{U_0}$, where x is the distance measured from the leading edge. By commencing the above mentioned set of transformations in the equations (5.8)-(5.11), the following sets of equations can be found which govern the steady flow field:

$$F''' + \frac{3}{4}FF'' + \frac{1}{2}(1 - F'^2) + Ri\left[(1-N)\Theta + N\Phi\right] = 0 \tag{5.18}$$
$$\frac{1}{Pr}\Theta'' + \frac{3}{4}F\Theta' = 0 \tag{5.19}$$
$$\frac{1}{Sc}\Phi'' + \frac{3}{4}F\Phi' = 0 \tag{5.20}$$

Corresponding boundary conditions are given by:

$$F = F' = 0, \quad \Theta = 1 \quad \eta = 0$$
$$F' = 1, \quad \Theta = 0, \quad \Phi = 0 \quad \eta \to \infty \tag{5.21}$$

For the unsteady flow field, the following transformations are introduced to attain the non similarity set of equations:

$$\psi_1(x,y) = \sqrt{\nu x^{\frac{3}{2}} U_0} G(\xi,\eta), \quad \theta_1(x,y) = T_0, \quad H(\xi,\eta) = C_0$$
$$\phi_1(x,y) = C_0 M(\xi,\eta), \quad \eta = y\sqrt{\frac{U_0}{\nu}} x^{-\frac{1}{4}} \tag{5.22}$$

where ψ_1 satisfies the equation (5.13)

Introducing these transformations, the following set of equations can be obtained which govern the unsteady flow:

$$G''' + \frac{3}{4}(FG'' + F''G) - F'G' + i\xi(1 - G') + 1 + Ri\,[(1 - N)H + NM] = \frac{1}{2}\xi\left(F'\frac{\partial G'}{\partial \xi} - F''\frac{\partial G}{\partial \xi}\right) \tag{5.23}$$

$$\frac{1}{Pr}H'' + \frac{3}{4}(FH' + G\Theta') - i\xi\ H = \frac{1}{2}\xi\left(F'\frac{\partial H}{\partial \xi} - \Theta'\frac{\partial G}{\partial \xi}\right) \tag{5.24}$$

$$\frac{1}{Sc}H'' + \frac{3}{4}(FM' + G\Theta') - i\xi\ M = \frac{1}{2}\xi\left(F'\frac{\partial M}{\partial \xi} - \Phi'\frac{\partial G}{\partial \xi}\right) \tag{5.25}$$

Boundary conditions to be satisfied:

$$G(\xi, 0) = G'(\xi, 0) = 0, \quad H(\xi, 0) = 1, \quad M(\xi, 0) = 1$$
$$G'(\xi, \infty) = 1, \quad H(\xi, \infty) = 0, \quad M(\xi, \infty) = 0 \tag{5.26}$$

5.3 Solution methodologies

Three different techniques have been brought into action to solve the governing equations. Implicit finite difference method is used to simulate both the steady and unsteady entire flow regime. Regular perturbation technique is applied to find the solutions near the leading edge and far from the leading edge, the solutions are obtained by applying asymptotic series solution method. The solution procedures are discussed in details in the following sections.

5.3.1 Extended Series solution (ESS) for small ξ

For small values of ξ, which corresponds to near the leading edge, we expand the functions G, H and M in powers of ξ as given below:

$$G(\xi,\eta)=\sum_{m=0}^{\infty}(2i\xi)^m\ G_m(\eta),\ \ H(\xi,\eta)=\sum_{m=0}^{\infty}(2i\xi)^m\ H_m(\eta),$$
$$M(\xi,\eta)=\sum_{m=0}^{\infty}(2i\xi)^m\ M_m(\eta) \tag{5.27}$$

Implementing these into the equations (5.24)-(5.26) and collecting the terms of similar powers of ξ, the following sets of equations and their corresponding boundary conditions can be obtained:

$$G_0'''+\frac{3}{4}\left[FG_0''+F''G_0\right]-F'G_0'+Ri\left[(1-N)\ H_0+N\ M_0\right]+1=0 \tag{5.28}$$
$$\frac{1}{Pr}H_0''+\frac{3}{4}\left[F\ H_0'+G_0\Theta'\right]=0 \tag{5.29}$$
$$\frac{1}{Sc}M_0''+\frac{3}{4}\left[F\ M_0'+G_0\Phi'\right]=0 \tag{5.30}$$

$$G_1'''+\frac{3}{4}F\ G_1''+\frac{5}{4}F''G_1-F'G_1'-\frac{1}{2}F'G_1'$$
$$+Ri\left[(1-N)H_1+NM_1\right]+\frac{1}{2}=\frac{1}{2}G_0' \tag{5.31}$$
$$\frac{1}{Pr}H_1''+\frac{3}{4}F\ H_1'+\frac{5}{4}\Theta'G_1-\frac{1}{2}F'H_1=0 \tag{5.32}$$
$$\frac{1}{Sc}M_1''+\frac{3}{4}F\ M_1'+\frac{5}{4}\Phi'G_1-\frac{1}{2}F'M_1=0 \tag{5.33}$$

$$G_m''' + \frac{3}{4}F\ G_m'' + \left(\frac{3}{4}+\frac{m}{2}\right)F''G_m - \left(1+\frac{m}{2}\right)F'G_m' + Ri\left[(1-N)H_m + N\ M_m\right] = \frac{1}{2}G_{m-1}' \tag{5.34}$$

$$\frac{1}{Pr}H_m'' + \frac{3}{4}F\ H_m' + \left(\frac{3}{4}+\frac{m}{2}\right)\Theta'G_m - \frac{m}{2}F'H_m = \frac{1}{2}H_{m-1} \tag{5.35}$$

$$\frac{1}{Sc}M_m'' + \frac{3}{4}F\ M_m' + \left(\frac{3}{4}+\frac{m}{2}\right)\Phi'G_m - \frac{m}{2}F'M_m = \frac{1}{2}M_{m-1} \tag{5.36}$$

$$G_m(0) = G_m'(0) = H_m(0) = M_m(0) = 0, \quad H_0(0) = 1, M_0(0) = 1$$

$$G_m'(\infty) = 1, \quad H_m(\infty) = 0, \quad M_m(\infty) = 0 \tag{5.37}$$

In the above equations (5.35)-(5.37), $m = 0, 1, 2, ...$ Evidently, equation (5.29) to equation.(5.37) are linear, but coupled, so these are solved independently pair-wise one after another. In this study, the implicit RungeKuttaButcher [92] initial value solver together with NachtsheimSwigert [91] iteration scheme is utilized to solve equation (5.29) to equation(5.37), up to $O(\xi^8)$.

5.3.2 Asymptotic series solutions (ASS) for large ξ

In the problems related to boundary-layer separation, the existence of the double layer owing to the coordinate expansion $\xi \to \infty$ is a common feature. In order to handle this situation in the framework of matched asymptotic expansion with a small parameter, an artificial parameter can be introduced or the co-ordinate undergoing the limit process may be considered a small or large parameter. This double layered boundary layer is observed in the far downstream of the flow region. The inside layer is a Stokes shear-wave motion, which oscillates with zero mean flow. The outer layer is a modified Blasius motion, which convects the mean flow to downstream.

Inner layer region

The region where the viscous force plays the significant role as the driving force is termed as the inner layer region. This region is concentrated near the surface of the vertical plate so that no slip boundary condition is assured to be satisfied. Riley [62] was the

first who revealed the inner boundary layer region where no slip boundary conditions were well preserved. In this region, as it is mentioned earlier, viscous forces are significantly dominant and have the same order of magnitude as that of boundary forces. In order to get the equations which are comparable with that of (5.24)-(5.26), the following scaled variables are introduced and the governing transformed equations are as follows:

$$\begin{aligned} &G(\xi,\eta) = \xi^{-\frac{1}{2}}\varphi(\xi,Y), \quad H(\xi,\eta) = H(\xi,Y) \\ &M(\xi,\eta) = M(\xi,Y), \quad Y = \xi^{\frac{-1}{2}}\eta \end{aligned} \tag{5.38}$$

$$\begin{aligned} &\frac{\partial^3\varphi}{\partial Y^3} + \frac{3}{4}\xi^{-\frac{1}{2}}F\frac{\partial^2\varphi}{\partial Y^2} + \xi^{-1}\left(1 - F'\frac{\partial\varphi}{\partial Y}\right) + \frac{1}{2}\xi^{-\frac{3}{2}}F''\varphi \\ &\quad + i\left(1 - \frac{\partial\varphi}{\partial Y}\right) + \ Ri\xi^{-1}\left[(1-N)H + NM\right] \\ &\quad = \frac{1}{2}\left[F'\left(\frac{\partial^2\varphi}{\partial Y\partial\xi} + \frac{Y}{2\xi}\frac{\partial^2\varphi}{\partial Y^2}\right) - \xi^{-\frac{1}{2}}F''\left(\frac{\partial\varphi}{\partial\xi} + \frac{Y}{2\xi}\frac{\partial\varphi}{\partial Y}\right)\right] \end{aligned} \tag{5.39}$$

$$\begin{aligned} &\frac{1}{Pr}\frac{\partial^2 H}{\partial Y^2} + \frac{3}{4}\xi^{-\frac{1}{2}}F'\frac{\partial H}{\partial Y} + \frac{1}{2}\xi^{-\frac{3}{2}}\theta'\varphi - iH \\ &\quad = \frac{1}{2}\left[F'\left(\frac{\partial^2\varphi}{\partial Y\partial\xi} + \frac{Y}{2\xi}\frac{\partial^2\varphi}{\partial Y^2}\right) - \xi^{-\frac{1}{2}}\theta'\left(\frac{\partial\varphi}{\partial\xi} + \frac{Y}{2\xi}\frac{\partial\varphi}{\partial Y}\right)\right] \end{aligned} \tag{5.40}$$

$$\begin{aligned} &\frac{1}{Sc}\frac{\partial^2 M}{\partial Y^2} + \frac{3}{4}\xi^{-\frac{1}{2}}F'\frac{\partial H}{\partial Y} + \frac{1}{2}\xi^{-\frac{3}{2}}\phi'\varphi - iM \\ &\quad = \frac{1}{2}\left[F'\left(\frac{\partial^2\varphi}{\partial Y\partial\xi} + \frac{Y}{2\xi}\frac{\partial^2\varphi}{\partial Y^2}\right) - \xi^{-\frac{1}{2}}\phi'\left(\frac{\partial\varphi}{\partial\xi} + \frac{Y}{2\xi}\frac{\partial\varphi}{\partial Y}\right)\right] \end{aligned} \tag{5.41}$$

For smaller values of η, the solutions for the functions F, Θ, Φ can be expanded in terms of power series of η as follows:

$$F = a_2\eta^2 + a_3\eta^3 + a_4\eta^4 + a_5\eta^5 \cdots, \tag{5.42}$$

$$\theta = 1 + b_1\eta + b_2\eta^2 + b_3\eta^3 + b_4\eta^4 + b_5\eta^5 \cdots, \tag{5.43}$$

$$\phi = 1 + c_1\eta + c_2\eta^2 + c_3\eta^3 + c_4\eta^4 + c_5\eta^5 \cdots \tag{5.44}$$

The solutions of the above equations (5.40)-(5.42) can be found as follows:

$$\varphi(\xi,Y)=\sum_{m=0}^{\infty}\xi^{-\frac{m}{2}}E_m(Y),\quad H(\xi,Y)=\sum_{m=0}^{\infty}\xi^{-\frac{m}{2}}L_m(Y)$$
$$M(\xi,Y)=\sum_{m=0}^{\infty}\xi^{-\frac{m}{2}}P_m(Y) \tag{5.45}$$

Replacing the above form into the equations (5.40)-(5.42) and equating the like powers of ξ, the following sets of equations can be obtained:

$$E_0'''-iE_0'=-i \tag{5.46}$$
$$E_1'''-iE_1'=0 \tag{5.47}$$
$$E_2'''-iE_2'=-\left\{1+Ri\left((1-N)L_0+NP_0\right)\right\} \tag{5.48}$$
$$E_3'''-iE_3'=-\frac{a_2}{4}\left(3Y^2E_0''-8YE_0'+4E_0\right)-Ri\left((1-N)L_1+NP_1\right) \tag{5.49}$$

$$\frac{1}{Pr}L_0''-iL_0=0 \tag{5.50}$$
$$\frac{1}{Pr}L_1''-iL_1=0 \tag{5.51}$$
$$\frac{1}{Pr}L_2''-iL_2=0 \tag{5.52}$$
$$\frac{1}{Pr}L_3''-iL_3=-\frac{1}{4}\left(3a_2Y^2L_0'+b_1\left(YE_0'+2E_0\right)\right) \tag{5.53}$$

$$\frac{1}{Sc}P_0''-iP_0=0 \tag{5.54}$$
$$\frac{1}{Sc}P_1''-iP_1=0 \tag{5.55}$$
$$\frac{1}{Sc}P_2''-iP_2=0 \tag{5.56}$$
$$\frac{1}{Sc}P_3''-iP_3=-\frac{1}{4}\left(3a_2Y^2P_0'+b_1\left(YE_0'+2E_0\right)\right) \tag{5.57}$$

The associated boundary conditions are:

$$E_m(0) = E'_m(0) = 0,\ E'_0(\infty) = 1 \tag{5.58}$$

$$E'_m(\infty) = 0,\ \text{for } m = 1, 2, \cdots \tag{5.59}$$

$$L_0(0) = 1,\ L_m(0) = L_m(\infty) = 0 \text{ for } m = 1, 2, \cdots \tag{5.60}$$

$$P_0(0) = 1,\ P_m(0) = P_m(\infty) = 0 \text{ for } m = 1, 2, \cdots \tag{5.61}$$

Solving the above set of equations, it can be obtained the values of $G''(\xi, 0),\ H'(\xi, 0),\ M'(\xi, 0)$ as:

$$\xi^{-\frac{1}{2}} G''(\xi, 0) = \sum_{m=0}^{\infty} \xi^{-\frac{m}{2}} E''_m(0) \tag{5.62}$$

$$\xi^{-\frac{1}{2}} H'(\xi, 0) = \sum_{m=0}^{\infty} \xi^{-\frac{m}{2}} L'_m(0) \tag{5.63}$$

$$\xi^{-\frac{1}{2}} M'(\xi, 0) = \sum_{m=0}^{\infty} \xi^{-\frac{m}{2}} P'_m(0) \tag{5.64}$$

where,

$$E''_0(0) = \sqrt{i},\ E''_1(0) = 0$$
$$E''_2(0) = \frac{1}{\sqrt{i}} \left[1 + Ri \left(\frac{1 - N}{\sqrt{Pr} + 1} + \frac{N}{\sqrt{Sc} + 1} \right) \right] \tag{5.65}$$
$$E''_3(0) = \frac{3}{16} a_2 i \tag{5.66}$$

$$L'_0(0) = -\sqrt{iPr},\ L'_1(0) = 0,\ L'_2(0) = 0 \tag{5.67}$$
$$L'_3(0) = -\frac{3}{16i} a_2 + \frac{b_1}{2i} \left[\frac{3}{2} - \sqrt{Pr} + \frac{Pr^{\frac{5}{2}}}{(1 - Pr)^2} + \frac{Pr(1 - 3Pr)}{2(1 - Pr)^2} \right] \tag{5.68}$$

$$P'_0(0) = -\sqrt{iSc},\ P'_1(0) = 0,\ P'_2(0) = 0 \tag{5.69}$$
$$P'_3(0) = -\frac{3}{16i} a_2 + \frac{c_1}{2i} \left[\frac{3}{2} - \sqrt{Sc} + \frac{Sc^{\frac{5}{2}}}{(1 - Sc)^2} + \frac{Sc(1 - 3Sc)}{2(1 - Sc)^2} \right] \tag{5.70}$$

Outer layer region

It is expected that, the viscous forces are absent in the outer layer region. It has been observed by some researchers that in the outer layer region, the convective and conductive terms of both thermal and concentration equations are of the same order of magnitude. New scaled variables $\hat{\delta} = \xi^{\frac{-1}{2}}$ is introduced in order to simulate this region and the following set of equations are obtained:

$$\hat{\delta}^2\ \bar{G}''' + \hat{\delta}^2\ \frac{3}{4}\left(F\bar{G}'' + F''\bar{G}\right) - \hat{\delta}^2\ F'\bar{G}' + i(1-\bar{G}') + Ri\hat{\delta}^2\ \left[(1-N)\bar{H} + N\bar{M}\right] + 1 = \frac{1}{4}\hat{\delta}^3\ \left(F''\frac{\partial\bar{G}}{\partial\hat{\delta}} - F'\frac{\partial\bar{G}'}{\partial\hat{\delta}}\right) \tag{5.71}$$

$$\hat{\delta}^2\ \frac{1}{Pr}\bar{H}'' + \hat{\delta}^2\ \frac{3}{4}\left(F\bar{H}' + \bar{G}\Theta'\right) - i\bar{H} = \frac{1}{4}\hat{\delta}^3\left(\Theta'\frac{\partial\bar{G}}{\partial\hat{\delta}} - F'\frac{\partial\bar{H}}{\partial\hat{\delta}}\right) \tag{5.72}$$

$$\hat{\delta}^2\ \frac{1}{Sc}\bar{M}'' + \hat{\delta}^2\ \frac{3}{4}\left(F\bar{M}' + G\Theta'\right) - i\bar{M} = \frac{1}{4}\hat{\delta}^3\ \left(\Phi'\frac{\partial\bar{G}}{\partial\hat{\delta}} - F'\frac{\partial\bar{M}}{\partial\hat{\delta}}\right) \tag{5.73}$$

The boundary conditions are same as equation (5.27). Suggested expansion for the functions $G,\ H$ and M are as follows:

$$G(\hat{\delta},\eta) = \sum_{m=0}^{\infty}\hat{\delta}^m\ \bar{G}_m(\eta),\quad H(\hat{\delta},\eta) = \sum_{m=0}^{\infty}(\hat{\delta})^m\ \bar{H}_m(\eta)$$
$$M(\hat{\delta},\eta) = \sum_{m=0}^{\infty}(\hat{\delta})^m\ \bar{M}_m(\eta \tag{5.74}$$

Replacing this expansion in equations (5.24)-(5.26), the equations for $\bar{G}_m,\ \bar{H}_m,\ \bar{M}_m^{'}s$ can be found by equating the similar powers of δ:

$$\bar{G}_0' = 1,\ \bar{G}_1' = 0,\ i\bar{G}_2' = \frac{3}{4}F''G_0 - F' + 1$$
$$i\bar{G}_3' = \bar{G}_1''' + \frac{3}{4}\left(FG_1'' - F'\bar{G}_1'\right) + \frac{1}{2}F''\bar{G}_1 + Ri\left((1-N)\bar{H}_1 + N\bar{M}_1\right)$$
$$i\bar{G}_{n+3}' = \bar{G}_{n+1}''' + \frac{3}{4}\left(F\bar{G}_{n+1}'' - F'\bar{G}_{n+1}'\right) + \frac{1}{2}F''\bar{G}_{n+1} + Ri\left((1-N)\bar{H}_{n+1} + N\bar{M}_{n+1}\right) \tag{5.75}$$

$$
\begin{aligned}
&i\bar{H}_0 = 0,\ i\bar{H}_1 = 0,\ iH_2 = \frac{3}{4}\Theta'\bar{G}_0,\ i\bar{H}_3 = \frac{1}{2}\Theta' G_1 \\
&-i\bar{H}_{n+3} + \frac{1}{Pr}\bar{H}''_{n+1} + \frac{3}{4}F'H'_{n+1} + \frac{1}{2}\Theta'\bar{G}_{n+1} + \frac{1}{4}F'\bar{H}_{n+1} = 0 \\
&i\bar{M}_0 = 0,\ i\bar{M}_1 = 0,\ iM_2 = \frac{3}{4}\Phi'\bar{G}_0,\ i\bar{M}_3 = \frac{1}{2}\Phi' G_1 \\
&-i\bar{M}_{n+3} + \frac{1}{Pr}\bar{M}''_{n+1} + \frac{3}{4}F'M'_{n+1} + \frac{1}{2}\Phi'\bar{G}_{n+1} + \frac{1}{4}F'\bar{M}_{n+1} = 0
\end{aligned} \tag{5.76}
$$

which are subject to the outer boundary conditions :

$$
\begin{aligned}
&\bar{G}'_0 \to 1 \text{ and } \bar{\mathrm{G}}'_{\mathrm{n}} \to 0 \text{ for } \ \eta \to \infty \ \ \bar{\mathrm{H}}_0(0) = 1,\ \bar{\mathrm{H}}_{\mathrm{m}}(0) = \bar{\mathrm{H}}_{\mathrm{m}}(\infty) = 0 \\
&\bar{M}_0(0) = 1,\ \bar{M}_m(0) = \bar{M}_m(\infty) = 0
\end{aligned} \tag{5.77}
$$

Solutions of the above equations are:

$$
\begin{aligned}
&\bar{G}_0 = \eta + C_0,\ \bar{G}_1 = C_1,\ \bar{G}_2 = i^{-1}\left(\frac{3}{4}\eta F' + \frac{3}{4}C_0F' - \frac{7}{4}F + \eta + C_2\right) \\
&\bar{G}_3 = i^{-1}\left(\frac{1}{2}C_1F' + C_3\right),\ \bar{H}_0 = 0,\ \bar{H}_1 = 0 \\
&\bar{H}_2 = i^{-1}\left(\frac{3}{4}\Theta'\bar{G}_0\right),\ \bar{H}_3 = i^{-1}\left(\frac{1}{2}\Theta'\bar{G}_1\right) \\
&\bar{M}_0 = 0,\ \bar{M}_1 = 0,\ \bar{M}_2 = i^{-1}\left(\frac{3}{4}\Theta'\bar{G}_0\right),\ \bar{M}_3 = i^{-1}\left(\frac{1}{2}\Theta'\bar{G}_1\right)
\end{aligned} \tag{5.78}
$$

The unknown constants $C'_n s$ are determined by the matching procedure which has been discussed in the following section.

Matching

From the solutions of the each functions of the outer expansions, some constants are introduced. Since each of the functions involving inner expansions are solved completely, the unknown constants can be settled on the principle of the matching:

$$
\lim_{Y\to\infty} G^i(\hat{\delta}, Y) = \lim_{\eta\to 0} G^o(\hat{\delta}, \eta).
$$

Carrying out the corresponding limit and neglecting the exponentially small terms, the following equations can be obtained for the inner layer region:

$$\begin{aligned} G^i(\hat{\delta}, Y) = 2^{\frac{-1}{2}}\hat{\delta}\left(-\frac{1}{\sqrt{i}}2^{\frac{1}{2}}\hat{\delta}^{-1}\eta + \hat{\delta}^2 C - 2^{\frac{1}{2}}i\hat{\delta}\eta\right) \\ 2^{\frac{-1}{2}}\hat{\delta}\left(+a_2 i\hat{\delta}\eta^2 + a_2 2^{\frac{1}{2}}\sqrt{i}\hat{\delta}^2\eta + \cdots\right) \end{aligned} \tag{5.79}$$

and solutions of the outer layer region is:

$$G^o(\hat{\delta}, \eta) = \eta + C_0 + \hat{\delta}C_1 + \hat{\delta}^2\left(\frac{1}{4}a_2\eta^2 i - \eta i + C_2\right) + \hat{\delta}^3/i\left(a_2 C_1\eta + C_3\right) + \cdots \tag{5.80}$$

Since each terms in equation (5.79) will correspond a term with the same power of $\hat{\delta}$ in equation (5.80). So by equating the similar terms from each of these equations, the unknown constants can be chosen as:

$$C_0 = 0,\ C_1 = -\frac{1}{\sqrt{2i}},\ C_2 = \frac{2\sqrt{2}-1}{4}a_2\eta^2 i,\ C_3 = \frac{C}{\sqrt{2}}i + a_2 i\sqrt{i}\eta - C_1 a_2\eta \quad etc.$$

where

$$C = \sqrt{i} + \frac{Ri(1-N)}{Pr-1}\left(1 + \frac{\sqrt{i}}{\sqrt{Pr}}\right) + \frac{Ri\ N}{Sc-1}\left(1 + \frac{\sqrt{i}}{\sqrt{Sc}}\right) \tag{5.81}$$

Using the equations (5.79) and (5.80) composite solutions for velocity, heat transfer and mass transfer can be attained.

5.3.3 Finite difference method (FDM) for all ξ

The solutions of the equations (5.19)-(5.21) associated with the boundary equation (5.22) and the equations (5.24)-(5.26) along with the boundary condition (5.27) are attained by applying regular finite difference method. The order of the differential equations are reduced by introducing some new variables for the first order derivative of the associated functions, for example, $F' = H$ etc. Because of introducing new variables, the order of the set of the equations (5.19)-(5.21) and equations (5.24)-(5.26) has been reduced into order two and the resulting two sets of second order partial differential equations are discretized by using the

forward difference formula. As a result of discretization, a system of tri-diagonal algebraic equations for momentum, temperature and concentration equations are formed. Details of the calculations are discussed in the following subsections.

Steady flow

The resulting momentum equation, energy equation and concentration equation for the steady flow field turned into system of tri-diagonal algebraic equations. Then these system of equations are solved by using TDMA (tri diagonal matrix solver algorithm). The form of the discretized momentum equation (5.18) is given below:

$$\begin{aligned}
&A_1 H_{i,j+1} + B_1 Hi, j + C_1 H_{i,j-1} = D_1, \quad \text{where} \\
&A_1 = \left[\frac{1}{(\triangle\eta)^2} + \frac{3}{4} \times \frac{1}{(2\triangle\eta)} F_{i,j}\right] \\
&C_1 = \left[\frac{1}{(\triangle\eta)^2} - \frac{3}{4} \times \frac{1}{(2\triangle\eta)} F_{i,j}\right] \\
&B_1 = -\left[\frac{2}{(\triangle\eta)^2)} + \frac{1}{2} H_{i,j}\right] \\
&D_1 = -\frac{1}{2} - Ri\left[(1-N)\ T_{i,j} + N\ M_{i,j}\right]
\end{aligned} \tag{5.82}$$

The temperature equation (5.19)is discretized as:

$$\begin{aligned}
&A_2 \Theta_{i,j+1} + B_2 \Theta i, j + C_2 \Theta_{i,j-1} = D_2, \quad \text{where} \\
&A_2 = \left[\frac{1}{Pr\ (\triangle\eta)^2} + \frac{3}{4} F_{i,j} \times \frac{1}{(2\triangle\eta)}\right] \\
&C_2 = \left[\frac{1}{Pr\ (\triangle\eta)^2} - \frac{3}{4} F_{i,j} \times \frac{1}{(2\triangle\eta)}\right] \\
&B_2 = \frac{2}{Pr(\triangle\eta)^2}, \quad D_2 = 0
\end{aligned} \tag{5.83}$$

And the discretized concentration equation (5.20) takes the form:

$$\begin{aligned} &A_3\Phi_{i,j+1} + B_3\Phi i,j + C_3\Phi_{i,j-1} = D_3, \quad \text{where} \\ &A_3 = \left[\frac{1}{Sc\ (\triangle\eta)^2} + \frac{3}{4}F_{i,j} \times \frac{1}{(2\triangle\eta)}\right] \\ &C_3 = \left[\frac{1}{Sc\ (\triangle\eta)^2} - \frac{3}{4}F_{i,j} \times \frac{1}{(2\triangle\eta)}\right] \\ &B_3 = \frac{2}{Sc(\triangle\eta)^2}, \quad D_3 = 0 \end{aligned} \tag{5.84}$$

Here, $1 \leq i \leq M$ and $2 \leq j \leq M-1$ denote the grid points along the η and ξ directions, respectively. $\triangle\xi = \xi_i - \xi_{i-1}$ is the step size in the i'th direction and $\triangle\eta = \eta_j - \eta_{j-1}$ determines the step size in the j'th direction. Finally $F_{i,j}$ is calculated from the relation:

$$F_{i,j} = F_{i,j-1} + \frac{1}{2}\triangle\eta(H_{i,j} + H_{i,j-1})$$

Corresponding boundary conditions take the form:

$$\begin{aligned} &F_{i,j} = H_{i,j} = 0, \quad \Theta_{i,j} = 1, \quad \Phi_{i,j} = 1 \\ &H_{M,j} \to 0, \quad \Theta_{M,j} \to 0, \quad \Phi_{M,j} \to 0 \end{aligned} \tag{5.85}$$

Unsteady Flow field

For fluctuating flow field, the real and imaginary parts of the governing equations are separated and discretized by following the similar method as mentioned above. Since the governing equations for the fluctuating flow field are coupled with steady equations, firstly the steady flow field is simulated and the corresponding calculated values are used as known values for solving the unsteady set of equations. The discretized form of the equations are presented below:

Real part of the Momentum equation (5.23):

$$
\begin{aligned}
&A_{11}UR_{i,j+1} + B_{11}URi,j + C_{11}UR_{i,j-1} = D_{11}, \quad \text{where} \\
&A_{11} = \left[\frac{1}{(\triangle\eta)^2} + \frac{3}{4}V_{i,j}\frac{1}{(2\triangle\eta)}\right] \\
&C_{11} = \left[\frac{1}{(\triangle\eta)^2} - \frac{\left(\frac{3+2\xi}{4(1+\xi)}V_{i,j} + \xi\ VX\right)}{(2\triangle\eta)}\right], \quad B_{11} = \frac{2}{(\triangle\eta)^2)} \\
&D_{11} = \frac{3}{4} \times\ UY \times\ VR + \xi \times\ UI + 1 + ri\left[(1-N)\ TR + N\ MR\right] \\
&\qquad + \frac{1}{2} \times\ \frac{\xi}{\triangle\ \xi}\left[U \times\ UR_{i,j} + UY\ \times\ (VR_{i,j} - VR_{i-1,j})\right]
\end{aligned} \tag{5.86}
$$

Imaginary part of the Momentum equation:

$$
\begin{aligned}
&A_{12}\ UI_{i,j+1} + B_{12}UIi,j + C_{12}UI_{i,j-1} = D_{12} \quad \text{where} \\
&A_{11} = \left[\frac{1}{(\triangle\eta)^2} + \frac{3}{4}V_{i,j}\frac{1}{(2\triangle\eta)}\right]
\end{aligned}
$$

$$
\begin{aligned}
&C_{11} = \left[\frac{1}{(\triangle\eta)^2} - \frac{\left(\frac{3+2\xi}{4(1+\xi)}V_{i,j} + \xi\ VX\right)}{(2\triangle\eta)}\right], \quad B_{11} = \frac{2}{(\triangle\eta)^2)} \\
&D_{11} = \frac{3}{4} \times\ UY \times\ VR + \xi \times\ UI + 1 + ri\left[(1-N)\ TI + N\ MI\right] \\
&\qquad + \frac{1}{2} \times\ \frac{\xi}{\triangle\ \xi}\left[U \times\ UI_{i,j} + UY\ \times\ (VI_{i,j} - VI_{i-1,j})\right]
\end{aligned} \tag{5.87}
$$

Real part of the Energy equation (5.24)

$$
\begin{aligned}
&A_{21}\theta R_{i,j+1} + B_{21}\theta Ri, j + C_{21}\theta R_{i,j-1} = D_{21}, \quad \text{where} \\
&A_{21} = -\left[\frac{1}{Pr\ (\triangle\eta)^2} + \left(\frac{3+2\xi}{4(1+\xi)}V_{i,j} + \xi\ VX\right)/(2\triangle\eta)\right] \\
&C_{21} = -\left[\frac{1}{Pr\ (\triangle\eta)^2} - \left(\frac{3+2\xi}{4(1+\xi)}V_{i,j} + \xi\ VX\right)/(2\triangle\eta)\right] \\
&B_{21} = \frac{2}{Pr(\triangle\eta)^2} + \frac{\xi}{\triangle\xi}U_{i,j} \\
&D_{21} = \frac{\xi}{\triangle\xi}U_{i,j}\theta R_{i-1,j} + \frac{\xi}{\triangle\xi}TY(VR_{i,j} - VR_{i-1,j}) \\
&\qquad + \xi^{1/2}(1+\xi)^{1/2}\ St\ \theta I_{i,j} + \xi\ UR_{i,j}\ TX
\end{aligned} \tag{5.88}
$$

Imaginary part of the Energy equation:

$$
\begin{aligned}
&A_{22}\theta I_{i,j+1} + B_{22}\theta Ii, j + C_{22}\theta I_{i,j-1} = D_{22}, \quad \text{where} \\
&A_{22} = -\left[\frac{1}{Pr\ (\triangle\eta)^2} + \left(\frac{3+2\xi}{4(1+\xi)}V_{i,j} + \xi\ VX\right)/(2\triangle\eta)\right]
\end{aligned}
$$

$$
\begin{aligned}
&C_{22} = -\left[\frac{1}{Pr\ (\triangle\eta)^2} - \left(\frac{3+2\xi}{4(1+\xi)}V_{i,j} + \xi\ VX\right)/(2\triangle\eta)\right] \\
&B_{22} = \frac{2}{Pr(\triangle\eta)^2} + \frac{\xi}{\triangle\xi}U_{i,j} \\
&D_{22} = \frac{\xi}{\triangle\xi}U_{i,j}\theta I_{i-1,j} + \frac{\xi}{\triangle\xi}TY(VI_{i,j} - VI_{i-1,j}) \\
&\qquad + \xi^{1/2}(1+\xi)^{1/2}\ St\ \theta I_{i,j} + \xi\ UI_{i,j}\ TX
\end{aligned} \tag{5.89}
$$

Real part of the concentration equation (5.25):

$$
\begin{aligned}
&A_{31}\phi R_{i,j+1} + B_{31}\phi R_{i,j} + C_{31}\phi R_{i,j-1} = D_{31}, \quad \text{where} \\
&A_{31} = -\left[\frac{1}{Sc\ (\triangle\eta)^2} + \left(\frac{3+2\xi}{4(1+\xi)}V_{i,j} + \xi\ VX\right)/(2\triangle\eta)\right]
\end{aligned} \tag{5.90}
$$

$$
\begin{aligned}
C_{31} &= -\left[\frac{1}{Sc\ (\triangle\eta)^2} - \left(\frac{3+2\xi}{4(1+\xi)}V_{i,j} + \xi\ VX\right)/(2\triangle\eta)\right] \\
B_{31} &= \frac{2}{Pr(\triangle\eta)^2} + \frac{\xi}{\triangle\xi}U_{i,j} \\
D_{31} &= \frac{\xi}{\triangle\xi}U_{i,j}\phi R_{i-1,j} + \frac{\xi}{\triangle\xi}TY(VR_{i,j} - VR_{i-1,j}) \\
&\quad + \xi^{1/2}(1+\xi)^{1/2}\ St\ \phi I_{i,j} + \xi\ UR_{i,j}\ CX
\end{aligned} \tag{5.91}
$$

Imaginary part of the Concentration equation

$$
\begin{aligned}
&A_{32}\phi I_{i,j+1} + B_{32}\phi I_{i,j} + C_{32}\phi I_{i,j-1} = D_{32}, \quad \text{where} \\
&A_{32} = -\left[\frac{1}{Sc\ (\triangle\eta)^2} + \frac{3+2\xi}{4(1+\xi)}V_{i,j}/(2\triangle\eta)\right]
\end{aligned} \tag{5.92}
$$

$$
\begin{aligned}
C_{32+} &= -\left[\frac{1}{Sc\ (\triangle\eta)^2} - \frac{3+2\xi}{4(1+\xi)}V_{i,j}/(2\triangle\eta)\right] \\
B_{32} &= \frac{2}{Sc(\triangle\eta)^2} + \frac{\xi}{\triangle\xi}U_{i,j} + \frac{1}{2(1+\xi)}U_{i,j} \\
D_{32} &= \frac{\xi}{\triangle\xi}U_{i,j}\phi I_{i-1,j} + \frac{\xi}{\triangle\xi}TY(VI_{i,j} - VI_{i-1,j}) \\
&\quad - \xi^{1/2}(1+\xi)^{1/2}\ St\ \phi R_{i,j}\xi\ UI_{i,j}\ CX
\end{aligned} \tag{5.93}
$$

In the above expressions, UX, VX, TX, CX represents the first order partial derivatives w.r.t ξ of the quantities U, V, T, C respectively and UY, VY, TY, CY are the partial derivatives of the respective measurement of the related values w.r.t η. Further, UR, VR, TR, MR are the measurement of the real part of the respective quantities and UI, VI, TI, MI are the measurement of the imaginary part of the corresponding quantities

In order to solve all the resulting sets of algebraic equations, TDMA (tridiagonal solver)is applied. The computation starts at $\xi = 0.0$ and then it marches up to $\xi = 2000$ using the step size $\triangle\xi = 0.01$. At every ξ_i station, the computations are iterated until the difference of the results of two successive iterations becomes less or equal to 10^{-6}.

5.4 Results and discussion

The present study is devoted to investigate the velocity of flow field, local heat transfer and mass transfer of a mixed convective unsteady flow due to double diffusion. Extensive parametric studies have been carried out in order to elucidate the vivid picture of the flow field. Influence of the parameters on the important quantities of physical interest are discussed and presented in this section. Results have been depicted in both tabular and graphical form for different values of the various parameters. In the Table 5.1, numerical

Table 5.1: Comparison of the values of amplitude and phase angels of the local shear stress, obtained by perturbation methods and finite difference method, while, Pr=0.7, Sc=0.94, w=0.5, Ri=1.0.

ξ	A_U		ϕ_U	
—-	FDF	ESS and ASS.	FDF	ESS and ASS
0.0000	1.7285	1.71659[1]	0.00000	0.00000[1]
0.0500	1.7320	1.71549[1]	5.0738	5.30589[1]
0.1001	1.7423	1.71220[1]	10.1093	9.21283[1]
0.1501	1.7592	1.70671[1]	15.0707	13.79736[1]
0.2502	1.7823	1.78903[1]	19.9239	16.08001[1]
0.3002	1.8448	1.78918[1]	29.2095	28.35452[1]
0.3502	1.8828	1.78715[1]	33.6054	31.74723[1]
0.4003	1.9243	1.74666[1]	37.8210	33.92143[1]
0.4503	1.9684	1.72822[1]	41.8533	36.07423[1]
0.5504	2.0143	1.60768[1]	45.7000	38.20373[1]
1.0078	2.4184	1.23616[2]	26.22925	26.55354[2]
4.0027	2.2728	2.1719[2]	35.96272	35.8813[2]
6.0040	2.6613	2.5534[2]	37.56064	39.6030[2]
8.0053	2.9873	2.9009[2]	43.57451	38.5850[2]
10.0067	3.2792	3.2172[2]	44.16434	39.4115[2]
12.0080	3.5559	3.5080[2]	44.43331	44.8022[2]
14.0093	3.8184	3.7781[2]	44.83141	44.8305[2]
15.0000	3.9429	3.9053[2]	44.90746	44.8417[2]

[1] stands for series solution and [2] stands for asymptotic solution

results for the shear stress obtained by different numerical techniques are presented against ξ. It can be observed from the table that the values of shear stress are in acceptable agreement obtained by different solution methodologies. It can also be observed that the values of shear stress increase monotonically as the values of ξ increases. That is, as it is

marched towards the downstream, monotonic increment of the values of shear stress are obtained. It can also be noticed that the increment of the values of Pr have also some effects on these quantities. It can also be marked that the value of phase angles reaches at the asymptotic value which is 45^0 as flow marches towards downstream.

Table 5.2: Comparison of the values of amplitude and phase angels of the shear stress, obtained by perturbation methods and finite difference method, while, Pr=0.7, Sc=0.94, w=0.5, Ri=2.0.

ξ	A_U		ϕ_U	
—-	FDF	ESS and ASS	FDF	ESS and ASS
0.0000	0.6933	0.69348[1]	0.00000	0.00000[1]
0.0500	0.6925	0.69266[1]	5.0738	5.7100[1]
0.1001	0.6903	0.69019[1]	6.9959	6.16754[1]
0.1501	0.6866	0.68608[1]	10.1247	9.25041[1]
0.2502	0.6752	0.67299[1]	15.9239	15.41251[1]
0.3002	0.6678	0.66405[1]	18.4475	18.49102[1]
0.3502	0.6595	0.65354[1]	20.8291	20.56744[1]
0.4003	0.6504	0.64150[1]	25.6943	24.64159[1]
0.4503	0.6409	0.64796[1]	28.8533	27.71350[1]
0.5504	0.6217	0.59655[1]	45.7000	33.85328[1]
1.0078	0.5940	0.59378[2]	45.2292	43.4615[2]
4.0027	1.6524	1.6206[2]	45.1104	43.7725[2]
6.0040	2.0416	2.0045[2]	45.4723	43.9807[2]
8.0053	2.3650	2.4735[2]	45.2715	44.2389[2]
10.0067	2.6470	2.7420[2]	45.1602	44.3927[2]
12.0080	2.9003	2.9865[2]	45.1004	44.4948[2]
14.0093	3.1328	3.2113[2]	45.0676	44.5675[2]
15.0000	3.2417	3.2353[2]	45.0571	44.5963[2]

[1] stands for series solution and [2] stands for asymptotic solution

Table 5.2 presents some values of amplitude and phase angles of local heat transfer of the unsteady flow field. The results have been produced with the constant values of Pr=0.7, Sc=0.94, w=0.5 and Ri=2.0. From the table 5.2, it can be seen that the amplitudes and phase angles of the shear stress are in good agreement with those calculated by different numerical methods. Here also, continuous increment is marked as the increment of the values of ξ. The phase angles are zero under quasi-steady condition, and monotonically approach towards the asymptotic value.

The effects of various parameters on the amplitude and phase angles of shear stress, local heat transfer and mass transfer rate have been depicted in the Figures 5.2-5.6. The Figure 5.2 inferred the effects of Prandtl number Pr on local heat transfer rate. The values of Pr have been ranged from 0.054 to 8.0 while all other associated parameters are taken as constant. Prandtl number ranging from 0.7 to 1.0 represents gases, 1 to 10 stands for water, 0.001 to 0.03 are for liquid metals and for oil these values are ranging from 50 to 2000. The graphs show that, as the values of Pr are increased the concerned quantities also become higher. For the phase angles, it can also be seen that the corresponding values are increased slowly but surely approach towards the asymptotic value of 45^0. The

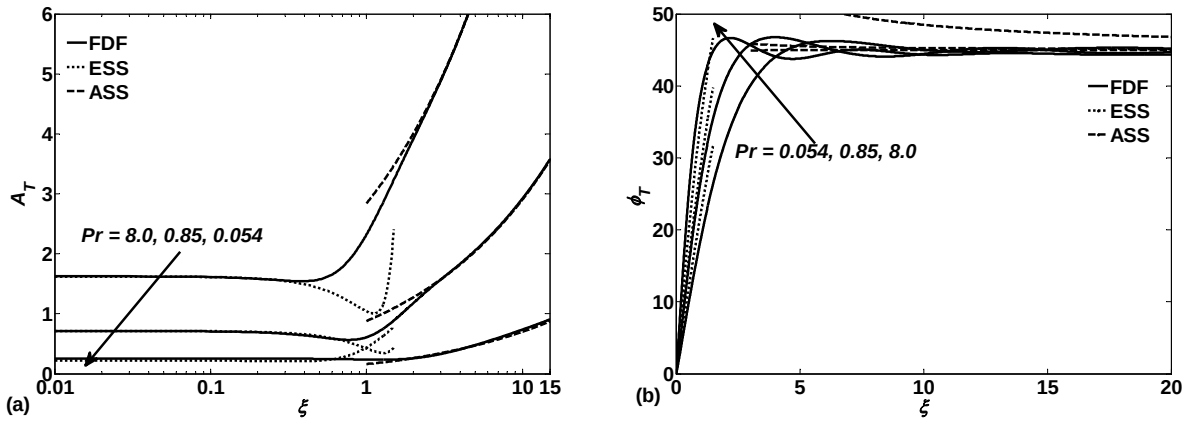

Figure 5.2: (a) Amplitude, (b) Phase angles of heat transfer for different values of Pr, while, Sc=0.94, Ri=1.0, w=0.5.

effects of the another diffusive parameter Sc on the local mass transfer has been depicted in Figure 5.3. Here range for the Schmidt number has been chosen from 0.22 to 1.76. The values of the Schmidt number, Sc are taken to represent the various species, benzene (1.76), carbondioxide (0.94), water vapor (0.60), and hydrogen (0.22). In this case, for both the values of amplitude and phase angle of local mass transfer, similar types of behaviour to local heat transfer can be monitored. The enhancement of the values of Sc, produces higher values of the amplitude of mass transfer. Phase angles of the mass transfer also attain its asymptotic value of 45^0 as flow is headed for downstream.

In Figures 5.4-5.6, the effects of the Richardson's number Ri on the values of amplitude and phase angles of shear stress, heat transfer and mass transfer have been presented. It

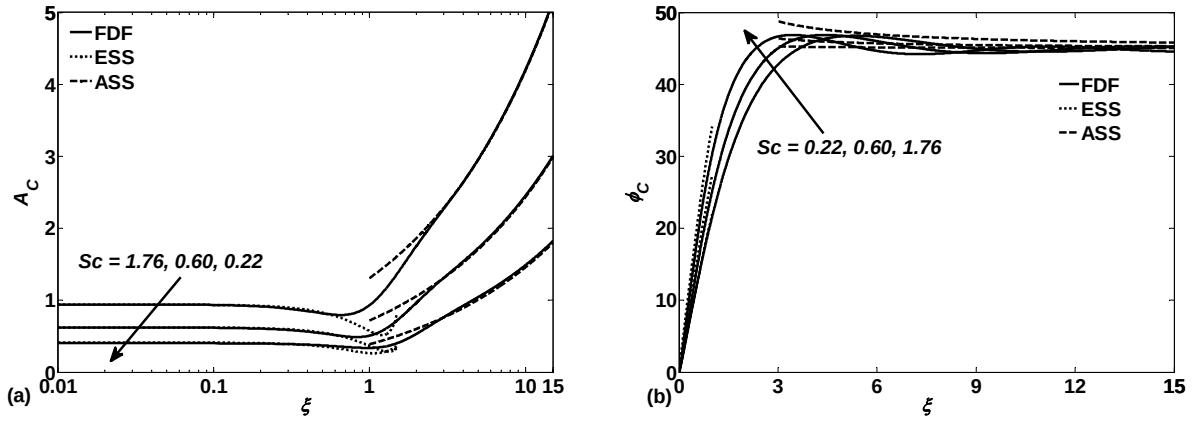

Figure 5.3: (a) Amplitude, (b) Phase angles, of mass transfer for different values of Sc, while, Pr=0.7, Ri=1.0, w=0.5.

can be seen from the Figure 5.4, the change of the values of Ri have significant effects on the value of amplitude and phase of shear stress. For higher values of Ri, the amplitudes of shear stress also become higher, where as, the corresponding values of the phase angles show the reverse behaviour. That is, smaller values of phase angle are observed for higher values of Ri. As the value of Ri becomes higher, both the mixed convection of the flow and heat transfer are enhanced and accordingly the amplitude of shear stress becomes higher. But the values of the phase angle are decreased because in the down stream region, the derivative of the local skin friction is higher than in the leading edge for smaller values of Ri.

Though, significant changes are not achieved for both the heat transfer rate and mass transfer rate in case of changing the values of Ri, but similar to the shear stress, amplitude of heat transfer and mass transfer are also boosted up little bit due to the increment of Ri. In both of the cases of heat and mass transfer, the phase angles become smaller as the values of Ri increase.

Transient shear stress, transient heat transfer and transient mass transfer at different values of ξ against the oscillation parameter ωt have been revealed in Figures 5.7-5.9. From the practical points of view, these quantities are important to study, because, these quantities may ruin a system. This is because, all these three quantities are unsteady in nature from leading edge to far down stream region. The definition for transient skin

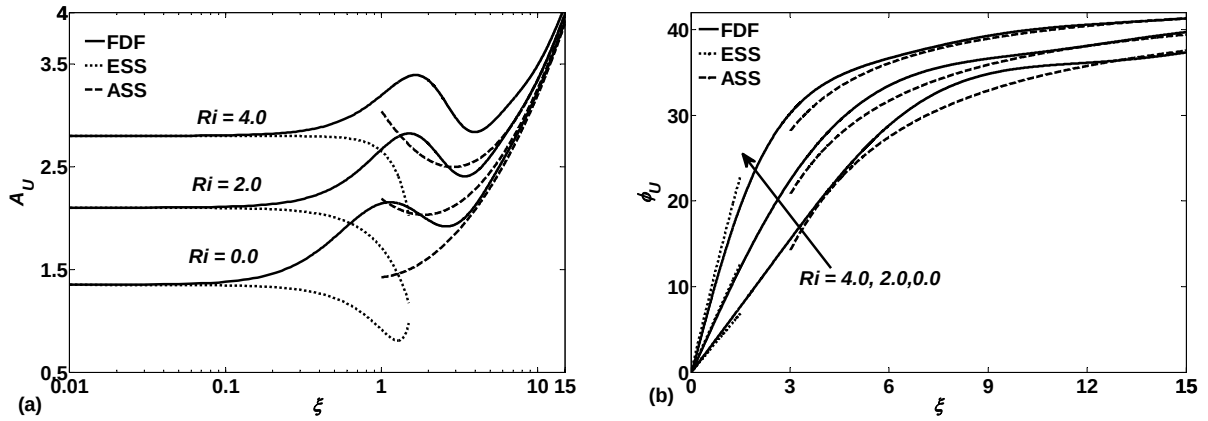

Figure 5.4: (a) Amplitude, (b) Phase angles of local shear stress for different values of Ri, while, Pr=0.70, Sc=0.94, w=0.5.

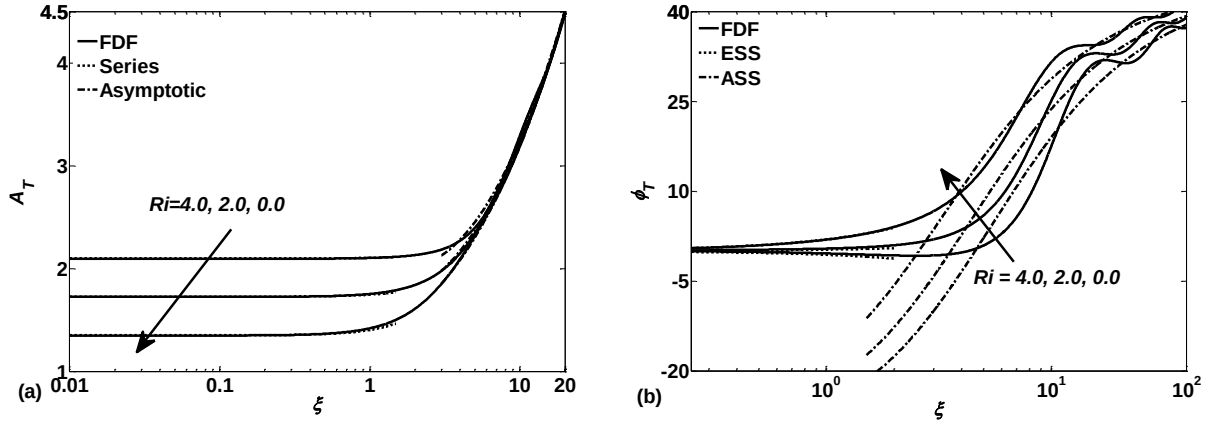

Figure 5.5: (a) Amplitude, (b) Phase angles of heat transfer for different values of Ri, while, Pr=0.70, Sc=0.94, w=0.5.

friction , τ, transient heat transfer q, and transient mass transfer m, have been taken as follows:

$$\tau = \tau_s + \varepsilon A_u \cos(\omega t + \phi_s)$$

$$q = q_s + \varepsilon A_t \cos(\omega t + \phi_t)$$

$$m = m_s + \varepsilon A_c \cos(\omega t + \phi_c)$$

where τ_s is the steady mean shear stress, q_s is the steady surface heat transfer rate and m_s is the steady surface mass transfer rate respectively. The values of τ_s , q_s, m_s

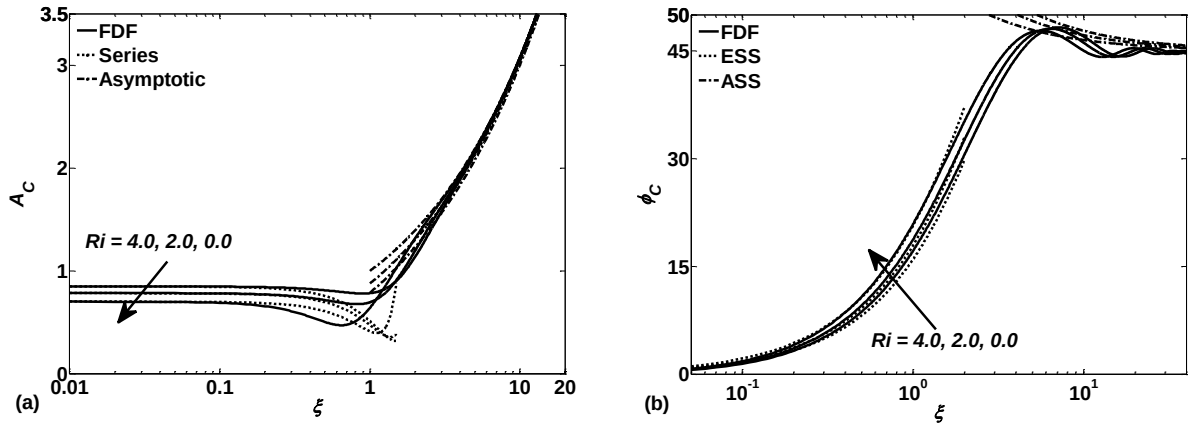

Figure 5.6: (a) Amplitude, (b) Phase angles of mass transfer for different values of Ri, while, Pr=0.70, Sc=.94, w=0.5.

are calculated first and then the required quantities are obtained accordingly from the simulations by using the implicit finite difference method for the entire regime. Each of the case, the values of Ri have been chosen as 1.0 and 4.0 and all other parameters are taken as Pr=0.7, Sc=0.94, w=0.5 respectively.

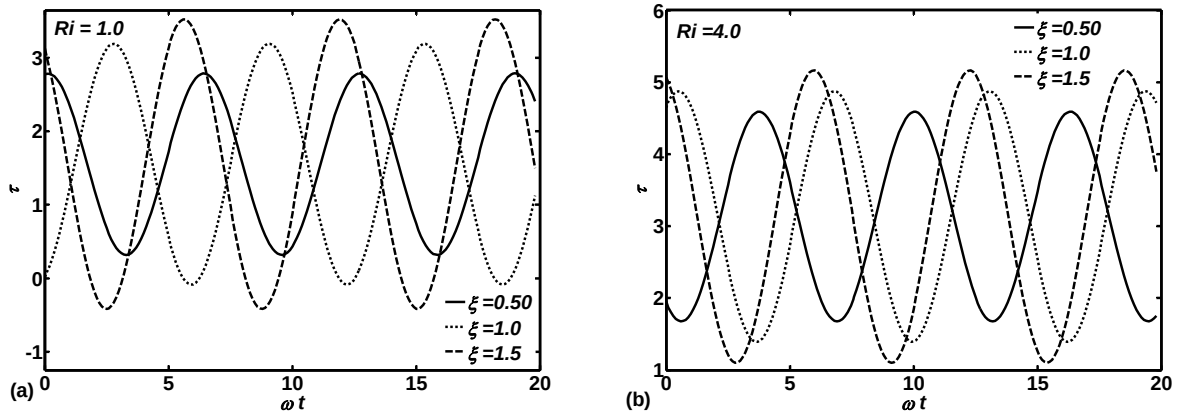

Figure 5.7: Transient shear stress for different values of ξ against ωt, while, Sc=0.94, Pr=0.7, w=0.5, Ri=1.0, 4.0.

From all these results, one can detect the phase shift of the oscillations of shear stress, heat transfer and mass transfer as the values of ξ is increased. Periodic maximum and minimum of the amplitude of the respective oscillations are also clearly perceived. It also

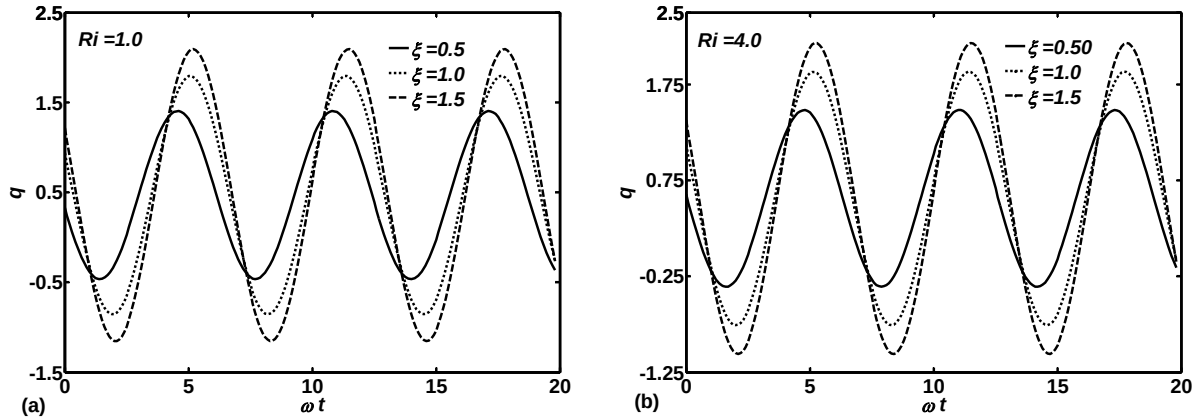

Figure 5.8: Transient heat transfer for different values of ξ against ωt, while, Sc=0.94, Pr=0.7, w=0.5, Ri=1.0, 4.0.

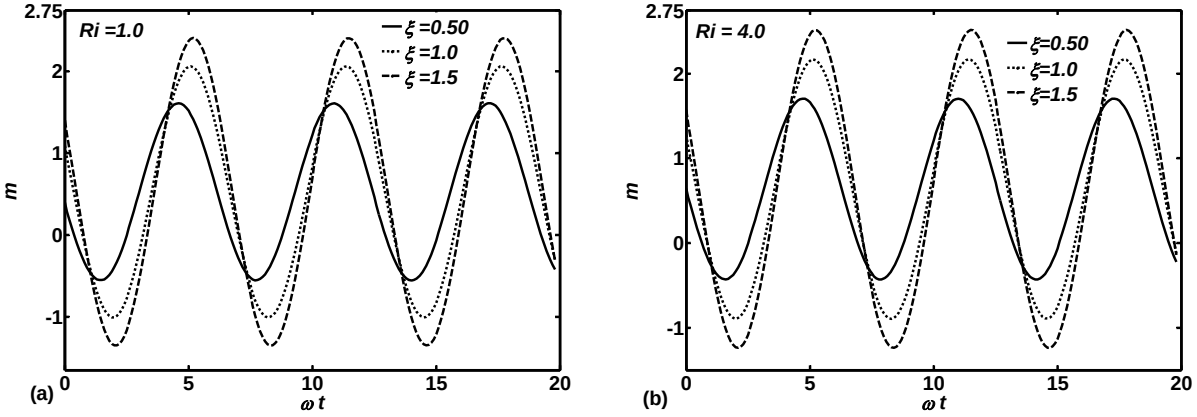

Figure 5.9: Transient mass transfer for different values of ξ against ωt, while, Sc=0.94, Pr=0.7, w=0.5, Ri=1.0, 4.0.

can be noticed that, as the value of Ri is increased from 1.0 to 4.0, the amplitude of the oscillations are also increased for the same values of ξ. Since the effect of mixed convection of flow, heat transfer and mass transfer is relatively stronger in the small ξ region, the intensity of oscillations dropped down quickly away from the leading edge for lower values of Ri. Moreover, it can be noted that, the amplitude of the oscillation of the shear stress is highest and corresponding lowest value is attained for the local mass transfer for the variation of different parameters.

5.5 Summary

Numerical calculations have been carried out in this present learning, in order to depict the parametric effects on different essential quantities. For the unsteady case, the corresponding quantities are illustrated as amplitude and phase angles. Important findings of the present investigation are listed below:

- From both graphical and tabular representation of the results, it can be concluded that, the amplitude of the surface heat transfer, surface mass transfer as well as the shear stress are increased along with the increment of all the parameters.
- The phase angles of the heat and mass transfer progressively attain the asymptotic value 45^0 with the increases of the local frequency parameter ξ.
- Moreover, for the transient shear stress, transient heat transfer and transient mass transfer, it can also be observed the higher amplitude of oscillations as the values of ξ increases.
- Lastly, the quick convergence of the simulations ensures the efficiency of the numerical method that has been implemented to simulate the flow field, in presence of conjugate buoyancy.

Chapter 6

Heat and mass transfer response in MHD natural convection flow due to oscillating surface temperature and concentration

6.1 Introduction

"MHD" flow which is termed as magnetohydrodynamics flow, arises when there is interaction of moving electrically conducting fluids with electric and magnetic fields. This kind of interaction can be observed in liquids, gases, two -phase mixtures, or plasmas. This kind of flow provides some very interesting phenomena with electro-fluid-mechanical energy conversion. Sometimes, flow involving electrically conducting fluid is also discussed as "cross-field" where a uniform fluid stream and a uniform magnetic field making a nonzero angel with it. In this type of flow, both the buoyancy and magnetic forces effects flow of electrically conducting fluid. Heating and flow control in metal processing, power generation from two phases mixtures or seeded high temperature gases, magnetic confinement of high temperature plasmas etc. are some very well known practical scientific and technical applications of this type of flow. Continuous development of MHD flow is opening new

horizon to the technical development. Most recent research have been conducting in MHD flow so that it can be used in seawater propulsion and control of turbulent boundary layers to reduce drag. MHD also applies quite well to astrophysics and cosmology.

In this present work, buoyancy driven magnetohydrodynamic flow along a vertical surface have been considered. It has also been taken into account that the surface temperature, surface species concentration and free stream velocity are time dependent. Both the surface temperature and species concentration have oscillations with small amplitude. The term "crossed-field" here has been used to describe a flow of electrically conducting fluid. Moreover, it has been assumed that in some undisturbed flow region , there is a uniform magnetic field making a non zero angle with it. This assumption assures that there must be an electric field in such region , directed perpendicularly to both the stream velocity and magnetic-field vectors. Some early research regarding the MHD flow reported that regardless of the strength of the applied magnetic field, the electromagnetic forces are negligibly important in some region very near to the leading edge of the plate, whilst far from the leading edge this sort of forces are significantly dominant. In this study, flow field for the entire region is simulated by applying finite difference method.

6.2 Formulation of the problem

In this work, consideration has been given to unsteady two dimensional magnetohydrodynamic natural convection flow of a viscous incompressible and electrically conducting fluid over a semi infinite vertical flat plate in presence of variable transverse magnetic field with uniform strength B_0. It is also assumed that both the surface temperature and the surface mass concentration oscillate with small amplitude about a mean value. The ambient fluid is maintained at uniform temperature and concentration , T_∞, C_∞ respectively. However, all the thermo- physical fluid properties are considered to be constant and viscous dissipation effect is neglected. Moreover, it is assumed that the ratio of thermal diffusivity and molecular diffusivity to magnetic diffusivity are small enough so that the perturbation can be avoided in the basic normal field. The coordinate system and flow configuration of the problem are shown in figure 6.1. Under the usual Boussinesq approximation along with

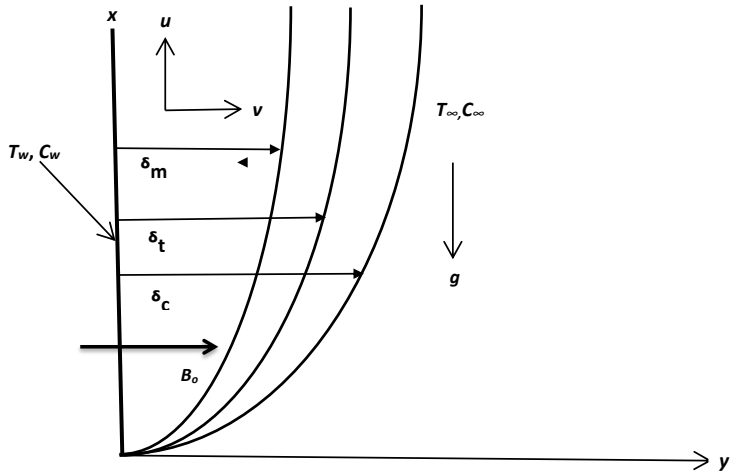

Figure 6.1: Configuration and coordinate of the flow field

the above mentioned assumptions, the boundary layer equations for mass, momentum and energy can be written as:

$$\frac{\partial \bar{u}}{\partial \bar{x}} + \frac{\partial \bar{v}}{\partial \bar{y}} = 0 \tag{6.1}$$

$$\frac{\partial \bar{u}}{\partial t} + \bar{u}\frac{\partial \bar{u}}{\partial \bar{x}} + \bar{v}\frac{\partial \bar{u}}{\partial \bar{y}} = \nu\frac{\partial^2 \bar{u}}{\partial \bar{y}^2} + g\beta_T\bar{T} + g\beta_C\bar{C} - \frac{\sigma_0 B_0^2}{\rho}\bar{u} \tag{6.2}$$

$$\frac{\partial \bar{T}}{\partial t} + u\frac{\partial \bar{T}}{\partial \bar{x}} + v\frac{\partial \bar{T}}{\partial \bar{y}} = \bar{\alpha}\frac{\partial^2 \bar{T}}{\partial \bar{y}^2} \tag{6.3}$$

$$\frac{\partial \bar{C}}{\partial t} + u\frac{\partial \bar{C}}{\partial \bar{x}} + v\frac{\partial \bar{C}}{\partial \bar{y}} = D\frac{\partial^2 \bar{C}}{\partial \bar{y}^2} \tag{6.4}$$

where $\bar{u}$ and $\bar{v}$ are the $\bar{x}$ and $\bar{y}$ components of velocity field, respectively, in the momentum boundary layer; $\bar{T} = T - T_\infty$ and $\bar{C} = C - C_\infty$ is the temperature and concentration in the thermal and concentration boundary layers respectively, ν is the kinematic viscosity of the fluid, σ the electrical conductivity, B_0 is the magnetic field normal to the plate, ρ the density of the fluid, g the acceleration due to gravity, α the thermal diffusivity, D is the molecular diffusivity, β_T, β_C are the coefficients of volume expansion due to temperature and concentration respectively. Associated boundary conditions are:

$$\begin{aligned} &y = 0 : u = v = 0, \quad \bar{T} = T_w, \quad \bar{C} = C_w, \\ &y = \infty : u(x, \infty, t) = v(x, \infty, t) = 0, \quad \bar{T} \to T_\infty, \bar{C} \to C_\infty \end{aligned} \tag{6.5}$$

where, $T_w = \theta_w(x)[1+\varepsilon\,(\exp i\omega t + c.c)]$, $C_w = \phi_w(x)[1+\varepsilon\,(\exp i\omega t + c.c)]$, $\theta_w(x)$ and $\phi_w(x)$ are, respectively the mean surface temperature and mean surface concentration; $\varepsilon(<< 1)$ is the amplitude and ω is the frequency of oscillations in the surface temperature and concentration.

The following dimensionless variables can be introduced to get a set of non dimensional governing equations:

$$\begin{aligned}
&\bar{u} = \frac{\nu G r_L^{1/2}}{L} u,\ \bar{v} = \frac{\nu G r_L^{1/2}}{L} v \\
&y = \frac{G r_L^{1/4}}{L}\bar{y},\ x = \frac{G r_L^{1/4}}{L}\bar{x},\ M = \frac{\sigma B_0^2}{\rho}\frac{L^2}{\nu} G r_L^{-\ 1/2} \\
&x = \frac{\bar{x}}{L},\ Gr_L = \frac{g\beta_T \Delta T L^3}{\nu^2},\ Gr_C = \frac{g\beta_C \Delta C L^3}{\nu^2} \\
&\theta = \frac{T - T_\infty}{T_w - T_\infty},\ \phi = \frac{C - C_\infty}{C_w - C_\infty}
\end{aligned} \tag{6.6}$$

Commencing the above set of non dimensional variables, some of which are dependent and some are independent, the equations (6.1)-(6.4) take the form:

$$\frac{\partial u}{\partial x} + \frac{\partial v}{\partial y} = 0 \tag{6.7}$$

$$\frac{\partial u}{\partial t} + u\frac{\partial u}{\partial x} + v\frac{\partial u}{\partial y} = \nu\frac{\partial^2 u}{\partial y^2} + g\beta_T\theta + g\beta_C\phi - Mu \tag{6.8}$$

$$\frac{\partial \theta}{\partial t} + u\frac{\partial \theta}{\partial x} + v\frac{\partial \theta}{\partial y} = \bar{\alpha}\frac{\partial^2 \theta}{\partial y^2} \tag{6.9}$$

$$\frac{\partial \phi}{\partial t} + u\frac{\partial \phi}{\partial x} + v\frac{\partial \phi}{\partial y} = D\frac{\partial^2 \phi}{\partial y^2} \tag{6.10}$$

" Since the geometry under consideration lacks an obvious length scale, non-dimensional parameters are best considerations with in respect to the distance from the leading edge x. This local variation of parameters reflecting the relative magnitudes of the forces involved at a given station is instrumental in formulating the problem in the form of suitable for numerical integration. In particular, the non-dimensional quantity, $\xi = M^2 x$ represents a local measures of the relative magnetic and buoyancy forces independent of viscous or com-

bined thermal and mass diffusion elements. Consequently, we seek to formulate the problem in terms of this fundamental dimensionless characteristic coordinate. " [65]. Equation (6.5) suggests the solutions of the equations (6.7)-(6.10) to be of the form:

$$\begin{aligned} &u(x,y,t) = u_0(x,y) + \varepsilon\,(\exp i\omega t + c.c)\,u_1(x,y),\;\; v(x,y,t) = v_0(x,y) + \varepsilon\,(\exp i\omega t = c.c)\,v_1(x,y) \\ &\bar{T}(x,y,t) = \theta_w(x,y)\,(\theta_0(x,y) + \varepsilon\,(\exp i\omega t = c.c)\,\theta_1(x,y)) \\ &\bar{C}(x,y,t) = \phi_w(x,y)\,(\phi_0(x,y) + \varepsilon\,(\exp i\omega t + c.c)\,\phi_1(x,y)) \end{aligned} \tag{6.11}$$

where u_0, v_0, θ_0 and ϕ_0 represent the steady mean flow. Considering these form of solutions, the steady mean flow is governed by the following set of equations:

$$\frac{\partial u_0}{\partial x} + \frac{\partial v_0}{\partial y} = 0 \tag{6.12}$$

$$u_0\frac{\partial u_0}{\partial x} + v_0\frac{\partial u_0}{\partial y} = \alpha\frac{\partial^2 u_0}{\partial y^2} + g\beta_T\theta_w(x)\theta_0 + g\beta_C\phi_w(x)\phi_0 - Mu_0 \tag{6.13}$$

$$u_0\frac{\partial \theta_0}{\partial x} + v_0\frac{\partial \theta_0}{\partial y} = \bar{\alpha}\frac{\partial^2 \theta_0}{\partial y^2} \tag{6.14}$$

$$u_0\frac{\partial \phi_0}{\partial x} + v_0\frac{\partial \phi_0}{\partial y} = \bar{\alpha}\frac{\partial^2 \phi_0}{\partial y^2} \tag{6.15}$$

Corresponding boundary conditions are:

$$\begin{aligned} &y = 0 : u_0 = v_0 = 0, \quad \theta_0 = \theta_w(x), \quad \phi_0 = \phi_w(x) \\ &y \to \infty : u_0 \to 0, \quad \theta_0 \to 0, \quad \phi_0 \to 0 \end{aligned} \tag{6.16}$$

The set of differential equations and corresponding boundary conditions, which govern the unsteady flow field are in the form of equations (6.17)-(6.21):

$$\frac{\partial u_1}{\partial x} + \frac{\partial v_1}{\partial y} = 0 \tag{6.17}$$

$$u_0\frac{\partial u_1}{\partial x} + u_1\frac{\partial u_0}{\partial x} + v_0\frac{\partial u_1}{\partial y} + v_1\frac{\partial u_0}{\partial y} + i\omega u_1 = \bar{\alpha}\frac{\partial^2 u_1}{\partial y^2} + g\beta_T\theta_w(x)\theta_1 + g\beta_C\phi_w(x)\phi_1 - Mu_1 \tag{6.18}$$

$$u_0\frac{\partial \theta_1}{\partial x} + u_1\frac{\partial \theta_0}{\partial x} + v_0\frac{\partial \theta_1}{\partial y} + v_1\frac{\partial \theta_0}{\partial y} + i\omega\theta_1 = \bar{\alpha}\frac{\partial^2 \theta_1}{\partial y^2} \tag{6.19}$$

$$u_0\frac{\partial \phi_1}{\partial x} + u_1\frac{\partial \phi_0}{\partial x} + v_0\frac{\partial \phi_1}{\partial y} + v_1\frac{\partial \phi_0}{\partial y} + i\omega\phi_1 = \bar{\alpha}\frac{\partial^2 \phi_1}{\partial y^2} \tag{6.20}$$

$$\begin{aligned} &y = 0 : u_1 = v_1 = 0, \quad \theta_1 = \theta_w(x), \quad \phi_1 = \phi_w(x) \\ &y \to \infty : u_1 \to 0, \quad \theta_1 \to 0, \quad \phi_1 \to 0 \end{aligned} \tag{6.21}$$

In the above equations, the parameters Pr, Sc, St have been introduced. The dimensionless parameter Pr, which is the Prandtl number, represents the ratio of momentum diffusivity to the thermal diffusivity. Sc, which is the Schmidt number, represents the ratio of momentum diffusivity to the momentum diffusivity and $St = \frac{\omega}{M}$ is the frequency parameter. The important quantities which are considered as of the utmost interest, are unsteady shear stress, surface temperature and surface concentration. These quantities can be calculated from the solutions of the equations (6.18)-(6.21) and (6.23)-(6.26). In this present study, these quantities are calculated and presented in terms of amplitude and phase angels. The following expressions are used to calculate the amplitude and phase of regarding quantities.

$$\begin{aligned} &A_u = \sqrt{(f_r'')^2 + (f_i'')^2}|_{\eta=0}, \ A_t = \sqrt{(\theta_r^2) + (\theta_i^2)}|_{\eta=0} \\ &A_c = \sqrt{(\phi_r^2) + (\phi_i^2)}|_{\eta=0} \qquad \text{and} \end{aligned} \tag{6.22}$$

$$\phi_u = \tan^{-1}(\frac{f_i''}{f_r''}),\ \phi_t = \tan^{-1}(\frac{\theta_i}{\theta_r})$$
$$\phi_c = \tan^{-1}(\frac{\phi_i}{\phi_r}) \tag{6.23}$$

where, (f_r, f_i) , (θ_r, θ_i) and (ϕ_r, ϕ_i) represent the real and imaginary part of $f_1(\xi, \eta)$, $\theta_1(\xi, \eta)$ and $\phi_1(\xi, \eta)$ respectively. The solution methodology for different parts of the flow field are discussed in brief in the following section.

6.3 Solution methodology

6.3.1 Steady Flow field

In order to solve the equations (6.12)-(6.16) by using the finite difference method, stream function formulation (SFF) have been implemented. By using, SFF, the dimensionless boundary layer equations (6.12)-(6.16) have been transformed into a system of equations, which are pertinent for the entire regime, i.e. from the leading edge to the downstream region. The following transformations are brought in, which were firstly introduced by Hunt and Wilks [80] for the semi infinite vertical flat plate:

$$\psi = x^{3/4}(1+\xi)^{-1/4}F(\eta, \xi),\quad \eta = x^{-1/4}(1+\xi)^{-1/4}y$$
$$\xi = M^2 x,\quad \theta = \Theta(\eta, \xi),\quad \phi = \Phi(\eta, \xi) \tag{6.24}$$

where ψ is the stream function which satisfy the continuity equation (6.12). With the help of these transformations, the equations (6.12)-(6.16) can be transformed into the following

set of non similarity equations:

$$\frac{\partial^3 F}{\partial \eta^3} + \frac{3+2\xi}{4(1+\xi)} F \frac{\partial^2 F}{\partial \eta^2} - \frac{1}{2(1+\xi)} \left(\frac{\partial F}{\partial \eta}\right)^2 - \xi^{1/2}(1+\xi)^{1/2} \frac{\partial F}{\partial \eta} + (1+\xi)(\Theta + N\Phi) = \xi \left(\frac{\partial F}{\partial \eta}\frac{\partial^2 F}{\partial \xi \partial \eta} - \frac{\partial^2 F}{\partial \eta^2}\frac{\partial F}{\partial \xi}\right) \tag{6.25}$$

$$\frac{1}{Pr}\frac{\partial^2 \Theta}{\partial \eta^2} + \frac{3+2\xi}{4(1+\xi)} F \frac{\partial \Theta}{\partial \eta} = \xi \left(\frac{\partial F}{\partial \eta}\frac{\partial \Theta}{\partial \xi} - \frac{\partial \Theta}{\partial \eta}\frac{\partial F}{\partial \xi}\right) \tag{6.26}$$

$$\frac{1}{Sc}\frac{\partial^2 \Phi}{\partial \eta^2} + \frac{3+2\xi}{4(1+\xi)} F \frac{\partial \Phi}{\partial \eta} = \xi \left(\frac{\partial F}{\partial \eta}\frac{\partial \Phi}{\partial \xi} - \frac{\partial \Phi}{\partial \eta}\frac{\partial F}{\partial \xi}\right) \tag{6.27}$$

Associated boundary conditions are:

$$F(0,\xi) = \frac{\partial F}{\partial \eta}(0,\xi) = 0,\ \Theta(0,\xi) = \Phi(0,\xi) = 1$$
$$\frac{\partial F}{\partial \eta}(\infty,\xi) \to 0,\ \Theta(\infty,\xi) \to\ 0,\ \Phi(\infty,\xi) \to 0 \tag{6.28}$$

For the sake of solving the above set of non-linear, coupled partial differential equations, a new variable $H = \frac{\partial F}{\partial \eta}$ has been introduced so that the above system of equations turned into second order partial differential equations:

$$\frac{\partial^2 H}{\partial \eta^2} + \frac{3+2\xi}{4(1+\xi)} F \frac{\partial H}{\partial \eta} - \frac{1}{2(1+\xi)} H^2 - \xi^{1/2}(1+\xi)^{1/2} H + (1+\xi)(\Theta + N\Phi) = \xi \left(H\frac{\partial H}{\partial \xi} - \frac{\partial H}{\partial \eta}\frac{\partial F}{\partial \xi}\right) \tag{6.29}$$

$$\frac{1}{Pr}\frac{\partial^2 \Theta}{\partial \eta^2} + \frac{3+2\xi}{4(1+\xi)} F \frac{\partial \Theta}{\partial \eta} = \xi \left(H\frac{\partial \Theta}{\partial \xi} - \frac{\partial \Theta}{\partial \eta}\frac{\partial F}{\partial \xi}\right) \tag{6.30}$$

$$\frac{1}{Sc}\frac{\partial^2 \Phi}{\partial \eta^2} + \frac{3+2\xi}{4(1+\xi)} F \frac{\partial \Phi}{\partial \eta} = \xi \left(H\frac{\partial \Phi}{\partial \xi} - \frac{\partial \Phi}{\partial \eta}\frac{\partial F}{\partial \xi}\right) \tag{6.31}$$

Along with the boundary conditions:

$$F(0,\xi) = H(0,\xi) = 0,\ \Theta(0,\xi) = \Phi(0,\xi) = 1$$
$$H(\infty,\xi) \to 0,\ \Theta(\infty,\xi) \to 0,\ \Phi(\infty,\xi) \to 0 \tag{6.32}$$

The above set of equations are discretized for numerical scheme by replacing the partial derivatives with back-ward difference formulas. The resulting momentum equation, energy equation and concentration equation have been turned into system of tri-diagonal algebraic equations. Then these system of equations have been solved by TDMA. The form of the discretized momentum equations (6.29)is given below:

$$
\begin{aligned}
&A_1\ H_{i,j+1} + B_1\ Hi,j + C_1\ H_{i,j-1} = D_1, \quad \text{where} \\
&A_1 = -\left[\frac{1}{(\triangle\eta)^2} + \frac{\left(\frac{3+2\xi}{4(1+\xi)}F_{i,j} + \frac{\xi}{\triangle\xi}(F_{i,j} - F_{i-1,j})\right)}{(2\triangle\eta)}\right] \\
&C_1 = -\left[\frac{1}{(\triangle\eta)^2} - \frac{\left(\frac{3+2\xi}{4(1+\xi)}F_{i,j} + \frac{\xi}{\triangle\xi}(F_{i,j} - F_{i-1,j})\right)}{(2\triangle\eta)}\right] \\
&B_1 = \frac{2}{(\triangle\eta)^2)} + \left(\frac{1}{2(1+\xi)} + \frac{\xi}{\triangle\xi}\right) H_{i,j} + \xi^{1/2}(1+\xi)^{1/2} \\
&D_1 = \frac{\xi}{\triangle\xi}H_{i,j}H_{i-1,j} + (1+\xi)(\Theta_{i,j} + N\Phi_{i,j})
\end{aligned}
\tag{6.33}
$$

For the energy equation (6.30), the discretized equation takes the form:

$$
\begin{aligned}
&A_2\Theta_{i,j+1} + B_2\Theta i,j + C_2\Theta_{i,j-1} = D_2, \quad \text{where} \\
&A_2 = -\left[\frac{1}{Pr\ (\triangle\eta)^2} + \left(\frac{3+2\xi}{4(1+\xi)}F_{i,j} + \frac{\xi}{\triangle\xi}(F_{i,j-F_{i-1,j}})\right)/(2\triangle\eta)\right] \\
&C_2 = -\left[\frac{1}{Pr\ (\triangle\eta)^2} - \left(\frac{3+2\xi}{4(1+\xi)}F_{i,j} + \frac{\xi}{\triangle\xi}(F_{i,j-F_{i-1,j}})\right)/(2\triangle\eta)\right] \\
&B_2 = \frac{2}{Pr(\triangle\eta)^2} + \frac{\xi}{\triangle\xi}H_{i,j},\ D_2 = \frac{\xi}{\triangle\xi}H_{i,j}\Theta_{i-1,j}
\end{aligned}
\tag{6.34}
$$

And for the concentration equation (6.31), the discretized equation takes the form:

$$\begin{aligned}
&A_3\Phi_{i,j+1} + B_3\Phi i,j + C_3\Phi_{i,j-1} = D_3, \quad \text{where} \\
&A_3 = -\left[\frac{1}{Sc\ (\triangle\eta)^2} + \left(\frac{3+2\xi}{4(1+\xi)}F_{i,j} + \frac{\xi}{\triangle\xi}(F_{i,j-F_{i-1,j}})\right)/(2\triangle\eta)\right] \\
&C_3 = -\left[\frac{1}{Sc\ (\triangle\eta)^2} - \left(\frac{3+2\xi}{4(1+\xi)}F_{i,j} + \frac{\xi}{\triangle\xi}(F_{i,j-F_{i-1,j}})\right)/(2\triangle\eta)\right] \\
&B_3 = \frac{2}{Sc(\triangle\eta)^2} + \frac{\xi}{\triangle\xi}H_{i,j},\ D_3 = \frac{\xi}{\triangle\xi}H_{i,j}\Phi_{i-1,j}
\end{aligned} \tag{6.35}$$

Here,$1 \leq i \leq M$ and $2 \leq j \leq M-1$ denote the grid points along the η and ξ directions, respectively. $\triangle\xi = \xi_i - \xi_{i-1}$ is the step size in the i'th direction and $\triangle\eta = \eta_j - \eta_{j-1}$ determines the step size in the j'th direction. Finally $F_{i,j}$ is calculated from the relation:

$$F_{i,j} = F_{i,j-1} + \frac{1}{2}\triangle\eta\ (H_{i,j} + H_{i,j-1})$$

For newly introduced function, corresponding boundary conditions take the form:

$$\begin{aligned}
&F_{i,j} = H_{i,j} = 0,\ \Theta_{i,j} = 1,\ \Phi_{i,j} = 1 \\
&H_{M,j} \to 0,\ \Theta_{M,j} \to 0,\ \Phi_{M,j} \to 0
\end{aligned} \tag{6.36}$$

6.3.2 Fluctuating flow field:

Using the similar set of transformations (equation 6.28) for the unsteady flow field, the following set of equations can be derived from equations (6.17)-(6.21):

$$\frac{\partial^3 f}{\partial \eta^3} + \frac{3+2\xi}{4(1+\xi)}\left(F\frac{\partial^2 f}{\partial \eta^2} + f\frac{\partial^2 F}{\partial \eta^2}\right) - \frac{1}{(1+\xi)}\left(\frac{\partial F}{\partial \eta}\frac{\partial f}{\partial \eta}\right)$$
$$-iSt\ \xi^{1/2}(1+\xi)^{1/2}\frac{\partial f}{\partial \eta} + (1+\xi)(\theta + N\phi) - \xi^{1/2}(1+\xi)^{1/2}\frac{\partial f}{\partial \eta}$$
$$= \xi\left(\frac{\partial f}{\partial \eta}\frac{\partial^2 F}{\partial \eta \partial \xi} + \frac{\partial F}{\partial \eta}\frac{\partial^2 f}{\partial \eta \partial \xi} - \frac{\partial^2 F}{\partial \eta^2}\frac{\partial f}{\partial \xi} - \frac{\partial^2 f}{\partial \eta^2}\frac{\partial F}{\partial \xi}\right) \tag{6.37}$$

$$\frac{1}{Pr}\frac{\partial^2 \theta}{\partial \eta^2} + \frac{3+2\xi}{4(1+\xi)}\left(F\frac{\partial \theta}{\partial \eta} + f\frac{\partial \Theta}{\partial \eta}\right) - iSt\ \xi^{1/2}(1+\xi)^{1/2}\frac{\partial \theta}{\partial \eta}$$
$$= \xi\left(\frac{\partial F}{\partial \eta}\frac{\partial \theta}{\partial \xi} + \frac{\partial f}{\partial \eta}\frac{\partial \Theta}{\partial \xi} - \frac{\partial \theta}{\partial \eta}\frac{\partial F}{\partial \xi} - \frac{\partial \Theta}{\partial \eta}\frac{\partial f}{\partial \xi}\right) \tag{6.38}$$

$$\frac{1}{Sc}\frac{\partial^2 \phi}{\partial \eta^2} + \frac{3+2\xi}{4(1+\xi)}\left(F\frac{\partial \phi}{\partial \eta} + f\frac{\partial \Phi}{\partial \eta}\right) - iSt\ \xi^{1/2}(1+\xi)^{1/2}\frac{\partial \phi}{\partial \eta}$$
$$= \xi\left(\frac{\partial F}{\partial \eta}\frac{\partial \phi}{\partial \xi} + \frac{\partial f}{\partial \eta}\frac{\partial \Phi}{\partial \xi} - \frac{\partial \phi}{\partial \eta}\frac{\partial F}{\partial \xi} - \frac{\partial \Phi}{\partial \eta}\frac{\partial f}{\partial \xi}\right) \tag{6.39}$$

Associated boundary conditions are:

$$f(0,\xi) = \frac{\partial f}{\partial \eta}(0,\xi) = 0, \quad \theta(0,\xi) = \phi(0,\xi) = 1$$
$$\frac{\partial f}{\partial \eta}(\infty,\xi) \to 0, \quad \theta(\infty,\xi) \to 0, \quad \phi(\infty,\xi) \to 0 \tag{6.40}$$

The equations (6.37)-(6.39) can now be decomposed into two sets of equations for representing the real and imaginary part by introducing $\frac{\partial f}{\partial \eta} = U$, and $U = U_R + iU_I$ etc. Then these two sets of equation can be discretized by following the similar approach, that has already been discussed in previous subsection. The discretized form of the equations (6.37)-(6.39) are presented below:

Real part of the Momentum equation:

$$A_{11}UR_{i,j+1} + B_{11}URi,j + C_{11}UR_{i,j-1} = D_{11}, \quad \text{where}$$

$$A_{11} = -\left[\frac{1}{(\triangle\eta)^2} + \frac{\left(\frac{3+2\xi}{4(1+\xi)}V_{i,j} + \xi\ VX\right)}{(2\triangle\eta)}\right]$$

$$C_{11} = -\left[\frac{1}{(\triangle\eta)^2} - \frac{\left(\frac{3+2\xi}{4(1+\xi)}V_{i,j} + \xi\ VX\right)}{(2\triangle\eta)}\right]$$

$$B_{11} = \frac{2}{(\triangle\eta)^2)} + \left(\frac{1}{(1+\xi)} + \frac{\xi}{\triangle\xi}\right)UR_{i,j} + \xi^{1/2}(1+\xi)^{1/2} - \xi\ UX$$

$$D_{11} = \frac{\xi}{\triangle\xi}\left(U_{i,j}UR_{i-1,j} + UY(VR_{i,j} - VR_{i-1,j})\right) + (1+\xi)(\theta R_{i,j} + N\phi R_{i,j})$$
$$+ \xi^{1/2}(1+\xi)^{1/2}\ St\ UI_{i,j} + \frac{3+2\xi}{4(1+\xi)}UY\ VR_{i,j} \qquad (6.41)$$

Imaginary part of the Momentum equation:

$$A_{12}\ UI_{i,j+1} + B_{12}UIi,j + C_{12}UI_{i,j-1} = D_{12}, \quad \text{where}$$

$$A_{12} = -\left[\frac{1}{(\triangle\eta)^2} + \frac{\left(\frac{3+2\xi}{4(1+\xi)}V_{i,j} + \xi\ VX\right)}{(2\triangle\eta)}\right]$$

$$C_{12} = -\left[\frac{1}{(\triangle\eta)^2} - \frac{\left(\frac{3+2\xi}{4(1+\xi)}V_{i,j} + \xi\ VX\right)}{(2\triangle\eta)}\right]$$

$$B_{12} = \frac{2}{(\triangle\eta)^2)} + \left(\frac{1}{(1+\xi)} + \frac{\xi}{\triangle\xi}\right)UR_{i,j} + \xi^{1/2}(1+\xi)^{1/2} - \xi\ UX$$

$$D_{12} = \frac{\xi}{\triangle\xi}\left(U_{i,j}UR_{i-1,j} + UY(VI_{i,j} - VI_{i-1,j})\right) + (1+\xi)(\theta I_{i,j} + N\phi I_{i,j})$$
$$- \xi^{1/2}(1+\xi)^{1/2}\ St\ UR_{i,j} + \frac{3+2\xi}{4(1+\xi)}UY\ VI_{i,j} \qquad (6.42)$$

Real part of the Energy equation:

$$
\begin{aligned}
&A_{21}\theta R_{i,j+1} + B_{21}\theta Ri,j + C_{21}\theta R_{i,j-1} = D_{21}, \quad \text{where} \\
&A_{21} = -\left[\frac{1}{Pr\ (\triangle\eta)^2} + \left(\frac{3+2\xi}{4(1+\xi)}V_{i,j} + \xi\ VX\right)/(2\triangle\eta)\right] \\
&C_{21} = -\left[\frac{1}{Pr\ (\triangle\eta)^2} - \left(\frac{3+2\xi}{4(1+\xi)}V_{i,j} + \xi\ VX\right)/(2\triangle\eta)\right] \\
&B_{21} = \frac{2}{Pr(\triangle\eta)^2} + \frac{\xi}{\triangle\xi}U_{i,j} \\
&D_{21} = \frac{\xi}{\triangle\xi}U_{i,j}\theta R_{i-1,j} + \frac{\xi}{\triangle\xi}TY(VR_{i,j} - VR_{i-1,j}) \\
&\qquad\qquad + \xi^{1/2}(1+\xi)^{1/2}\ St\ \theta I_{i,j} + \xi\ UR_{i,j}\ TX
\end{aligned} \tag{6.43}
$$

Imaginary part of the Energy equation:

$$
\begin{aligned}
&A_{22}\theta I_{i,j+1} + B_{22}\theta Ii,j + C_{22}\theta I_{i,j-1} = D_{22}, \quad \text{where} \\
&A_{22} = -\left[\frac{1}{Pr\ (\triangle\eta)^2} + \left(\frac{3+2\xi}{4(1+\xi)}V_{i,j} + \xi\ VX\right)/(2\triangle\eta)\right] \\
&C_{22} = -\left[\frac{1}{Pr\ (\triangle\eta)^2} - \left(\frac{3+2\xi}{4(1+\xi)}V_{i,j} + \xi\ VX\right)/(2\triangle\eta)\right] \\
&B_{22} = \frac{2}{Pr(\triangle\eta)^2} + \frac{\xi}{\triangle\xi}U_{i,j}
\end{aligned} \tag{6.44}
$$

$$
\begin{aligned}
&D_{22} = \frac{\xi}{\triangle\xi}U_{i,j}\theta I_{i-1,j} + \frac{\xi}{\triangle\xi}TY(VI_{i,j} - VI_{i-1,j}) \\
&\qquad\qquad + \xi^{1/2}(1+\xi)^{1/2}\ St\ \theta I_{i,j} + \xi\ UI_{i,j}\ TX
\end{aligned} \tag{6.45}
$$

Real part of the concentration equation:

$$
\begin{aligned}
&A_{31}\phi R_{i,j+1} + B_{31}\phi R_{i,j} + C_{31}\phi R_{i,j-1} = D_{31}, \quad \text{where} \\
&A_{31} = -\left[\frac{1}{Sc\ (\triangle\eta)^2} + \left(\frac{3+2\xi}{4(1+\xi)}V_{i,j} + \xi\ VX\right)/(2\triangle\eta)\right] \\
&C_{31} = -\left[\frac{1}{Sc\ (\triangle\eta)^2} - \left(\frac{3+2\xi}{4(1+\xi)}V_{i,j} + \xi\ VX/\right)(2\triangle\eta)\right] \\
&B_{31} = \frac{2}{Pr(\triangle\eta)^2} + \frac{\xi}{\triangle\xi}U_{i,j} \\
&D_{31} = \frac{\xi}{\triangle\xi}U_{i,j}\phi R_{i-1,j} + \frac{\xi}{\triangle\xi}TY(VR_{i,j} - VR_{i-1,j}) \\
&\qquad\qquad + \xi^{1/2}(1+\xi)^{1/2}\ St\ \phi I_{i,j} + \xi\ UR_{i,j}\ CX
\end{aligned} \tag{6.46}
$$

Imaginary part of the Concentration equation:

$$
\begin{aligned}
&A_{32}\phi I_{i,j+1} + B_{32}\phi I_{i,j} + C_{32}\phi I_{i,j-1} = D_{32}, \quad \text{where} \\
&A_{32} = -\left[\frac{1}{Sc\ (\triangle\eta)^2} + \frac{3+2\xi}{4(1+\xi)}V_{i,j}/(2\triangle\eta)\right] \\
&C_{32} = -\left[\frac{1}{Sc\ (\triangle\eta)^2} - \frac{3+2\xi}{4(1+\xi)}V_{i,j}/(2\triangle\eta)\right] \\
&B_{32} = \frac{2}{Sc(\triangle\eta)^2} + \frac{\xi}{\triangle\xi}U_{i,j} + \frac{1}{2(1+\xi)}U_{i,j} \\
&D_{32} = \frac{\xi}{\triangle\xi}U_{i,j}\phi I_{i-1,j} + \frac{\xi}{\triangle\xi}TY(VI_{i,j} - VI_{i-1,j}) \\
&\qquad\qquad - \xi^{1/2}(1+\xi)^{1/2}\ St\ \phi R_{i,j}\xi\ UI_{i,j}\ CX
\end{aligned} \tag{6.47}
$$

The solution procedures of the above sets of discretized equations (6.41)-(6.43) are exactly similar to which is described in chapter 5.

6.4 Results and discussion

In this present study, the conjugate effect of thermal and mass diffusion on natural convection flow has been elucidated by numerical simulations in presence of a strong cross magnetic field. As boundary condition, the surface velocity, temperature and concentration are assumed to be of small amplitude oscillation. The form of this type of boundary

condition suggests the decomposition of the governing equations into two parts which are time dependent and time independent respectively. In this present investigation, these two sets of equations are simulated separately. Since the solutions of time dependent set of equations are coupled with the time independent ones, the equations governing the steady state flow is solved firstly, then the simulated results are considered as known values while the unsteady set of equations are solved. Stream function formulation has been implemented in order to convert the governing equations for both steady and unsteady part into nonsimilar equations. Then the equations are solved via implicit finite difference method along with tridiagonal solver. All the important parameters, for example, the buoyancy ratio parameter w, the Prandtl numberPr, the Schmidt number Sc, the Strouhal number, St have been taken into consideration and extensive simulations carried out so that the insight of the flow field in conjunction with heat and mass transfer can be revealed. Throughout the simulations, the values of Prandtl number and Schmidt number are chosen both small and large. For the steady case, the values of Schmidt numbers have chosen comparatively small, ranging from 0.22 to 1.76. For the unsteady case, the values of Pr is taken relatively small while the values of Sc were varying from 10 to 50. This is because, combination of small Prandtl number and higher Schmidt number represents the liquid metals. The liquid metals have significant industrial and technical applications. Since the liquid metals are non flammable, non-toxic and environmental friendly, these are used in source exchanger, electronic pumps, ambient heat exchanger as well as the fuel of heat engines. Sodium-alloys, bismuth, lead-bismuth are used in nuclear plant as heat transfer fluids. Moreover, mercury play a vital role as heat reducer in reactor plant. Presently, the smallest value of Pr has been chosen 0.054 which represents the lithium [65]- [67].

At the very outset of the investigations, in order to validate the present numerical simulations, the results are produced similar to [65], by considering the similar assumption and comparative results are presented in Table 6.1. Hunt and Wilks [80] studied the same problem considering no mass diffusion and Sadia *et al.* [65]- [67] extended the problem considering mass diffusion along with thermal diffusion. In both the cases, the surface temperature and concentration are considered as constants respectively. Here, the heat

Table 6.1: Values of the shear stress and heat transfer, for the steady flow, obtained by finite difference method, while, Pr=0.7, N=0.0.

ξ	Skin friction coefficient			Heat transfer coefficient		
	Wilks	Sadia *et al.* [66]	Present	Wilks	Sadia *et al.* [66]	Present
0.01	0.3447	0.3441	0.3449	1.2962	1.2972	1.2924
0.05	0.4953	0.4923	0.4908	0.8412	0.8404	0.8459
0.10	0.5722	0.5645	0.5683	0.6919	0.6909	0.6914
0.20	0.6544	0.6380	0.6391	0.5641	0.5610	0.5680
1.00	0.7654	0.7189	0.7127	0.4227	0.4147	0.4133
2.00	0.8459	0.8471	0.8588	0.3335	0.3334	0.3315
4.00	0.9184	0.9169	0.9170	0.2581	0.2582	0.2576
6.00	1.0101	1.0125	1.0170	0.1647	0.1649	0.1603
8.00	1.0288	1.0319	1.0356	0.1452	0.1455	0.1469
10.00	1.0418	1.0456	1.0430	0.1314	0.1317	0.1320
12.00	1.0515	1.0560	1.0547	0.1209	0.1212	0.1263
14.00	1.0591	1.0641	1.0647	0.1209	0.1212	0.1233
16.00	1.0651	1.0708	1.0765	0.1059	0.1062	0.1047

transfer, mass transfer and the shear stress are observed in presence of small amplitude oscillations at the surface with the regarding quantities.

6.4.1 Steady flow field

It has been mentioned earlier that the parametric studies for both steady and unsteady flow fields are carried out and results are presented both in tabular and graphical forms. Some numerical values of shear stress, heat transfer and mass transfer are listed in Table 6.2 against the values of ξ for two different values of Sc=1.76 and 0.22 which corresponds to benzene and carbondioxide respectively. The values of Pr and the buoyancy ratio parameter w were taken 0.7 and 0.5 respectively. From the table it can be observed that, for higher values of ξ, i.e. as it is marched towards the down stream the values of both heat transfer and mass transfer coefficients get smaller where as the values of shear stress become higher. The values of mass transfer coefficient get enhanced because of the increment of the values of Sc and heat transfer coefficients diminishes as it is expected. Figure 6.2-6.3 presents the effects of Pr, Sc and N on heat transfer and mass transfer. During the study of effect

Table 6.2: Values of the shear stress, heat transfer, and Mass transfer for the steady flow, obtained by finite difference method for Sc=1.76, 0.22, while, Pr=0.7,N=0.5.

ξ	Sc=1.76			Sc=0.22		
	Shear stress	Heat Transfer	Mass Transfer	Shear stress	Heat transfer	Mass transfer
0.1004	0.8443	0.5973	0.5991	0.8611	0.5197	0.4303
0.2008	0.9652	0.4566	0.4707	0.9853	0.4006	0.3242
0.3012	1.0379	0.3925	0.4123	1.0601	0.3465	0.2760
0.4016	1.0892	0.3536	0.3770	1.1128	0.3137	0.2466
0.5020	1.1282	0.3266	0.3526	1.1528	0.2909	0.2263
0.6024	1.1591	0.3064	0.3344	1.1845	0.2739	0.2110
0.7028	1.1843	0.2905	0.3201	1.2103	0.260	0.1990
0.8032	1.205	0.2775	0.3085	1.2318	0.2495	0.1892
0.9036	1.2233	0.2666	0.2987	1.2499	0.2402	0.1810
1.0040	1.2387	0.2573	0.2903	1.2655	0.2323	0.1740
3.0120	1.3595	0.1789	0.2185	1.3842	0.1650	0.1161
5.0201	1.3932	0.1518	0.1917	1.4096	0.1457	0.1004
7.0281	1.4099	0.1364	0.1758	1.4233	0.1334	0.0908
9.0361	1.4203	0.1261	0.1647	1.4345	0.1222	0.0823
15.0602	1.4373	0.1078	0.1441	1.4468	0.1082	0.0718
17.0683	1.4408	0.1037	0.1394	1.4523	0.1012	0.0667
20.0803	1.4449	0.0988	0.1336	1.4550	0.0971	0.0640

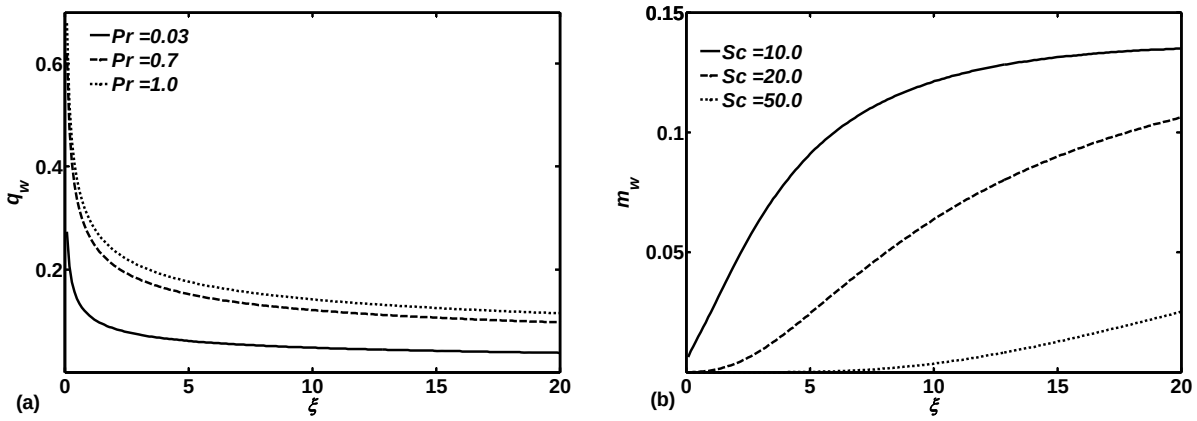

Figure 6.2: (a) Heat transfer, (b) mass transfer of steady flow field for different values of Pr, and Sc respectively, while, w=0.5.

of Prandtl number on heat transfer, the values of other parameters are kept constant. In this case, the value of Sc is taken 10.0, the buoyancy ratio parameter N is chosen 0.5 and the values of Pr are taken 0.03, 0.7 and 1.0 which represents liquid metals, air at 20^0 C at 1 atm. pressure and water respectively. Figures 6.2(a) and 6.2(b) show the

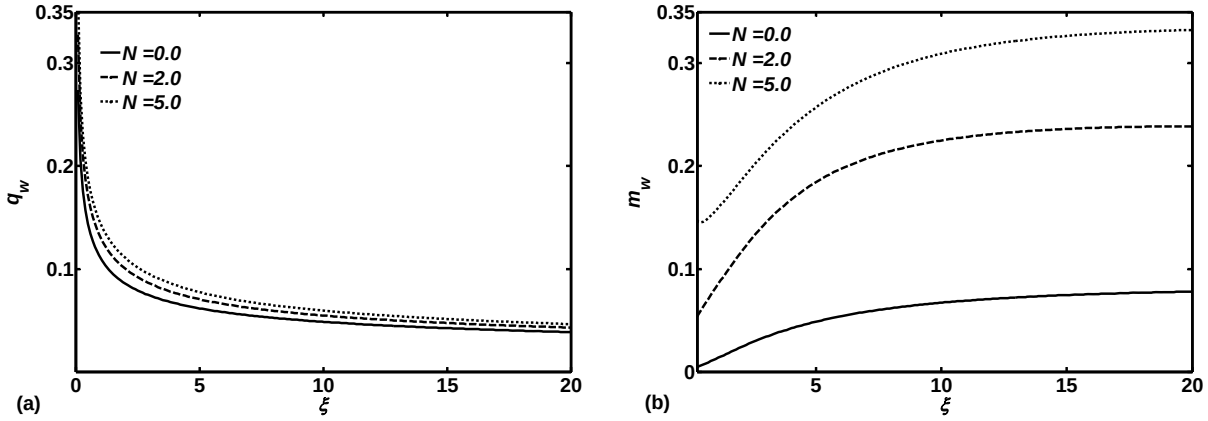

Figure 6.3: (a) Heat transfer, (b) Mass transfer of steady flow field for different values of N, while, Pr=0.054, Sc=10.0.

effect of different Prandtl number on heat transfer and Schimdt number on mass transfer respectively. For studying the effects of Prandtl number on heat transfer, different values of Prandtl numbers are chosen representing liquid metals, air and water where as during the case of Schimdt number a combination of lower Prandtl number and relatively higher values of Schmidt number (10 to 50)have been chosen. This is because small Prandtl number and

large Schmidt number is the usual characteristic of liquid metals. Since, now a days liquid metals are one of the most important component, specially in nuclear power plants and heat exchanger, this type of combinations are made for investigation. From the graphs it can be observed that the increment of both Prandtl number and Schmidt number leads to declination of heat and mass transfer respectively.

Figures 6.3(a) and 6.3(b) present the effect of buoyancy ratio parameter N on heat and mass transfer. From the graphs it can be inferred that, as the values of N goes higher the values of both heat and mass transfer increase. The value of N=0.0 indicates that the flow field is solely dominated by thermal diffusion where as the other values of N ensure the combined buoyancy force due to thermal and mass diffusion and positive values of N indicates that the upward buoyancy force near the surface becomes more dominant.

6.4.2 Fluctuating flow field

The governing equations of the unsteady flow field are also solved by the implicit finite difference method for the entire regime and the results are expressed in terms of amplitude and phase angles of heat transfer, mass transfer and shear stress as these quantities have great interest from engineering point of view. Likewise the steady flow, here also parametric studies have been carried out broadly. The new dimensionless frequency parameter, Strouhal number, St has been commenced here in order to characterize the unsteadiness and oscillation of the flow field in presence of magnetic field.

In the Table 6.3, some values of amplitude and phase angles of shear stress, heat transfer and mass transfer are listed against the locally varying parameter ξ. Tridiagonal matrix solver is used to solve the discretized equations. Starting from zero, ξ is stride out till 50 and iterations are carried out till the difference between two successive iterated results that are smaller than 10^{-6}. Results on the table show that the amplitudes of heat transfer, mass transfer and shear stress increase along with the values of ξ. The phase angles of both heat and mass transfer approach towards the asymptotic value 45^0. Near the very leading edge, i.e. for very very small values of ξ some undulation of the values of the phase angles can be observed but as the values of ξ become higher, the corresponding values of phase angle

Table 6.3: Values of the amplitude and phase angles of shear stress, heat transfer, and mass transfer for the unsteady flow obtained by finite difference method, while, Pr=0.7, Sc=0.60, N=0.5,N=0.5, St=0.5.

ξ	Heat Transfer		Mass Transfer		Shear stress	
	Amplitude	Phase angles	Amplitude	Phase angles	Amplitude	Phase angles
0.0000	0.0489	0.0000	0.0474	0.0000	1.2475	0.0000
0.1010	0.3481	44.6099	0.5480	47.2802	1.0575	13.1416
0.2020	0.4211	45.1063	0.6525	45.6489	1.0821	15.1466
0.3030	0.4737	45.0457	0.7371	44.6980	1.1146	16.5484
0.4040	0.5186	44.8199	0.8138	44.6173	1.1495	17.8173
0.5051	0.5596	44.7434	0.8761	44.7876	1.1869	18.8600
0.6061	0.5960	44.7926	0.9324	44.7689	1.2237	19.7017
0.7071	0.6293	44.8154	0.9844	44.8291	1.2598	20.3999
0.8081	0.6603	44.8387	1.0325	44.8295	1.2945	20.9779
0.9091	0.6894	44.8554	1.0781	44.8534	1.3281	21.4760
1.0101	0.7171	44.8702	1.1212	44.8597	1.3606	21.8987
3.5354	1.2017	44.9527	1.8787	44.9308	1.9768	25.0809
5.0505	1.4116	44.9582	2.2069	44.9300	2.2589	25.4179
7.0707	1.6499	44.9586	2.5794	44.9223	2.5854	25.6126
9.0909	1.8576	44.9561	2.9040	44.9116	2.8740	25.7119
13.0303	2.2068	44.9479	3.4500	44.8877	3.3647	25.8205
16.0606	2.4416	44.9406	3.8169	44.8681	3.6971	25.8772
18.0808	2.5863	44.9354	4.0431	44.8547	3.9025	25.9098
20.0000	2.7166	44.9303	4.2468	44.8419	4.0878	25.9386

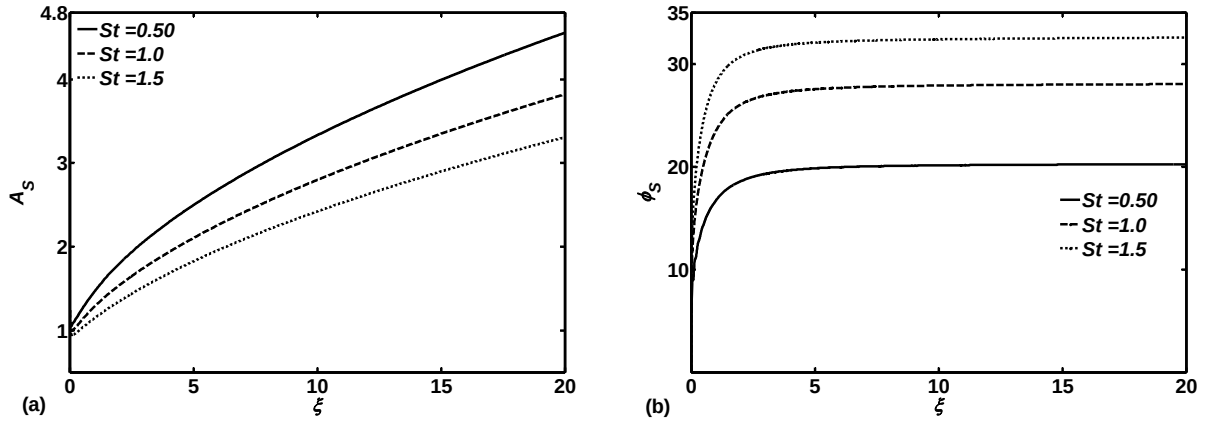

Figure 6.4: (a) Amplitude, (b) Phase angles of shear stress for different values of St, while, Pr=0.054, Sc=10.0, N=0.5.

tends to the regarding asymptotic value.

The effects of Prandtl number Pr on the heat transfer is picturised in Figure 6.4. To depict this effect the simulations are done with Sc=10.0,N=0.5,St=0.5. Both the values of amplitude and phase angles of heat transfer enhanced with the values of Pr. The values of phase angles do not vary much along with the variations of the values of ξ and Pr.

Figure 6.5 shows the effect of Sc on mass transfer. During these simulations, the combinations of Pr and Sc are made to represent the liquid metals. It can be observed from the figures that similar to Pr here also the amplitude of the mass transfer coefficient increase with the increment of the value of Sc. The values of the phase angle of mass transfer do not vary much with the variation of the values of Sc but for the higher value of Sc, near the leading edge small fluctuation can be detected but as it is headed for the downstream, the corresponding values reach to it's asymptotic value which is 45^0.

Figures 6.6-6.8 explicate the effect of Strouhal number St on shear stress, heat transfer and mass transfer respectively. The figure (6.6) clearly illustrates that, for lower St, higher amplitude of shear stress is found and the values increase monotonically as the locally varying parameter ξ is increased. But highest value of phase angle is achieved for the highest value of St, i.e. as the value of St goes up, the values of the phase angle are also boosted up. For both the heat transfer and mass transfer cases, it can be concluded from the figures that, the values of the amplitude of the heat transfer and mass transfer coefficients attain

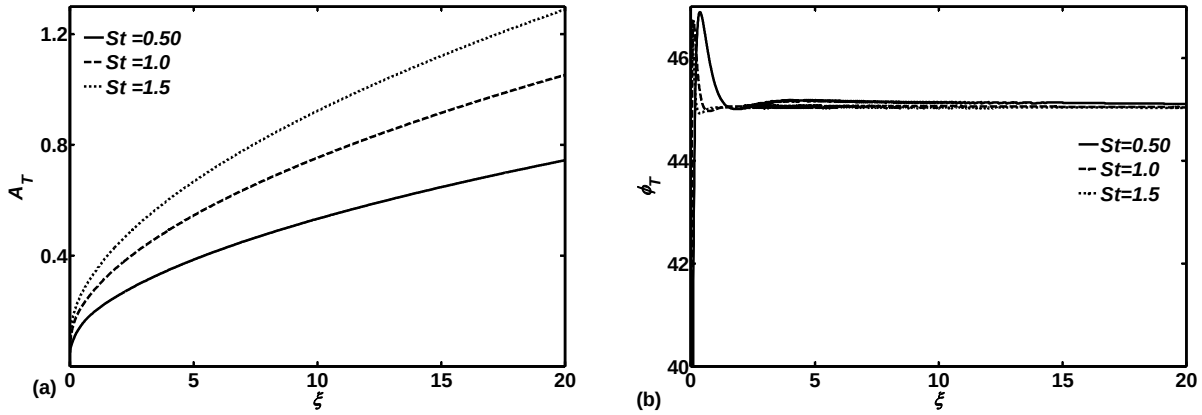

Figure 6.5: (a) Amplitude, (b) Phase angles of heat transfer for different values of St, while, Pr=0.054, Sc=10.0, N=0.5.

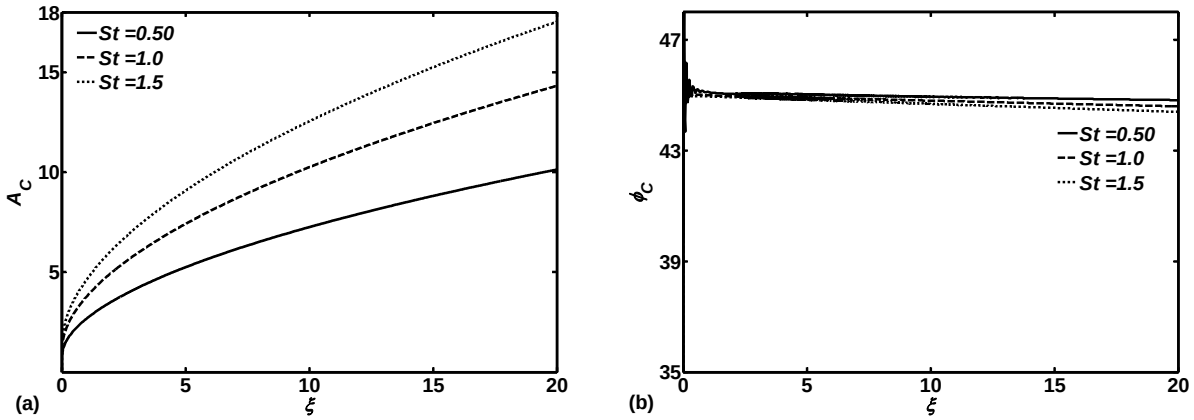

Figure 6.6: (a) Amplitude, (b) Phase angles of mass transfer for different values of St, while, Pr=0.054, Sc=10.0, N=0.5.

the higher values as St is raised up. For the liquid metal case, it can also be noted that the values of mass transfer is larger than the heat transfer though the patterns are similar. For both circumstances, the values of phase angle once again arrive at their asymptotic value.

Finally, Figure 6.9 depicts the effect of N on shear stress. Here only the positive values of N have been taken into account which serve the higher upward buoyancy than the downward buoyancy in the leading edge. From the graphs it can be detected that higher the values of N, higher the value of amplitude of shear stress is. For relatively higher values of$N$ little swinging of the values of both amplitude and phase angle can be noted near the leading edge but for higher values of ξ, the values get stable and start increasing along with

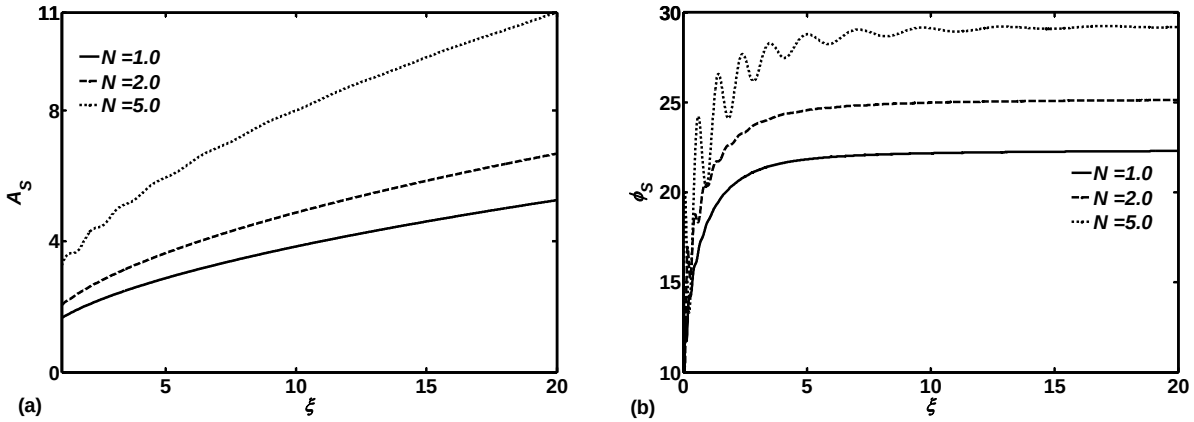

Figure 6.7: (a) Amplitude, (b) Phase angles of shear stress for different values of N, while, Pr=0.054, Sc=10.0, St=0.5.

the increment of ξ.

6.5 Summary

The aim of the present work is to study both the steady and unsteady natural convection flow in presence of strong cross magnetic field. Moreover, time dependent boundary conditions have been imposed on free stream velocity, surface heat transfer and surface mass concentration. All-encompassing parametric studies have revealed the following important points regarding this type of flow:

- For both the steady and unsteady cases, increment of the values of Prandtl number Pr enhance the heat transfer rate. For unsteady case, asymptotic values for both the amplitude and phase angles can be achieved as the simulations march towards the trail edge of the flow field.

- Mass transfer rate is increased along with the increment of the values of Schmidt number Sc. In this case also, the asymptotic values of the phase angle of the mass transfer rate, which is 45^0 is attained right after the leading edge.

- Study of the dimensionless frequency parameter St shows that both the heat transfer and mass transfer rate is enhanced due to the enhancement of the values of St whilst

both the amplitude and phase angles of shear stress is decreased due to the increment of *St*.

- Only the positive values of N have been taken into account and it is worth noting that higher the values of N, the values of amplitude and phase angles of shear stress also become higher.

Chapter 7

Heat and mass transfer response along horizontal circular heated cylinder for mixed convection flow

7.1 Introduction

Both in natural and artificial flow situation, there is almost always unsteadiness occurs and examples of unsteady free and mixed convection flow are in abundant. In natural convection flow, the fluid movement is created by the warm fluid itself and also a process in which the fluid motion is occurred by buoyancy effects. Buoyancy forces arise due to density gradients within the fluid caused by the temperature field itself. The transport processes due to double diffusion occurs both in nature and many engineering applications. Some very important examples of engineering applications of double diffusive flow include chemical reactions in reactor chamber, chemical vapor deposition of solid layers, combustion of atomized liquid fuels and dehydration operations in chemical and foundry plants etc. Recent significant development in computing techniques and tools have opened up a new horizon in studying fluid flow problems which are involved with some complicated geometry. These type of fluid flow have considerable involvement with the interaction of applicable phenomena. For example, flow over tubes in nuclear reactors and cylindrical

heating elements are very much related to the free convection over vertical or horizontally placed cylinders. Though in nature and many engineering applications, double diffusive flow occurs frequently, less attention has been given to the study of unsteady flow due to double diffusion. Moreover, only the search of similarity solutions have attracted much attention. This is because similarity formulation transform easily the transport equations into a set of ordinary differential equations which can be solved numerically for different values of the parameters involved.

This present study is devoted to investigate unsteady, double diffusive, mixed convective flow along an infinite horizontal cylinder. Alike to any double diffusive study, the governing equations of the flow field is simulated for two different diffusive parameters, Pr and Sc. The values of these two parameters depend on the nature of the fluid and on the physical mechanisms governing the diffusion of the heat and chemical species. As the most important fluids are atmospheric air and water, most of the results that have been produced here is calculated by taking the value of $Pr = 0.71$ against ξ and Sc is chosen as 0.22 (due to presence of H_2 as the chemical species). To derive the governing equations, the boussinesq approximations are made, that is, it is assumed that the fluid property variations are limited to firstly the density which is taken into account only in so far as its effects the buoyancy term and secondly the viscosity. Based on the conservation principle, the governing equations are expressed in terms of vorticity, stream function, energy equation and concentration equation. During the numerical computation, similar solutions of [82] and [83] are produced and compared with the present results to validate the model simulation.

7.2 Formulation of the problem

In this work, consideration has been given to unsteady two dimensional mixed convection flow of a viscous incompressible fluid over a circular cylinder. The cylinder is considered as heated and placed horizontally in a uniform stream with its axis perpendicular to the oncoming flow direction. The cylinder surface has maintained with isothermal and isoconcentration surface with constant temperature T_s and concentration C_s. The ambient

fluid is maintained at uniform temperature and concentration, T_∞, C_∞ respectively and free stream velocity is taken as U_∞. However, all the thermo- physical fluid properties are considered to be constant and viscous dissipation effect is neglected. The flow configuration of the problem and the coordinate system is shown in figure 7.1.

Under the usual Boussinesq approximation together with the above assumptions, the

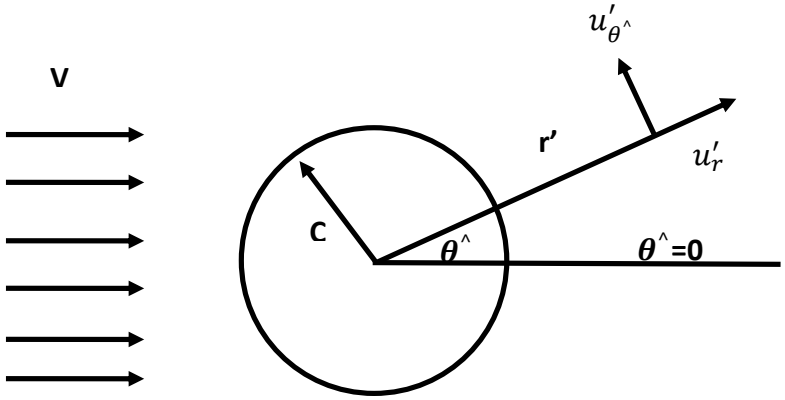

Figure 7.1: Configuration of the model

conservation equations for mass, momentum , energy and concentration can be written as:

$$\nabla^2 \Psi = -\Omega \tag{7.1}$$

$$\begin{aligned} \frac{\partial \zeta'}{\partial t'} + v'_{r'}\frac{\partial \zeta'}{\partial r'} + \frac{v_{\hat{\theta}'}}{r'}\frac{\partial \zeta'}{\partial \hat{\theta}} &= \nu \nabla^2 \zeta' \\ -\left(\frac{1}{\rho}\right)\left(\frac{\partial F_{\hat{\theta}}}{\partial r'} - \frac{1}{r'}\frac{\partial F_r}{\partial \hat{\theta}} + \frac{F_{\hat{\theta}}}{r'} + \frac{\partial M_{\hat{\theta}}}{\partial r'} - \frac{1}{r'}\frac{\partial M_r}{\partial \hat{\theta}} + \frac{M_{\hat{\theta}}}{r'}\right) & \end{aligned} \tag{7.2}$$

$$\zeta' = \nabla^2 \Psi' \tag{7.3}$$

$$\frac{\partial T}{\partial t'} + v'_{r'}\frac{\partial T}{\partial r'} + \frac{v_{\hat{\theta}'}}{r'}\frac{\partial T}{\partial \hat{\theta}} = \left(\frac{\kappa}{\rho c_p}\right)\nabla^2 T \tag{7.4}$$

$$\frac{\partial C}{\partial t'} + v'_{r'}\frac{\partial C}{\partial r'} + \frac{v_{\hat{\theta}}}{r'}\frac{\partial C}{\partial \hat{\theta}} = \left(\frac{\mu}{\rho c_m}\right)\nabla^2 C \tag{7.5}$$

where,

$$\nabla^2 = \frac{\partial^2}{\partial r'^2} + \frac{1}{r'}\frac{\partial}{\partial r'} + \frac{1}{r'^2}\frac{\partial^2}{\partial \hat{\theta}^2} \tag{7.6}$$

and

$$v'_{r'} = \frac{1}{r'}\frac{\partial \Psi'}{\partial \hat{\theta}}, \quad v'_{\hat{\theta}} = -\frac{\partial \Psi'}{\partial r'} \tag{7.7}$$

In the above set of equations, t' is the time, $v'_{r'}$ and $v'_{\hat{\theta}}$ are the velocities in the r' and $\hat{\theta}$ directions. All other Greek symbols, for example, $\nu,\ \kappa,\ ,\mu,\ \rho$ stands for kinematic viscosity, thermal conductivity, molecular conductivity and density respectively. $c_p,\ c_m$ represent the specific heat and specific concentration respectively. $F_{r'}$ and $F_{\hat{\theta}}$ are the radial and transverse components of the body force due to thermal diffusion and $M_{r'}$ and $M_{\hat{\theta}}$ are due to molecular diffusion which are defined in the following forms:

$$\begin{aligned} F_{r'} &= \rho g \beta_T (T - T_\infty) \sin\hat{\theta}, \quad F_{\hat{\theta}} = \rho g \beta (T - T_\infty) \cos\hat{\theta} \\ M_{r'} &= \rho g \beta_C (C - C_\infty) \sin\hat{\theta}, \quad M_{\hat{\theta}} = \rho g \beta (C - C_\infty) \cos\hat{\theta} \end{aligned} \tag{7.8}$$

For determining the boundary conditions, only half of the plane can be considered. This is because, flow is symmetric about a vertical plane passing through the axis of the cylinder. The following boundary conditions should be satisfied accordingly:

$$\begin{aligned} &u = v = \Psi = 0, \quad \Omega = -\frac{\partial^2 \Psi}{\partial r^2} \\ &T = 1,\ C = 1 \ \text{ on the cylinder surface and} \\ &\Psi = v = \Omega = \frac{\partial T}{\partial \hat{\theta}} = \frac{\partial C}{\partial \hat{\theta}} = 0 \ \text{ on the lines of symmetry} \end{aligned} \tag{7.9}$$

Moreover, the following conditions are derived in the inflow and outflow region respectively:

$$\begin{aligned} v = \frac{\partial \Psi}{\partial r'} = 0 = T = C, \quad \Omega = -\frac{1}{r'^2}\frac{\partial^2 \Psi}{\partial \hat{\theta}^2} \\ v = \frac{\partial \Psi}{\partial r'} = 0, \quad \Omega = -\frac{1}{r^2}\frac{\partial^2 \Psi}{\partial \hat{\theta}^2} \end{aligned} \tag{7.10}$$

The vorticity Ω and the stream function Ψ are related to the velocity field by:

$$\Omega = -\frac{1}{r'}\left(r'\frac{\partial v'}{\partial r'} + v' - \frac{\partial u'}{\partial \hat{\theta}}\right) \tag{7.11}$$

The following relation is defined to understand the correlation between the vorticity ζ', stream function Ψ' :

$$\zeta' = -\frac{1}{r'}\left(r'\frac{\partial v_{\hat{\theta}'}}{\partial r'} + v_{\hat{\theta}} - \frac{\partial v'_r}{\partial \hat{\theta}}\right) \tag{7.12}$$

In order to make the above set of equations, dimensionless, the following dimensionless quantities have been introduced:

$$\begin{aligned} v_r = \frac{v'_{r'}}{V},\ v_\theta = \frac{v'_\theta}{V},\ r = \frac{r'}{a},\ t = t'\frac{V}{a}, \Psi = \frac{\Psi'}{aV} \\ \zeta = \zeta'\frac{a}{V},\ \phi = \left(\frac{T - T_\infty}{T_w - T_\infty}\right),\ \varphi = \left(\frac{C - C_\infty}{C_w - C_\infty}\right) \end{aligned} \tag{7.13}$$

The velocity of the free stream has been considered as V. Introducing this dimensionless quantities, the transformed equations can be found as:

$$\begin{aligned} \frac{\partial \zeta}{\partial t} + v_r\frac{\partial \zeta}{\partial r} + \frac{v_{\hat{\theta}}}{r}\frac{\partial \zeta}{\partial \hat{\theta}} = \left(\frac{2}{Re}\right)\nabla^2\zeta \\ -\frac{Gr}{2Re^2}\left(\cos\hat{\theta}\frac{\partial \phi}{\partial r} - \frac{\sin\hat{\theta}}{r}\frac{\partial \phi}{\partial \hat{\theta}} + \cos\hat{\theta}\frac{\partial \varphi}{\partial r} - \frac{\sin\hat{\theta}}{r}\frac{\partial \varphi}{\partial \hat{\theta}}\right) \end{aligned} \tag{7.14}$$

$$\frac{\partial \phi}{\partial t} + v_r\frac{\partial \zeta}{\partial r} + \frac{v_{\hat{\theta}}}{r}\frac{\partial \phi}{\partial \hat{\theta}} = \frac{2}{Re\ Pr}\nabla^2\phi \tag{7.15}$$

$$\frac{\partial \varphi}{\partial t} + v_r\frac{\partial \zeta}{\partial r} + \frac{v_{\hat{\theta}}}{r}\frac{\partial \varphi}{\partial \hat{\theta}} = \frac{2}{Re\ Sc}\nabla^2\varphi \tag{7.16}$$

where,

$$\begin{aligned} Re = \frac{2aV}{\nu},\quad Pr = \frac{\mu\ c_p}{\kappa},\quad Sc = \frac{D}{\lambda},\quad Gr = Gr_T + Gr_C \\ Gr_T = \frac{g\beta(2a)^3(T - T_\infty)}{\nu^2},\quad Gr_C = \frac{g\beta(2a)^3(C - C_\infty)}{\nu^2} \end{aligned}$$

7.3 Solution methodology

The set of vorticity-stream function equations together with energy and concentration equations have been solved by using implicit finite difference method. The modified polar coordinates have been introduced as $(\xi,\ \theta)$, where, $\xi = \ln(r/a)$ and accordingly the gov-

erning equations (7.14)-(7.16) are transformed into:

$$e^{2\xi}\frac{\partial\Omega}{\partial t} = \frac{2}{Re}\left(\frac{\partial^2\Omega}{\partial\xi^2} + \frac{\partial^2\Omega}{\partial\hat{\theta}^2}\right) - \frac{\partial\psi}{\partial\hat{\theta}}\frac{\partial\Omega}{\partial\xi} + \frac{\partial\psi}{\partial\xi}\frac{\partial\Omega}{\partial\hat{\theta}} - e^{\xi}\frac{Gr}{2Re^2}\left[\cos\hat{\theta}\frac{\partial\phi}{\partial\xi} - \sin\hat{\theta}\frac{\partial\phi}{\partial\hat{\theta}}\right] \tag{7.17}$$

$$e^{2\xi}\Omega = \frac{\partial^2\Psi}{\partial\xi^2} + \frac{\partial\Psi}{\partial\hat{\theta}^2} \tag{7.18}$$

$$e^{2\xi}\frac{\partial\phi}{\partial t} = \frac{2}{Re\ Pr}\left(\frac{\partial^2\phi}{\partial\xi^2} + \frac{\partial^2\phi}{\partial\hat{\theta}^2}\right) - \frac{\partial\psi}{\partial\hat{\theta}}\frac{\partial\phi}{\partial\xi} + \frac{\partial\psi}{\partial\xi}\frac{\partial\phi}{\partial\hat{\theta}} \tag{7.19}$$

$$e^{2\xi}\frac{\partial\varphi}{\partial t} = \frac{2}{Re\ Pr}\left(\frac{\partial^2\varphi}{\partial\xi^2} + \frac{\partial^2\phi}{\partial\hat{\theta}^2}\right) - \frac{\partial\psi}{\partial\hat{\theta}}\frac{\partial\varphi}{\partial\xi} + \frac{\partial\psi}{\partial\xi}\frac{\partial\varphi}{\partial\hat{\theta}} \tag{7.20}$$

where, $u' = e^{-\xi}\frac{\partial\Psi}{\partial\hat{\theta}}$, $v' = -e^{-\xi}\frac{\partial\Psi}{\partial\xi}$ and the corresponding boundary conditions are :

$$\Psi = \frac{\partial\Psi}{\partial\xi} = 0,\ \phi = \varphi = 1 \text{ at } \xi = 0$$
$$e^{-\xi}\frac{\partial\Psi}{\partial\hat{\theta}} \to \cos\hat{\theta},\ e^{-\xi}\frac{\partial\Psi}{\partial\xi} \to \sin\hat{\theta},\ \text{as } \xi \to \infty \tag{7.21}$$

The above set of equations (7.17)-(7.20) are discretized by using forward and central difference scheme. The resultant system of equations are solved by using Gaussian elimination method. For the whole computational domain, a uniform grid in both ξ and $\hat{\theta}$ directions are used and the iterative procedure is stopped to obtain the final vorticity, temperature and concentration distribution when the difference in computing these quantities in the latest iteration is less than 10^{-5}. Such grid and criteria make efficient use of both computational time and space.

7.4 Results and discussion

Mixed convection flow due to double diffusion from a hot horizontal circular cylinder have been investigated in this present problem. Since the vorticity field along with the heat and mass transfer is effected by the parameters Re, Gr_T/Re^2, Gr_C/Re^2, and also the flow direction, extensive exploration is made and the results are presented in terms of contour

plot for stream function, isothermal lines, isoconcentration lines. Graphical representation of local Nusselt number, average Nusselt number, Sherwood number, average Sherwood number have also been made based on the numerical simulation. To validate the numerical simulations of the present model, calculated values are qualitatively compared with the published results, [82]. As mentioned above in this case the full sets of transport equations are solved instead of boundary layer equations. This is because, even for small Re, the boundary layer thickness is significantly large. Moreover, boundary layer approximation is no longer valid in the wake region, i.e. in the region following the point of separation. Finally, when $Gr/Re^2 \sim O(1)$, then there is no method available to estimate accurately enough the velocity distribution outside the boundary layer region. In this present study, to explicate and discuss the local and average Nusselt numbers, the definitions for the respective quantities are used as given below:

$$Nu = \frac{2ah}{k}, \quad anu = \frac{2a\overline{h}}{k} \tag{7.22}$$

where, h and $\overline{h}$ represents the local and average heat transfer coefficients and these quantities are calculated as:

$$h = \frac{\dot{q}}{(T_s - T_\infty)}, \quad \overline{h} = \frac{1}{2\pi}\int_0^{2\pi} h \; d\hat{\theta}, \quad \dot{q} = -k\left(\frac{\partial T}{\partial r'}\right)_{r'=a} \tag{7.23}$$

where, $\dot{q}$ is the rate of heat transfer per unit area. Likewise, the local Sherwood number, average Sherwood number are also computed by using the rate of mass transfer per unit area, the surface mass concentration and ambient concentration of the fluid field as:

$$\begin{aligned} sh &= \frac{2ac}{D}, \quad ssh = \frac{2a\overline{c}}{D} \\ c &= \frac{\dot{m}}{(C_s - C_\infty)}, \quad \overline{c} = \frac{1}{2\pi}\int_0^{2\pi} c \; d\hat{\theta}, \quad \dot{m} = -D\left(\frac{\partial C}{\partial r'}\right)_{r'=a} \end{aligned} \tag{7.24}$$

where, c and $\overline{c}$ stand for local and average mass transfer coefficients.

Since, the coefficient of heat and mass transfer depend on the Reynolds number, Re, Grashof numbers Gr_T, Gr_C, Prandtl number Pr, Schmidt number Sc, the influence of

all these parameters have been studied carefully and the calculated results are presented graphically. Formation of velocity, temperature and concentration boundary layer around the cylinder surface in course of time have also been observed closely and the required time for attaining steady state condition also monitored. Present model have been studied extensively in three different juncture and the results are presented in the following sections.

7.4.1 Validation of the model

In order to validate the present model simulation, similar solutions of [82] for local Nusselt number, average Nusselt number, stream function, isotherm have been produced along with the referenced model assumptions. Since the referenced results were calculted only for thermal diffusion, during the present simulation, the value of Gr_C is considered as zero so that no mass transfer is taken into account and the present model turned into similar to that of [82]. Contour plot for stream function and isotherm are presented here and compared qualititavely with that of [82]. It can be observed from Figures 7.2-7.3, there is an excellent agreement between the present simulation and the results published in [82].

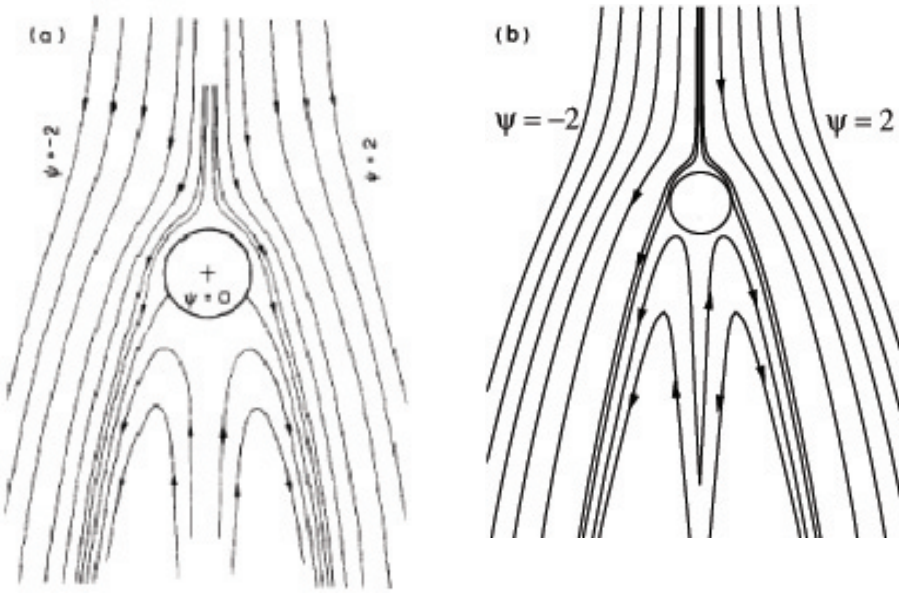

Figure 7.2: Contours of the stream function for $Gr_T = 100$, while, $Gr_C = 0$, Re=20.

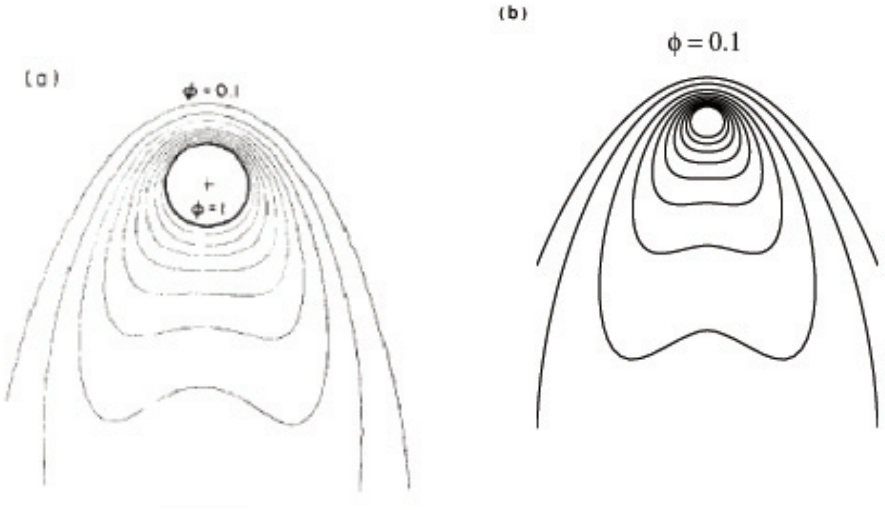

Figure 7.3: Contours of the isotherm for $Gr_T = 100$, while, $Gr_C = 0$, Re=20.

7.4.2 Heat transfer and mass transfer rate

In this section, parametric studies of velocity temperature and concentration fields have been performed and graphical representation of the results are depicted in terms of contour, Nusselt number and Sherwood number. Moreover, in the boundary conditions, stated at the very out set of this study, the value of ϵ is taken as zero. As a result, there is no oscillation in the surface quantities. The effect of thermal Grashof number, Gr_T, on local Nusselt number(Nu) and average Nusselt number (anu) are illustrated in Figures 7.4-7.5. From the figures, it can be viewed that just right after heating the cylinder, the average nusselt number attain its maximum value and as time passed by, this value decreased and accomplished its asymptotic value which is about 2.0. It can also be perceived that the value of local Nusselt number reaches its maximum value near the front stagnation point($x = \pi$)and after that the value starts decreasing. Moreover, the value of local Nusselt number increases significantly as long as the value of Gr_T increases.

The effect of concentration diffusion parameter, Sc, on local and average Sherwood number are illustrated in Figures 7.6-7.7. As it is expected, higher values of Sc, produces higher value of the related quantities. Local optimum value is noted for the local Sherwood number for each values of Sc. In this present study as well, the same values of Sc, as used in the previous chapters were chosen and while varying this quantity, the remaining

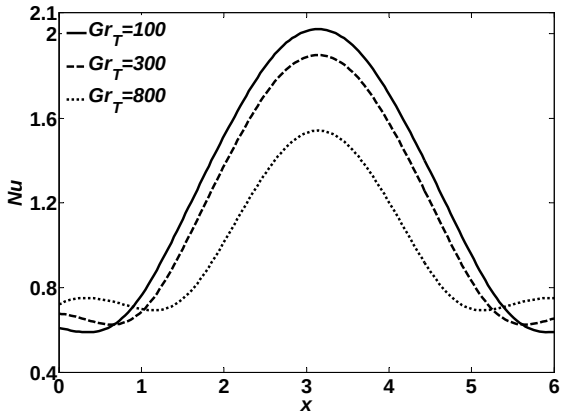

Figure 7.4: Local Nusselt number around the cylinder, while, $Gr_T = 100, Gr_C = 0.0$, Re=20.

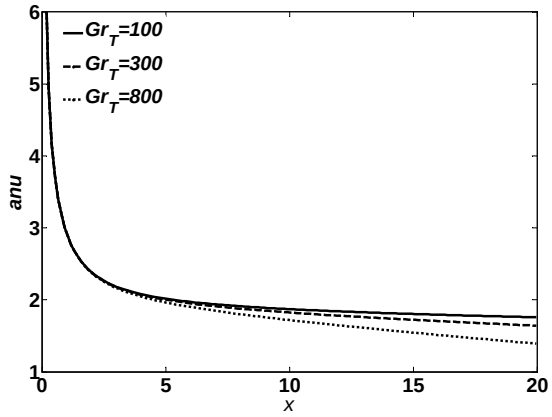

Figure 7.5: Average Nusselt number around the cylinder, while, $Gr_T = 100, Gr_C = 0.0$, Re=20.

parameters are kept constant.

The vorticity distribution around the cylinder surface for different values of Gr_T/Re^2 is presented in Figure 7.8. It is comprehensible from the figure that, as the value of Gr_T/Re^2 becomes higher, the surface vorticity, and accordingly the velocity gradient at the surface becomes remarkably higher. This is obvious, because, buoyancy forces are dominant near the surface and as a result of this, the pressure near the cylinder surface is less and region of suction is produced.

The contour plot of stream function for different values of Gr_T and Gr_C are presented in Figures 7.9-7.10. It can be depicted from the figures that the effects of both Gr_T and

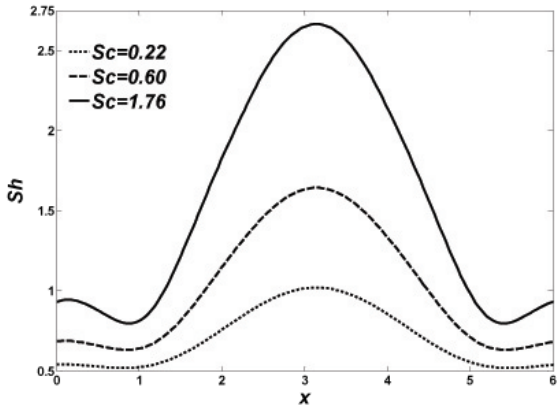

Figure 7.6: Local Sherwood number for different values of Sc around the cylinder, while, $Gr_T = 100, Gr_C = 100.0$, Re=20.

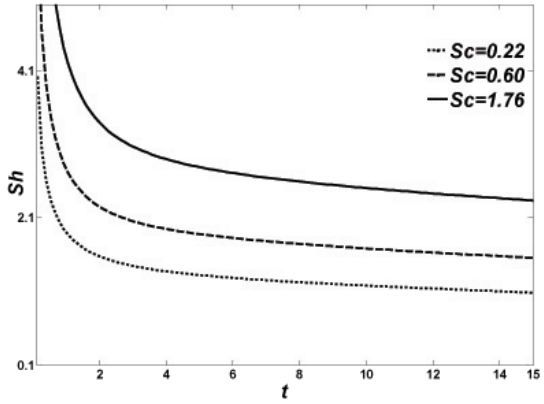

Figure 7.7: Average Sherwood number for different values of Sc around the cylinder, while, $Gr_T = 100, Gr_C = 100.0$, Re=20.

Gr_C are quite significant in velocity boundary layer. To visualize the effect of Gr_T on the stream function, contours of the stream function for $Gr_T = 100,\ 400$ and 800 are drawn. It can be observed from the contours that higher values of Gr_T produces recirculation region in the flow field more significantly than the relatively smaller values. To predict the effect of Gr_C on the velocity boundary layer, the values of $Gr_T,\ Re$ were chosen as 100 and 20 respectively and the values of Gr_C were chosen as 100, 200 and 300 respectively. These contour plot of the stream function show that, increasing value of Gr_C results in reduction of wake length and gradually it vanishes completely.

Contours of the isotherm for different values of Gr_T are plotted in Figure 7.11. From

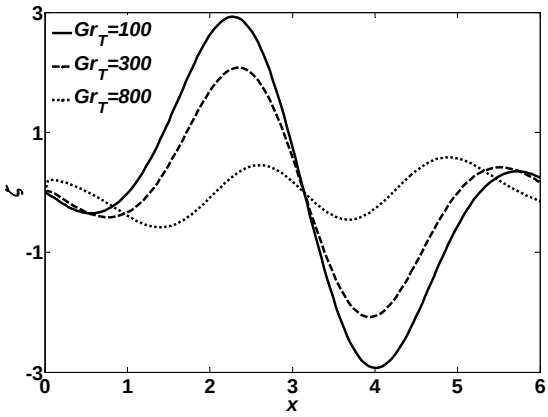

Figure 7.8: Vorticity distribution around the cylinder, while, Gr_T=100, Re=5.

these figures, it is clear that there is notable effect of this parameter on isotherm pattern. These contour plots indicate that there is higher temperature gradient for higher values of Gr_T and results in higher rate of heat transfer. Since, this parameter is directly act as an influential parameter to effect the velocity field also, the formation of recirculation region is effected by it and as a result heat transfer rate from the surface is noteworthy.

7.5 Summary

Mixed convection flow along a horizontal hot cylinder have been investigated in this present study. Numerical simulations have been carried out for solving the full set of transport equations which are regarded as vorticity-stream function formulation. The important findings for this model study are listed below:

- Full Navier-Stokes equation in the form of vorticity-stream function along with energy and concentration equations have been solved.

- The variations of vorticity, Nusselt number and Sherwood number are calculated over the whole cylinder surface. The zone beyond the point of separation has also been taken into account.

- Study of the dimensionless parameters, Pr, and Sc show that the heat and mass transfer rate enhance due to the enhancement of the values of Pr and Sc.

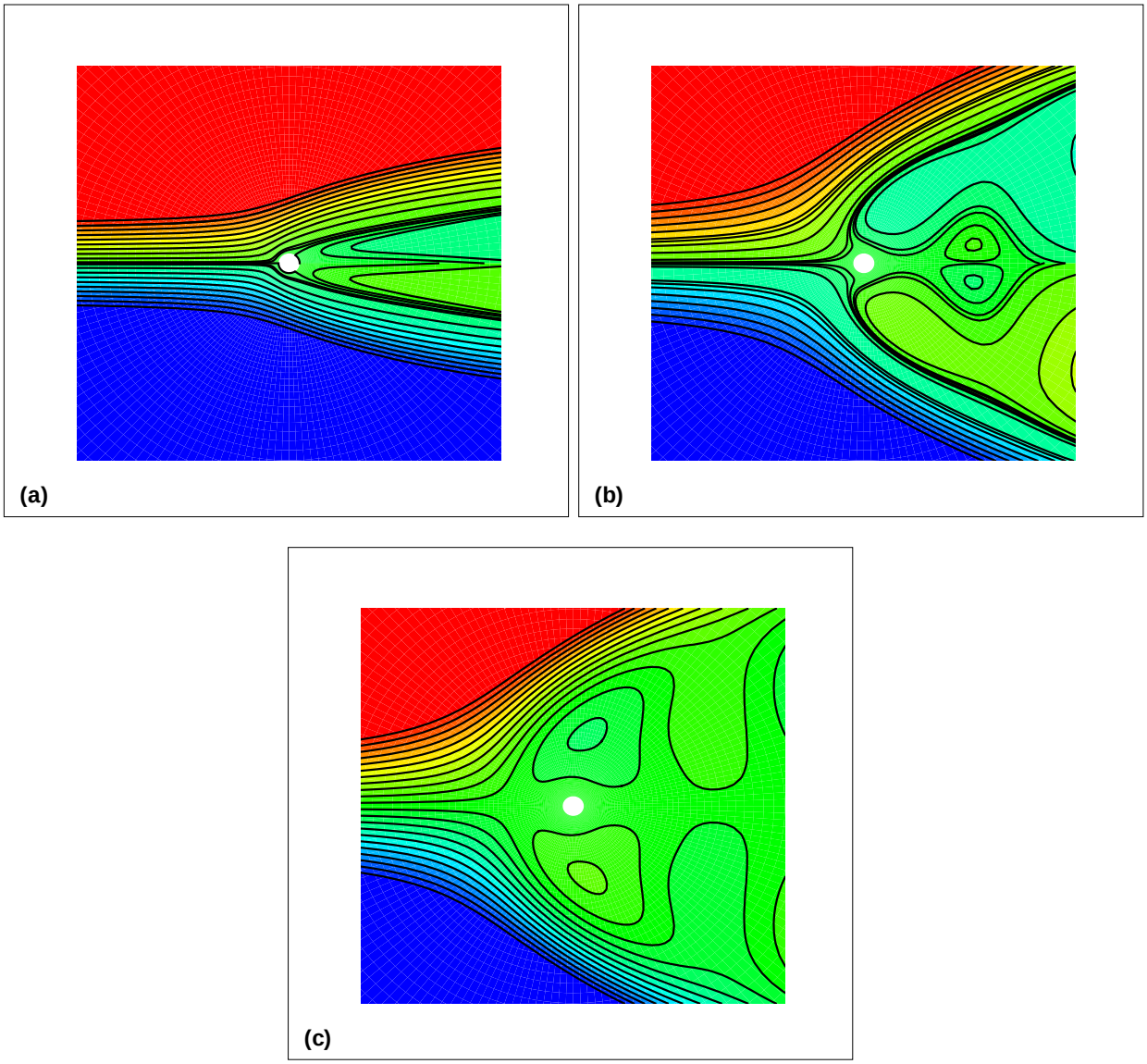

Figure 7.9: Contours of the stream function for (a) $Gr_T = 100$, (b) $Gr_T = 400$, (c) $Gr_T = 800$, while, $Gr_C = 100.0$, Re=20.

- Average Nusselt number and Sherwood number against time are predicted and it has been observed that after a while these two quantities attain their asymptotic values.
- Stream lines for different values of temperature and concentration Grashof number Gr_T and Gr_C have been plotted and depicted significant effects on velocity field.
- From the contours of isotherms and isoconcentration for different values of thermal Grashof number Gr_T and concentration Grashof number Gr_c, different patterns of wake regions are observed and for higher values of Gr_T and Gr_C, bigger size of the wake regions are formed.
- The length of the wake region is increased due to the increment of the oscillating parameter ϵ.
- For changing the direction of the forced flow, completely different patterns of the vortex region is formed, as a result, the surface heat and mass transfer rate are also effected.
- Both the heat and mass transfer rate is increased when the temperature and concentration diffusion parameters Pr and Sc are boosted up.

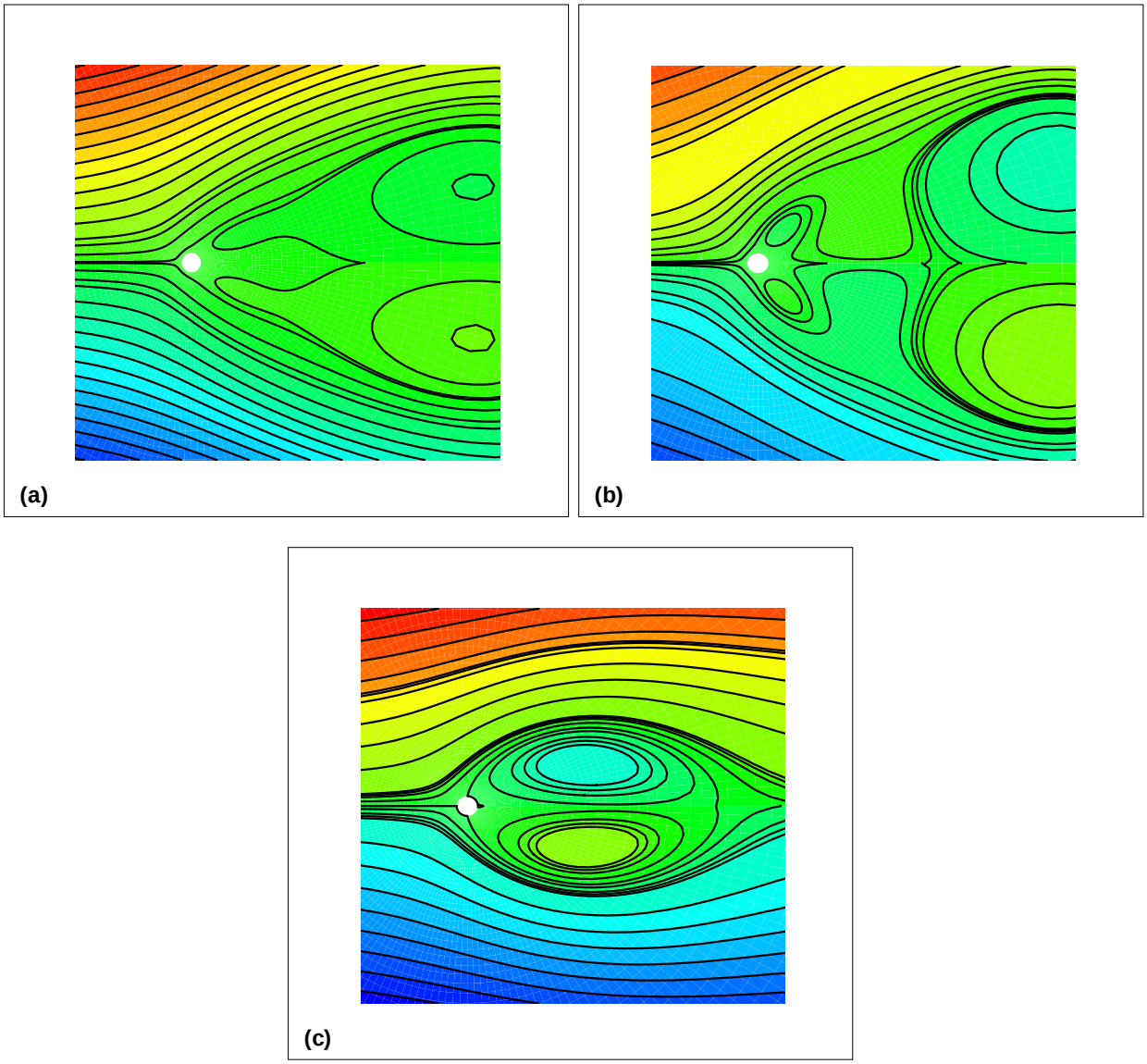

Figure 7.10: Contours of the stream function for (a) $Gr_C = 100$, (b) $Gr_C = 200$, (c) $Gr_C = 400$, while, $Gr_T = 100.0$, Re=20.

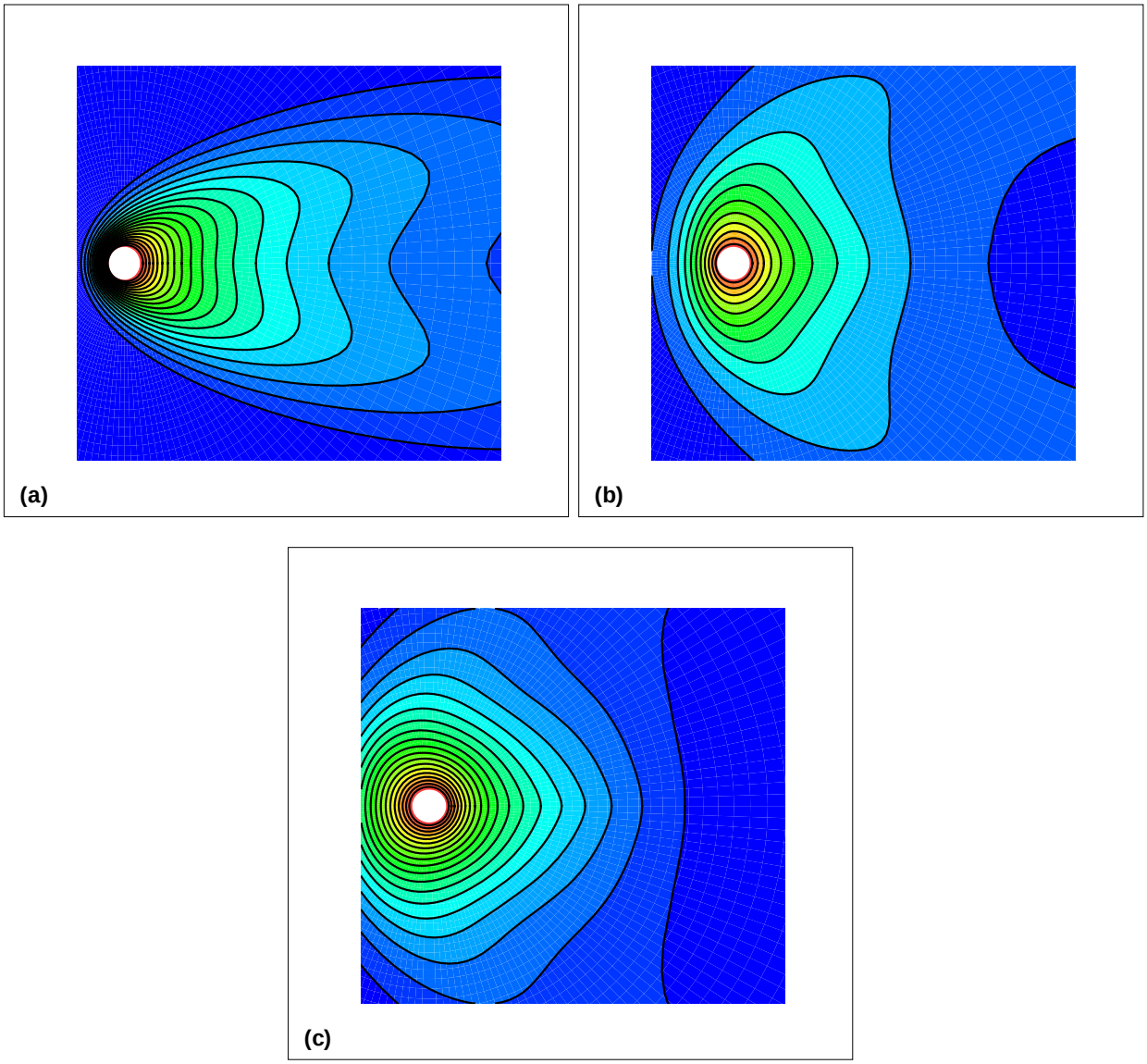

Figure 7.11: Contours of the isotherm for (a) $Gr_T = 100$, (b) $Gr_T = 400$, (c) $Gr_T = 800$, while, $Gr_C = 100.0$, Re=20.

Chapter 8

Study of mixed convection flow along circular cylinder with oscillating surface temperature and concentration

8.1 Introduction

Study of conjugate heat and mass transfer along blunt bodies have significant importance in both theoretical and practical points of view. Flow due to double diffusion along isolated circular cylinder have been paid noteworthy attention because of versatile engineering applications. Some very important engineering applications, where this type of flow plays essential role are: drying of different materials (paper, textiles, film, veneer materials etc.), cooling of glass, plastic and industrial devices from turbine blades to electronic circuits, anemometry and chemical or radioactive contamination/purification process etc.

Recent significant development in computing techniques and tools have opened up a new horizon in studying fluid flow problems which are involved with some complicated geometry. These types of fluid flow have considerable involvement with the interaction of applicable phenomena. For example, flow over tubes in nuclear reactors and cylindrical

heating elements are very much related to the free convection over vertically or horizontally placed cylinders.

Steady forced convection flow due to heat and species concentration along circular cylinder in laminar cross flow have been studied by number of researchers. Amongst them, Dennis *et al.* [90] was the one who investigated this type of flow considering low Reynolds numbers. Boundary layer flow of a viscous incompressible fluid over an isothermal cylinder of elliptic cross section of various eccentricities was studied by Jaman *et al.* [75]- [76]. In this paper, two configuration of the ellipse, termed as blunt (major axis is horizontal) and slender (major axis is vertical) were taken into account and transformed governing equations were solved by using finite difference technique together with Keller-box elimination method. A brief literature citation similar to the present work has been presented in chapter 1.

To study the unsteady mixed convective flow along a infinite horizontal cylinder is the subject of this chapter. In fact, present study wishes to extend the idea presented in the previous chapter. Here only the boundary conditions for surface heat and mass transfer have been changed. It is assumed that, both the surface temperature and species concentration have small amplitude oscillation. The rest of the assumptions, configuration as well as the solution procedure are exactly similar to previous work. Alike to any double diffusive study, the governing equations of the flow field is simulated for two different diffusive parameters, Pr and Sc. Here also, to derive the governing equations, the boussinesq approximations are made, that is, it has been assumed that the fluid property variations are limited to firstly the density which is taken into account only in so far as its effects the buoyancy term and secondly the viscosity. Based on the conservation principle, the governing equations are expressed in terms of vorticity, stream function, energy equation and concentration equation.

8.2 Formulation of the problem

Since the flow configuration, all the thermo and physical fluid properties of the problem are kept exactly same as the problem discussed in chapter 7, details elucidation of this config-

uration and model assumptions are avoided here. By taking all the related assumptions of the model problem, and by using exactly the similar type of dimensionless quantities, the governing equations of the associated flow field can be written as:

$$\frac{\partial \zeta}{\partial t} + v_r \frac{\partial \zeta}{\partial r} + \frac{v_{\hat{\theta}}}{r} \frac{\partial \zeta}{\partial \hat{\theta}} = \left(\frac{2}{Re} \right) \nabla^2 \zeta$$
$$- \frac{Gr}{2Re^2} \left(\cos\hat{\theta} \frac{\partial \phi}{\partial r} - \frac{\sin\hat{\theta}}{r} \frac{\partial \phi}{\partial \hat{\theta}} + \cos\hat{\theta} \frac{\partial \varphi}{\partial r} - \frac{\sin\hat{\theta}}{r} \frac{\partial \varphi}{\partial \hat{\theta}} \right) \tag{8.1}$$

$$\frac{\partial \phi}{\partial t} + v_r \frac{\partial \zeta}{\partial r} + \frac{v_{\hat{\theta}}}{r} \frac{\partial \phi}{\partial \hat{\theta}} = \frac{2}{Re\ Pr} \nabla^2 \phi \tag{8.2}$$

$$\frac{\partial \varphi}{\partial t} + v_r \frac{\partial \zeta}{\partial r} + \frac{v_{\hat{\theta}}}{r} \frac{\partial \varphi}{\partial \hat{\theta}} = \frac{2}{Re\ Sc} \nabla^2 \varphi \tag{8.3}$$

where,

$$Re = \frac{2aV}{\nu}, \quad Pr = \frac{\mu\ c_p}{\kappa}, \quad Sc = \frac{D\ c_m}{\lambda}, \ Gr = Gr_T + Gr_C$$
$$Gr_T = \frac{g\beta(2a)^3(T - T_\infty)}{\nu^2}, \quad Gr_C = \frac{g\beta(2a)^3(C - C_\infty)}{\nu^2}, \tag{8.4}$$

The boundary conditions are:

$$v_r = v_{\hat{\theta}} = 0, \ \phi = \varphi = 1 \ \text{ at } \ r = 1$$
$$v_r \to (1 + \epsilon\ \sin\ t)\cos\hat{\theta}, \ v_{\hat{\theta}} \to -(1 + \epsilon\ \sin\ t)\sin\hat{\theta} \ \text{ as } \ \zeta \to 0 \tag{8.5}$$
$$\phi \to 0, \ \varphi \to 0, \ \text{ as } \ r \to \ \infty$$

These boundary conditions are derived from the no slip, isothermal and iso concentration conditions on the cylinder surface together with the free stream conditions away from it.

8.3 Solution methodology

The set of vorticity-stream function together with energy and concentration equation have been solved by using implicit finite difference method. Here also the same type of modified polar coordinates as that has been used in previous chapter are introduced as $(\xi, \hat{\theta})$ where,

$\xi = \ln(r/a)$. Thus the governing equations (8.1)-(8.3) are transformed into:

$$e^{2\xi}\frac{\partial \Omega}{\partial t} = \frac{2}{Re}\left(\frac{\partial^2 \Omega}{\partial \xi^2} + \frac{\partial^2 \Omega}{\partial \hat{\theta}^2}\right) - \frac{\partial \psi}{\partial \hat{\theta}}\frac{\partial \Omega}{\partial \xi} + \frac{\partial \psi}{\partial \xi}\frac{\partial \Omega}{\partial \hat{\theta}} - e^{\xi}\frac{Gr}{2re^2}\left[\cos\hat{\theta}\frac{\partial \phi}{\partial \xi} - \sin\hat{\theta}\frac{\partial \phi}{\partial \hat{\theta}}\right] \tag{8.6}$$

$$e^{2\xi}\Omega = \frac{\partial^2 \Psi}{\partial \xi^2} + \frac{\partial \Psi}{\partial \hat{\theta}^2} \tag{8.7}$$

$$e^{2\xi}\frac{\partial \phi}{\partial t} = \frac{2}{Re\ Pr}\left(\frac{\partial^2 \phi}{\partial \xi^2} + \frac{\partial^2 \phi}{\partial \hat{\theta}^2}\right) - \frac{\partial \psi}{\partial \hat{\theta}}\frac{\partial \phi}{\partial \xi} + \frac{\partial \psi}{\partial \xi}\frac{\partial \phi}{\partial \hat{\theta}} \tag{8.8}$$

$$e^{2\xi}\frac{\partial \varphi}{\partial t} = \frac{2}{Re\ Pr}\left(\frac{\partial^2 \varphi}{\partial \xi^2} + \frac{\partial^2 \phi}{\partial \theta^2}\right) - \frac{\partial \psi}{\partial \theta}\frac{\partial \varphi}{\partial \xi} + \frac{\partial \psi}{\partial \xi}\frac{\partial \varphi}{\partial \theta} \tag{8.9}$$

where, $u' = e^{-\xi}\frac{\partial \Psi}{\partial \theta},\ v' = -e^{-\xi}\frac{\partial \Psi}{\partial \xi}$ and the corresponding boundary conditions are :

$$\begin{aligned}
&\Psi = \frac{\partial \Psi}{\partial \xi} = 0, \phi = \varphi = 1 \ \text{ at } \ \xi = 0 \\
&e^{-\xi}\frac{\partial \Psi}{\partial \theta} \to (1 + \epsilon\ \sin\ t)\cos\theta,\ e^{-\xi}\frac{\partial \Psi}{\partial \xi} \to (1 + \epsilon\ \sin\ t)\sin\theta,\ \xi\ \to 0 \\
&\phi \to 0,\ \varphi \to 0 \ \text{ as } \ \xi \to \infty
\end{aligned} \tag{8.10}$$

Exactly similar simulation technique that is applied for the previous model studied in chapter 7, came into action here and for the whole computational domain a uniform grid in both ξ and θ directions are used and the iterative procedure is stopped to obtain the final vorticity, temperature and concentration distribution when the difference in computing the these quantities in the latest iteration is less than 10^{-5}. This type of grid selection and iteration execution criterion were efficient in terms of both space and computational time.

8.4 Results and discussion

It has already been declared that all the assumptions are kept similar to those described in the model in chapter 7, except some changes with the boundary conditions are made in present study. Therefore, all the parameters effecting the flow field remain same. Therefore, parametric studies varying the parameters, $Re,\ Gr_T/Re^2,\ Gr_C/Re^2$, carried out as

well as the flow direction is taken into account. Calculated results are presented in terms of contour plot of stream function, isothermal lines and isoconcentration lines. Moreover, local Nusselt number, average Nusselt number, Sherwood number, average Sherwood number are also calculated to predict the heat and mass transfer. In this present study also, to explicate and discuss the local and average Nusselt numbers, the similar type of definitions, as discussed in the previous chapter, are used. Present model have been studied all-embracing manner and the results are presented in the following section.

In the present chapter, all results by varying different important parameters are illustrated by considering small amplitude of oscillation in the boundary temperature and concentration. Since the direction of the forced flow is another important parameter which influence the flow field as well as the heat and mass transfer, here both the positive and negative direction of forced flow have considered. When the flow direction is considered as vertically upward, the flow is termed as parallel flow and for vertically downward forced flow, the flow is termed as contra flow. To elucidate the effect of this fact on the entire flow regime, the Grashof number due to thermal and mass diffusion are taken as both positive and negative.

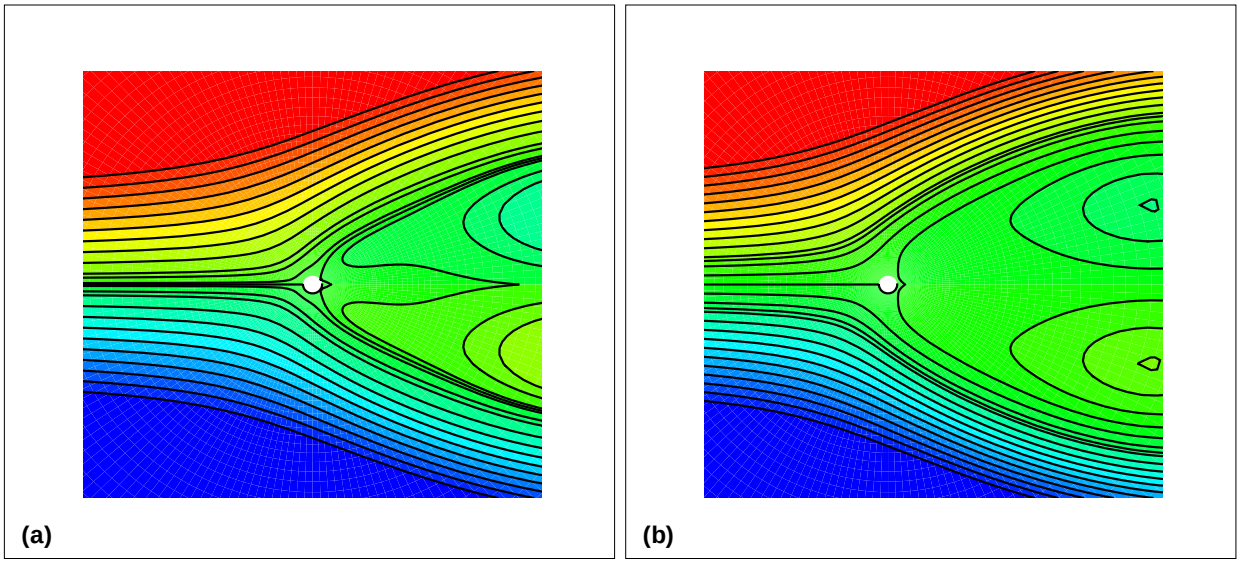

Figure 8.1: Contours of the stream function for (a) $\epsilon = 0.10$, (b) $\epsilon = 0.20$, while, $Gr_T = 100.0$, $Gr_C = 100.0$, Re=20.

The effect of various values of small amplitude of the oscillation ϵ in stream function,

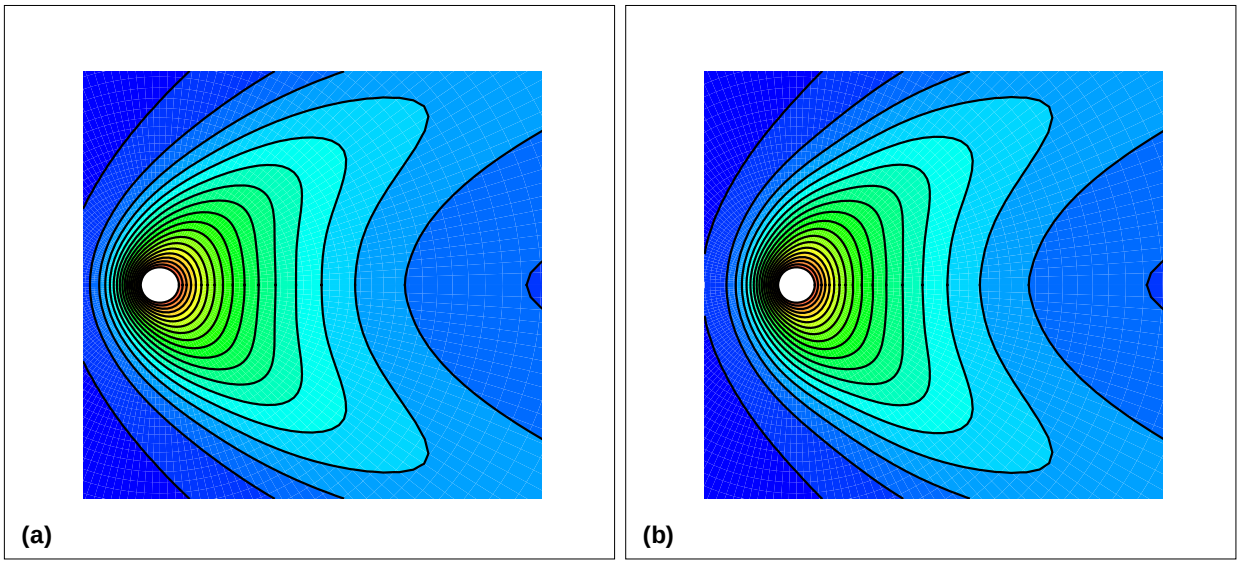

Figure 8.2: Contours of the isotherm for (a) $\epsilon = 0.10$, (b) $\epsilon = 0.20$, while, $Gr_T = 100.0$, $Gr_C = 100.0$, Re=20.

surface temperature and surface concentration is portrayed in Figures 8.1-8.3. The values of ϵ are taken as 0.1, 0.2 and 0.3 respectively while the values of both thermal and concentration grashof numbers Gr_T and Gr_C are considered as 100. The values of the Prandtl number Pr and Schmidt number Sc are taken as 0.7 and 0.60 respectively and the value of Re is chosen as 0.20. It is observed different shapes and sizes of the recirculation regions for different values of ϵ, for the contours of stream function, isotherms and isoconcentrations. For higher values of ϵ the reattachment lengths get bigger and for all the cases, the velocity, temperature and concentration fields are symmetrical about the line $\theta = 0$.

Figure 8.4, shows the contours of the stream function for different values of thermal grashof number Gr_T. The contours show that, for relatively lower values of Gr_T the wake is formed in the downstream side of the cylinder. The size of the vortex region becomes bigger as the value of Gr_T is increased and in the vortex region the heat and mass transfer from the cylinder surface occur due to natural convection. Once again, from recirculation region to main stream, the heat and mass transfer arise for conduction.

Figure 8.5 show the effect of Prandtl number Pr on the local Nusselt number around the surface of the cylinder and the average Nusselt number for different time steps. From the graph of the average Nusselt number it can be inferred that, for higher values of Pr,

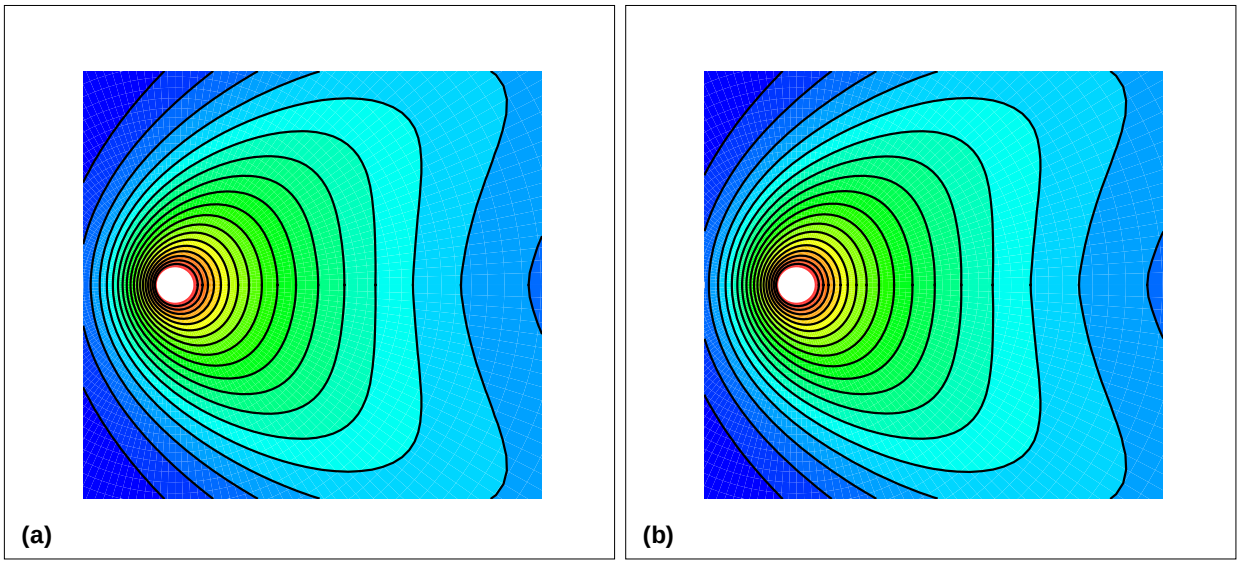

Figure 8.3: Contours of the isoconcentration for (a) $\epsilon = 0.10$, (b) $\epsilon = 0.20$, while, $Gr_T = 100.0$, $Gr_C = 100.0$, Re=20.

higher rate of surface heat transfer occurred and as time passes, the average heat transfer rate reaches to the asymptotic value. For comparatively higher value of $Pr = 5.0$, it takes little longer time to achieve the asymptotic value of average heat transfer. For local heat transfer rate, it can be observed that an absolute maximum value occurs in each case and these maximum values are noted near the front stagnation point, i.e. when $\theta = 180^0$. For higher value of $Pr = 5.0$, the behaviour of local Nusselt number is slightly different, as there can be detected a local maximum value near the rear stagnation point ($\theta = 0$), then it goes downwards for a little while and then starts to increase to reach up to its maximum value.

For different values of the Schmidt number Sc, it can also be detected exactly the similar types of behaviour in local and average mass transfer rate in terms of Sherwood number and average Sherwood number. To depict the effects of Schmidt number, the values of Sc are chosen as 0.22, 0.60 and 1.76 when the value of Pr is taken as 0.70. Similar to average local and average heat transfer, there can also be noted higher rate of mass transfer for higher values of Sc.

Another important factor that effects the both heat and mass transfer is the direction of the forced flow. For the contra flow, i.e. for different negative values of thermal Grashof

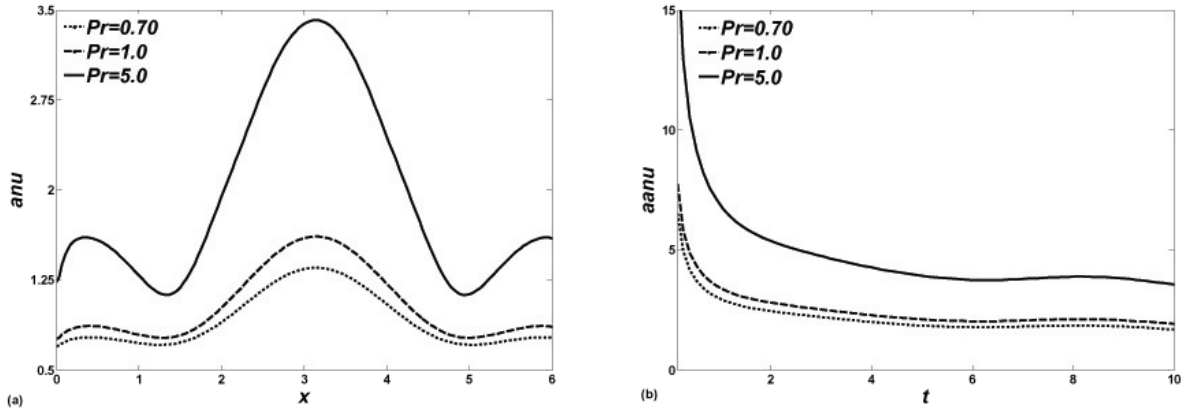

Figure 8.4: (a) Local Nusselt number (b) Average Nusselt number, around the cylinder, while, $Gr_T = 100,\ Gr_C = 0.0,\ Re$=20, ϵ=0.0.

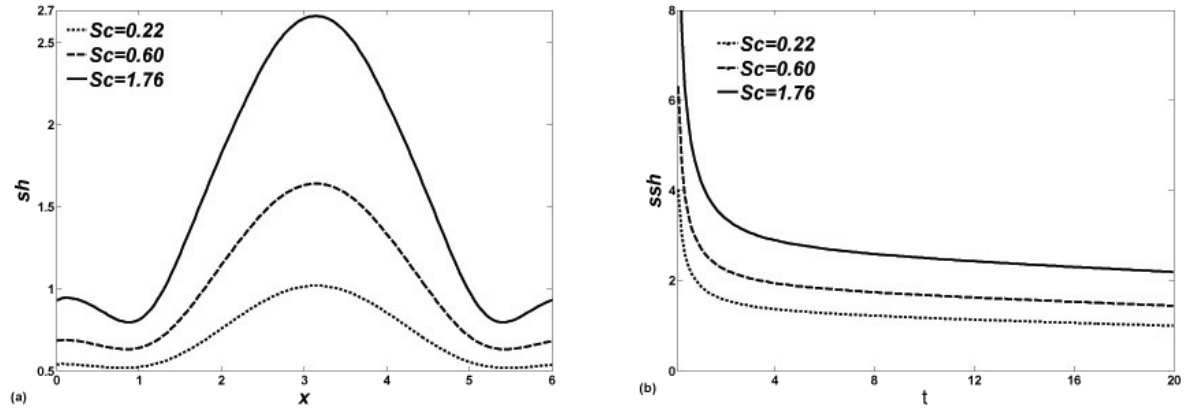

Figure 8.5: (a) Local Sherwood number (b) Average Sherwood number, around the cylinder, while, $Gr_T = 100,\ Gr_C = 0.0,\ Re$=20, $\epsilon = 0.0$.

number, Gr_T the contours of stream function, temperature and concentration are plotted in Figures 8.6-8.7. From the figures, it is clear that completely different patterns of wake regions have formed for velocity, temperature and species concentration. For higher values of Gr_T , the longer length of the recirculation regions are scrutinized. From the pattern of the wake regions, it can be described that, fluid flow inside the recirculation zone is segregated from the main stream and both the heat and mass transfer in this region is caused through the wake boundaries. Moreover, in these regions, heat and mass transfer from the surface of the cylinder is influenced by natural convection where the buoyant forces due to

thermal and mass diffusion are dominant.

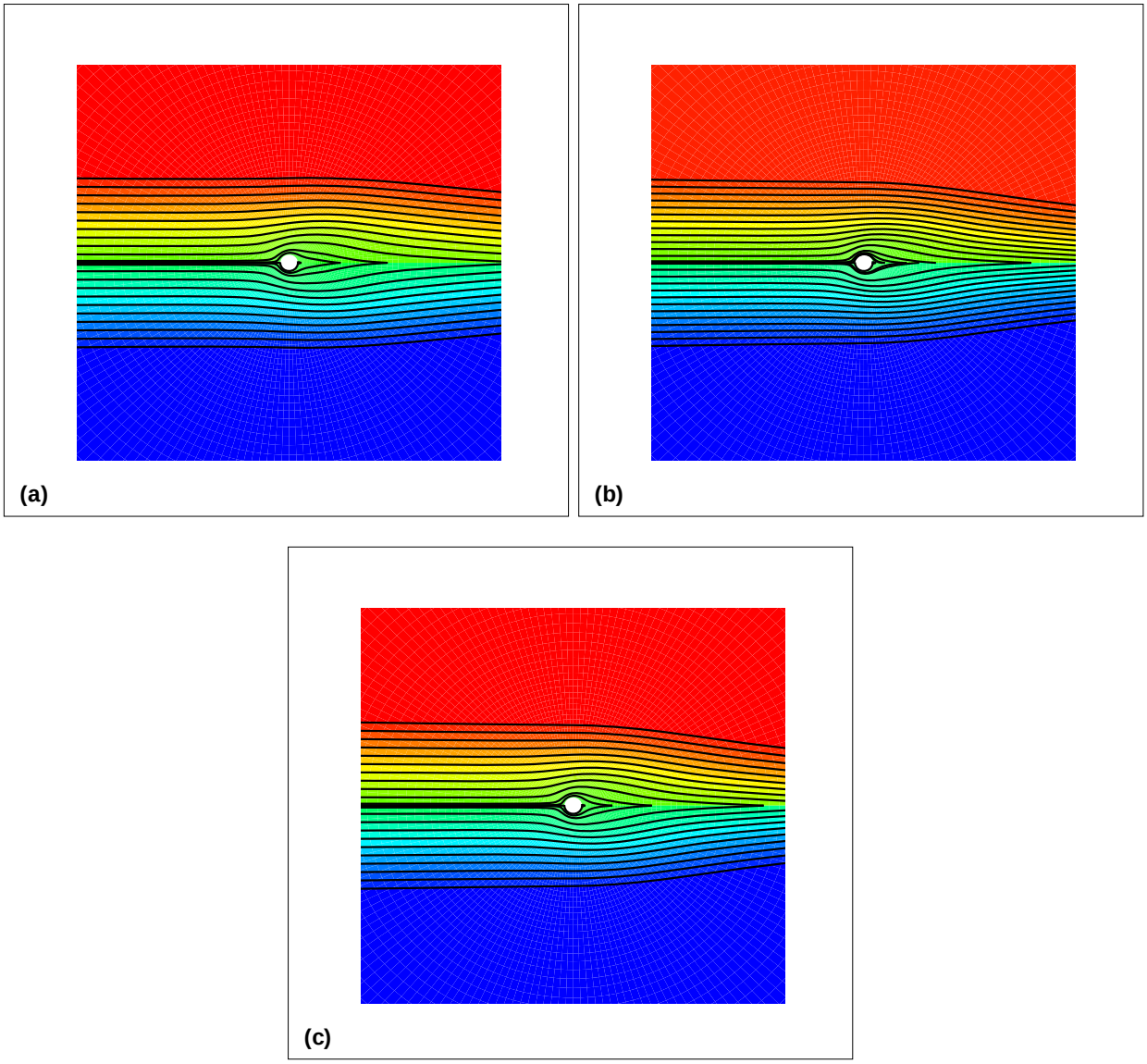

Figure 8.6: Contours of the stream function for (a) $Gr_T = -100$, (b) $Gr_T = -300$, (c) $Gr_T = -800$, while, $Gr_T = 100.0$ Re=20, ϵ =0.0.

8.5 Summary

Mixed convection flow along a horizontal cylinder have been investigated assuming that the surface temperature, surface concentration and free stream velocity have small amplitude

oscillation. Vorticity-stream function formulation have been used to derive the governing equation of the flow field. Because of the oscillation in the surface temperature and species concentration, some changes in the streamlines, isotherm lines and isoconcentration lines, compare to those discussed in the previous chapter were observed and depicted in graphical forms. Some important findings based on numerical simulations are listed below:

- Study of the dimensionless parameter Sc shows that the mass transfer rate is enhanced due to the enhancement of the values of Sc. Similar manners of heat transfer coefficient can also be noted due to the increment of Prandtl number Pr.

- Average Nusselt number and Average Sherwood number against time are predicted and it has been observed that after a while these two quantities attain their asymptotic values.

- Stream lines for different values of concentration Grashof number Gr_C have been plotted and depicted significant effect on velocity field.

- From the contours of isotherms and isoconcentration for different values of thermal Grashof number Gr_T and concentration Grashof number Gr_c it can be observed different patterns of wake regions and for higher values of Gr_T and Gr_C , bigger size of the wake regions are formed.

- The length of the wake region is increased due to the increment of the oscillating parameter ϵ.

- For changing the direction of the forced flow, completely different patterns of the vortex region is formed, as a result, the surface heat and mass transfer rate are also effected.

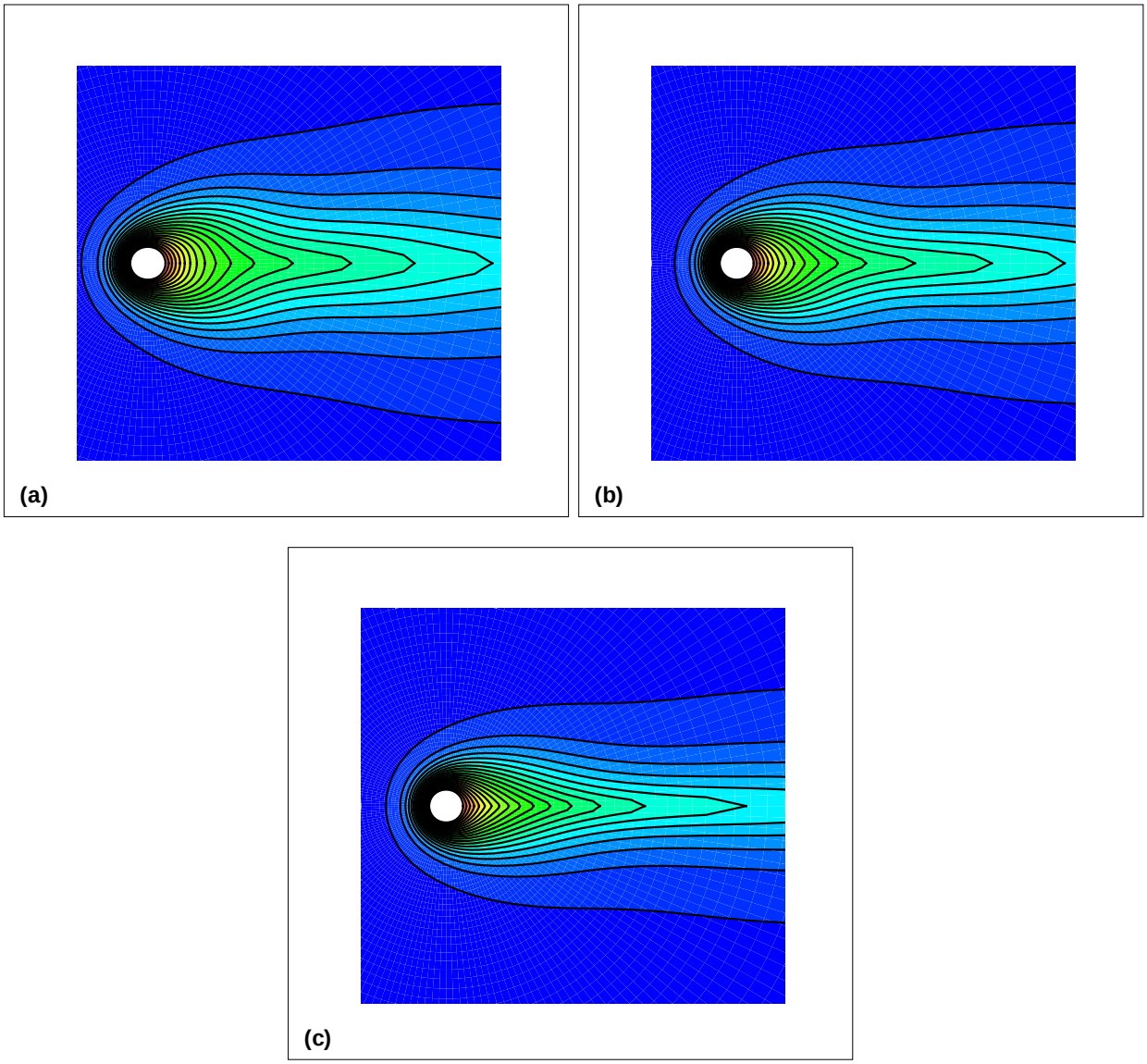

Figure 8.7: Contours of the isotherm for (a) $Gr_C = -100$, (b) $Gr_C = -300$, (c) $Gr_C = -800$, while, $Gr_T = 100.0$ Re=20, ϵ =0.0.

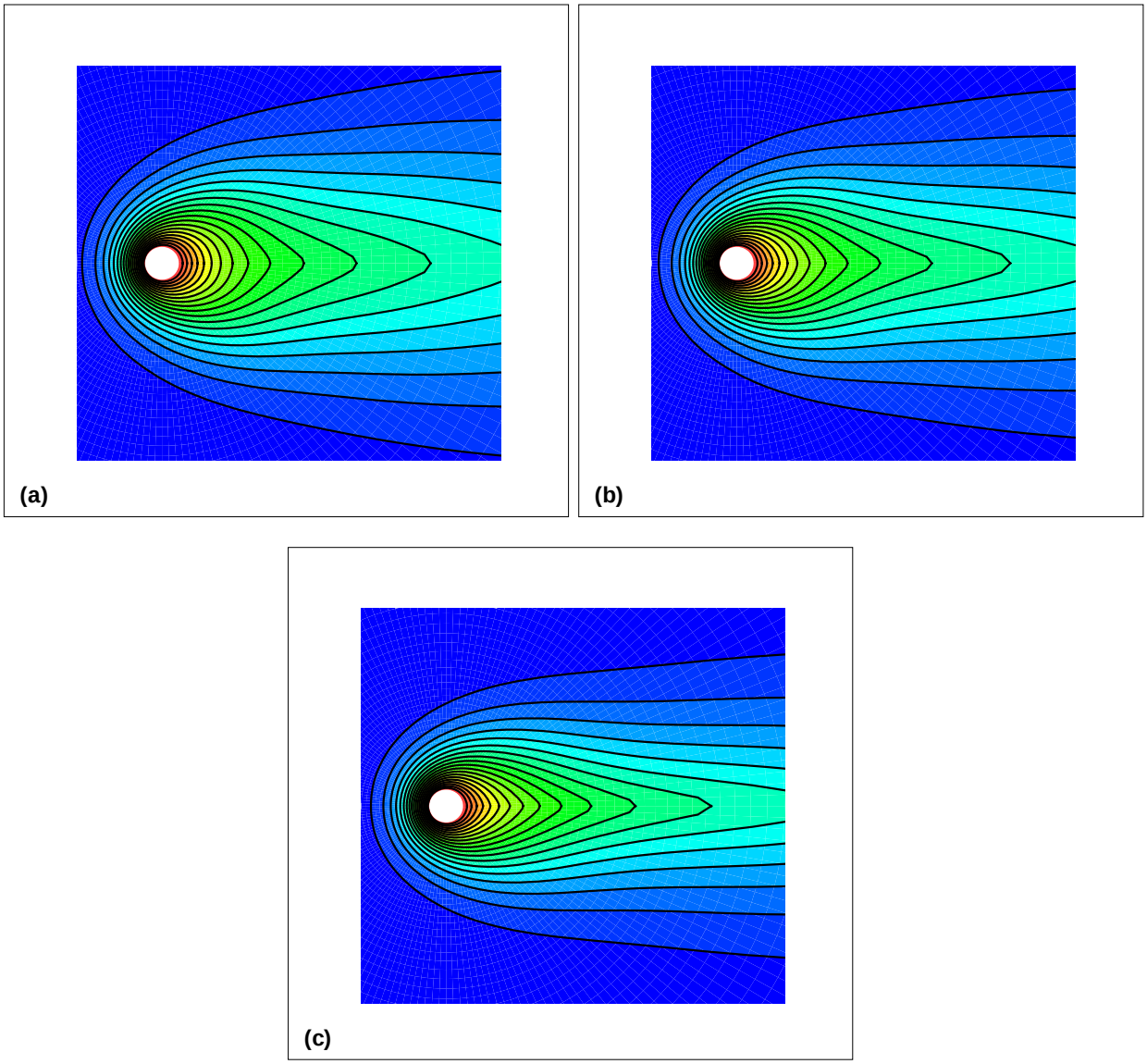

Figure 8.8: Contours of the isotherm for (a) $Gr_C = -100$, (b) $Gr_C = -300$, (c) $Gr_C = -800$, while, $Gr_T = 100.0$ Re=20, ϵ =0.0.

Chapter 9

Conclusion

The main perseverance of this dissertation is to study different types of flow along flat plate, wedge and cylindrical surfaces. Dissimilar convection processes have been considered for different cases. In addition, flow is taken as two dimensional, laminar, incompressible and viscous. In most of the model studies, it is assumed that buoyancy effect occur due to both thermal and mass diffusion. The presence of species concentration introduce two extra parameters into the problems, namely, w and Sc. Oscillating surface heat and mass boundary conditions have been applied for each instances. Present works sought to determine how the presence of nonuniform surface temperature and species concentration on the surface alters the convection-diffusion boundary layer flow. Since the flows with the buoyancy forces arising from combination of temperature and species concentration effects of comparable magnitude are in abundant in both natural and engineering applications, now a days double diffusive flow is investigated with greatest importance. There are many interesting aspects of such flows, for example, resulting transport characteristics, results of the opposition of the two effects, influence of the combined effect on the stability of laminar flows, the effects of values of the relative transport parameters the Prandtl number and the Schmidt number. During the investigations of each case, all these important parameters are pondered and their effects on the entire flow field have been studied.

During the studies of two dimensional, laminar, incompressible viscous flow along vertical flat plate, boundary layer approximations and Boussinesque approximations are made

and governing equations are developed accordingly. But when the flow along cylindrical surfaces are studied, the orientation of the cylinder is taken as horizontal and full sets of Navier-Stoke's equations in terms of vorticity and stream function are solved.

With the aim of studying heat and mass transfer, the regarding coefficients are calculated in terms of dimensionless quantities, such as, Nusselt number, Sherwood number. Since, these quantities are closely related to velocity and frictional force, the wall shear stress is also computed in terms of skin friction. All these dimensionless quantities are presented in terms of amplitude and phase angles. Both tabular and graphical representations are made to explicate the computed results. Most important parameters, such as, Prandtl number, Schmidt number, Strouhal number etc., that influence the entire flow fields, are taken into account and their effects are studied in details by taking different ranges of each of these parameters.

Different numerical techniques are applied to solve the governing equations of the flow field. With the purpose of validating the present numerical simulations, results obtained from different numerical techniques are compared and sometimes, the results are compared with some experimental findings and some published results. During the numerical simulations, convergence is assured by continuing iteration until the difference of the results of two successive iterations becomes less or equal to 10^{-6}.

Flow along vertical flat plate is studied in chapter 3. Fluid flow along a vertical wedge is contemplated in chapter 4 and 5. In chapter 6 of this dissertation, buoyancy driven magnetohydrodynamic flow along a vertical surface have been considered in presence of strong magnetic field. It has been assumed that in some undisturbed flow region , there is a uniform magnetic field making a nonzero angle with it. In the model flow, studied in chapter 6 and 7, consideration has been given to unsteady two dimensional mixed convection flow of a viscous incompressible fluid over a heated circular cylinder. The cylinder is placed horizontally in a uniform stream with its axis perpendicular to the oncoming flow direction. Important findings for each case are listed at the end of each chapters.

From the overall observations, it can be concluded that the amplitudes of the surface heat and mass transfer coefficient increase regardless of the Prandtl number, Pr, and

Schmidt number, Sc, the buoyancy parameter w, and the exponent parameter n. The phase angles for both the surface heat and mass flux increase monotonically towards the asymptotic value for all values of the governing physical parameters.

For the flow along horizontal heated cylinder, recirculation region of different sizes and shapes are discerned for different values of thermal grashof number Gr_T as well as concentration grashof number Gr_C. Higher values of both these parameters result into larger recirculation region, therefore higher reattachment length is calculated. Because of larger size of the recirculation region, both heat and mass transfer in the surface are increased.

From the analysis of heat and mass transfer along with wall shear stress, it can be inferred a complex correlation among the flow pattern, wall shear stress, surface heat and mass transfer enhancement. Nonuniform heat and mass boundary conditions also introduce some interesting feature in the flow field.

Future works:

First of all, the possible and accessible extension of the present works can undergo experimental and analytical investigation. As further improvement of the present work, each model can be extended for compressible flow. The variable viscosity can also be incorporated so that all these studies can be fit into broader areas of engineering applications. Moreover, some other physical parameters, such as: radiation effect, chemical reactions, phase changes etc. can also be studied with all these prescribed models. All these modeled flow can be studied for more complicated geometry. The calculated results and observations can be incorporated with some relevant industrial and engineering problems and optimization can be achieved for real world applications. Moreover the unsteady natural, forced and mixed convection flow problems discussed here can surely be extended to the transient state problems as well.

Appendix A

Keller-Box Method

In this section the detailed description of the numerical scheme, which is effectively used to solve various boundary layer problems under different geometries with significant physical circumstances is presented. To solve these nonlinear parabolic partial differential equations, Keller box method is effectively used. This method was initially introduced by [94] and subsequently this idea was further exposed by many researchers. Since the mathematical formulation is already considered in the particular chapters, here only the steps which are incorporated in this numerical scheme are discussed, specifically for the problem (3.30)-(3.32) and similar steps has been followed for other sets of equations.

The development of the algorithm of implicit finite difference method together with Keller-box scheme is worked out on the non-similarity equations (3.30)-(3.32) satisfying the boundary conditions (3.33). These equations are as follows

$$F''' + p_1 F F'' - p_2 (F')^2 + p_3 \Theta + p_4 \Phi = 0 \tag{A.1}$$

$$\frac{1}{Pr}\Theta'' + p_1 F \Theta' - p_5 F' \Theta = 0 \tag{A.2}$$

$$\frac{1}{Sc}\Phi'' + p_1 F \Phi' - p_5 F' \Phi = 0 \tag{A.3}$$

$$F(0) = F'(0) = 0, \Theta'(0) = \Phi'(0) = -1$$
$$F'(\infty) = \Theta(\infty) = \Phi(\infty) = 0 \tag{A.4}$$

where

$$p_1 = \frac{n+4}{5}, \quad p_2 = \frac{2n+3}{5}, \quad p_3 = (1-w), \quad p_4 = w, \quad p_5 = \frac{4n+1}{5} \tag{A.5}$$

The procedure can be initiated by writing the system of equations. (A.1)-(A.4) in terms of system of first order equations as given below:

$$F' = u \tag{A.6}$$

$$u' = v \tag{A.7}$$

$$\Theta' = p \tag{A.8}$$

$$\Phi' = q \tag{A.9}$$

$$v' + p_1 F v - p_2 u^2 + p_3 \Theta + p_4 \Phi = 0 \tag{A.10}$$

$$\frac{1}{Pr} p' + p_1 F p - p_5 \Theta = 0 \tag{A.11}$$

$$\frac{1}{Sc} q' + p_1 F q - p_5 \Phi = 0 \tag{A.12}$$

The corresponding boundary conditions take the form

$$\begin{gathered} f(0,\xi) = u(0,\xi) = 0, \quad \Theta(0,\xi) = -1, \quad \Phi(0,\xi) = -1 \\ u(\infty,\xi) \to 0, \quad \Theta(\infty,\xi) \to 0, \quad \Theta(\infty,\xi) \to 0 \end{gathered} \tag{A.13}$$

The net points are expressed as

$$\begin{gathered} \xi^0 = 0, \quad \xi^n = \xi^{n-1} + k_n, \quad n = 1, 2, \ldots, N \\ \eta_0 = 0, \quad \eta_j = \eta_{j-1} + m_j, \quad j = 1, 2, \ldots, J, \quad \eta_J = \eta_\infty \end{gathered} \tag{A.14}$$

where k_n and m_j are the variable mesh width. Now we approximate the physical quantities $(F,\ u,\ v,\ \Theta,\ p,\ \Phi,\ q)$ at each point (ξ^n, η_j) of the net by $(F^n,\ u^n,\ v^n,\ \Theta^n,\ p^n, \Phi^n,\ q^n)$,

which are denoted by net functions.

We initiate discretization process by writing the finite difference approximations of the ordinary differential equations (A.6)-(A.9) for the midpoint $(x^n, \eta_{j-1/2})$ using centered difference derivatives. Thus, we get

$$\begin{aligned}
\frac{F_j^n - F_{j-1}^n}{m_j} &= \frac{u_j^n + u_{j-1}^n}{2} = u_{j-1/2}^n \\
\frac{u_j^n - u_{j-1}^n}{m_j} &= \frac{v_j^n + v_{j-1}^n}{2} = v_{j-1/2}^n \\
\frac{\Theta_j^n - \Theta_{j-1}^n}{m_j} &= \frac{p_j^n + p_{j-1}^n}{2} = p_{j-1/2}^n \\
\frac{\Phi_j^n - \Phi_{j-1}^n}{m_j} &= \frac{q_j^n + q_{j-1}^n}{2} = q_{j-1/2}^n
\end{aligned} \tag{A.15}$$

For the partial differential equations (A.10)-(A.12), the finite difference forms are approximated by centering about the midpoint $(\xi^{n-1/2}, \eta_{j-1/2})$. This can be accomplished in two steps. Firstly, we center the partial differential equations (A.10)-(A.12) about the point $(\xi^{n-1/2}, \eta)$ without specifying η. Let $L_1,\ L_2$ and L_3 be the notations for left hand side (LHS) of the equations (A.10)-(A.12) respectively. Therefore the finite difference approximations to the equations (A.10)-(A.12) can be written as

$$\begin{aligned}
\frac{L_1^n + L_1^{n-1}}{2} &= 0 \\
\frac{L_2^n + L_2^{n-1}}{2} &= 0 \\
\frac{L_3^n + L_3^{n-1}}{2} &= 0
\end{aligned} \tag{A.16}$$

The above set of equation (A.16)can also be written in the form

$$(v^{'})^n + p_1(Fv)^n - p_2(u^2)^n + p_3\Theta^n + p_4\Phi^n = -L_1^{n-1} \tag{A.17}$$

$$\frac{1}{Pr}(p^{'})^n + p_1(Fp)^n - p_5(u\Theta)^n = -L_2^{n-1} \tag{A.18}$$

$$\frac{1}{Sc}(q^{'})^n + p_1(Fq)^n - p_5(u\Phi)^n = -L_3^{n-1} \tag{A.19}$$

where

$$\begin{aligned} L_1^{n-1} &= \left[v^{'} + p_1 F v - p_2 u^2 + p_3 \Theta - p_4 \Phi\right]^{n-1} \\ L_2^{n-1} &= \left[\frac{1}{Pr} p^{'} + p_1 (F p) - p_5 (u \Theta)\right]^{n-1} \\ L_3^{n-1} &= \left[\frac{1}{Sc} q^{'} + p_1 (F q) - p_5 (u \Phi)\right]^{n-1} \end{aligned} \tag{A.20}$$

By centering the equations (A.17)-(A.19) about the point $(\xi^{n-1/2}, \eta_{j-1/2})$.

$$\frac{(v_j^n - v_{j-1}^n)}{m_j} + p_1 (F v)_{j-1/2}^n - p_2 (u_{j-1/2}^n)^2 + p_3 \Theta_{j-1/2}^n + p_4 \Phi_{j-1/2}^n = -(L_1)_{j-1/2}^{n-1} \tag{A.21}$$

$$\frac{1}{Pr} \frac{(p_j^n - p_{j-1}^n)}{m_j} + p_1 (F p)_{j-1/2}^n + p_5 (u \Theta)_{j-1/2}^n = -(L_2)_{j-1/2}^{n-1} \tag{A.22}$$

$$\frac{1}{Sc} \frac{(q_j^n - q_{j-1}^n)}{m_j} + p_1 (F q)_{j-1/2}^n + p_5 (u \Phi)_{j-1/2}^n = -(L_3)_{j-1/2}^{n-1} \tag{A.23}$$

where

$$\begin{aligned} (L_1)_{j-1/2}^{n-1} &= \left[\frac{(v_j - v_{j-1})}{m_j} + p_1 F_{j-1/2} v_{j-1/2} - p_2 (u_{j-1/2})^2 + p_3 \Theta_{j-1/2} + p_4 \Phi_{j-1/2}\right]^{n-1} \\ (L_2)_{j-1/2}^{n-1} &= \left[\frac{1}{Pr} \frac{(p_j - p_{j-1})}{m_j} + p_1 F_{j-1/2} p_{j-1/2} - p_5 \Theta_{j-1/2} u_{j-1/2}\right]^{n-1} \\ (L_3)_{j-1/2}^{n-1} &= \left[\frac{1}{Sc} \frac{(q_j - q_{j-1})}{m_j} + p_1 F_{j-1/2} q_{j-1/2} - p_5 \Phi_{j-1/2} u_{j-1/2}\right]^{n-1} \end{aligned} \tag{A.24}$$

The equations in (A.15), (A.21)-(A.23) are evaluated for $j = 1, 2, \cdots, J$ at a given n. The boundary conditions at $\xi = \xi^n$ are

$$F_0^n = u_0^n = v_0^n = 0, \quad \Theta_0^n = 1, \quad \Phi_0^n = 1, \quad u_J^n = 0, \quad \Theta_J^n = 0, \quad \Phi_J^n = 0 \tag{A.25}$$

Equations in (A.15) and (A.21)-(A.23) form a system of equations in which $(F_j^n, u_j^n, v_j^n, \Theta_j^n, p_j^n, \Phi_j^n, q_j^n)$ for $0 \leq j \leq J$ are unknowns and the quantities $(F_j^{n-1}, u_j^{n-1}, v_j^{n-1}, \Theta_j^{n-1}, p_j^{n-1}, \Phi_j^{n-1}, q_j^{n-1})$ are already known for $0 \leq j \leq J$.

It is to be noted that $(L_1)_{j-1/2}^{n-1}$, $(L_2)_{j-1/2}^{n-1}$, $(L_3)_{j-1/2}^{n-1}$ involve only known quantities if it is assumed that the solution is known on $\xi = \xi^{n-1}$. Introducing Newton's method by linearizing the system of equations (A.15), (A.20)- (A.23). For the higher order iterates, consider

$$\begin{aligned} F_j^{(i+1)} &= F_j^{(i)} + \delta F_j^{(i)} \\ u_j^{(i+1)} &= u_j^{(i)} + \delta u_j^{(i)} \\ v_j^{(i+1)} &= v_j^{(i)} + \delta v_j^{(i)} \\ \Theta_j^{(i+1)} &= \Theta_j^{(i)} + \delta \Theta_j^{(i)} \\ p_j^{(i+1)} &= p_j^{(i)} + \delta p_j^{(i)} \\ \Phi_j^{(i+1)} &= \Phi_j^{(i)} + \delta \Phi_j^{(i)} \\ q_j^{(i+1)} &= q_j^{(i)} + \delta q_j^{(i)} \end{aligned} \tag{A.26}$$

Substituting the expressions (A.26) in to equations (A.15) and (A.20)-(A.23) and dropping the terms that are quadratic in $(\delta F_j^n, \delta u_j^n,\ \delta v_j^n, \delta \Theta_j^n,\ \delta p_j^n, \delta \Phi_j^n, \delta q_j^n)$, the following set of equations after some algebraic manipulations can be formed

$$\delta F_j^{(i)} - \delta F_{j-1}^{(i)} - \frac{1}{2} m_j \left(\delta u_j^{(i)} + \delta u_{j-1}^{(i)} \right) = (r_1)_{j-1/2} \tag{A.27}$$

$$\delta u_j^{(i)} - \delta u_{j-1}^{(i)} - \frac{1}{2} m_j \left(\delta v_j^{(i)} + \delta v_{j-1}^{(i)} \right) = (r_5)_{j-1/2} \tag{A.28}$$

$$\delta \Theta_j^{(i)} - \delta \Theta_{j-1}^{(i)} - \frac{1}{2} m_j \left(\delta p_j^{(i)} + \delta p_{j-1}^{(i)} \right) = (r_6)_{j-1/2} \tag{A.29}$$

$$\delta \Phi_j^{(i)} - \delta \Phi_{j-1}^{(i)} - \frac{1}{2} m_j \left(\delta q_j^{(i)} + \delta q_{j-1}^{(i)} \right) = (r_7)_{j-1/2} \tag{A.30}$$

$$\begin{aligned} &(a_1)_j \delta v_j^{(i)} + (a_2)_j \delta v_{j-1}^{(i)} + (a_3)_j \delta F_j^{(i)} + (a_4)_j \delta F_{j-1}^{(i)} + (a_5)_j \delta u_j^{(i)} + (a_6)_j \delta u_{j-1}^{(i)} \\ &+ (a_7)_j \delta \Theta_j^{(i)} + (a_8)_j \delta \Theta_{j-1}^{(i)} + (a_9)_j \delta p_j^{(i)} + (a_{10})_j \delta p_{j-1}^{(i)} + (a_{11})_j \delta \Phi_j^{(i)} + (a_{12})_j \delta \Phi_{j-1}^{(i)} \\ &+ (a_{13})_j \delta q_j^{(i)} + (a_{14})_j \delta q_{j-1}^{(i)} = (r_2)_{j-1/2} \end{aligned} \tag{A.31}$$

$$(b_1)_j\delta p_j^{(i)} + (b_2)_j\delta p_{j-1}^{(i)} + (b_3)_j\delta F_j^{(i)} + (b_4)_j\delta F_{j-1}^{(i)} + (b_5)_j\delta u_j^{(i)} + (b_6)_j\delta u_{j-1}^{(i)}$$
$$+ (b_7)_j\delta v_j^{(i)} + (b_8)_j\delta v_{j-1}^{(i)} + (b_9)_j\delta\Theta_j^{(i)} + (b_{10})_j\delta\Theta_{j-1}^{(i)} + (b_{11})_j\delta\Phi_j^{(i)} + (b_{12})_j\delta\Phi_{j-1}^{(i)} \quad \text{(A.32)}$$
$$+ (b_{13})_j\delta q_j^{(i)} + (b_{14})_j\delta q_{j-1}^{(i)} = (r_3)_{j-1/2}$$

$$(c_1)_j\delta q_j^{(i)} + (c_2)_j\delta q_{j-1}^{(i)} + (c_3)_j\delta F_j^{(i)} + (c_4)_j\delta F_{j-1}^{(i)} + (c_5)_j\delta u_j^{(i)} + (c_6)_j\delta u_{j-1}^{(i)}$$
$$+ (c_7)_j\delta v_j^{(i)} + (c_8)_j\delta v_{j-1}^{(i)} + (c_9)_j\delta\Theta_j^{(i)} + (c_{10})_j\delta\Theta_{j-1}^{(i)} + (c_{11})_j\delta p_j^{(i)} + (c_{12})_j\delta p_{j-1}^{(i)} \quad \text{(A.33)}$$
$$+ (c_{13})_j\delta\Phi_j^{(i)} + (c_{14})_j\delta\Phi_{j-1}^{(i)} = (r_4)_{j-1/2}$$

where

$$(a_1)_j = \frac{1}{m_j} + \frac{p_1}{2}F_j^i, \quad (a_2)_j = -\frac{1}{m_j} + \frac{p_1}{2}F_{j-1}^i$$
$$(a_3)_j = \frac{p_1}{2}v_j^i, \quad (a_4)_j = \frac{p_1}{2}v_{j-1}^i, \quad (a_5)_j = -\frac{p_2}{2}u_j^i, \quad (a_6)_j = -\frac{p_2}{2}u_{j-1}^i,$$
$$(a_7)_j = \frac{p_3}{2}, \quad (a_8)_j = \frac{p_3}{2}, \quad (a_9)_j = 0, \quad (a_{10})_j = 0,$$
$$(a_{11})_j = \frac{p_4}{2}, (a_{12})_j = \frac{p_4}{2}, (a_{13})_j = 0, \quad (a_{14})_j = 0,$$

$$(b_1)_j = \frac{1}{Pr\ m_j} + \frac{p_1}{2}F_j^i, \quad (b_2)_j = -\frac{1}{Pr\ m_j} + \frac{p_1}{2}F_{j-1}^i$$
$$(b_3)_j = \frac{p_1}{2}p_j^i, \quad (b_4)_j = \frac{p_1}{2}p_{j-1}^i, \quad (b_5)_j = -\frac{p_5}{2}\ \Theta_{j-1/2}^i, \quad (b_6)_j = -\frac{p_5}{2}\ \Theta_{j-1/2}^i,$$
$$(b_7)_j = 0, \quad (b_8)_j = 0, \quad (b_9)_j = -\frac{p_5}{2}u_{j-1/2}^i, \quad (b_{10})_j = -\frac{p_5}{2}u_{j-1/2}^i$$
$$(b_{11})_j = \quad (b_{12})_j = \quad (b_{13})_j = 0, \quad (b_{14})_j = 0,$$

$$(c_1)_j = \frac{1}{Sc\ m_j} + \frac{1}{2}p_1F_j^i, \quad (c_2)_j = -\frac{1}{Sc\ m_j} + \frac{p_1}{2}F_{j-1}^i$$
$$(c_3)_j = \frac{p_1}{2}q_j^i, \quad (c_4)_j = \frac{p_1}{2}q_{j-1}^i, \quad (c_5)_j = -\frac{p_5}{2}\ q_{j-1/2}^i, \quad (c_6)_j = -\frac{p_5}{2}\ q_{j-1/2}^i,$$
$$(c_7)_j = 0, \quad (c_8)_j = 0, \quad (c_9)_j = 0, \quad (c_{10})_j = 0,$$
$$(c_{11})_j = 0, \quad (c_{12})_j = 0, \quad (c_{13})_j = -\frac{p_5}{2}\ u_{j-1/2}^i, \quad (c_{14})_j = -\frac{p_5}{2}\ u_{j-1/2}^i$$

$$
\begin{aligned}
(r_1)_{j-1/2} &= \left(F_{j-1}^{n}\right)^{(i)} - \left(F_{j}^{n}\right)^{(i)} + m_j \left(u_{j-1/2}^{n}\right)^{(i)} \\
(r_5)_{j-1/2} &= \left(u_{j-1}^{n}\right)^{(i)} - \left(u_{j}^{n}\right)^{(i)} + m_j \left(v_{j-1/2}^{n}\right)^{(i)} \\
(r_6)_{j-1/2} &= \left(\Theta_{j-1}^{n}\right)^{(i)} - \left(\Theta_{j}^{n}\right)^{(i)} + m_j \left(p_{j-1/2}^{n}\right)^{(i)} \\
(r_7)_{j-1/2} &= \left(\Phi_{j-1}^{n}\right)^{(i)} - \left(\phi_{j}^{n}\right)^{(i)} + m_j \left(q_{j-1/2}^{n}\right)^{(i)} \\
(r_2)_{j-1/2} &= -\left[\frac{1}{m_j}\left(v_j^n - v_{j-1}^n\right) + p_1 (Fv)_{j-1/2}^{n} - p_2 (u^2)_{j-1/2}^{n} + p_3 \Theta_{j-1/2}^{n} + p_4 \Phi_{j-1/2}^{n}\right]^{i} - (L_1)_{j-1/2}^{n-1} \\
(r_3)_{j-1/2} &= -\left[\frac{1}{Pr\ m_j}\left(p_j^n - p_{j-1}^n\right) + p_1 \left(Fp\right)_{j-1/2}^{n} - p_5 u_{j-1/2}^{n} \Theta_{j-1/2}^{n}\right]^{i} - (L_2)_{j-1/2}^{n-1} \\
(r_4)_{j-1/2} &= -\left[\frac{1}{Sc\ m_j}\left(q_j^n - q_{j-1}^n\right) + p_1 \left(Fq\right)_{j-1/2}^{n} - p_5 u_{j-1/2}^{n} \Phi_{j-1/2}^{n}\right]^{i} - (L_3)_{j-1/2}^{n-1}
\end{aligned}
\tag{A.34}
$$

The boundary conditions becomes

$$
\delta F_0 = \delta u_0 = \delta u_0 = 0, \quad \delta\Theta_0 = 1, \quad \delta\Phi_0 = 1, \quad \delta u_J = 0, \quad \delta\Theta_J = 0, \quad \delta\Phi_J = 0 \tag{A.35}
$$

The structure of the linearized system of differential equations (A.27)-(A.33) is a block tridiagonal structure which can be solved with the help of block elimination method.

Appendix B

Implicit Finite Difference Method Along with Gaussian Elimination Method

The governing equations of the boundary layer problems can also be solved with the help of implicit finite difference method which has various advantages. First of all, this technique is comparatively easier to implement and also can be firmly applied to problems having complex physical situations and easily enhanced to cover the influence of variable properties of the fluid. The development of the algorithm of implicit finite difference method together with Gaussian elimination technique is worked out on the partial differential equations (6.29)-(6.31) satisfying the boundary conditions (6.32) as well as some other sets of equation. The detailed description of this technique for the equations (6.29)-(6.31)together

with the boundary condition (6.32) is presented here.

$$\frac{\partial^2 H}{\partial \eta^2} + \frac{3+2\xi}{4(1+\xi)} f \frac{\partial H}{\partial \eta} - \frac{1}{2(1+\xi)} H^2 - \xi^{1/2}(1+\xi)^{1/2} H + (1+\xi)(\Theta + N\Phi) = \xi \left(H \frac{\partial H}{\partial \xi} - \frac{\partial H}{\partial \eta} \frac{\partial F}{\partial \xi} \right) \tag{B.1}$$

$$\frac{1}{Pr} \frac{\partial^2 \Theta}{\partial \eta^2} + \frac{3+2\xi}{4(1+\xi)} F \frac{\partial \Theta}{\partial \eta} = \xi \left(H \frac{\partial \Theta}{\partial \xi} - \frac{\partial \Theta}{\partial \eta} \frac{\partial F}{\partial \xi} \right) \tag{B.2}$$

$$\frac{1}{Sc} \frac{\partial^2 \Phi}{\partial \eta^2} + \frac{3+2\xi}{4(1+\xi)} F \frac{\partial \Phi}{\partial \eta} = \xi \left(H \frac{\partial \Phi}{\partial \xi} - \frac{\partial \Phi}{\partial \eta} \frac{\partial F}{\partial \xi} \right) \tag{B.3}$$

Along with the boundary conditions:

$$F(0,\xi) = H(0,\xi) = 0,\ \Theta(0,\xi) = \Phi(0,\xi) = 1$$
$$H(\infty,\xi) \to 0,\ \Theta(\infty,\xi) \to 0,\ \Phi(\infty,\xi) \to 0 \tag{B.4}$$

An under relaxation iterative procedure is chosen for the finite difference technique. Subscripts i and j are used to represent nodes in the ξ and η directions respectively and $1 \le i \le L$ and $2 \le j \le L-1$. Now the expressions of the partial differential equations of mass, momentum and energy given in (6.29)-(6.31) in finite difference quotients are implemented. The discretization procedure is carried out for numerical scheme using central difference for diffusion terms and backward difference for the convection terms. Equations (B1)-(B3) can be written as

$$\frac{H_{i,j+1} - 2H_{i,j} + H_{i,j-1}}{(\triangle\eta)^2} + P_1 F_{i,j} \frac{H_{i,j+1} - H_{i,j-1}}{2\triangle\eta} - P_2 H_{i,j}^2 - P_3 H_{i,j} + P_4 \left(\Theta_{i,j} + N\Phi_{i,j}\right) = \xi \left[H_{i,j} \left(\frac{H_{i,j} - H_{i-1,j}}{\triangle\xi} \right) - \left(\frac{F_{i,j} - F_{i-1,j}}{\triangle\xi} \right) \left(\frac{H_{i,j+1} - H_{i,j-1}}{2\triangle\eta} \right) \right] \tag{B.5}$$

$$\frac{1}{Pr} \frac{\Theta_{i,j+1} - 2\Theta_{i,j} + \Theta_{i,j-1}}{(\triangle\eta)^2} + P_1 F_{i,j} \frac{\Theta_{i,j+1} - \Theta_{i,j-1}}{2\triangle\eta} = \xi \left[H_{i,j} \left(\frac{\Theta_{i,j} - \Theta_{i-1,j}}{\triangle\xi} \right) - \left(\frac{F_{i,j} - F_{i-1,j}}{\triangle\xi} \right) \left(\frac{\Theta_{i,j+1} - \Theta_{i,j-1}}{2\triangle\eta} \right) \right] \tag{B.6}$$

$$\begin{aligned}&\frac{1}{Sc}\frac{\Phi_{i,j+1}-2\Phi_{i,j}+\Theta_{i,j-1}}{(\triangle\eta)^2}+P_1F_{i,j}\frac{\Phi_{i,j+1}-\Phi_{i,j-1}}{2\triangle\eta}\\&=\xi\left[H_{i,j}\left(\frac{\Phi_{i,j}-\Phi_{i-1,j}}{\triangle\xi}\right)-\left(\frac{F_{i,j}-F_{i-1,j}}{\triangle\xi}\right)\left(\frac{\Phi_{i,j+1}-\Phi_{i,j-1}}{2\triangle\eta}\right)\right]\end{aligned}\tag{B.7}$$

Associated boundary conditions are

$$\begin{aligned}\eta_1=0:\quad & F_{1,j}=H_{1,j}=0,\quad \Theta_{1,j}=1,\quad \Phi_{1,j}=1\\ \eta_L\to\infty:\quad & H_{L,j}\to 0,\quad \Theta_{L,j}\to 0,\quad \Phi_{L,j}\to 0,\end{aligned}\tag{B.8}$$

where

$$P_1=\frac{3+2\xi}{4(1+\xi)},\quad P_2=\frac{1}{2(1+\xi)},\quad P_3=\xi^{1/2}(1+\xi)^{1/2},\quad P_4=(1+\xi)\tag{B.9}$$

Finally (B.5)-(B.7) leads to a system of algebraic equations. Momentum equation (B.5) gives

$$\begin{aligned}&A_1\ H_{i,j-1}+B_1\ H_{i,j}+C_1\ H_{i,j+1}=D_1,\quad \text{where}\\&C=-\left[\frac{1}{(\triangle\eta)^2}+\frac{\left(\frac{3+2\xi}{4(1+\xi)}F_{i,j}+\frac{\xi}{\triangle\xi}(F_{i,j}-F_{i-1,j})\right)}{(2\triangle\eta)}\right]\\&A=-\left[\frac{1}{(\triangle\eta)^2}-\frac{\left(\frac{3+2\xi}{4(1+\xi)}F_{i,j}+\frac{\xi}{\triangle\xi}(F_{i,j}-F_{i-1,j})\right)}{(2\triangle\eta)}\right]\\&B=\frac{2}{(\triangle\eta)^2)}+\left(\frac{1}{2(1+\xi)}+\frac{\xi}{\triangle\xi}\right)H_{i,j}+\xi^{1/2}(1+\xi)^{1/2}\\&D=\frac{\xi}{\triangle\xi}H_{i,j}H_{i-1,j}+(1+\xi)(\Theta_{i,j}+N\Phi_{i,j})\end{aligned}\tag{B.10}$$

It can be noted that for every value of i the unknown quantities are $H_{i,j+1}$, $H_{i,j}$ and $H_{i,j-1}$ for $j=2,3,4,\cdots,L-1$ leads to a set of $L-2$ equations with $L-2$ unknowns ($H_{i,2}$, $H_{i,3}$, $\cdots$, $H_{i,L-2}$ and $H_{i,L-1}$). The set of equations in (B.10) can be expressed in the form of

following matrix

$$\begin{pmatrix} B_{1,2} & C_{1,2} & 0 & 0 & \cdots & 0 & 0 & 0 \\ A_{1,3} & B_{1,3} & C_{1,3} & 0 & \cdots & 0 & 0 & 0 \\ 0 & A_{1,4} & B_{1,4} & C_{1,4} & \cdots & 0 & 0 & 0 \\ \vdots & \vdots & \vdots & \vdots & \ddots & \vdots & \vdots & \vdots \\ \vdots & \vdots & \vdots & \vdots & \ddots & \vdots & \vdots & \vdots \\ 0 & 0 & 0 & 0 & \cdots & A_{1,L-2} & B_{1,L-2} & C_{1,L-2} \\ 0 & 0 & 0 & 0 & \cdots & 0 & A_{1,L-1} & B_{1,L-1} \end{pmatrix} \begin{pmatrix} H_{i,2} \\ H_{i,3} \\ H_{i,4} \\ \vdots \\ \vdots \\ H_{i,L-2} \\ H_{i,L-1} \end{pmatrix} = \begin{pmatrix} D_{1,2} \\ D_{1,3} \\ D_{1,4} \\ \vdots \\ \vdots \\ D_{1,L-2} \\ D_{1,L-1} \end{pmatrix} \tag{B.11}$$

For the energy equation, (B.6)the discretized equation takes the form:

$$\begin{aligned} &A_2\Theta_{i,j-1} + B_2\Theta_{i,j} + C_2\Theta_{i,j+1} = D_2, \quad \text{where} \\ &C_2 = -\left[\frac{1}{Pr\ (\triangle\eta)^2} + \left(\frac{3+2\xi}{4(1+\xi)}F_{i,j} + \frac{\xi}{\triangle\xi}(F_{i,j-F_{i-1,j}})\right)/(2\triangle\eta)\right] \\ &A_2 = -\left[\frac{1}{Pr\ (\triangle\eta)^2} - \left(\frac{3+2\xi}{4(1+\xi)}F_{i,j} + \frac{\xi}{\triangle\xi}(F_{i,j-F_{i-1,j}})\right)/(2\triangle\eta)\right] \\ &B_2 = \frac{2}{Pr(\triangle\eta)^2} + \frac{\xi}{\triangle\xi}H_{i,j},\ D_2 = \frac{\xi}{\triangle\xi}H_{i,j}\Theta_{i-1,j} \end{aligned} \tag{B.12}$$

Here again for each value of i the unknown variables are $\Theta_{i,j-1}$, $\Theta_{i,j}$ and $\Theta_{i,j+1}$ for $j = 2, 3, 4, \cdots, L-1$ leads to a set of $L-2$ equations with $L-2$ unknowns ($\Theta_{i,2}$, $\Theta_{i,3}$, $\cdots$, $\Phi_{i,L-2}$ and $\Phi_{i,L-1}$). The set of equations in (B.12) can be expressed in the form of following matrix

$$\begin{pmatrix} B_{2,2} & C_{2,2} & 0 & 0 & \cdots & 0 & 0 & 0 \\ A_{2,3} & B_{2,3} & C_{2,3} & 0 & \cdots & 0 & 0 & 0 \\ 0 & A_{2,4} & B_{2,4} & C_{2,4} & \cdots & 0 & 0 & 0 \\ \vdots & \vdots & \vdots & \vdots & \ddots & \vdots & \vdots & \vdots \\ \vdots & \vdots & \vdots & \vdots & \ddots & \vdots & \vdots & \vdots \\ 0 & 0 & 0 & 0 & \cdots & A_{2,L-2} & B_{2,L-2} & C_{2,L-2} \\ 0 & 0 & 0 & 0 & \cdots & 0 & A_{2,L-1} & B_{2,L-1} \end{pmatrix} \begin{pmatrix} \Phi_{i,2} \\ \Phi_{i,3} \\ \Phi_{i,4} \\ \vdots \\ \vdots \\ \Phi_{i,L-2} \\ \Phi_{i,L-1} \end{pmatrix} = \begin{pmatrix} D_{2,2} \\ D_{2,3} \\ D_{2,4} \\ \vdots \\ \vdots \\ D_{2,L-2} \\ D_{2,L-1} \end{pmatrix} \tag{B.13}$$

And for the concentration equation the discretized equation takes the form:

$$\begin{aligned}
&A_3\Phi_{i,j-1} + B_3\Phi_{i,j} + C_3\Phi_{i,j+1} = D_3, \quad \text{where} \\
&C_3 = -\left[\frac{1}{Sc\ (\triangle\eta)^2} + \left(\frac{3+2\xi}{4(1+\xi)}F_{i,j} + \frac{\xi}{\triangle\xi}(F_{i,j-F_{i-1,j}})\right)/(2\triangle\eta)\right] \\
&A_3 = -\left[\frac{1}{Sc\ (\triangle\eta)^2} - \left(\frac{3+2\xi}{4(1+\xi)}F_{i,j} + \frac{\xi}{\triangle\xi}(F_{i,j-F_{i-1,j}})\right)/(2\triangle\eta)\right] \\
&B_3 = \frac{2}{Sc(\triangle\eta)^2} + \frac{\xi}{\triangle\xi}H_{i,j},\ D_3 = \frac{\xi}{\triangle\xi}H_{i,j}\Phi_{i-1,j}
\end{aligned} \tag{B.14}$$

Here the unknown quantities are $\Phi_{i,j-1}$, $\Phi_{i,j}$ and $\Phi_{i,j+1}$ for each value of i while $j = 2, 3, 4, \cdots, L-1$ leads to a set of $L-2$ equations with $L-2$ unknowns ($\Phi_{i,2}$, $\Phi_{i,3}$, $\cdots$, $\Phi_{i,L-2}$ and $U_{i,L-1}$). The set of equations in (B.14) can be expressed in the form of following matrix

$$\begin{pmatrix}
B_{3,2} & C_{3,2} & 0 & 0 & \cdots & 0 & 0 & 0 \\
A_{3,3} & B_{3,3} & C_{3,3} & 0 & \cdots & 0 & 0 & 0 \\
0 & A_{3,4} & B_{3,4} & C_{3,4} & \cdots & 0 & 0 & 0 \\
\vdots & \vdots & \vdots & \vdots & \ddots & \vdots & \vdots & \vdots \\
\vdots & \vdots & \vdots & \vdots & \ddots & \vdots & \vdots & \vdots \\
0 & 0 & 0 & 0 & \cdots & A_{3,L-2} & B_{3,L-2} & C_{3,L-2} \\
0 & 0 & 0 & 0 & \cdots & 0 & B_{3,L-1} & C_{3,L-1}
\end{pmatrix}
\begin{pmatrix}
\Phi_{i,2} \\ \Phi_{i,3} \\ \Phi_{i,4} \\ \vdots \\ \vdots \\ \Phi_{i,L-2} \\ \theta_{i,L-1}
\end{pmatrix} =
\begin{pmatrix}
D_{3,2} \\ D_{3,3} \\ D_{3,4} \\ \vdots \\ \vdots \\ D_{3,L-2} \\ D_{3,L-1}
\end{pmatrix} \tag{B.15}$$

Finally $F_{i,j}$ is calculated from the relation:

$$F_{i,j} = F_{i,j-1} + \frac{1}{2}\triangle\eta\ (H_{i,j} + H_{i,j-1})$$

It is to be noted that the implicit formulas used here are found to be unconditionally stable. The discretized equations obtained in (B.11), (B.14) and (B.15) are respectively solved for $H_{i,j}$, $\Theta_{i,j}$ and $\Phi_{i,j}$, whose coefficient matrices are tridiagonal in nature. Such system of equations can be solved via Gaussian elimination technique or more effectively by Thomas Algorithm which is the innovation of Gauss elimination. In this method, the lower diagonal is eliminated initially. The details of the algorithm is given below for the

system of equations (B.11).

Applying Gauss elimination technique to (B.11) in order to eliminate the lowest diagonal term which results in an upper bi-diagonal form of the equations as given below

$$\begin{aligned}
H_{i,2} + \tfrac{C_{1,2}}{\hbar_2} H_{i,3} &= \varphi_2 \\
H_{i,3} + \tfrac{C_{1,3}}{\hbar_3} H_{i,4} &= \varphi_3 \\
\vdots \qquad\qquad \vdots & \\
H_{i,L-2} + \tfrac{C_{1,L-2}}{\hbar_{L-2}} H_{i,L-1} &= \varphi_{L-2} \\
H_{i,L-1} &= \varphi_{L-1}
\end{aligned} \tag{B.16}$$

It can be seen that the last equation in (B.16) only contains one unknown and remaining unknown variables is obtained from the penultimate equations in the above system, *i.e.*

$$\begin{aligned}
H_{i,L-1} &= \varphi_{L-1} \\
H_{i,j} &= \varphi_i - \frac{C_{1,i}}{\hbar_i} H_{i,j+1} \quad \text{for} \quad j = L-2, L-3, \cdots, 2
\end{aligned} \tag{B.17}$$

This leads to an explicit solution provided that $\hbar$'s are known. $\hbar$'s can be obtained from the following relation

$$\begin{aligned}
\hbar_2 &= B_{1,2} \\
\hbar_j &= B_{1,j} - A_{1,j} \frac{C_{1,j-1}}{\hbar_{j-1}} \quad \text{for} \quad j = 3, 4, \cdots, L-1
\end{aligned} \tag{B.18}$$

Similarly, φ's are acquired from the following

$$\begin{aligned} \varphi_2 =& \frac{D_{1,2}}{\hbar_2} \\ \varphi_j =& \frac{D_{1,j} - A_{1,j}\varphi_{j-1}}{\hbar_j} \quad \text{for} \quad j = 3, 4, \cdots, L-1 \end{aligned} \tag{B.19}$$

Similar steps are followed in order to apply Gaussian elimination technique on the system of equations (B.14) and (B.15). In the numerical procedure the iterative scheme operates along with an under relaxation factor. The under relaxation factor is used when the equations are nonlinear in nature and it lies between 0 and 1. During present simulation this factor is take to be 0.5 and it enhanced the convergence rate while solving the coupled equations. This numerical procedure comes out to be the most suitable technique when the convergence criteria leads to an oscillatory pattern and ultimately tends to overshoot the plausible final solution.

Bibliography

[1] S.Ostrach, " Natural Convection with combined driving forces ", *Physico Chem.Hydrodyn.*, vol.1, pp. 233-247, 1980.

[2] H.E.Huppert, J.S. Turner, " Double diffusive convection ", *J. Fluid. Mech.*, vol.106, pp. 299-329, 1981.

[3] B. Gebhart, L.Pera, " The nature of vertical natural convection flows resulting from the combined buoyancy effects of thermal and mass diffusion ", *Int. J. of Heat and Mass Transfer*, vol.14, pp. 2025-2050, 1971.

[4] A. Bejan, " Convection heat transfer ", New York, Wiley, 1984.

[5] A. Mongruel, M. Cloitre, C. Allain, " Scaling of boundary layer flows driven by double-diffusive convection ", *Int. J. Heat and Mass Transfer*, vol.39, pp. 3899-3910, 1996.

[6] J. S. Turner, "Buoyancy effects in fluids", Cambridge, Cambridge Univ. Press.

[7] B. Gebhart, "Natural convection flows and stability", *Adv. Heat Transfer*, vol. 9, pp. 273-348, 1973.

[8] A. Nakayama, " PC-Aided numerical heat transfer and convective flow", Tokyo, CRC press, 1995.

[9] R.J.Goldstein, R.J. Volino, " Onset and development of natural convection above a suddenly heated horizontal surface", *J. Heat Transfer*, vol.117, pp. 808-821, 1995.

[10] M.A. Hossain, "Simulteneous heat and mass transfer on oscillatory free convection boundary layer flow " *Int. J. Energy Res.*, vol.12, pp. 205-216, 1988.

[11] K.R. Khair, A. Bejan, " Mass transfer to natural convection boundary-layer flow driven by heat transfer", *J. Heat Transfer*, vol.107, pp. 979-981, 1985.

[12] H.T.Lin, C.M. Wu, " Combined heat and mass transfer by laminar natural convection flow from a vertical plate", *Heat Mass Transfer*, vol.30, pp. 369-376, 1992.

[13] H.T.Lin, C.M.Wu, " Combined heat and mass transfer by laminar natural convection flow from a vertical plate with unheated flux and concentration ", *Heat Mass Transfer*, vol.32, pp. 293-299, 1995.

[14] T.S.Chen Yuh, " Combined heat and mass transfer in natural convection on inclined surfaces ", *Numer. Heat Transfer*, vol.2, pp. 233-250, 1979.

[15] W.J. Minkowycz, P.Cheng, "Local non similar solutions for free convection with uniform lateral mass flux in porous medium ", *Lett. Heat Mass transfer*, vol.9, pp. 159-168, 1982.

[16] D. Angirasa, G.P. Peterson, I. Pop, " Combined heat and mass transfer by natural convection with opposing buoyancy effects in a fluid saturated porous medium", *Int. J. Heat and Mass Transfer*, vol.40, pp. 2755-2773, 1997.

[17] S.Hussain, M.A.Hossain, M.Wilson , " Natural Convection Flow from a Vertical Permeable Flat Plate with Variable Surface Temperature and Species Concentration " , *Engineering computations*, vol.17, Issue 7, pp. 789-812, 2000.

[18] M.A. Hossain, S.K.Das, and D.A.S.Rees, " Heat transfer response of free convection flow from a vertical heated plate to an oscillating surface heat flux " *Acta Mechanica*, vol.126, pp. 101-113, 1998.

[19] M.J.Lighthill, "The response of laminar skin-friction and heat transfer to fluctuations in the stream velocity ", *Proc. Roy. Soc*, vol.27, pp. 1-23, 1954.

[20] R.S.Nanda, V.P.Sharma, " Free Convection Laminar boundary layers in oscillatory flow ". *J. Fluid. Mech*, vol.15, pp. 419-428, 1963.

[21] S.Eshghy, V.S. Arpaci, J.A. Clark, " The effect of longitudinal oscillation on free convection from vertical surface", *J. Appl. Mech.*, vol.32, pp. 183-191, 1965.

[22] P.K. Muhuri, M.K. Maiti, " Free convection oscillatory flow from a horizontal plate ", *Int. J. Heat Mass transfer*, vol.10, pp. 717-732, 1967.

[23] M.A. Hossain, " Simultaneous heat and mass transfer on oscillatory free convection boundary layer flow ", *Int. J. Energy Research*, vol.12, pp. 761-769, 1988.

[24] M.A. Hossain, I.Pop, K. Vafai, " Combined free convection heat and mass transfer above a near horizontal surface in a porous medium", *Hybrid Methods in Engineering*, vol.1, pp. 87-102, 1999.

[25] R.C.Ackerberg, J.H. Philips, " The unsteady boundary layer on a semi-infinite flat plate due to small fluctuations in the magnitude of the free stream velocity", *J. Fluid Mech*, vol.51, part-I, pp. 137-157, 1972.

[26] O.V. Trevisan, A. Bejan, " Combined heat and mass transfer by natural convection in a vertical enclosure", *J. Heat Transfer*, vol.109, pp. 104-111, 1987.

[27] M. A. Hossain, S.Hussain, D.A.S.Rees, " Influence of fluctuating surface temperature and concentration on natural convection flow from a vertical flat plate ", *ZAMM*, vol.81, Issue 10, pp. 699-709, 2001.

[28] Hiroshi Ishigaki, " Periodic Boundary layer near a two -dimensional stagnation point", *J. of Fluid. Mech.*, vol.43, pp. 477-486, 1970.

[29] Hiroshi Ishigaki, " An exact periodic solution of the energy equation ", *J. of Fluid. Mech.*, vol.50, pp. 657-668, 1971.

[30] Hiroshi Ishigaki, " Skin friction and surface temperature of an insulated flat plate fixed in a fluctuating stream ", *J. of Fluid. Mech.*, vol.46, pp. 165-175, 1971.

[31] Hiroshi Ishigaki, " The effect of oscillation on flat plate heat transfer", *J. of Fluid. Mech.*, vol.47, pp. 537-546, 1971.

[32] Hiroshi Ishigaki, " Heat transfer in a periodic boundary layer near a two-dimensional stagnation point", *J. of Fluid. Mech.*, vol.56, pp. 619-627, 1972.

[33] M. B.Glauert, " The laminar boundary layer on oscillating plates and cylinders" , *J. Fluid Mech*, vol.1, pp. 97-110, 1955.

[34] M. B. Glauert, " Oscillatory flow past a magnetize plate ", *J. Fluid Mech.*, vol.12, pp. 625-637, 1962.

[35] K. Gerstan, " Heat transfer in laminar boundary layers with oscillating outer flow ", AGARBograph, vol.97, pp. 423-475, 1965.

[36] M. Kumari, R.S.R. Gorla, " Combined convection along a non-isothermal wedge in a porous medium", *J. Heat Mass Transfer*, vol.32, pp.-393-398, 1997.

[37] M.A. Hossain, M.S. Munir, M.Z. Hafiz, H.S. Takhar, " Flow of a viscous incompressible fluid of temperature dependent viscosity past a permeable wedge with uniform surface heat flux", *Heat Mass Transfer*, vol.36, pp. 333-341, 2000.

[38] M. Kumari, H.S. Takhar, G. Nath, " Mixed convection flow over a vertical wedge embedded in a highly porous medium", *J. Heat Mass Transfer*, vol.37, pp. 139-146, 2001.

[39] R. Kandasamy, I. Muhaimin , A.B. Khamis, " Thermophoresis and variable viscosity effects on MHD mixed convective heat and mass transfer past a porous wedge in the presence of chemical reaction" , *Heat Mass Transfer*, vol.45, pp. 703-712, 2009.

[40] P.C. Sinha, P. Singh, " Transient free convection flow due to the arbitrary motion of a vertical plate ", *Proc. Camb. Phil. Soc.*, vol.67, pp. 677-688, 1970.

[41] N.C. Roy, M.A.Hossain, S. Hussain, " Unsteady laminar mixed convection boundary layer flow near a vertical wedge due to oscillations in the free-stream and surface temperature", *Int. J. of Applied Mechanics and Engineering* , vol. 21, No.1, pp. 169-186, 2016.

[42] R. Eichhorn, "The effect of mass transfer on free convection", *ASME J. Heat Transfer*, vol.82, pp. 260-263, 1960.

[43] E.M. Sparrow, R.D. Cess, " Free convection with lowing and suction ",*Int. J. Heat Mass Transfer*, vol.83, pp. 387-389, 1961.

[44] J.H.Merkin, " The effects of blowing and suction on free convection boundary layers ", *Int. J. Heat Mass Transfer* , vol.18, pp. 237-244, 1975.

[45] P.G.Parikh, R. Moffat, W. Kays, D.Bershader, " Free convection over a vertical porous plate with transpiration", *Int.J. Heat Mass Transfer*, vol.17, pp. 1465-1474, 1974.

[46] J.P.Hartnett, E.R.G.Eckert, " Mass transfer cooling in a laminar boundary layer with constant fluid properties ", (1975),*ASME J. Heat Transfer*, vol.79, pp. 247-254, 1975.

[47] E.M. Sparrow, J.B. Starr, " The transpiration cooling flat plate with various thermal and boundary condition ",*Int. J. Heat Mass Transfer*, vol.9, pp. 508-510, 1960.

[48] T.T. Kao, " Laminar free convection with suction or blowing along a vertical surface ", *AIChE J.*, vol.28, pp.338-341, 1982.

[49] M. Vedhanayagam, R.A Altenkirch, R. Eichhorn, " A transformation of the boundary-layer equations for free convection past a vertical flat plate with arbitrary blowing and wall temperature variation ", *Int. J. Heat Mass Transfer*, vol.23, pp. 1286-1288.

[50] H.T. Lin, W.S. Yu, " Free convection on horizontal plate with blowing and suction ", *ASME, J. Heat Transfer*, vol.110, pp. 793-796, 1988.

[51] S. Tsuruno, I. Iguchi, " Prediction of combined free and forced convective heat transfer along a vertical plate with uniform blowing ", *ASME, J. Heat Transfer*, vol.102, pp. 168-170, 1980.

[52] R.M. Terril, " Laminar boundary layer flow near separation with and without suction", *Phil. Trans. Royal Society*, vol.9, pp. 55-100, 1960.

[53] M.D. kelleher, K.T. Yang, " Heat transfer response of laminar free convection boundary-layers along vertical heated plate to surface temperature", *ZAMP*, vol.19, pp. 31-44, 1968.

[54] K.T. Yang, " Possible similarity solutions for laminar free convection on vertical plates and cylinders ", *J. Appl. Mech.*, vol. 82, pp. 230-236, 1960.

[55] M.A. Hossain, " Effect of transpiration on combined heat and mass transfer in mixed convection along a vertical plate", *Int. J. Energy Res.*, vol.16, pp. 761-769, 1992.

[56] M.A. Hossain, K.C.A. Alam, D.A.S. Rees, " MHD free and forced convection boundary layer flow along a vertical porous plate ", *Appl. Mech. Engr.*, vol.2, pp. 33-51, 1997.

[57] S. Kimura, A. Bejan, " The heat line visualization of convective heat transfer", *J. Heat Transfer*, vol.105, pp. 916-919, 1983.

[58] S.K. Aggarwal, A. Mahpara, " Use of heat line for unsteady buoyancy-driven flow in a cylindrical enclosure ", *J. Heat Transfer*, vol.111, pp. 576-578, 1989.

[59] H.I. Abu Mulaweh, " A review of research on laminar mixed convection flow over backward and forward-facing steps ", Int. J. Thermal Sciences , vol.42(9), pp. 897-909, 2003.

[60] M.A. Hossain, A.C. Mandal, " Effects of mass transfer and free convection on the unsteady MHD flow past a vertical porous plate with constant suction ", *Int. J. Energy Research*, vol.10, Issue.4, pp. 409-416, 1986.

[61] K.R. Sing, T.G. Cowling, " Thermal convection in magnetohydrodynamic boundary layer ", *J.Mech. Appl. Math.*, vol.16, pp. 1-5, 1963.

[62] N. Riley, " Magnetohydrodynamic free convection ", *J. Fluid. Mech.*, vol.18, pp. 247-267, 1964.

[63] H.K. Kuiken, " Magnetohydrodynamic free convection in a strong cross field ", *J. Fluid. Mechanics*, vol.40, pp. 21-38, 1970.

[64] G. Palani, U. Srikanth, " MHD flow past a semi infinite vertical plate with mass transfer ", *Nonlinear Anal: Model. Control*, vol.14, pp. 345-356, 2009.

[65] S. Siddiqa, M.A. Hossain , " Conduction-Convection-Radiation effects on the flow of optically dense grey fluid over a horizontal circular disk", *J. Eng. Phys. thermophys.*, vol.85, pp. 627-636, 2012.

[66] S. Siddiqa, M.A. Hossain, I.Pop, " Conjugate thermal and mass diffusion effect on natural convection flow in presence of strong cross magnetic field", *Int.J. of Heat and Mass Transfer*, vol.55, pp. 5120-5132, 2012.

[67] S. Siddiqa, M.A. Hossain, S.C. Saha, " Double diffusive magneto-convection fluid flow in a strong cross magnetic field with uniform surface heat and mass flux ", *J. Heat Transfer*, vol.134, Art. No. 114506 (9 pages), 2012.

[68] M. A. Hossain, H. Banu and R. A. Begum, " Effects of viscous dissipation and free convection currents on the flow of an electrically conducting fluid past an accelerated vertical porous plate", *Astrophysics and Space Sciences*, vol.113, pp. 269-279 1985.

[69] M.A. Hossain, I.Pop, M. Ahmed, " MHD free convection flow from an isothermal plate inclined at a small angle to the horizontal ", *J.of Theor. Appl. Fluid. Mech.* vol.1, pp. 194-207, 1996.

[70] A. Zeeshan, R. Ellahi, " Series solutions of non-linear partial differential equations with slip boundary conditions for non-Newtonian MHD fluid in porous space ", *J. Appl. Math. Inf. Sci*, vol.7(1), pp. 253-261, 2013.

[71] J.H. Merkin, " Free convection boundary layers on cylinders of elliptic cross section ", *J. of Heat Transfer*, vol.99, pp. 453-457, 1977.

[72] M.A. Hossain, M. A. Alim, " Effect of thermal radiation on natural convection over cylinders of elliptic cross section ", *Acta Mechanica*, vol.129, pp. 177-186, 1998.

[73] D.A. Saville, S.W. Churchill, " Laminar free convection in boundary layers near horizontal cylinders and vertical axisymmetric bodies", *J. Fluid. Mech.*, vol. 29, pp. 391-399, 1967.

[74] F.N.Lin, B.T. Chao ," Laminar free convection over two-dimensional and axisymmetric bodies of arbitrary contours" *J. Heat Transfer, Trans. ASMF. Series C*, vol.96, pp. 435-442, 1974.

[75] M. K. Jaman, M.A. Hossain, " Fluctuating free convection flow along heated horizontal circular cylinders". *Int. J.Fluid Mech. Res.*, vol.36, pp. 207-230, 2009.

[76] M. K. Jaman , M.A. Hossain, " Effect of fluctuations surface temperature on natural convection flow over cylinders of elliptic cross section ", *The open transport phenomena Journal*, vol.2, pp. 35-47, 2010.

[77] D. B.Ingham, " The magnetogasdynamic boundary layer for a thermally conducting plate", *Quart. J. Mech. and Applied Math*, vol.20, Pt.3, 1967.

[78] G.Wilks, " Magnetohydrodynamic free convection about a semi infinite vertical plate in a strong cross-field ", *J. Appl.Math. Phys.*, vol.27, pp. 621-631, 1976.

[79] M.A. Hossain, " Viscous and joule heating on MHD free convection flow with variable plate temperature ", *Int. J. of. Heat and Mass Transfer*, vol.35, pp. 3485-3487, 1992.

[80] R. Hunt, G. Wilks, " Low Prandtl number magnetohydrodynamic natural convection in a strong cross field ", *Numer. Heat Transfer* , vol.4, pp. 303-316, 1981.

[81] G. Wilks, R. Hunt, " Magnetohydrodynamic free convection flow about a semi infinite plate at whose surface heat flux is uniform ", *ZAMP*, vol.35, pp. 34-49, 1984.

[82] H.M.Badr, " A theoretical study of laminar mixed convection from a horizontal cylinder in a cross stream", *Int. J.Heat Mass Transfer.*,vol.26, no. 5, pp. 639-653, 1983.

[83] F.M.Mahfouz, H.M.Badr, " Flow structure in the wake of a rotationally oscillating cylinder", *Journal of Fluids Engineering.*, vol.122, pp. 290-300, 2000.

[84] H.M.Badr, " Laminar combined convection from a horizontal cylinder-parallel and contra flow regime", *Int. J.Heat Mass Transfer.*, vol.27,no. 1, pp. 15-27, 1984.

[85] P. wang, R. Kahawita, D.L. Nguyen, " Transient laminar convection from horizontal cylinders ", *Intl. J. of Heat and Mass Transfer*, vol.34, no.6, pp. 1429-1442, 1991.

[86] B.Fornberg, " A numerical study of steady viscous flow past a circular cylinder", *J. Fluid Mech.*, vol.98, part.4, pp. 819-855, 1980.

[87] H. D. Nguyen, P. Seungho, R.W.Douglass, " Unsteady mixed convection about a rotating circular cylinder with small fluctuations in the free stream velocity", *Int.J.Heat Mass Transfer.*, vol.39, no.3, pp. 511-525, 1996.

[88] Chin-Hsiang Cheng, Jing-Lia Hong, Win Aung, " Numerical prediction of lock-on effect on convective heat transfer from a transversely oscillating circular cylinder", *Int. J.Heat Mass Transfer.*, vol.40, no.8, pp. 1825-1834, 1997.

[89] J.Patterson, J.Imberger, " Unsteady natural convection in a rectangular cavity", *J. Fluid Mech.*, vol.100, part.1, pp. 65-86, 1980.

[90] S.C.R. Dennis, J.D.Hudson, N. Smith, " Steady laminar forced convection from a circular cylinder at low Reynolds number ", *Physics Fluids*, vol.2, pp-933-940, 1967.

[91] P. R. Nachtsheim and P. Swigert, " Satisfaction of asymptotic boundary conditions in numerical solution of the system of non-linear equations of boundary layer type ", NASA TND-3004, 1965.

[92] J.C. Butcher, " Runge-Kutta method ", *Math.Com*, vol.18, pp. 50-55, 1964.

[93] H.B. Keller, " Numerical methods in boundary layer theory", *Annul. Rev. Fluid. Mech.*, vol.10, pp. 417-433, 1978.

[94] T.Cebeci, P. Bardshaw, " Physical and computational aspects of convective heat transfer ", Springer-Velag, NY, 1984.

[95] H.Schlichting, K.Gersten, " Boundary -Layer Theory ", *Springer*, 2000.

[96] H.K.Versteeg, W.Malalasekera, " An introduction to Computational Fluid Dynamics ", *Longmann Scientific and Technical*, 1995.

[97] I.Pop, D.B.Ingham, " Convective Heat Transfer: Mathematical and Computational Modeling of Viscous Fluids and Porous Media ", *Peragamon* , 2001.

[98] T.Cebeci, P.Bradshaw, " Momentum transfer in boundary layers ", *Hemisphere publishing Corporation*, 1977.

[99] C.A.J. Fletcher, " Computational Techniques for fluid dynamics ", Vol. 1,2., Springer-Verlag, Berlin.

[100] Sadia Siddiqa, " On Convection Flow of Viscous Fluid Along a Surface with and without Radiation Effect", Ph.D thesis, COMSASTS Institute of information and Technology,